THE UNIVERSITY *of* EDINBURGH

Nanoparticles and Atherosclerosis:

Resolving the Paradox

Jennifer B Raftis

Presented for the degree of Doctor of Philosophy

University of Edinburgh

2013

Declaration

I hereby declare that the thesis presented has been composed only by me the undersigned. The work contained within this thesis has been performed wholly by me except in certain circumstances, for which the contributors and level of contribution are clearly indicated.

I also declare that the work presented herein has not been submitted for any other degree or professional qualification.

Jennifer B Raftis

To Pat and Rena Raftis

(Dad and Mam)

Acknowledgements

I would like to first and foremost like to thank my team of supervisors Dr Nick Mills, Dr Rodger Duffin and Professor Ken Donaldson; though I never went as far as praying to them they were the holy trinity of supervisors. Nick for his endless enthusiasm in the face of any data, Rodger for always being ready to help with anything and Ken “The Don” Donaldson, godfather of particle toxicology he put many things in perspective; they have been an endless source of inspiration, knowledge, kindness, realism, time and modesty. It was a privilege working with all of them. I am looking forward to continuing to work together on projects in the future.

I would like to thank the Department of Health for supporting these studies through the award of Policy Research Programme Nanotechnologies (PR-NT-0208-10025) and the BHF Programme Grant (RG/05/003). I would like to take this opportunity to say a special thanks to everyone that works under the BHF Programme Grant in particular the inspirational Professor David Newby (Professor of Cardiology and Consultant Cardiologist),who has been an invaluable support throughout my project; he makes a very difficult job look easy. I have been very fortunate to be involved with this group during my project; they are a dynamic, remarkable group of people who always keep the bigger picture in mind. I would like to thank Dr Andrew Lucking, Dr Jeremy Langrish, Dr Mark Miller, Dr Katie Shaw, Dr Anoop Shah, Dr Shirjel

Alam, Dr Nikhil Joshi, Steve McLean and last but not least Dr Amanda Hunter.

I would like to thank both past and present members of the ELEGI Colt Laboratories, MRC/University of Edinburgh Centre for inflammation research, Professor Bill MacNee, Dr Ellen Drost, Dr Craig Poland, Dr Fiona Murphy, Dr Anja Schinwald, Jen McLeish, Dr Wan-Seob Cho, Catherine McGuinnes, Dr Roberto Rabinovich, Dr Santiago Giavedoni, Dr Gourab Choudhury and Dr Ramzi Lakhdar. The CIR in general is a great place to do a PhD, everybody was ready and willing to help whether or not it was in their best interests, I would like to say a special thanks to Professor Adriano Rossi, Professor Ian Dransfield, Professor Sarah Howie, Dr Jillian Stephen, Mark Marsden, Bob Morris and his histology team. A special thanks has to go to Fiona Rossi and Shonna Johnston for their endless patience and optimistic approach to everybody around them, they made my life a lot easier, though I don't think they can say the same about me. I would like to thank Steve Mitchell for help with the electron microscopy work.

I would like to thank all the dedicated staff at the Clinical Research Facility (CRF) at the Royal Infirmary of Edinburgh who were endlessly accommodating to the ever changing needs of research and unaccountably calm in the face of last minute changes. They created a friendly and entertaining working environment and I look forward to any work I have to carry out there in the future. I would particularly like to thank Finny Patterson,

Sharon Cameron, Tracey Edminston and Heather Spence. I would also like to say a special thank you to the volunteers who willingly gave up their time and blood for my research, I am truly grateful, as well as all the phlebotomists in the CIR.

On a more personal note I would not have been able to complete this work without the support of some very good friends I have made along the way, Jillian Stephen and Siobhán Ní Choileáin for providing much light relief mainly in the form of dinners and pints, Amanda Hunter for trips to Starbucks and entertainment whilst stripping pigs. Outside of work I would like to thank Elizabeth Ludvigsen, Caitlin Smith, Jonathan Rush and Luke Morgan, for always appearing to be interested in what I did. I would like to thank Riley Briggs for his help and being a welcome distraction over the past year.

I would like to thank my family, my Father Pat, Mother Rena, Sisters Emma, Caroline and Sean (my brother from another mother) whom I dedicate this thesis too. It sounds trite, but I could and would not have done this without them. My sister Emma in particular knows what doing a PhD is like as we started ours around the same time and she has been an invaluable sounding board throughout the whole process.

Abstract

Air pollution is increasingly recognised as an important and modifiable risk factor for cardiovascular disease. Exposure is associated with a range of adverse cardiovascular events including hospital admissions with angina and myocardial infarction, and with cardiovascular death. The main arbiter of these adverse health effects appears to be combustion-derived nanoparticles that incorporate reactive organic and transition metal components. Through the induction of cellular oxidative stress and pro-inflammatory pathways, these nanoparticles exert detrimental effects on platelets, vasculature and myocardium, and can augment the development and progression of atherosclerosis.

Over the last 10 years there has been remarkable progress in the development of targeted engineered nanoparticles as contrast agents to enhance cellular and molecular imaging. Ultra-small paramagnetic iron oxide (USPIO) nanoparticles (<100 nm) produce disruptions in the magnetic field of magnetic resonance imaging (MRI) scanners, and a decrease in image intensity in areas where the particles accumulate. USPIO particles are phagocytosed by cells of the monocyte-macrophage system throughout the body including within atheromatous plaques. USPIOs have regulatory approval in the United Kingdom for imaging lymph nodes in breast and prostate cancer as well as FDA approval for parenteral iron-replacement

therapy in chronic kidney disease. There is great interest in developing USPIO and other nanoparticle contrast agents for imaging atherosclerosis.

The delivery of engineered nanoparticles (ENPs) directly into the bloodstream to provide enhanced imaging of the unstable atheromatous plaque may assist in the diagnosis of plaque rupture and may ultimately permit targeted delivery of therapies directly to the site of vascular injury. However, these particles once blood-borne may alter monocyte-macrophage function and activate circulating platelets with adverse effects on clinical outcomes. Previously it has been shown that inhalation of combustion-derived nanoparticles results in increases in platelet-monocyte aggregation and thrombus formation in healthy volunteers. These combustion derived nanoparticles share structural similarities with engineered nanoparticles designed for intravascular infusion. This raises an obvious paradoxical question: can engineered nanoparticles designed for medical use mediate similar effects to combustion derived nanoparticles in susceptible populations?

My thesis addresses this question and describes a series of complimentary experimental and clinical studies to investigate the effects of engineered nanoparticles on platelet function and thrombogenesis using commercial and clinically available nanoparticles. I found that cationic nanoparticles caused platelet activation and aggregation in vitro, whereas, anionic nanoparticles caused inflammation and up-regulated adhesion molecule ICAM-1 in

monocyte derived macrophages indicating that nanoparticles have different toxicological properties in different biological conditions. Using an ex vivo model of thrombus formation, the Badimon chamber, I observed that USPIO nanoparticles added to flowing native whole blood in an extra-corporeal circuit increased platelet rich thrombus formation under high shear conditions compared to saline control in healthy volunteers. These studies were repeated in patients with abdominal aortic aneurysms who received intra-venous systemic infusions of USPIO to enhance MRI imaging. I demonstrated up-regulation in markers of platelet activation and more platelet rich thrombus formation in the Badimon chamber one hour following systemic delivery of USPIO.

In summary I have demonstrated that medical nanoparticles influence platelet activation in patients with cardiovascular disease and have pro-thrombotic effects in an ex-vivo model of in both healthy persons and susceptible patients. In light of this data and to ensure the safe future development of engineered nanoparticles for medical use platelet activation assays and follow-up monitoring of patients should be considered routine in both the developmental and clinical stages of engineered nanoparticle use.

Contents

Table Index

Figure Index

Abbreviations

AAA	Abdominal Aortic Aneurysm
ACS	Acute coronary syndrome
ADME	Adsorption, distribution, metabolism and elimination
APC	Allophycocyanin
CD62P	P-selectin
CDNP	Combustion derived nanoparticles
DLS	Dynamic light scattering
ELISA	Enzyme-linked immunosorbant assay
ENP	Engineered Nanoparticle
EPR	Electron paramagnetic resonance
FITC	Fluorescein isothiocyanate
FMT	Fluorescence-mediated tomography
HBSS	Hank's Balanced Salt Solution (HBSS)
ICAM	Intracellular adhesion molecule
ICPMS	Inductively coupled plasma mass spectrometry
IL-	Interleukin
IMDM	Iscove's modified Dulbecco's medium
Kcps	kilo counts per second
LPS	Lipopolysaccharide
$MDM_{ø}$	Monocyte-derived macrophages
MMP	Matrix metalloproteinase
MRI	Magnetic resonance imaging

PBMC	Peripheral blood mononuclear cells
PBS	Phosphate buffered saline
PE	Phycoerythrin
PEG	Polyethylene glycol
PET	Positron-emission tomography
PFA	Paraformaldehyde
PM10	Particulate Matter
PPACK	D-Phenylalanine-L-prolyl-L-arginine chloromethyl ketone
PPP	Platelet poor plasma
PRP	Platelet-rich plasma
PSC	Polyglucose sorbitol carboxymethylether
PSGL-1	P-selectin glycoprotein ligand-1
RES	Recticuloendothelial system
SPECT	Single-photon-emission computed tomography
SPIO	Superparamagnetic particles of iron oxide
TEM	Transmission electron microscope
Tempone-H	1 hydroxyl-2,2,6,6-tetramethyl-4-oxo-piperdine
TNFα	Tumour necrosis factor alpha
TRAP-6	Thrombin Receptor Activating Peptide-6
USPIO	Ultrasmall superparamagnetic particles of iron oxide
WP	Washed platelets
ZP	Zeta Potential

Chapter 1 **Introduction**

Much of the following chapter has been adapted from Chapter 8, p139-156 "Cardiovascular Effects" of the book "*Adverse Effects of Engineered Nanomaterials*" written by Jennifer B Raftis, edited by Nick Mills and Rodger Duffin.

1.1 *Cardiovascular Disease*

Cardiovascular disease is the most common cause of death worldwide in both men and women. As societies become more developed, and the standard of living improves, cardiovascular disease increases in prevalence as less people die early in life from communicable disease due to improvements in healthcare. Life expectancy also increases and cardiovascular disease is more common in older persons. Increasing knowledge and treatment of cardiovascular risk factors has led to a decline in mortality rates in developed countries however the problem continues to escalate globally because rates in developing countries are increasing rapidly.

1.1.1 **Atherothrombosis**

Atherothrombosis is a complex inflammatory disease and is classified according to plaque composition (van Gils et al. 2009). Plaque development, rupture and subsequent thrombosis involve a number of inflammatory processes including endothelial dysfunction, leukocyte recruitment and migration, platelet activation, matrix metalloproteinase (MMP) activity, and degradation of the fibrous cap resulting in plaque rupture and thrombosis (Slevin et al. 2008).

The following image taken from Sanz and Fayad 2008 (Sanz and Fayad 2008) depicts normal endothelium on the left and the development and rupture of an atherosclerotic lesion on the right hand side.

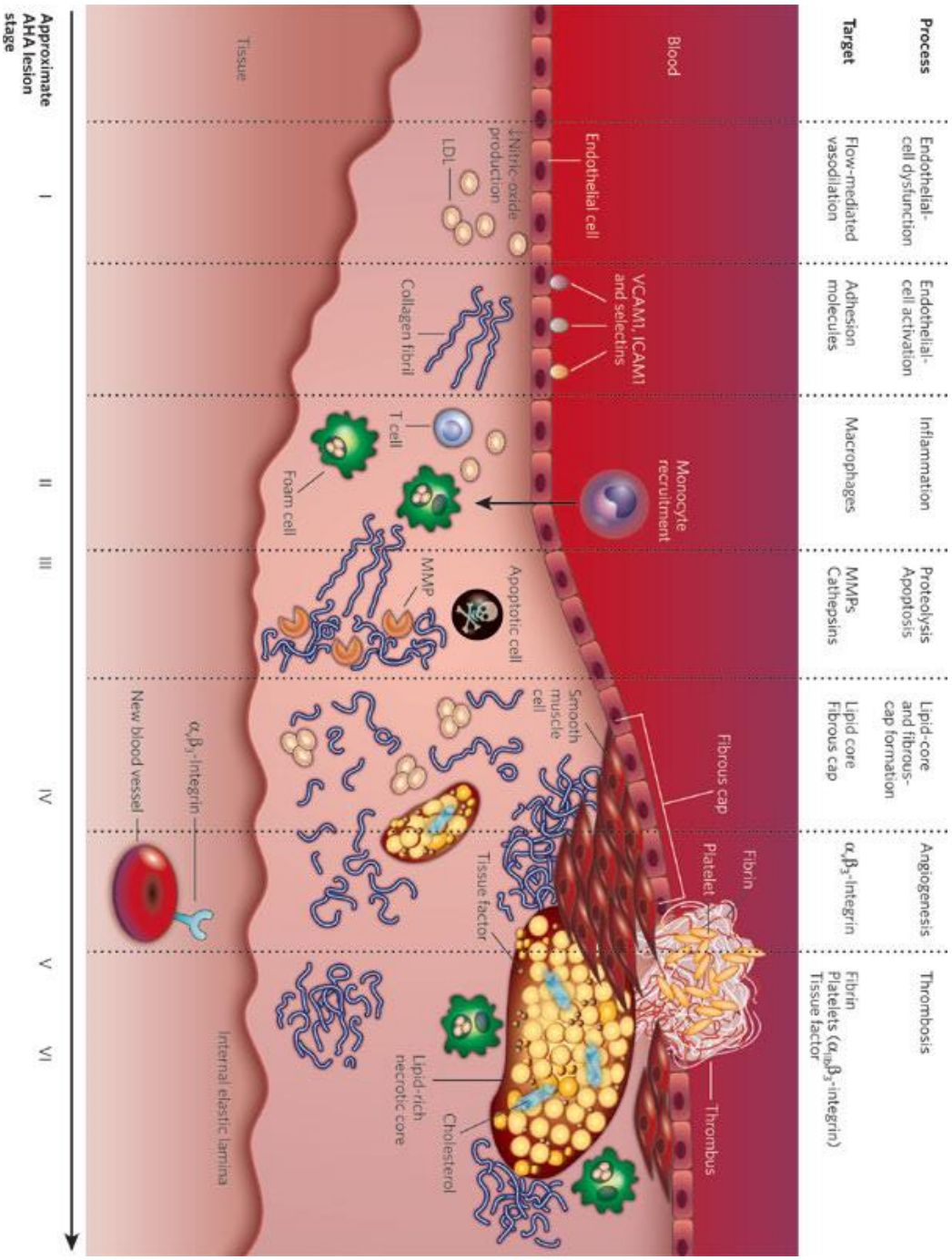

Figure 1-1 Atherosclerotic Lesion Development

1.1.2 **Cardiovascular Risk**

Successful therapies and strategies for prevention of cardiovascular disease are dependent on identification of individuals at risk using clinical risk scores based on age, sex, blood pressure, serum cholesterol and cigarette smoking (Viera and Sheridan 2010;Wang 2011). While these risk scores are used widely and identification of traditional risk factors is the basis of most primary prevention screening policies, these calculators are imperfect; the majority of persons presenting with an adverse cardiac event have no prior history or any established risk factors (Wang 2011). The converse is also true, many patients with risk factors do not go on to develop atherothrombotic disease or have an acute cardiovascular event.

Cardiovascular risk is not a static entity and fluctuates hour to hour and day to day. There are many contributing factors to our cardiovascular risk some of which are:

- Age
- Gender
- Physical Activity
- Genetics
- Diet
- Blood Cholesterol
- Blood Pressure

- Weight
- Stress
- Air Pollution

All these factors combine, at any one time, to determine how likely it is that an individual will suffer an adverse cardiovascular event.

An alternative and perhaps preferable strategy would be to identify individuals with early atherosclerotic disease in an attempt to modify the course of the disease and prevent the clinical consequences of plaque rupture, thrombosis, and infarction. Clinical and experimental research has focused on the identification of novel biomarkers that could indicate the early development of atherothrombotic disease. Before a biomarker is introduced as a diagnostic tool in clinical practice, it must satisfy the following criteria: it must be highly specific, easy to measure, provide novel information about the disease, and reflect disease burden accurately helping the clinician decide on an appropriate course of treatment. These basic criteria are not easily met for a heterogeneous condition like atherothrombosis. Imaging strategies that target these pathological processes in atherosclerotic plaque development may provide more sensitive methods to monitor disease progression, permit early detection of the disease, and have a role in the assessment of treatment efficacy. The ability to identify plaque structure and function/activity would allow the clinician to identify those individuals at highest risk of plaque rupture.

1.2 *Nanoparticles*

1.2.1 **Nanotechnology**

Nanotechnology aims at the development of nanoparticles (particles with at least one dimension less than 100nm; ENP) and other nanomaterials such as nanosurfaces and nanomatrices with novel properties not found in the same material in its bulk form. Nanotechnology is currently being applied in all manner of commercial industries to confer unique properties on products or improve those existing ones. One of the potentially most significant applications is in the field of medicine. A huge number of studies are underway to determine the usefulness of ENPs and nanosurfaces in a variety of medical fields and they are likely to have a big impact in areas such as diagnostics, medical imaging and treatment (Linkov et al. 2008) allowing for a movement towards personalised patient medicine. Concomitant with the development of nanotechnology a new discipline of nanotoxicology has emerged.

1.2.2 **Nanotoxicology**

Nanotoxicology assesses the potential risks of both naturally occurring and anthropogenic NPs; it serves to ensure the safety and continued development of nanotechnology whilst protecting consumers, workers and

the environment (Donaldson et al. 2004). The novel nature of ENPs is not taken into account under American, European or British medical product legislation. Whilst we may come to realise in the future that it is unnecessary to legislate ENP separately a more cautious approach seems warranted during early use. This should avoid unexpected outcomes and also increase public confidence in their safety when their use becomes widespread. Nanotechnology has advanced rapidly and is now a platform for many medical applications such as drug delivery (Wang et al. 2011), imaging (Yilmaz et al. 2011a) and diagnosis of disease (Hamzah et al. 2011). A number of questions have been raised about the safety of introducing large numbers of ENPs (Rosner and Auerbach 2011a) to potentially vulnerable patients (Donaldson and Seaton 2007). ENPs intended for clinical application should be rigorously tested with assessments taking into consideration the unique toxicology profile of nanoscale materials (Stone et al. 2007). The diversity of medical ENPs with respect to size, surface area, composition and surface properties, and the rapid pace of their development and commercialization, poses significant challenges to traditional toxicological paradigms (Gupta and Gupta 2005). With so many variables and no agreed standards for safety it may be difficult to fully characterise the effects of ENPs before clinical use (Walker and Bucher 2009).

1.3 *Diagnostic and therapeutic applications of nanoparticles in cardiovascular disease*

ENPs are unique in terms of their size and structure. Their small size allows them to interact with the body at a molecular level and confers upon them a high surface area to volume ratio. They can be manufactured to have different shapes, sizes, structures, surface functionalization and coatings, allowing them to be specifically targeted to a biomarker of disease (Song et al. 2010). The ability to understand and manipulate the properties of nanomaterials will ultimately determine their usefulness in nanomedicine (Cormode et al. 2009). The following table, adapted from Kim et al 2010 (Kim et al. 2010), gives examples of nanomaterials intended for clinical use:

Table 1-1 nanomaterials intended for clinical use

Nanomaterial	Commercial Name	Application	Target	Adverse Effects	Manufacturer	Current Status
Iron oxide	Endorem	MRI	Liver	Back pain, vasodilation	Bayer Schering	FDA approved
	Resovist	MRI	Liver	None	Bayer Schering	FDA approved
	Combidex	MRI	Lymph nodes	None	Advanced Magnetics	In phase 3 clinical trials
	Nano Therm	Cancer therapy	Various	Acute urinary retention	MagForce	In phase 3 clinical trials
	Feraheme	Iron replacement therapy	RES macrophages of the liver, spleen and bone marrow	Diarrhea, nausea, dizziness, hypotension, constipation, peripheral edema anaphylactic-type reactions, cardiac arrest, Tachycardia, angioedema, ischemic myocardial events.	AMAG Pharmaceuticals	FDA approved
Gold	Verigene	In vitro diagnostics	Genetic	N/A	Nanosphere	FDA approved
	Aurimmune	Cancer therapy	Various	Fever	CytImmune Sciences	Phase 2 clinical trials
Nanoshells	Auroshell	Cancer therapy	Head and Neck	Under investigation	Nanospectra Biosciences	Phase 1 clinical trials
Protein	Abraxane	Cancer therapy	Breast	Cytopenia	Abraxis Bioscience	FDA approved
Liposome	Doxil/Caelyx	Cancer therapy	Various	Hand-foot syndrome, stomatitis	Ortho Biotech	FDA approved
Polymer	Oncaspar	Cancer therapy	Acute lymphoblastic leukemia	Urticaria, rash	Rhône-Poulenc Rorer	FDA approved
	CALAA-01	Cancer therapy	Various	Mild renal toxicity	Calando	Phase 2 clinical trials
Dendrimer	VivaGel	Microbicide	Cervicovaginal	Abdominal pain, dysuria	Starpharma	Phase 2 clinical trials
Micelle	Genexol-PM	Cancer therapy	Various	Peripheral sensory neuropathy, neutropenia	Samyang	Phase 4 clinical trials

Nanomaterial synthesis has progressed rapidly in recent years and has generated complex state-of-the-art nanoscale structures with diverse and complex functionalities (Cormode, Skajaa, Fayad, & Mulder 2009). The ability to construct such nanomaterials has led to the development of multi-modal and multi-functional ENPs to facilitate magnetic resonance imaging (MRI), computed tomography (CT) and positron-emission tomography (PET) or for targeted drug delivery (Kim et al. 2011). The development of such ENPs has led to the terms “theragnostic” or “theranostic” to describe an ENP that can be used both for diagnostic and therapeutic applications (Cormode, Skajaa, Fayad, & Mulder 2009;Schladt et al. 2011).

The application of nanotechnology to medical imaging is an exciting new frontier in medical science. To date only a handful of ENPs are used routinely in the clinic (Rosner and Auerbach 2011b;Weidner et al. 2011), but many more are in development or under investigation in clinical trials (Kim, Rutka, & Chan 2010). As a research tool, ENM are invaluable (Mulder et al. 2007). Unlike traditional imaging strategies, ENP based or molecular imaging modalities enable us to study the underlying mechanisms of disease *in vivo* to identify the biological, chemical and genetic factors contributing to the disease (McCarthy et al. 2010). On a simpler level, ENPs have been used to improve the effectiveness of current clinical diagnostic tools. For example, SPIONs are used as a contrast agent in patients undergoing magnetic resonance imaging (MRI) to improve spatial resolution.

Imaging as a diagnostic tool has gained importance over the years and is now indispensable in the clinic. Systems such as PET, single-photon-emission computed tomography (SPECT), fluorescence reflectance imaging, fluorescence-mediated tomography (FMT), fibre-optic microscopy, optical frequency-domain imaging, will provide the future platforms for non-invasive molecular cardiovascular imaging. Comprehensive reviews of the nanomaterials in development for cardiovascular imaging are available elsewhere (Jaffer et al. 2006a;Jaffer et al. 2006b;Nahrendorf et al. 2008;Nahrendorf et al. 2009a;Sosnovik et al. 2008).

1.3.1 **Superparamagnetic iron oxide nanoparticles**

In 1985, Stark et al used MRI to determine the quantitative relationship between relaxation rates and iron levels in patients with iron overload (Stark et al. 1985) and it was quickly deduced that the increase in T2 relaxation rates in these patients could be artificially replicated and used to provide contrast in MRI (Renshaw et al. 1986). MRI imaging has been used to assess the extent of damage after a myocardial infarct or to monitor peripheral vascular disease (Uppal and Caravan 2010). SPIONs were originally used to provide contrast when imaging liver (Fukukura et al. 2010), spleen (Beduneau et al. 2009) and lymph nodes (Weidner, van Lin, Dinter, Rozema, Schoenberg, Wenz, Barentsz, & Lohr 2011) as this is where these particles naturally accumulated. With improvements in ENP production iron-

oxide ENPs were designed to be more biocompatible with increased circulation times to assist with MRI (Krombach et al. 2002a). Particle size and surface coating can be modified to target SPIONs to different sites. Larger particles, 50-150 nm in diameter, predominantly produce a signal decrease and are used as contrast media for imaging the liver and spleen. Smaller particles, less than 20 nm, are distributed more widely and can improve the identification of lymph nodes (Harisinghani et al. 1997;Harisinghani et al. 2003) or assist in the characterization of vulnerable atherosclerotic plaque. SPIONs have been used to enhance plaque imaging in a number of experimental models of atherosclerosis (Briley-Saebo et al. 2008;Klug et al. 2008;Klug et al. 2009;Sigovan et al. 2009), however the clinical studies published to date are less consistent (Morishige et al. 2010;Richards et al. 2011;Tang et al. 2008;Yilmaz et al. 2011b).

Macrophages are the most common target for molecular imaging agents as there is a large body of evidence implicating them in the disease and, as a naturally phagocytic cell; they tend to scavenge foreign material without much manipulation. Several experimental studies have demonstrated that SPIONs or ultra-small paramagnetic iron oxide ENPs (USPIONs) can localise to atherosclerotic plaques and can be used to evaluate its metabolic state (Klug, Gert, Thomas, Christan, Marco, Elisabeth, Volker, Rommel, Eberhard, Peter, & Wolfgang 2009;Kooi et al. 2003a;Richards, Semple, Macgillivray, Gray, Langrish, Williams, Dweck, Wallace, McKillop, Chalmers, Garden, & Newby 2011;Schmitz et al. 2001a;Trivedi et al. 2004). Targeted molecular

imaging has been shown to result in localisation of ENPs within macrophage in atherosclerotic plaque (Kooi, Cappendijk, Cleutjens, Kessels, Kitslaar, Borgers, Frederik, Daemen, & van Engelshoven 2003a;Ruehm et al. 2001a;Trivedi et al. 2003a).

Other applications of SPIONs include the assessment of myocardial perfusion (Jing et al. 2008;Krombach et al. 2002b) and characterisation of aortic aneurysms (Richards, Semple, Macgillivray, Gray, Langrish, Williams, Dweck, Wallace, McKillop, Chalmers, Garden, & Newby 2011). SPIONs with a modified coating have also been used in molecular imaging, such as receptor-directed imaging (Eck et al. 2010), cell labeling for in-vivo monitoring of stem cell migration (Thu et al. 2009), and in labelling gene constructs for localization in gene therapy studies (Zhao et al. 2010).

1.3.2 **Design and synthesis of SPIONs**

For molecular imaging purposes SPIONs need to be biocompatible, low-toxicity, have a high magnetic moment, high colloidal stability, uniform particle size and the ability to bind various types of biological molecules (Lodhia et al. 2010a). The particle surface, functionalization or coating acts as the interface between the body and the core of the ENP often acting as a barrier to stabilise the core thus ultimately determining the reactivity and solubility of the ENP core (Mahmoudi et al. 2011a). Often the surface

monolayer is used to target the core molecule to a specific site of interest. Drug delivery to a specific area of the body without the associated systemic side effects is one of the most attractive attributes of a ENP- based drug delivery platform (Mahmoudi, Sant, Wang, Laurent, & Sen 2011a). Delivery of SPION's to a specific region of interest or disease state is dictated by their surface functionalization (Uppal et al. 2011;Uppal & Caravan 2010).

For the most part SPIONs are in development as MRI contrast agents, which relies on them having a high saturation magnetism value measured as electromagnetic units per gram (Lodhia, Mandarano, Ferris, Eu, & Cowell 2010a;Lodhia et al. 2010b). This value will determine the overall effectiveness of the contrast agent. Relaxation rates are a measure of the ability of a contrast agent to enhance the relaxation rate of water protons (H^1). SPIONs with high T2 values have faster relaxation rates. Properties that affect the magnetisation value of a SPION include size and aggregation with the highest values occurring in particles between 6-20nm in diameter. When each particle is separate it will act independently, which increases the net magnetism per unit mass. The more particles aggregate the lower their magnetisation values and surface coatings are often used to prevent aggregation.

Research focusing on understanding the various interactions of SPIONs with the glycocalyx and biomolecules *in vivo* (i.e. protein corona) may lead to novel SPIONs with optimum surface properties that might overcome the

problems of toxicity (see below) and permit more successful targeting (Mahmoudi et al. 2011b;Shaw and Murthy 2010). Examples of SPIONs in development or in clinical use are given below (adapted from Lodhia et al) (Lodhia, Mandarano, Ferris, Eu, & Cowell 2010a):

Table 1-2 SPIONs and their application in clinical medicine

Name	Status	Application	Administration	Relaxivities $mmol^{-1}sec^{-1}$	Coating	Core size (nm)
Lumirem and Gastromark	USA and Europe	GI	Oral	T2-72 T1-3.2	Silica	300
Abdoscan	Europe	GI	Oral	N/A	Polystyrene	300
Endorem/ Feriedex	USA	Liver/Spleen	IV	T2-98.3 T1-23.9	Dextran	5.6
Resovist	Withdrawn from some markets	Liver/Spleen	IV	T2-151.0 T1-25.4	Carbo-Dextran	4.2
Sinerem/ Combidex	Clinical trial	Lymph node Bone Marrow	IV	T2-44.1 T1-21.6	Dextran	4-6
Clariscan	Discontinued	Perfusion/ angiography	IV	T2-35 T1-20	Carbohydrate-PEG	5-7
Supravist	Preclinical	Perfusion Lymph node Bone Marrow	IV	T2-57 T1-7.3	Carbo-Dextran	3-5
MION 46	Preclinical	Angiography Lymph node Tumour Infarction	IV	N/A	Dextran	4-6
Feraheme	USA	Iron replacement therapy	IV	N/A	Polyglucose sorbitol carboxymethylether	

1.3.3 **Particokinetics of parenteral delivery of nanomaterials for medical applications**

Toxicokinetic studies are intended to define parameters under which a xenobiotic is to be studied and the particle equivalent is particokinetics. Ideal mass balance particokinetics aims to have information that is comparable from one study to another defining the adsorption, distribution, metabolism and elimination (ADME) of the xenobiotic (Buchanan et al. 1997). Relative to the amount of literature available on the applications of ENPs in medicine, there is little in the way of particokinetic data concerning the fate of such particles following exposure (Lewinski et al. 2008). With ENP, not only do we have to consider whether the particles themselves are inherently toxic, but also how they interact with molecular structures and how, or if, they redistribute and clear from organs and tissues.

When used in drug delivery, ENPs are often employed to increase specificity of drug delivery and improve persistence of the parent drug in the body (Li and Huang 2008). In a situation where the ENP increases drug circulation it is important to monitor particokinetics to predict potential parent drug toxicity and side effects which may be substantially altered once the drug is associated with a ENP (Li & Huang 2008). Characteristics of the ENP such as size, surface area, charge and surface chemistry as well as the method by which they are introduced (intravenous, inhalation, sub-dermal injection,

ingestion into the gut etc.) determine the ultimate fate of the ENP once inside the body. Medical ENP themselves are usually made of materials deemed biologically safe and are generally not the drugs themselves, merely a delivery vehicle as is the case with drug-loaded liposomes. They may also serve as a means of visualising pathological processes and lesions in life as is the case with nanoparticulate contrast agents. The behaviour of ENP cannot be determined from their bulk properties since relatively low toxicity materials in their bulk form display novel properties, even toxicity, when presented in the nano-scale. Therefore it is very important to rigorously test nanomaterials composed of a material even if it has been found to be low toxicity in bulk form and in fact the nano-form may arguably be seen as a new materials with unknown properties. Kinetic studies of ENPs used in medicine have been carried out, but no single consensus has emerged on what determines their fate.

1.3.3.1 Surface dependent distribution

Surface characteristics are one of the main factors in determining whether or not a particle will be cleared by the recticuloendothelial system (RES) after intra-venous administration (Al-Jamal et al. 2009). When hydrophobic ENPs are injected intra-venously they are rapidly opsonised by blood serum proteins and cleared from the circulation by the RES resulting in significant losses from circulation. However this opsonisation can be limited by

alteration of the surface coatings of the ENPs. The most common method of prolonging circulation is conjugation of the ENP with polyethylene glycol (PEG) polymer, providing the particle with steric hindrance to opsonisation or phagocytosis (Li & Huang 2008) and allowing the 'PEG-ylated' form to remain in the circulation for much longer thus increasing their potential for interaction with blood components. A number of studies have demonstrated altered distribution patterns based on modification of the surface coating. He (He et al. 2008) compared three silica ENPs each with a different surface ligand attached, -OH, -COOH and PEG. The PEG-ylated particles showed longer circulation times and a reduced uptake by the RES. Beduneau (Beduneau, Ma, Grotepas, Kabanov, Rabinow, Gong, Mosley, Dou, Boska, & Gendelman 2009) covalently conjugated IgG molecules to the surface of SPIONs showing accelerated uptake by monocytes and enhanced retention *in vivo* without affecting monocyte viability. This technique could be very useful in the monitoring and tracking of disease progression. It is clear that surface modification has the ability to alter distribution and clearance patterns of ENPs in the body, with small changes in surface moiety resulting in big differences in behaviour of these particles in the body (van Tilborg et al. 2008), (Jayagopal et al. 2007). Berry (Berry et al. 2003) demonstrated the need for increased understanding of ENP-cell interactions and how quickly they can be altered through surface modification. In the study the same ENPs were made with either a dextran or albumin polymer coating which significantly altered the pattern of ENP uptake by fibroblasts. The dextran ENPs were endocytosed and caused eventual cell death, whereas the

albumin-coated particles showed only signs of partial endocytosis and induced cell proliferation. This demonstrates the need to determine particle and coating activity as a whole and recognition of particles coatings in ultimately determining biodistribution patterns and determine biological activity.

1.3.3.2 Size Dependent Distribution

Others have suggested that size determines the final location of particles injected into the bloodstream (De Jong et al. 2008). This is likely to be true to an extent but is probably most relevant in those with an underlying condition such as atherosclerosis. Normally, in a healthy individual, the endothelium is very effective at preventing extravasation of ENPs due to the presence of tight junctions between endothelial cells (<2nm). However when the endothelium is compromised, as is the case in atherosclerosis, the normally tight junctions become more permeable and could potentially allow passage of ENPs in to underlying matrix, with unknown consequences. The final destination of particles in the body has been reported to be directly related to their size, with larger particles, >100nm, accumulating in the spleen due to its discontinuous endothelium with large fenestrations. Smaller particles, <100nm, accumulate in the liver passing through the fenestrated endothelium and finally taking up residence in the underlying parenchymal cells. Kinetic studies with gold ENPs show a size-dependent pattern of distribution. A

study by De Jong (De Jong, Hagens, Krystek, Burger, Sips, & Geertsma 2008) investigated a range of gold ENPs, administered intravenously in rats and found that biodistribution was dependent on particle size. The smallest particles (10nm) showing the most widespread organ distribution with 0.3% crossing the blood-brain barrier and high concentrations of all particles remaining in circulation after 24 hours, which could result in further accumulation in the organs. A similar study (Semmler-Behnke et al. 2008) in rats compared two particle sizes, both in the ultrafine range, 1.4nm and 18nm gold ENPs. The clearance of 1.4nm gold occurred via the kidneys and hepatobillary system whereas no such clearance was observed for the 18nm particles. They also reported accumulation of the larger particles in the liver and spleen, whereas no such organ-specific accumulation was seen for the 1.4nm particles.

1.3.3.3 Localisation to Atherosclerotic Plaques

Targeted molecular imaging has been shown to result in localisation of ENPs to atherosclerotic plaques (Kooi et al. 2003b),(Trivedi et al. 2003b), (Ruehm et al. 2001b). So it is known, with certainty that intravenously delivered ENPs deposit in the atherosclerotic plaque, but their ability to influence the atherosclerotic lesion development remains uncertain. Macrophages are the most commonly chosen target for molecular imaging as there is a large body of evidence implicating them in atherosclerosis and as naturally phagocytic

cells they tend to internalise foreign material. A study by Amirbekian (Amirbekian et al. 2007a) showed that enhancements seen in MRI scans with macrophage scavenger receptor (MSR) targeted gadolinium micelles (100nm) were directly related to macrophage content of the atheromas whereas gadolinium uptake was not seen with untargeted Gd-micelles. A study by (Schmitz et al. 2001b) showed that carboxydextran-coated USPIOs accumulated in endothelial cells and macrophages within atherosclerotic plaques in rabbits and followed up this work with a clinical study (Schmitz et al. 2002). Trivedi (Trivedi, King-Im, Graves, Cross, Horsley, Goddard, Skepper, Quartey, Warburton, Joubert, Wang, Kirkpatrick, Brown, & Gillard 2004) also showed accumulation of USPIO in carotid atheromas in macrophages in 7 out of 8 patients treated with Sinerem. The distinct pathologies of atherosclerotic plaques provide a highly sensitive way of imaging disease progression, allowing for early detection of the disease, and providing a useful tool in the assessment of the success of treatment. There is a clear need to develop a consensus on the ultimate fate and toxicity of intravenously administered ENPs and gain a better understanding of the mechanisms through which ENPs adversely affect cardiovascular outcomes.

The following table breaks down the size-dependent biodistribution of systemic ENPs:

Table 1-3 Size based ENP biodistribution

Hydrodynamic Diameter	Tissue Uptake	Renal Excretion
>30nm	Rapidly cleared by reticuloendothelial system (RES)	Not excreted by kidneys, excretion involves degradation of NP in RES tissue
10-30nm	Longer circulation time leads to increased uptake by non RES tissues.	Little, <5%, excretion by renal system excretion involves degradation of NP in RES tissue
4-10nm	Longer circulation time leads to increased uptake by non RES tissues.	Renal clearance increases as particle size decreases.
<4nm	Uptake in most cell types for particles not excreted by kidneys	Rapid clearance of nanoparticles by kidneys with retention of between 5-10% of injected dose

(Hirn et al. 2011;Semmler-Behnke, Kreyling, Lipka, Fertsch, Wenk, Takenaka, Schmid, & Brandau 2008)

1.4 *Nanoparticles and Cardiovascular Disease*

1.4.1 **Adverse effects of combustion derived nanoparticles in cardiovascular disease**

There have been many epidemiological and experimental studies demonstrating the adverse health effects of PM_{10} with the majority of investigators identifying the 'ultrafine' or nanoparticulate component as the most toxic of airborne pollutants (;Donaldson et al. 1997;Geiser et al. 2005;Mills et al. 2008b). These adverse effects are in the lungs, causing exacerbations of their condition in individuals with COPD and asthma and in the cardiovascular system, causing deaths and hospitalisations from heart attacks and strokes (Brook et al. 2002;Delfino et al. 2005;Mills et al. 2007a;Mills et al. 2009). These studies have raised concerns about the potential for ENPs to exert similar adverse health effects. These cardiovascular effects are thought to be mediated by particle induced oxidative stress and inflammation leading to vascular dysfunction, impaired fibrinolysis, and changes in the autonomic regulation of heart rate and rhythm (Langrish et al. 2008;Mills, Donaldson, Hadoke, Boon, MacNee, Cassee, Sandstrom, Blomberg, & Newby 2009). In support of this contention, CDNPs have been shown to be prothrombotic (Mills et al. 2007b) and may contribute to the formation of atherosclerotic plaques. Whilst CDNPs differ greatly in chemical composition compared to ENPs they share similarities in other

characteristics considered toxicologically significant, such as size and surface area; It is therefore plausible that ENPs will exert similar pro-inflammatory and pro-thrombotic effects, especially those manufactured for direct intravenous administration as a contrast agent in medical imaging (Donaldson 2006;Donaldson & Seaton 2007).

Given the huge amount of published data implicating CDNPs in the pathogenesis of cardiovascular diseases (Donaldson et al. 2005) an understanding of the cardiovascular toxicology of ENPs intended for medical use is essential to ensure their safe future use.

1.4.2 **Toxicity of nanoparticles in cardiovascular disease**

It is not surprising that a number of recent reviews focusing on the effects of occupational exposure to ENM have raised concerns that they could have similar health implications as CDNP (Castranova 2011;Eisen et al. 2011;Moller et al. 2011a). Resolution of these issues will require a collaborative approach between industry, government, academic researchers, and clinicians. In addition to occupational exposure to ENM the direct exposures to ENPs through medical use in susceptible populations is of immediate concern. ENM, unlike, pharmacological therapies are not routinely tested to determine their effect on the cardiovascular system prior to clinical use. All of these ENPs, not just those intended for the diagnosis and treatment of cardiovascular disease, have the potential to interact with cells

associated with disease progression. There have been no observational studies linking exposure to ENM and cardiovascular events, but a number of pre-clinical studies have reported that exposure to nanomaterials, directly or indirectly, can cause endothelial dysfunction and platelet activation, and may plausibly contribute to ischemic heart disease (McGuinnes et al. 2011;Sun et al. 2011;Zhu et al. 2010;Zhu et al. 2011a).

The schematic diagram below identifies mechanisms and potential targets for ENPs in circulation.

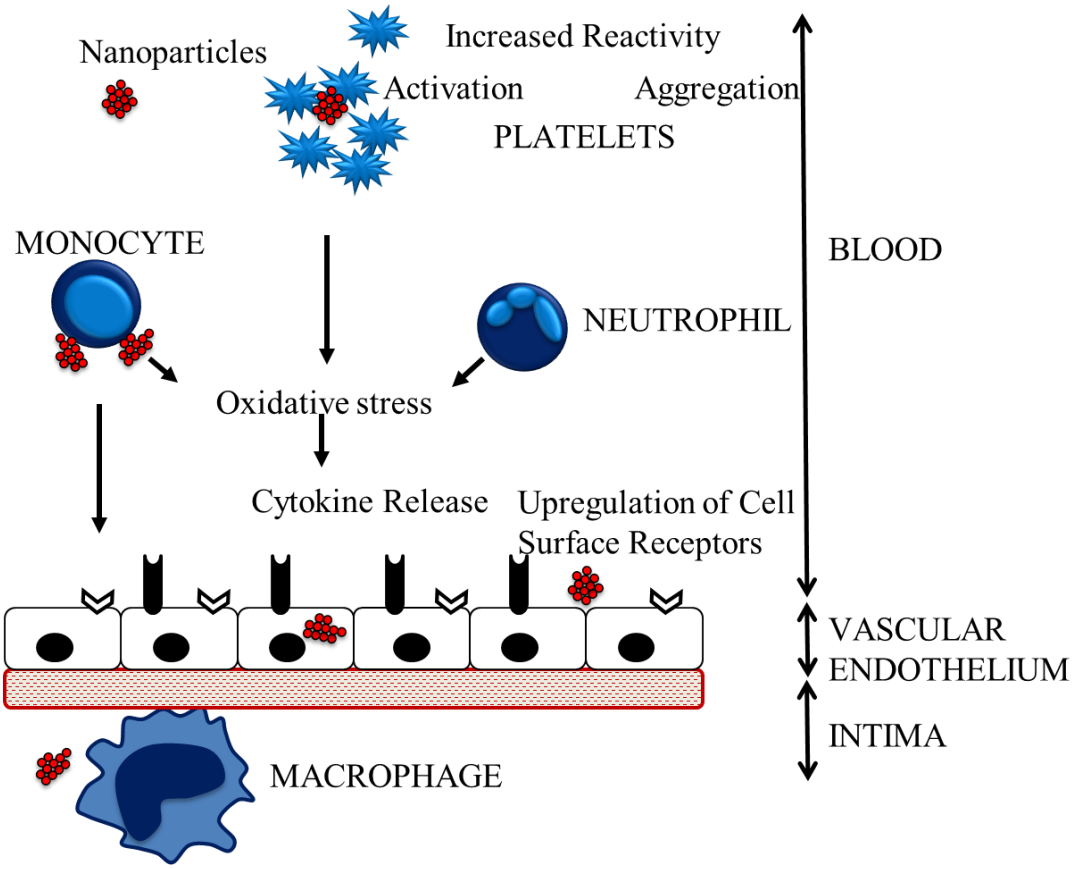

Figure 1-2 Targets for ENPs after intravenous injection

1.4.3 **In vitro studies**

Cardiovascular disease is a complex and dynamic process with many contributing factors and therefore a single *in vitro* model to study the adverse effects of ENM on cardiovascular system is unlikely to emerge. However, platelets, platelet-monocyte aggregation and the vascular endothelium have emerged as useful *in vitro* test systems, given their key role in the pathogenesis of coronary and ischemic heart disease (Neun and Dobrovolskaia 2011) (Bihari et al. 2010)

Compatibility of ENPs with blood components is important and a number of studies have employed assays of erythrocyte haemolysis (Lu et al. 2009), platelet aggregation and activation (Radomski et al. 2005), and platelet-leukocyte aggregation (McGuinnes, Duffin, Brown, Mills, Megson, MacNee, Johnston, Lu, Tran, Li, Wang, Newby, & Donaldson 2011). Direct and indirect toxicity to the cardiovascular system can be determined using cell lines with assays of oxidative stress, inflammation, and cell death (Dick et al. 2003). Whether observations from these *in vitro* models apply *in vivo* or in the clinic is uncertain, and in the absence of any standards for the assessment of the cardiovascular toxicity of ENM the role of *in vitro* assessments remain controversial.

Recent studies have shown that ENPs can interact with platelets causing activation, aggregation (McGuinnes, Duffin, Brown, Mills, Megson, MacNee, Johnston, Lu, Tran, Li, Wang, Newby, & Donaldson 2011;Miller et al. 2009b;Radomski, Jurasz, onso-Escolano, Drews, Morandi, Malinski, & Radomski 2005). Surface charge has been shown to be a critical determinant in platelet-ENP activation (McGuinnes, Duffin, Brown, Mills, Megson, MacNee, Johnston, Lu, Tran, Li, Wang, Newby, & Donaldson 2011). When studying the impact of ENM on a complex multisystem disease it is important to take into consideration potential downstream, indirect effects as well as direct toxicity. Shaw et al (Shaw et al. 2011) demonstrated that CDNPs induce moderate toxicity and inflammatory effects on endothelial cells following direct treatment. These effects were, however, amplified when endothelial cells were exposed to conditioned supernatant from monocyte-derived macrophages (MDMØ) exposed to CDNP due to the release of cytokines from CDNP -exposed macrophages. This approach utilising co-culture and other techniques that model the secondary effects of CDNPs (Inoue and Takano 2010;Ishii et al. 2005;Porter et al. 2007), could be very useful in studying the cardiovascular effects of nanomaterials. Nanomaterials are increasingly being used in cell tracking to monitor disease progression (Jendelova et al. 2004;Jing, Yang, Duan, Xie, Chen, Li, & Tan 2008;Voura et al. 2004). It is no longer sufficient to assess the potential toxicity of ENPs on the cell carriers alone; it is essential that these cells do not become ‘time bombs’ capable of releasing pro-inflammatory mediators in a vulnerable atherosclerotic plaque.

1.4.4 **In vivo studies**

In vivo studies carried out in susceptible animals have contributed significantly to our understanding of cardiovascular disease. In the ApoE knock-out mouse CDNP instilled into the lungs increases atherogenesis (Lucking et al. 2008;Tornqvist et al. 2007). Indeed ENM such as carbon nanotubes and TiO_2 can accelerate plaque progression in susceptible animal models (Moller, Mikkelsen, Vesterdal, Folkmann, Forchhammer, Roursgaard, Danielsen, & Loft 2011a). Mills & Miller et al exposed healthy human volunteers to dilute diesel exhaust, pure carbon ENPs, filtered diesel exhaust, or filtered air, in a randomized double blind cross-over study demonstrating that the adverse vascular effects of diesel exhaust could be attributed mainly to the nanoparticulate component and not to the associated gaseous pollutants (Mills et al. 2011). Observations *in vivo* were replicated *in vitro* using wire-myography providing a rationale for testing the effects of ENM on vascular function before introduction to the clinic.

1.4.5 **Ex vivo studies**

Ex-vivo studies have been very informative in modelling the effects of CDNP on cardiovascular disease. They allow measurements to be taken in tissues or artificial environments outside the organism, but with as little as possible deviation from natural conditions with no risk to the patient. *Ex-vivo*

techniques have not been used widely to study the effects of ENM on the cardiovascular system due to the need for specialist equipment, training, and the high cost involved. However, given the potential to generate meaningful data in the near patient setting these systems are worthy of consideration. *Ex vivo* techniques also side-step possible ethical issues associated with exposing healthy or diseased populations to the unknown effects of ENPs. Traditional *ex-vivo* models have assessed the direct effects of CDNP in isolated vessels to assess vasomotor dysfunction. This chapter does not intend to review previous studies as they have largely focused on CDNP however this topic is very well covered by many comprehensive reviews (Moller, Mikkelsen, Vesterdal, Folkmann, Forchhammer, Roursgaard, Danielsen, & Loft 2011a) and the findings can be applied to the study of the adverse effects of nanomaterial (Moller et al. 2011b).

As many medical ENPs in development are for use in populations considered particularly vulnerable, it would be desirable to model this *ex vivo*. The Badimon chamber is an *ex vivo* model of deep arterial injury and thrombus formation used previously to study the effects of diesel exhaust inhalation on thrombosis in man (Lucking, Lundback, Mills, Faratian, Barath, Pourazar, Cassee, Donaldson, Boon, Badimon, Sandstrom, Blomberg, & Newby 2008;Lundback et al. 2009). The chamber permits an assessment of thrombus formation in whole native blood without the need for anti-coagulants or exposure of the patient to the compounds being tested. While

principally used to assess the impact of novel antithrombotic agents it can be modified to assess the effects of ENM on thrombosis.

1.5 *The Paradox*

We are regularly exposed to nanoparticles from numerous sources both natural and anthropogenic. The effect of exposure to environmental particles has been widely studied with particular attention to the 'ultrafine' or CDNP (Li et al. 1997;Mills et al. 2008a). It is from such studies that most of our information pertaining to ENP toxicology has been extrapolated. Although CDNPs display significant differences in chemical makeup to ENPs they share similarities in characteristics considered toxicologically significant such as size and surface area. CDNP's have been shown to be prothrombotic in man (Mills et al. 2007c) and directly contribute to the formation of atherosclerotic plaques in experimental models (Campen et al. 2010). These CDNPs share properties with ENPs intended for direct administration to patients. This raises an obvious paradox regarding the prothrombotic capabilities of ENPs, especially those manufactured for intravenous administration.

It is therefore highly likely that exposure to some ENPs trigger acute cardiovascular events in those who are most vulnerable. I hypothesise that ENPs delivered directly into the blood will activate platelets and monocytes resulting in increased thrombosis.

1.5.1 **Aims**

The primary aim is to evaluate the effects of engineered nanoparticles on platelet funtion and thrombosis. The role of surface chemistry and charge in determining any prothrombotic effects was evaluated.

The following specific research questions are addressed:-

- Do engineered nanoparticles directly induce platelet activation *in vito*?

- Are the effects of engineered nanoparticles determined principally by: particle charge or surface chemistry?

- Do engineered nanoparticles induce platelet activation and thrombus formation in an ex-vivo model of thrombus formation?

- Do engineered nanoparticles delivered systemically through intra-venous infusion induce platelet activation and thrombus formation in patients?

Chapter 2 **Nanoparticle Panel**

2.1 *Abstract*

ENP characterisation is necessary to establish understanding and control of ENP synthesis and applications. For toxicological purposes knowing the parameters of what you are testing is essential for developing a structure activity relationship. This has proved difficult in ENP toxicology as no one characteristic; test or model has been shown to reliably predict toxicity. The ENPs selected for this study are a mixture of clinical and high-grade non-clinical SPIONs and two charged polystyrene latex beads used as a model for the toxicity of positively or negatively charged ENPs. The significance of this study is to identify and establish the physical parameters of the ENPs in subsequent studies and identify which characteristics contribute to their toxicity.

2.2 *Nanoparticle Panel*

2.2.1 **Feraheme**

Feraheme (AMAG pharmaceuticals) is an iron replacement product for the treatment of anaemia in adults. It is classified as a USPION and is coated with polyglucose sorbitol carboxymethylether (PSC). The overall colloidal particle size was 17-31 nm in diameter. Each mL of the colloidal Feraheme® contained 30 mg of elemental iron and 44 mg of mannitol. The formulation is isotonic with an osmolality of 270-330 mOsm/kg. The PSC coating, designed to delay release of the bioactive iron from plasma components until it has been cleared by the RES of the liver spleen and bone marrow. According to the manufacturer the iron is released from the iron-carbohydrate complex within vesicles in the macrophages and either enters the intracellular storage iron pool (e.g. ferritin) or transferred to plasma transferrin for transport to erythroid precursor cells for incorporation into haemoglobin. Feraheme® designed for delivery as an undiluted intravenous injection administered at a rate of up to 1mL/sec (30mg/sec) as a bolus injection. The recommended dose is an initial 510 mg intravenous injection followed by a second 510 mg intravenous injection 3 to 8 days later.

2.2.2 **Nanomag®-D-spio:**

SPIONs prepared by precipitation of iron oxide in the presence of dextran. Functionalized nanomag®-D-spio consists of about 55-85% (w/w) iron oxide in a matrix of dextran (40.000 Da). Nanomag®-D-spio are produced under controlled hygienic conditions. Hygiene areas are classified according to the ICH Q7A Good Manufacturing Praxis for drugs, the European GMP guideline for Good Manufacturing Praxis for drugs and investigational products, and according to DIN EN ISO 14644-1 for clean rooms and related clean room areas – Part 1: Classification of the air purity (ISO 14644-1:1999). All water is filtered through 0.2 µm filters and is routinely checked for microbiological contamination. The ENPs used in this project were Nanomag®-D-spio $–NH_2$, -COOH and plain all 20nm in size according to the manufacturer.

2.2.3 **Endorem**

Endorem™ (AMAG pharmaceuticals, Inc., Guerbet S.A.) was a black to reddish-brown aqueous colloid of superparamagnetic iron oxide associated with dextran for intravenous administration as a MRI contrast medium for the detection of liver lesions that are associated with an alteration in the RES. Endorem™ is taken up by macrophages, found only in healthy liver cells but not in most tumours. Tissues such as metastases, primary liver cancer, cysts and various benign tumours, adenomas and hyperplasia retain their native

signal intensity, so the contrast between normal and abnormal tissue is increased. The recommended dosage for Endorem™ is 4 mg/kg. Endorem™ is made up of dextran-coated iron oxide particles with a size distribution between 120 and 180 nm according to the manufacturer and an iron concentration of 0.2 mol/l. Before Endorem™ received approval in Germany and other European countries, clinical trials were performed in Japan, the USA, and Europe. At a dose of 10 micromole Fe/kg (Japan, USA) and 15 micromole Fe/kg (Europe).

2.2.4 **Polystyrene Latex Beads**

Polystyrene latex ENPs has various applications in research. In this study they were used as model ENPs to assess the effects of charge on toxicity.

2.2.5 **Carboxylated Beads**

Polybead® Carboxylate Microspheres 0.05µm are monodisperse polystyrene microspheres that contain surface carboxyl groups. These microspheres are packaged as 2.5% solids (w/v) aqueous suspensions.

2.2.6 **Aminated Beads**

Latex beads, amine-modified polystyrene, fluorescent blue are monodisperse polystyrene microspheres that contain surface amine groups. These microspheres are packaged as 2.5% solids (w/v) aqueous suspensions.

2.3 *Materials and Methods*

2.3.1 **Particle Sizing**

All ENPs were sized by dynamic light scattering (DLS) with a 90 plus Particle Size Analyzer (Brookhaven Instruments Corporation). All ENPs were suspended in sterile water (Milli-Q Academic, Millipore, MA, USA), water with 10% human serum, saline (Baxter Healthcare, Eng) and saline with 10% human serum at 1mg/mL and bath sonicated (Fisherbrand FB11002, 40 kHz) for 5 minutes prior to sizing. ENPs were further diluted 1:300 in sterile water or saline, as appropriate, prior to measurement. Solutions were adjusted to give a count rate of between 50-300kcps (kilo counts per second).

2.3.2 **Zeta-Potential**

The electrophoretic mobility or zeta potential of the sample was measured in a 1 mL clear zeta potential cuvette (DTS1060, Malvern) using a Malvern Zetasizer Nano-ZS according to the manufacturer's recommendations and converted into the zeta potential by applying the Henry equation. The data were collected and analysed with the Dispersion Technology software 4.20 (Malvern) producing histograms for the particles size as a number distribution or diagrams for the zeta potential as a distribution versus total counts. ENPs

were measured in water, water with 10% human serum, saline, and saline with 10% human serum.

2.3.3 **Transmission Electron Microscopy**

ENPs were suspended in sterile water (Milli-Q Academic, Millipore, MA, USA) at a concentration of 1mg/mL and sonicated for 5 minutes (Fisherbrand FB11002, 40 kHz). ENPs were further diluted 1:100 in sterile water. A drop (5µL) of this solution was loaded onto a 1 x 2 mm copper slot grid with a support film of Formvar/carbon (Agar Scientific, Essex, UK), covered and allowed to dry overnight @37˚C and visualized using a Philips CM120 transmission electron microscope (TEM).

2.3.4 **Electron Paramagnetic Resonance**

Electron paramagnetic resonance (EPR) was utilized to detect intrinsic free radical generation from the iron oxide ENPs used in this study. An EPR spectrometer (Miniscope MS200, Magnettech GmBH, Berlin) was used to detect electrons present in free radicals via alterations in electromagnetic energy. Due to the volatility of these free-radicals a spin-trap is used to capture them prior to measurement. There are many spin-traps available depending on the free-radical to be measured. In this case 1 hydroxyl-

2,2,6,6-tetramethyl-4-oxo-piperdine (Tempone-H; Alexis Co., Bingham, UK) was chosen to detect the generation of superoxide, peroxyl and peroxynitrite radicals (Miller et al. 2009a). The spin-adduct formed results in a characteristic three event EPR spectrum shown below:

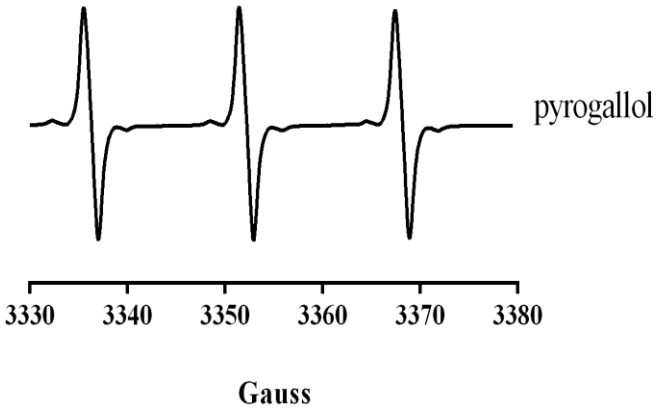

Figure 2-1Tempone-H spectrum

Samples were prepared at 50µg/mL in Hank's Balanced Salt Solution (HBSS) (PAA Laboratories Ltd., UK) with the addition of 1mM Tempone-H and incubated for 1-hour at 37˚C. Positive (Pyrogallol 100µM) and negative (HBSS) controls were employed to show both that the EPR spectrometer was calibrated and the HBSS used was not contaminated. All samples were transferred immediately after incubation to glass micropipettes (intraMARK BLAUBRAND, rand GmBH +CO KG, Wertheim, Germany) sealed with Cristaseal™ (VWR International, Lutterworth, UK). The spectrometer was set-up using the following settings: microwave frequency, 9.3-9.55 Hz;

microwave power, 20 mW; modulation frequency, 100 kHz; modulation amplitude, 1500mG; Centre field, 3365 G; sweep width, 50 G; sweep time, 30 sec; number of passes, 1. The EPR intensity was measured at 60 minutes and a numerical value (arbitrary scale) calculated using Miniscope software (version 6.51; Magnettech, Berlin, Germany) based on the area under the curve of the first event of the first three-event spectrum generated as previously described (Miller, Borthwick, Shaw, McLean, McClure, Mills, Duffin, Donaldson, Megson, Hadoke, & Newby 2009a).

2.3.5 **Nanoparticle Protein Affinity**

ENPs were incubated with human serum, made by re-calcification of platelet rich plasma, for 30 mins @37˚C. ENP serum suspensions were centrifuged @14,000*g* for 10 mins, the supernatant removed and ENP pellets washed with 1 mL deionised (DI) water. The wash cycle was repeated 5 times after which proteins associated with the ENP pellet were reduced using the NuPAGE® Novex® Bis-Tris Mini Gel system (Invitrogen™, life technologies™) according to manufacturer's instructions. Samples were diluted 1:12 in DI water before loading in the gel. Post- staining of the protein gels was carried out with SilverXpress® Silver Staining Kit as per manufacturer's instructions. Gels were assessed qualitatively for ENP-protein binding.

2.3.6 **Statistics**

Data are expressed as mean ± SEM unless otherwise stated. Statistical analysis was performed with GraphPad Prism (GraphPad Software, La Jolla, CA, USA) using one-way ANOVA Dunnett's test as appropriate to compare ENP treatment with control. Statistical significance was taken at $P<0.05$.

2.4 *Results*

Table 2-1 Commercially Available ENPs used in the studies

Name	Core	Manufacturer Size (nm)	Coating	Manufacturer
Feraheme® USPIO	Iron-oxide	17-31	PSC	AMAG
Endorem® SPIO	Iron-oxide	150	Dextran	Guebert
Nanomag®D-spio USPIO	Iron-oxide	20	Dextran	Micromod
USPIO-COOH		20	Dextran—COOH	Micromod
USPIO-NH_2		20	Dextran-NH_2	Micromod
Polystyrene Beads	Latex	50	COOH	Polysciences
	Latex	50	NH_2	Sigma Aldrich

All ENPs were chosen for their current and potential use in nanomedicine. A range of iron oxide ENP with various surface coatings and functionalisations.

Table 2-2 ENP characteristics measured in-house.

Nanoparticle	ZP (mv) Water	ZP (mv) Water 10% Serum	ZP (mv) Saline 0.9%	ZP (mv) Saline +10% Serum	SIZE (nm) Saline +10% Serum
Feraheme USPIO	-3.39±1.54	-20.18±1.73	-7.4±0.3	-20.18±1.73	30.15±0.52
Endorem SPIO	-19.76±1.07	-16.92±1.44	-15.267±3.01	-10.67±0.32	82.74±0.43
Nanomag®D-SPIO USPIO	-0.18±0.29	-12.34±0.59	-1.3±0.1	-20.18±1.73	30.15±0.52
USPIO-COOH	-13.5±0.69	-17.06±2.42	-6.4±0.2	-17.06±2.42	38.05±0.38
USPIO-NH_2	-1.31±1.27	-12.88±1.52	1.8±0.2	-12.88±1.52	43.48±0.25
Polystyrene Beads Poly-COOH	-28.54±6.129	-19.96±0.91	-14.00±1.91	-9.72±1.01	72.73±0.29
Poly-NH_2	25.76±1.909	0.079±0.149	12.10±1.04	-10.80±0.60	48.93±0.77

ENP size was measured in saline with 10% human serum. ENP size correlated well with the published manufacturer's sizes. ZP is a measure of the electrophoretic potential of a particle in a solution. As ZP is heavily dependent on the solution in which the ENP is suspended it was important to measure the value in a biologically relevant fluid. Here ZP was measured in water and saline with or without human serum. ZP varied widely depending on the solution in which they were suspended, the addition of serum greatly reducing the ZP most likely due to the adsorption of protein (which are

negatively charged), onto their surfaces. All ENP had a negative zeta potential in water and water with 10% serum apart from the aminated beads. In the slightly acidic saline mimicking inter-lysosomal conditions the negatively charged ENP were less negative than when measured in water whereas both the aminated ENP were positively charged. All ENP were negatively charged in the saline with 10% serum. Data represent mean±SEM, n=6-10.

Figure 2-2 Inherent free-radical generation of ENP

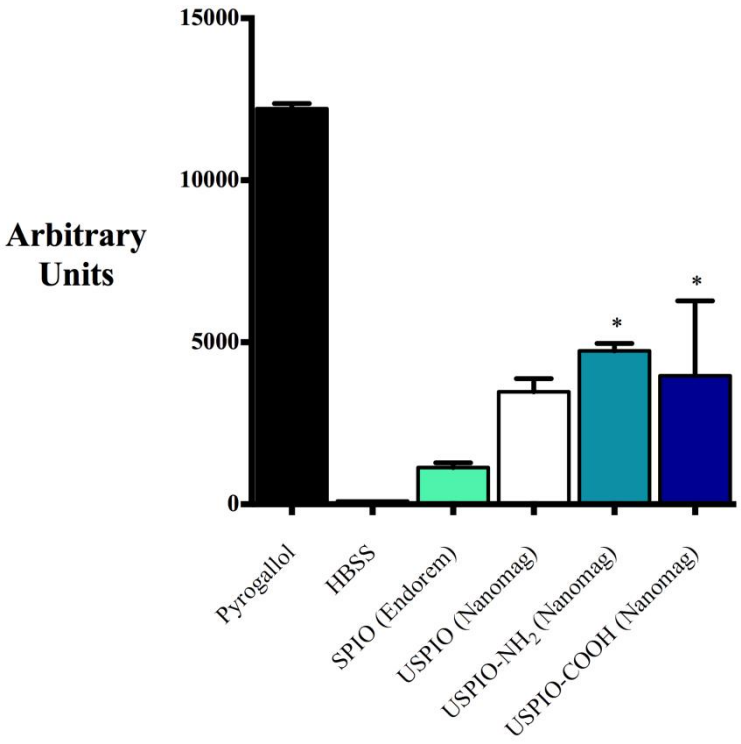

Unpaired electrons on the surface of the ENPs were measured using EPR. The aminated (USPIO-NH_2) and carboxylated (USPIO-COOH) iron oxide ENPs showed significant generation of free radicals superoxide, peroxyl and peroxynitrite. Data is mean±SEM, n=3-5. Pyrogallol is a positive control and HBSS a negative control.

Figure 2-3 Transmission Electron Micrographs of Iron-Oxide ENPs

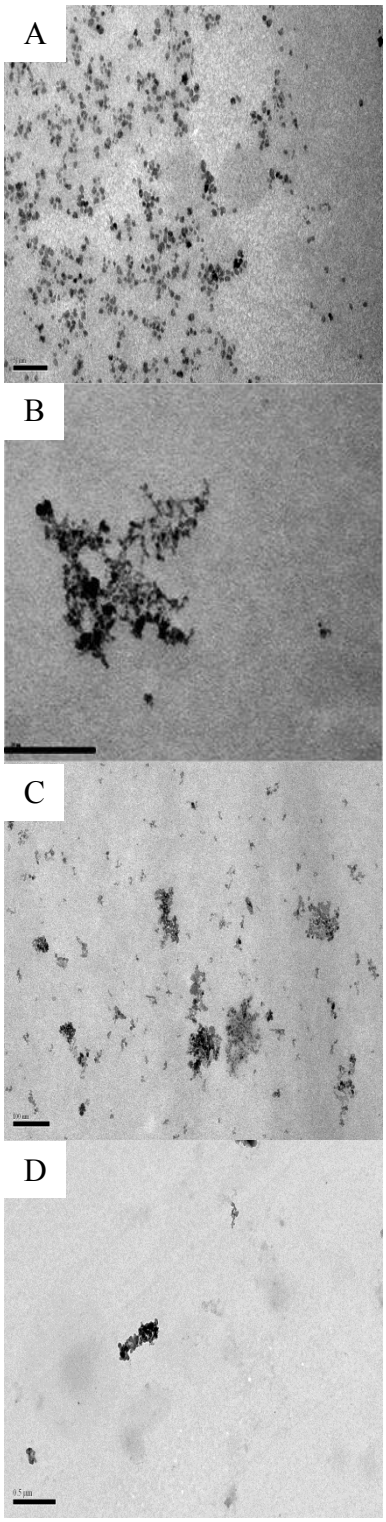

Transmission electron micrographs of iron oxide ENPs on copper grids were imaged to determine the morphology and aggregation state of the ENP. All ENP were well dispersed but appeared to be made up of aggregates of much smaller ENP Feraheme (A) 50nm scalebar, Endorem (B) scale bar 100nm, Nanomag-NH_2 (C) scale bar 100nm, Nanomag-COOH (D) scale bar 500nm.

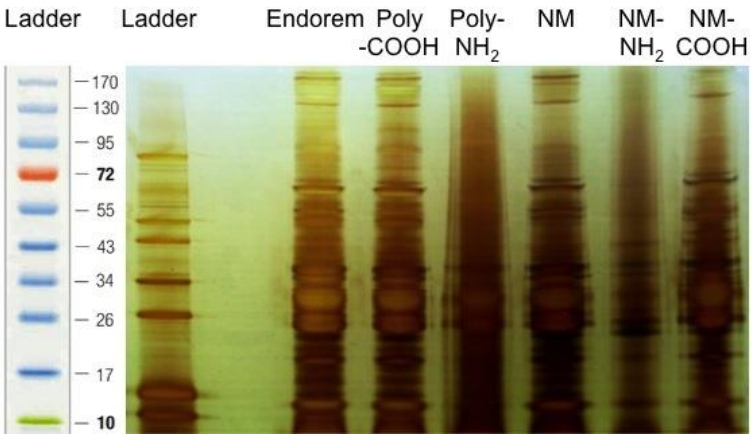

Figure 2-4 Protein Binding to ENPs

Gradient gel electrophoresis of protein attached to ENP surface after a 20min incubation in human serum. It appears that whilst all the ENP bound serum proteins the quantity was dependent on the surface functionalisation. The unmodified and carboxylated ENPs seemed to bind more proteins from the serum compared to the amine- modified ENPs.

2.5 *Discussion*

Many types of ENPs are being tested for use in medical applications, particularly as platforms for imaging and drug delivery. For these applications, cellular uptake is usually a prerequisite and is dictated by a number of factors including size and surface characteristics such as charge. The different uptake preferences of phagocytic and non-phagocytic cells for cationic and anionic ENPs may influence the efficacy and selectivity of ENPs for drug delivery and imaging (Yang et al. 2012).

SPIONs or ultrasmall SPIONs were chosen for this study as they are currently the most widely used ENP in a clinical setting and their use will only become more widespread in the future. Like most ENPs SPIONs can be produced in tight size ranges and specific functionality. Though not used clinically at the moment many functionalized SPIONs are in development for clinical use (Lamanna et al. 2011;Maity et al. 2012;Yang et al. 2011) in an attempt to target an area of interest e.g. atheroma (Michalska et al. 2012), instead of relying on passive uptake. This will be achieved through accurate chemical modification of the ENP surface and understanding the nano-bio interface. ENPs and their interaction with their biological structures, leading to the formation of a corona, is a huge area of research and is not addressed comprehensively in this study but as with all researchers studying the toxicity of ENPs the properties considered most like to confer toxicity were

measured, including; size, charge, free-radical generation and protein binding.

All iron oxide ENPs used in this study were considered low toxicity (Appendix I: Cytotoxicity). This study shows the effect of choice of suspension liquid is critical when determining the zeta potential of ENPs. This is not a new finding (Cho et al. 2012) but highlights the need to test ENPs in a relevant solution. Medical ENPs will not be delivered to the patient in water as it is not physiological and are much more likely to be delivered in saline, as is the case with Endorem™ or undiluted as supplied in a sugar/carbohydrate solution, e.g. mannitol, as is the case with Feraheme®.

Electrostatic forces have been shown in some case to govern the internalization of viruses (Taylor and Sansom 2010). It could be hypothesized that due to the similar physical, size, characteristics ENP entry into cells could be influenced by the same forces. Both positively and negatively charged ENPs bind serum and albumin, but affinity differs between surfaces. In this study both of the positively charged ENPs bound protein to a lesser extent than the unmodified and carboxylated ENPs. Similar findings have been previously reported (Jin and Kim 2012) and may account for the increased cellular uptake and increased cytotoxicity displayed by the cationic ENPs (Appendix I&II) as their positively charge surfaces are not masked and free to interact with negatively charged cell membranes. Some have suggested positively charged ENPs cause pores to form in cells mediating

their uptake and cytotoxicity (Frohlich 2012). A recent review, by Frölich 2012, summed up ENP uptake suggesting that cationic surface charge correlates with higher cellular uptake and greater cytotoxicity in non-phagocytic cells; cause plasma-membrane disruption and cell death whereas anionic ENPs are more easily ingested and are more cytotoxic to phagocytic cells such as macrophages. It was clear from this study that differently charged ENPs adsorbed serum proteins to different degrees. ENP-protein interactions are important if we are to make ENPs with specificity for particular sites within the body. From a chemistry point of view functionalising the ENP surface is not a major hurdle. Trying to design an ENP to target a specific area of the body through surface functionalisation without the homing molecules becoming masked by self-proteins will be the next big challenge in nano-medicine.

The spin-trap tempone-H was used to monitor free radical generation at the surface of the ENPs. Iron is essential for many biological processes but too much or too little in ionic form can in turn lead to disease. The body is good at dealing with an excess of iron in its elemental form but ENPs pose a longer term risk as they are retained and have the potential to produce free radicals as seen in this study which in turn can lead oxidative stress. The aminated and carboxylated iron oxide ENPs showed significant generation of free radicals superoxide, peroxyl and peroxynitrite. The functionalisation may disrupt the surface of the ENPs making them more reactive and prone to spontaneous free-radical generation. It has previously been shown in our

group that the polystyrene ENPs used in this study do not generate free radicals (McGuinnes, Duffin, Brown, Mills, Megson, MacNee, Johnston, Lu, Tran, Li, Wang, Newby, & Donaldson 2011) but have significantly different toxicological profiles based on their surface derivitisation.

The following studies discuss the toxicity and biological effects of the ENPs described in this chapter relating where we can their structure with their biological effects.

Chapter 3 *In Vitro* Effects of Engineered Nanoparticles

3.1 *Abstract*

This study was designed to test the hypothesis that ENPs can cause platelet activation and induce an inflammatory state in monocyte derived macrophage cells ($MDM_{\emptyset}$) in vitro. Blood from healthy volunteers (n=5-10) was mixed with increasing concentrations of SPIO, USPIO, USPIO-NH_2, USPIO-COOH, Poly-NH_2 and Poly-COOH nanoparticles (described in chapter 2). Blood was analysed by flow cytometry for the following markers of platelet activation: platelet-leukocyte aggregation, platelet surface p-selectin, platelet surface glycoprotein IIb/IIIa via PAC-1 binding. Platelet response to agonists TRAP-6 and Thrombin was determined by pre-treating platelets with SPIO, USPIO-NH_2 and USPIO-COOH using flow cytometry and calcium influx respectively. Poly-NH_2 beads significantly activated platelets in all assays tested as did USPIO-NH_2 nanoparticles Pre-treatment of platelets with all ENPs increased the sensitivity to TRAP-6, as measured by platelet surface p-selectin and PAC-1 binding, and thrombin, measured by calcium influx, suggesting that ENPs induce a hyper-reactive state.

Monocyte derived macrophages ($MDM_{\emptyset}$) isolated from human blood (n=4) were treated with SPIO, USPIO, USPIO-NH_2, USPIO-COOH and assessed

for inflammatory responses and ENP uptake. USPIO-COOH significantly increased levels of IL-8 pg/mL in cell culture supernatants over a 72-hour period as well as intercellular adhesion molecule ICAM-1. None of the other ENPs had an effect on $MDM_{Ø}$. Engineered nanoparticles with differing surface chemistries activated platelets and induced a pro-inflammatory state in $MDM_{Ø}$ in a dose dependent manner.

3.2 *Introduction*

As described in chapter one the paradox which exists between CDNPs contributing to CV risk and ENPs that are in development for the diagnosis and treatment of cardiovascular disease is one which needs to be resolved to ensure the safe continuation of their use in a clinical setting. Though the exact mechanisms by which CDNP mediate their adverse effect is unclear it has recently been established that it is the NP component that is driving the effect (Mills, Miller, Lucking, Beveridge, Flint, Boere, Fokkens, Boon, Sandstrom, Blomberg, Duffin, Donaldson, Hadoke, Cassee, & Newby 2011).

Thrombosis plays a central role in the pathogenesis of atherothrombotic disease. As well as contributing to initiation of disease, thrombosis at the site of a disrupted under coronary flow can cause vessel occlusion, resulting in an infarct or coronary event. Platelets are the key players in thrombosis and anti-platelet therapy is common in the treatment of cardiovascular disease (Grove 2012) ameliorating to some extent both platelet-platelet adhesion and platelet-leukocyte interactions. It has been shown previously that exposure to diesel exhaust increases platelet activation and enhances thrombus formation in the Badimon chamber (Lucking, Lundback, Mills, Faratian, Barath, Pourazar, Cassee, Donaldson, Boon, Badimon, Sandstrom, Blomberg, & Newby 2008).

Increasingly platelet-leukocyte binding, platelet-monocyte in particular, has been shown to be a sensitive marker of platelet activation and inflammation (Passacquale et al. 2011). Inflammation and atherothrombotic disease have been well documented (Libby et al. 2002) and anything that increases the inflammatory burden within a system could have adverse cardiovascular effects. Previous work has suggested that ENPs can activate platelets based on their surface charge (Jones et al. 2012b) and induce inflammation in cells involved in the pathogenesis of cardiovascular disease (Rehberg et al. 2012a).

3.2.1 **Hypothesis**

I hypothesise that ENPs (described in chapter 2) can activate platelets *in vitro* and induce an inflammatory state in $MDM_{ø}$ cells dependent on their charge and surface chemistry.

3.2.2 **Aims**

- To test the effects of surface chemistry and charge on platelet aggregation and activation in response to ENPs.

- To determine whether ENPs increase platelet sensitivity to known agonists TRAP-6 and thrombin.

- To determine whether ENP can induce a pro-inflammatory state in MDMØ cells over a 72-hour period.

3.3 *Materials and methods*

3.3.1 **Nanoparticle Panel**

Table 3-1Panel of Nanoparticles used in *in Vitro* studies

Name	Core	Manufacturer Size (nm)	Coating	Manufacturer
Endorem® SPIO	Iron-oxide	150	Dextran	Guebert
Nanomag®D-spio USPIO	Iron-oxide	20	Dextran	Micromod
USPIO-COOH		20	Dextran—COOH	Micromod
USPIO-NH_2		20	Dextran-NH_2	Micromod
Polystyrene Beads Poly-COOH	Latex	50	COOH	Polysciences
Poly-NH_2	Latex	50	NH_2	Sigma Aldrich

3.3.2 **Blood sampling**

Healthy non-smoking volunteers participated in this study. Subjects taking regular medication or with inter-current illness were excluded. The study was performed with the approval of the local research ethics committee, in accordance with the Declaration of Helsinki, and with the written informed consent of each participant. Blood was drawn by clean venepuncture of a large antecubital vein using a 19-gauge needle. Care was taken to ensure a smooth blood draw without venous stasis. The first 2ml was discarded and blood was taken without a tourniquet. Unless otherwise stated, blood was

collected into tubes containing the direct thrombin inhibitor, D-Phenylalanine-L-prolyl-L-arginine chloromethyl ketone (PPACK, Cambridge Biosciences). Tubes were gently inverted to ensure mixing of whole blood with anticoagulant.

3.3.3 **Platelet leukocyte binding**

Immunolabelling and flow cytometry were performed in whole blood to avoid centrifugation and washing steps, which can lead to artifactual platelet activation (Harding et al. 2007). Aliquots of whole blood (60µl) were incubated with a suspension of ENPs at 7-times final concentration (20µl) and antibody cocktail (anti-CD14-R-phycoerythrin(PE), anti-CD42a-Fluorescein isothiocyanate (FITC), anti-CD16-APC(Allophycocyanin) (60µl) for 25-minutes (mins) at room temperature; samples were fixed and red blood cells lysed by the addition of 1.5mls FACS-Lyse solution (Becton Dickinson) unless otherwise stated. Isotype matched controls were used to set the monocyte and neutrophil gates. Samples were analysed using a Becton-Dickinson FACS Calibur flow cytometer and data analysed using FlowJo version 7.5 (Treestar, Oregon, USA). All samples were analysed within 24 hours (hrs) unless otherwise stated. Monocytes were identified based on their forward and side scatter characteristics and then by triggering on FL-2 to identify CD14-PE positive monocytes and exclude large granular lymphocytes. For each measurement a minimum of 2,500 monocytes were

collected. Platelet-monocyte aggregates were defined as CD14/CD42a positive cells. Neutrophils were identified based on forward and side scatter characteristics and triggering on the FL-4 channel. Platelet-neutrophil aggregates were defined as CD16/CD42a positive cells. All results are expressed as percentage of +ve events as previously described (Harding, Din, Sarma, Jessop, Weatherall, Fox, & Newby 2007).

Plot A shows gating of monocytes based on their characteristic side and forward scatter. CD14+ monocytes were then selected from this gate shown in plot B. Plot C Fl2/Fl1 shows cells that stained with FITC-CD42a antibody and Pe-CD14 antibody Plot shows cells in the FL1 positive FL2 positive quadrant. These cells are platelet-monocyte aggregates.

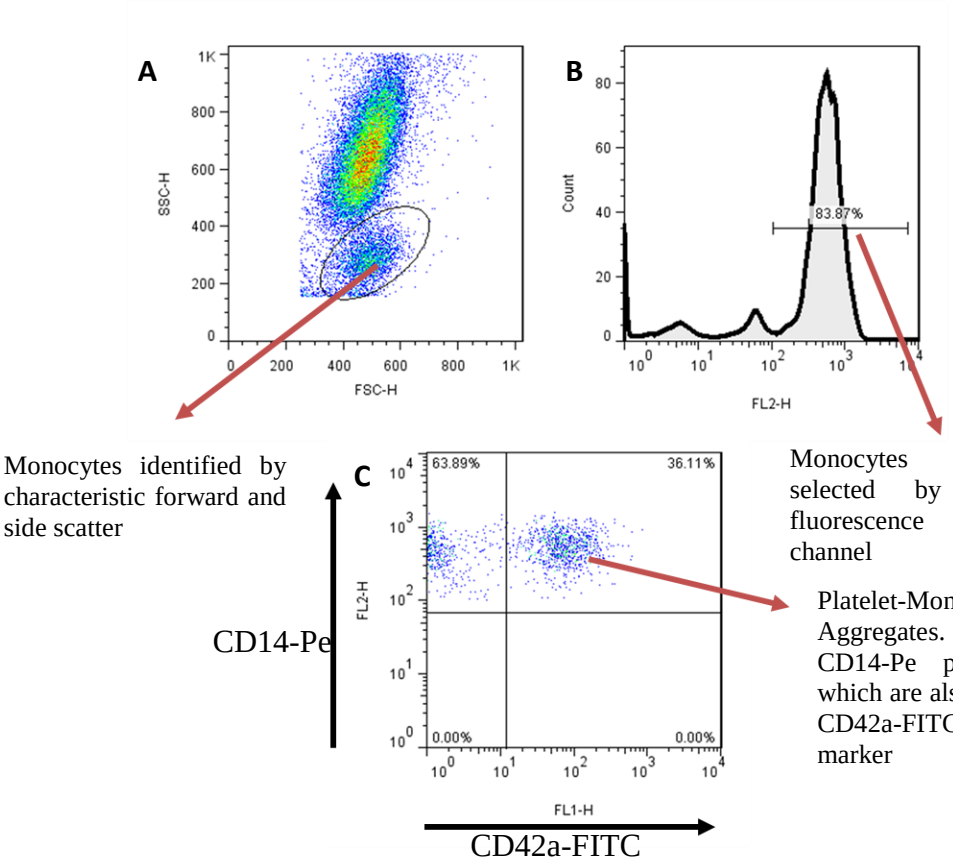

Figure 3-1 Flow Cytometry Scatter Plots Showing Platelet-Monocyte Aggregation.

Plot A shows gating of neutrophils based on their characteristic side and forward scatter. CD16+ neutrophils were then selected from the gate shown in plot B. Plot C Fl2/Fl1 shows cells that stained with FITC-CD42a antibody and Pe-CD16 antibody Plot shows cells in the FL1 positive FL2 positive quadrant. These cells are platelet-neutrophil aggregates.

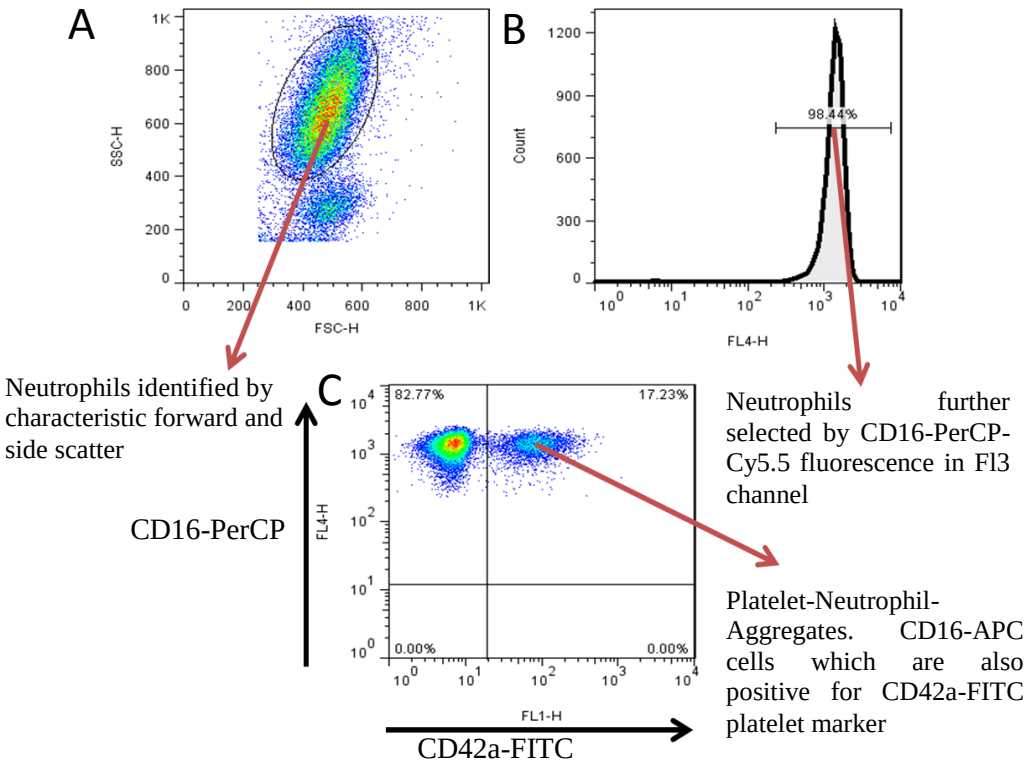

Figure 3-2 Flow Cytometry Scatter Plots Showing Platelet-Neutrophil Aggregation.

3.3.4 **Platelet activation**

Immunolabelling and flow cytometry were performed in whole blood. Aliquots of whole blood (5µl) were incubated with a suspension of ENPs (10µl) at 2.5-times final concentration and antibody cocktail CD42b-APC , CD62-p- (PE) and PAC-1- fluorescein isothiocyanate (FITC) (BD Pharmigen) (10µl) for 25 mins at room temperature and fixed with 800µl 1% paraformaldehyde (PFA). Samples were analysed using a Becton-Dickinson FACS Calibur flow cytometer with platelets gated by characteristic forward and side scatter properties and CD42a expression using appropriate isotype controls. The CD14/CD42a +ve, aminated bead treated populations were sorted into 1ml of medium. A further 5ml of PBS Phosphate Buffered Saline (Sigma Dorset, UK) was added to each tube and the samples were centrifuged at 1200rpm for 10 minutes. The cells were re-suspended in 50µl of PBS, which was then transferred to a slide and allowed to dry overnight in the dark, prior to being mounted in Moviol and viewed by Confocal microscopy Zeiss LSM Confocal Microscope with 488nm Laser with Hg lamp and UV Filter set for bead emission.

3.3.5 **Platelet Hyper-reactivity**

3.3.6 **Flow Cytometry**

Immunolabelling and flow cytometry were performed in platelet-rich plasma (PRP) derived from whole blood by centrifugation (Mistral 3000*i*) (200 *g*) without brake or acceleration for 20 mins. Platelet rich plasma was incubated with ENP for 10 mins on an orbital shaker. Thrombin Receptor Activating Peptide-6 (TRAP-6) was then added to each sample at a final concentration of 10µM. Samples were incubated with antibody cocktail (CD62-p-PE/PAC-1-FITC) (10µl) for 20 mins and fixed with 500µl of 1% PFA. Platelets were gated based on characteristic forward and side scatter properties.

3.3.7 **Calcium influx**

Washed platelets (WP) were derived from PRP by centrifugation (1200 g, 10 mins) in the presence of 300 ng/ml prostacyclin (PGI2) to prevent activation. WP were resuspended in PGI2-free HBSS buffer (without calcium and magnesium) and Fura-2 acetoxymethyl ester (Fura-2 AM; 2 mM), and incubated at 37°C for 30 mins. Following incubation, platelets were diluted to their original volume with HBSS, PGI2 added (300 ng/ml), and the mixture centrifuged (1200 g, 10 min). The supernatant was aspirated and discarded

to remove excess extracellular Fura-2 AM, and the loaded platelets re-suspended in HBSS buffer to the original volume. All fluorescence measurements were obtained using a Perkin-Elmer LS50B luminescence spectrometer (Perkin Elmer, Berkshire, U.K.). Fluorescence was measured at 371C, with excitation wavelengths of 340 and 380nm and an emission wavelength of 510 nm. Aliquots (1 ml) of Fura-2 AM loaded WP were equilibrated at 37°C before the addition of SPIO to a final volume of 50 µg/ml and 25 µg/ml; platelet nanoparticle mixtures were co-incubated for 5 min. At 5 min platelets were diluted with 2 mL HBSS with Ca2+/Mg2+ at 37°C and 10µl of thrombin was added to a final concentration of 1 U/mL and fluorescence monitored over a 5 minute period.

3.3.8 **Platelet Aggregometry**

Aggregometry was carried out based on a method adapted from Armstrong et al 2009 (Armstrong et al. 2009). Blood was taken as described and centrifuged at 135g for 15mins to prepare PRP. PRP was maintained at 37°C throughout all experiments and was used within 3 hours of collection. Platelet poor plasma (PPP) was prepared by further centrifugation at 13,000g for 15 mins. ENPs were prepared in 0.9% saline to four times the desired final concentration and added to a 96 well plate. 75µl PRP was added to the wells of the 96-well plate which was then immediately placed in a Biotek, Synergy HT plate reader set to read absorbance at 605nm every 30s for 16min

between vigorous shaking at 37°C. Changes in absorbance were converted to % aggregation by reference to the absorbance's of PRP only and PPP-ENP control readings. TRAP-6 was used as a positive control. Digital images of aggregates were taken with a Cannon Powershot A640.

% Aggregation = 100 - [(PRP – PPP.ENP control)/ (PRP-PPP)*100]

3.3.9 **Monocyte isolation**

Citrated whole blood was centrifuged (200 *g*; 20 min) and PRP aspirated. Leukocytes were separated from erythrocytes by dextran sedimentation and then further divided into peripheral blood mononuclear cells (PBMC) and granulocyte populations by centrifugation through a discontinuous Percoll® (Pharamcia, UK) gradient (720 *g*; 20 min). PBMC were harvested at the 55:68% interface and re-suspended in phenol red free Iscove's modified Dulbecco's medium (IMDM) supplemented with penicillin and streptomycin (both 100 U/mL). Enrichment for monocytes was performed by selective adherence to 48-well ($2x10^6$ cells/well) tissue culture plates for one hour (37°C; 5% CO2). Adherent monocytes were washed three times in phosphate buffered saline (PBS) and differentiated into $_{MDMØ}$ for 5 days in IMDM containing 10% autologous serum prepared by recalcification of PRP. Medium was replaced every 2-3 days.

3.3.10 **Monocyte derived macrophage**

Flowcytometry was used to determine cell viability and intracellular adhesion molecule (ICAM-1) expression in $_{MDM\emptyset}$. An anti-human CD54-APC antibody (Biolegend®) was used to stain $_{MDM\emptyset}$ for ICAM-1. Following treatment with ENP or media only, untreated media only control cells (and their supernatants containing any non-adherent cells) were removed from tissue culture plates using cell detachment solution (Accutase™:*Innovative Cell Technologies, Inc*.). Recovered cell suspensions were incubated for 20 min with anti-human CD54, washed in PBS, and resuspended in HBSS containing prior to analysis by BD Fortessa flow cytometer (Beckman Coulter, USA) equipped with DIVA data acquisition software. ICAM-1 expression was defined as the mean fluorescent intensity of APC.

3.3.11 **Cytokine analysis**

$_{MDM\emptyset}$ supernatants (cell-free) were collected, clarified by centrifugation to remove any remaining ENP (13,000 g; 10 min) and analysed by enzyme-linked immunosorbant assay (ELISA) for cytokine content as described below. Interleukin 8 (IL-8) concentrations were measured by ELISA (R&D Biosciences, UK) according to the manufacturer's instructions in $_{MDM\emptyset}$ cell supernatants. Briefly, cell culture supernatants were harvested, clarified by centrifugation, frozen immediately and stored at -70°C until analysed. Optical

densities were recorded by Dynatech MXR microplate reader (Dynatech Laboratories; USA), and the concentration of each cytokine calculated from a standard curve produced from serial dilutions of the appropriate cytokine. All standards and samples were assayed in duplicate.

3.3.12 **Confocal microscopy MDMØ**

Monocytes were isolated as above and added to an 8-well chamber slide (NUNC) at $4x10^6$ cells/mL. Cells were allowed to differentiate for 5-6 days as above. $MDM_{Ø}$ were treated with ENP suspensions made up in IMDM with 10% autologous serum for 24hrs. Cells were washed three times with PBS then fixed in ice-cold 100% methanol for 10 mins at -20°C. Excess methanol was removed and cells were permeabilized with ice-cold acetone for 1min at -20°C. Cells were blocked with 1% bovine serum albumin in PBS for 1hr before staining with anti-CD54-APC antibody (20µl per million cells) for 1hr. Cells were washed three times with PBS, dried, and mounted with vectashield-DAPI mounting media before viewing with a Leica SP5 confocal laser scanning microscope.

3.3.13 **Electron microscopy**

NP uptake by MDMØ was assessed using transmission electron microscopy (TEM). MDMØ were isolated and plated as described above on plastic coverslips (Thermanox®; Nunc, USA) in 24-well plates. Following NP exposure (100µg for 24hrs), coverslips were removed and fixed for 1-2hrs in 0.1 M sodium cacodylate buffer containing 3% glutaraldehyde. Coverslips were then fixed in 1% osmium tetroxide, embedded in araldite resin and cut into ultra-thin sections (60 nm thick) before viewing in a Philips CM12 transmission electron microscope.

3.3.14 **Statistics**

Data are expressed as mean± SEM unless otherwise stated. Statistical analysis was performed with GraphPad Prism (GraphPad Software, La Jolla, CA, USA) using one-way ANOVA with post-hoc Dunnett's compare ENP treatment with control. Statistical significance was taken at $P \leq 0.05$

3.4 Results

3.4.1 **Nanoparticles**

The nanoparticles used in this study were chosen for their relevance to clinically used ENP (see chapter 2). A range of doses were selected from 500µg/mL to 62µg/mL. The doses may seem high but they were chosen to encompass realistic final blood concentrations and maximal point of injection concentrations. As this is primarily a toxicological safety study the top doses are beyond what a patient would be exposed to clinically.

3.4.2 **Platelet Activation**

The most striking effects on platelet-leukocyte binding were seen with the positively charged ENPs. Both the Poly-NH_2 and the USPIO-NH_2 caused significant increases in platelet-monocyte (Fig 3-3, Fig 3-4) and platelet-neutrophil aggregation (Fig 3-5, Fig 3-6). No such increases were seen after treatment with either the un-functionalised or the carboxylated ENPs suggesting it is most likely an effect of the positive charge. Confocal microscopy images of whole blood treated with aminated beads revealed positively charged NP aggregated with platelets and bound to monocytes.

Platelet surface p-selectin, which mediates platelet-leukocyte binding through binding PSGL-1, was significantly increased by the Poly-NH_2 (Fig 3-7) and to

a lesser extent by the USPIO-NH_2 (Fig3-6) and Poly-COOH (Fig 3-7). P-selectin is shed rapidly from the cell surface so may not be as robust a marker of platelet activation as PMA which had a more consistent dose-dependent response. PAC-1 binding was increased by Poly-NH_2, the top dose of USPIO-NH_2 and the Poly-COOH however PAC-1 is a later marker of platelet activation and requires full α-body de-granulation and requires potent activation.

Platelet aggregometry was carried out in a 96-well plate Fig 3-12 shows a dose response to TRAP-6 demonstrating the technique is consistent, giving a characteristic platelet aggregation response. After 20 min only the Poly-NH_2 ENP caused significant increase in platelet aggregation (Fig 3-11). The aggregates can be seen in the wells indicated by red arrows in Fig 3-12.

3.4.3 **Platelet Hyper-reactivity**

The response of platelets to known agonist is an important test of their function. Any deviation from a normal response can manifest as a clinical condition. Here platelets that had been incubated with SPIO, USPIO-NH_2 and USPIO-COOH showed increased sensitivity to agonists TRAP-6 and thrombin.

Platelets treated with ENPs showed a lower threshold for activation and increased sensitivity to TRAP-6 measured by surface p-selectin and PAC-1 binding (Fig 3-13). This phenomenon was also demonstrated by measuring calcium influx in response to thrombin in platelets that had been pre-treated with ENP compared to saline treated platelets (Fig 3-14). Incubation with the nanoparticles alone (Fig 3-7, 3-9) showed some moderate increases in platelet activation but even nanoparticles that could not activate platelets showed here that they increased their sensitivity to agonists lowering their threshold of activation.

3.4.4 **MDMØ Inflammation**

MDMØ were incubated with SPIO, USPIO, USPIO-NH_2 and USPIO-COOH for 24 and 72-hours. The ENP were tolerated well by the cells and displayed no cytotoxic effects (see Appendix I). The most prominent effect was seen after treatment with the USPIO-COOH which caused an up-regulation in ICAM-1 detected by flow cytometry and confocal microscopy, comparable to that of the potent inflammagen LPS (Fig 3-13). This coincided with increased release of IL-8 from the USPIO-COOH treated cells (Fig 3-16, Fig 3-17) which persisted over the 72-hour period. No effects were seen after treatment with the other ENP suggesting it may be a carboxylic specific effect. While no specific mechanism was studied to account for this unique carboxylic driven effect the TEMs suggested that the USPIO-COOH were

taken up more readily by the cells which resulted in higher intracellular concentrations of the particles (Fig3-15). TNF-α, IL-1β, IL-6 and VCAM were measured by ELISA and flow cytometry respectively but were not significantly increased. It is possible they would be detected at an earlier time point.

3.4.5 **Platelet Activation**

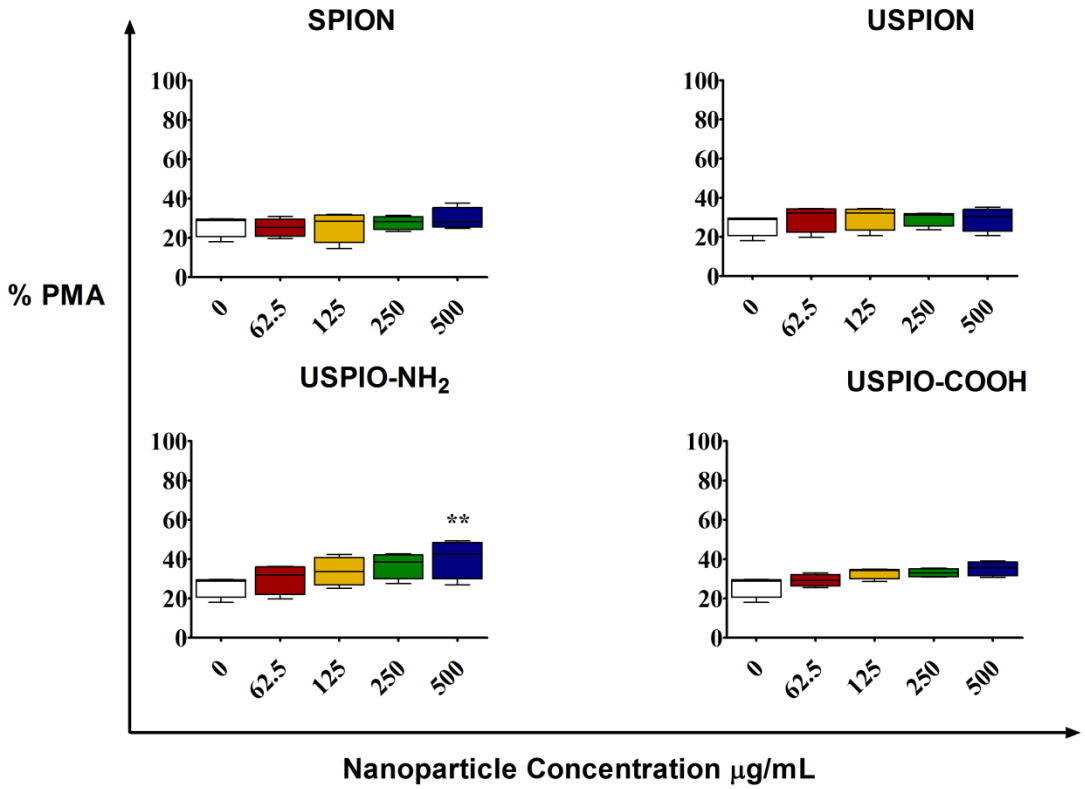

Figure 3-3. Platelet-Monocyte Aggregates in whole blood after incubation with iron-oxide ENPs. The data suggest that surface charge may affect the extent to which ENP's can activate platelets, positively charged, aminated particles being the most potent. Data represent mean ± SEM of 4-6 individual experiments.

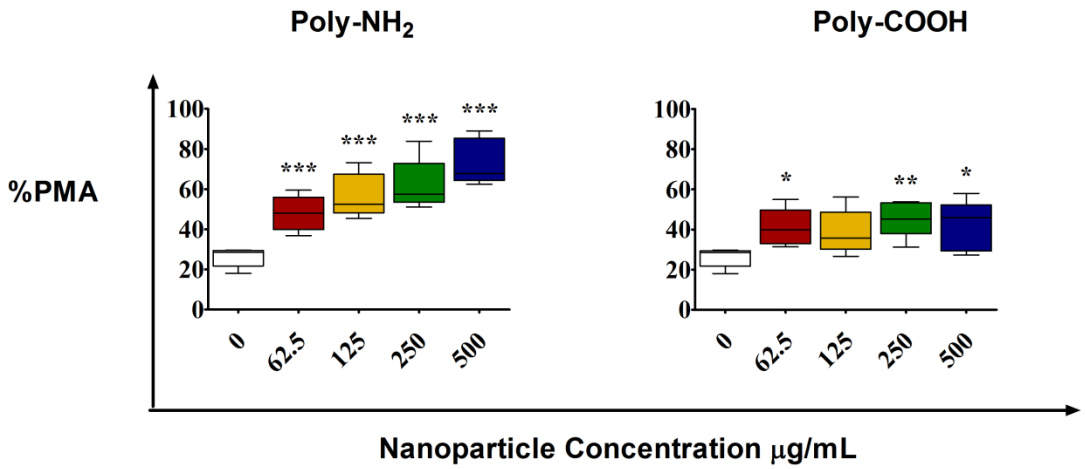

Figure 3-4 Platelet-Monocyte Aggregation in Whole blood *in vitro* after incubation with polystyrene beads. The data support the theory that positively charged ENP are more potent platelet activators than negatively charged ENP. Data represent mean ± SEM of 4-6 individual experiments.

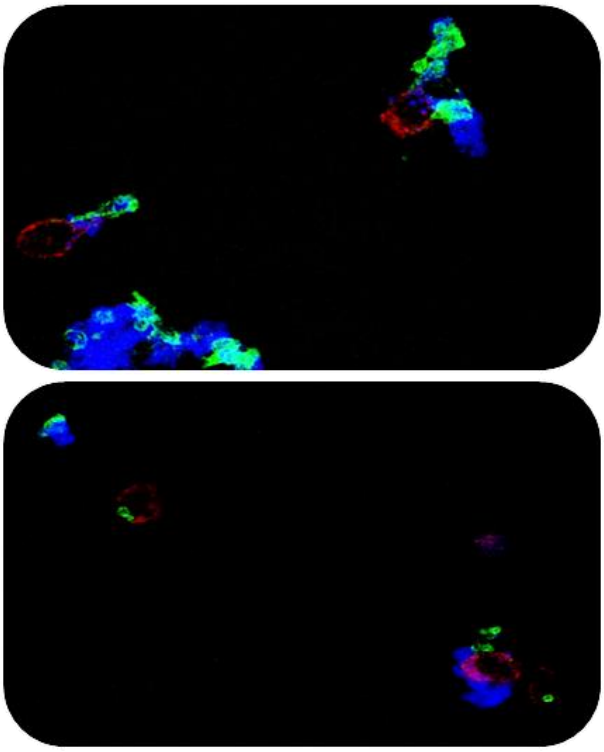

Figure 3-5 Confocal microscopy of platelet monocyte nanoparticle aggregates. Platelet (green), monocyte (red), nanoparticle (blue) aggregates isolated from whole blood. The nanoparticles appear to bind to and activate platelets which then in-turn bind to circulating monocytes. Images are representative.

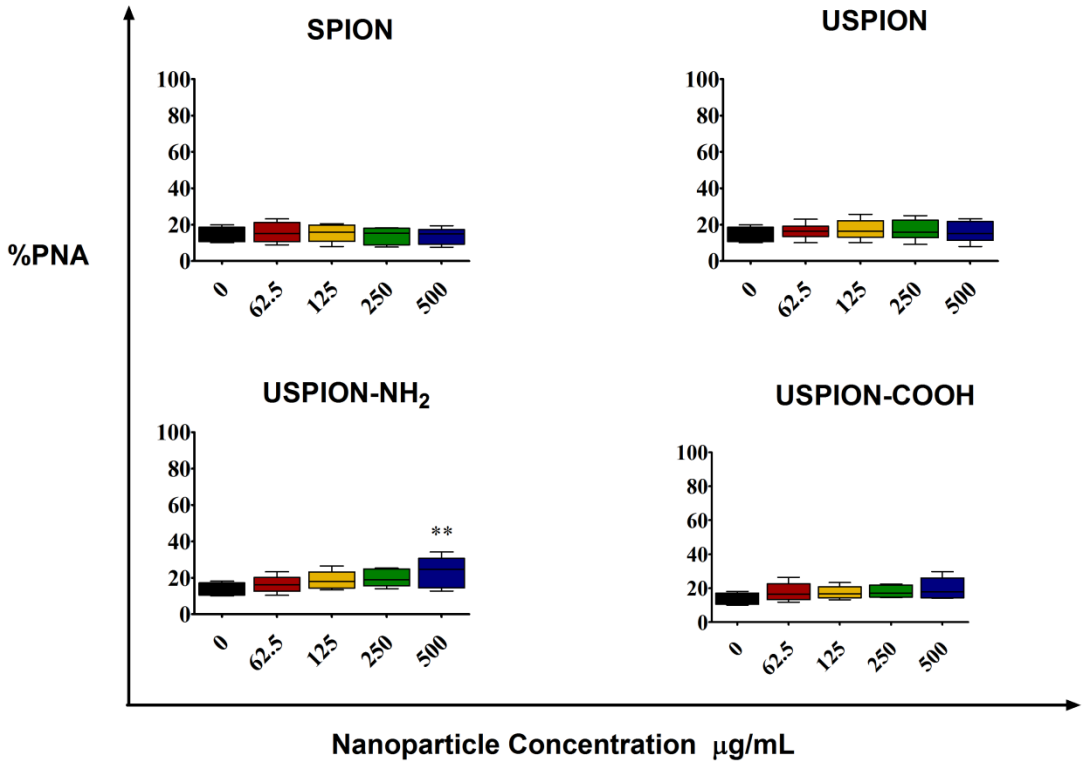

Figure 3-6 Platelet-Neutrophil Aggregates in whole blood *in vitro* after incubation with iron-oxide nanoparticles. The data suggest that surface charge may affect the extent to which ENP's can activate platelets, positively charged, aminated particles being the most potent as they were with the PMA. Data represent mean ± SEM of 4-6 individual experiments.

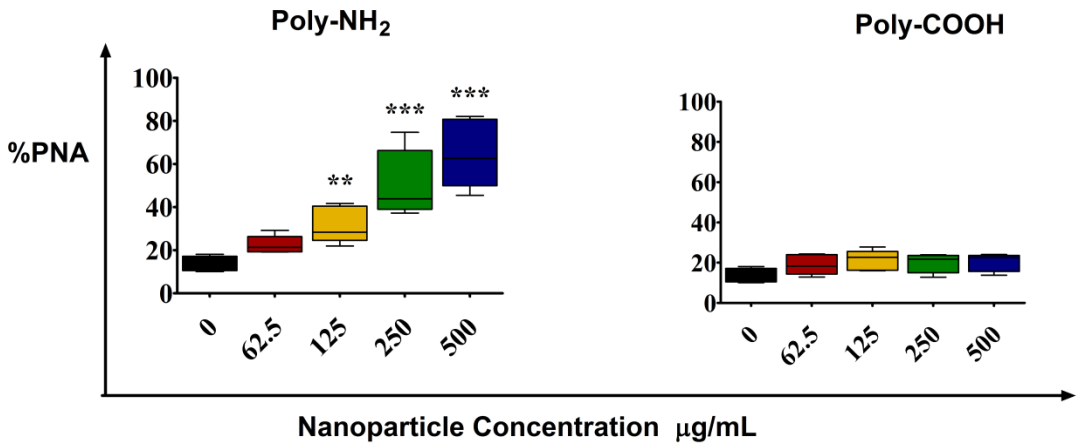

Figure 3-7 Platelet-Neutrophil Aggregation in Whole blood in vitro after incubation with polystyrene beads. The data support the theory that positively charged ENP are more potent platelet activators than negatively charged ENP. Data represent mean ± SEM of 4-6 individual experiments.

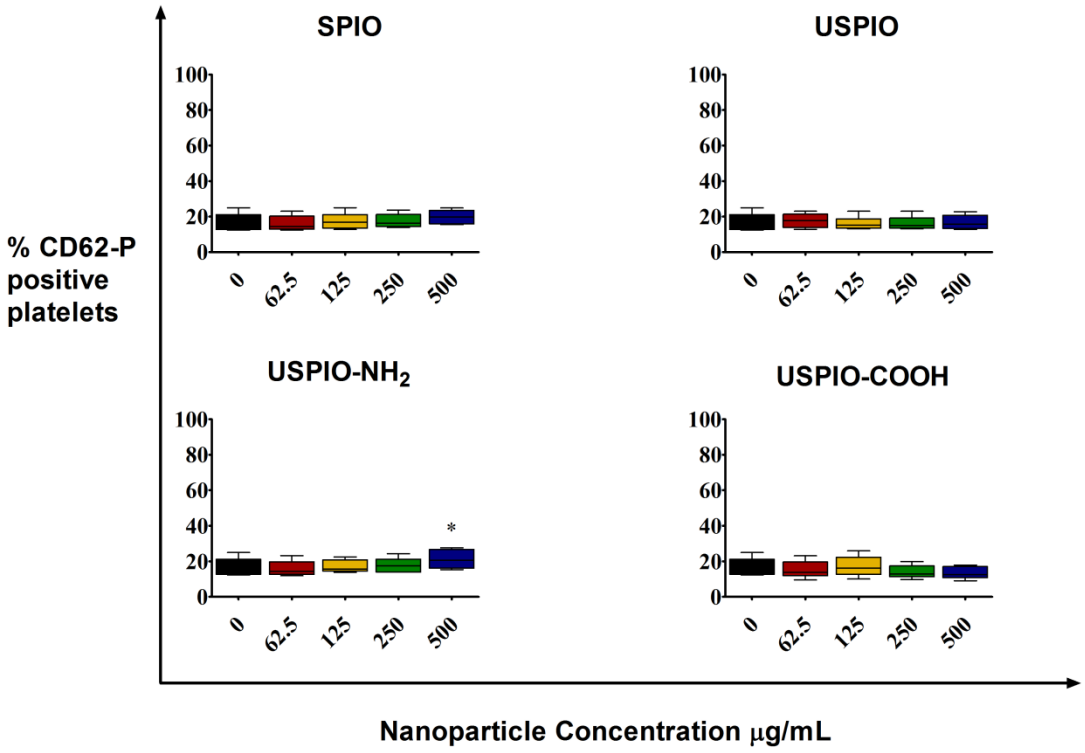

Figure 3-8 Platelet Surface P-selectin Expression after incubation with iron-oxide nanoparticles. P-selectin was significantly increased after incubation with USPIO-NH_2 but not SPIO, USPIO, or USPIO-COOH. Data represent mean±SEM of 4-6 individual experiments.

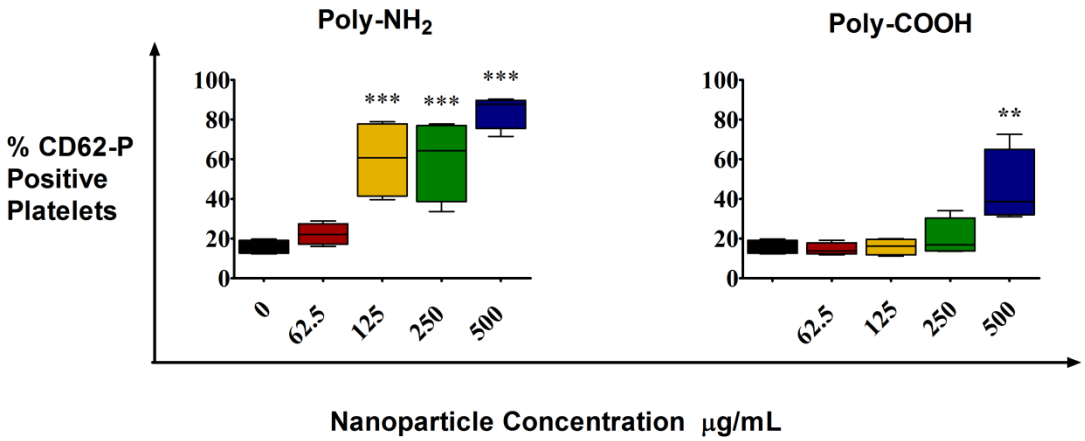

Figure 3-9 Platelet Surface P-selectin Expression after incubation with polystyrene beads. The Poly-NH_2 beads were potent platelet activators increasing platelet surface p-selectin in a dose dependent manner. The Poly-COOH beads had an effect at the highest dose. Data represent mean±SEM of 4-6 individual experiments.

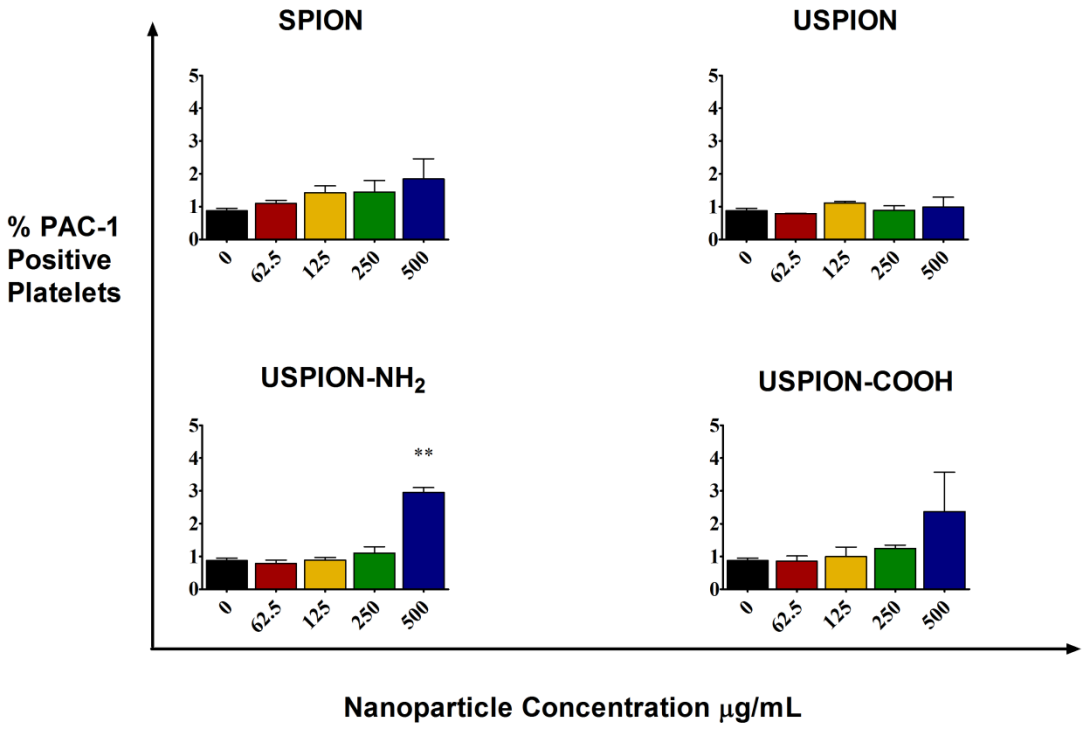

Figure 3-10 Binding of PAC-1 to platelet surface after incubation with iron-oxide nanoparticles. Though PAC-1 binding was low (<5%) slight increases were seen with the USPIO-NH_2. Data represent mean±SEM of 3 individual experiments.

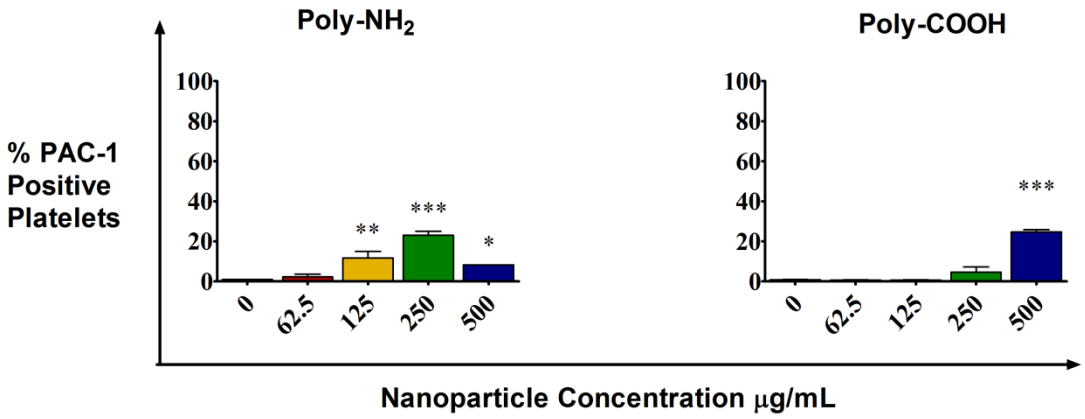

Figure 3-11 Binding of PAC-1 to platelet surface after incubation with polystyrene beads. A bigger increase in PAC-1 binding was seen with the beads again the aminated nanoparticles were more potent platelet activators. Data represent mean±SEM of 3 individual experiments.

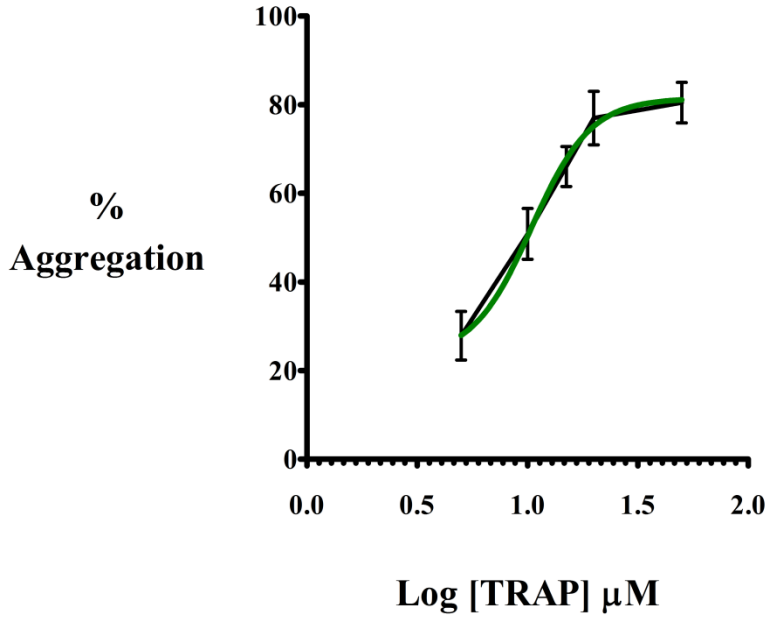

Figure 3-10 Platelet Aggregation in platelet rich plasma in response to the agonist Thrombin Receptor Activating Peptide 6 (TRAP-6) at 20 minutes.

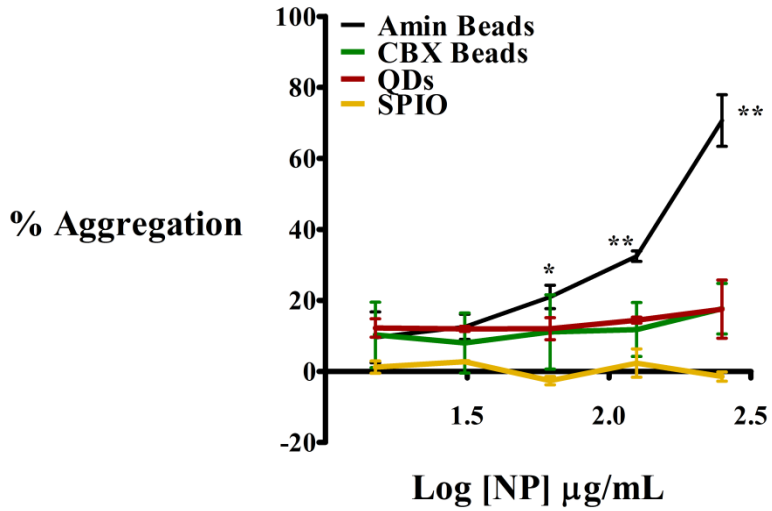

Figure 3-11 Platelet Aggregation in platelet rich plasma in response to ENPs. The positively charged aminated beads caused a dose dependent increase in platelet aggregation. Data represent mean±sem, n=5.

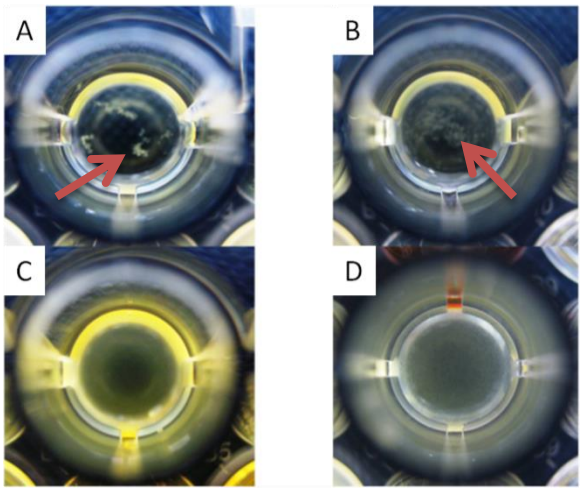

Figure 3-12 Images of platelet aggregates in 96 well plate showing aggregates indicated by red arrows, after 20 minutes incubation with A) TRAP-6, B) Aminated beads, C) Saline, D) Carboxylated beads.

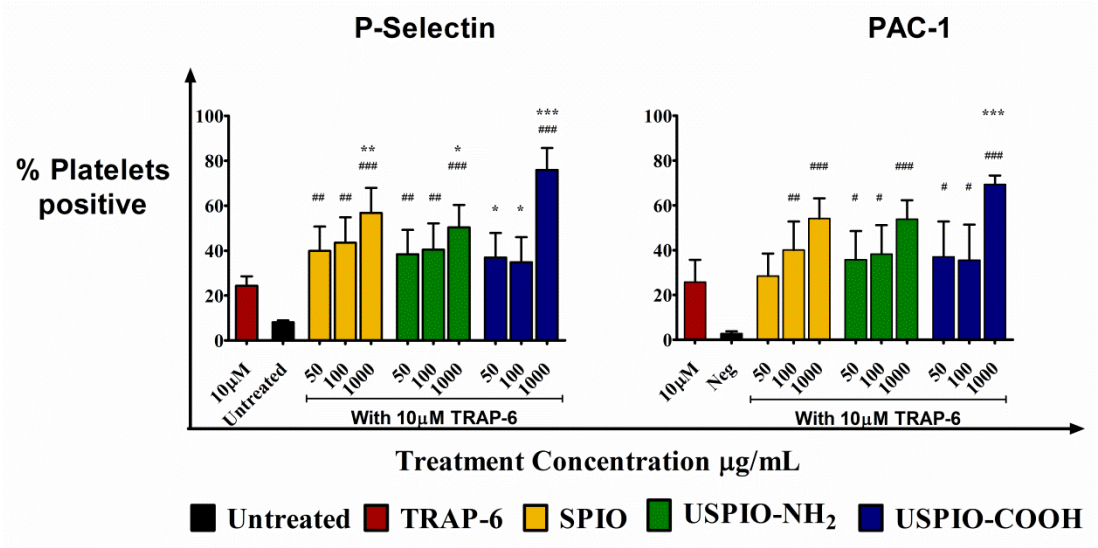

Figure 3-13 Platelet Hyper-reactivity. Platelet surface p-selectin and PAC-1 were significantly increased compared to the untreated control when co-incubated with nanoparticles and 10μm TRAP-6 (denoted by #). Significant increases were also seen when comparing TRAP-6 alone to TRAP-6 nanoparticle co-incubations (denoted by *). Data represent mean ± sem, n=5 for p-selectin, n=4 for PAC-1.

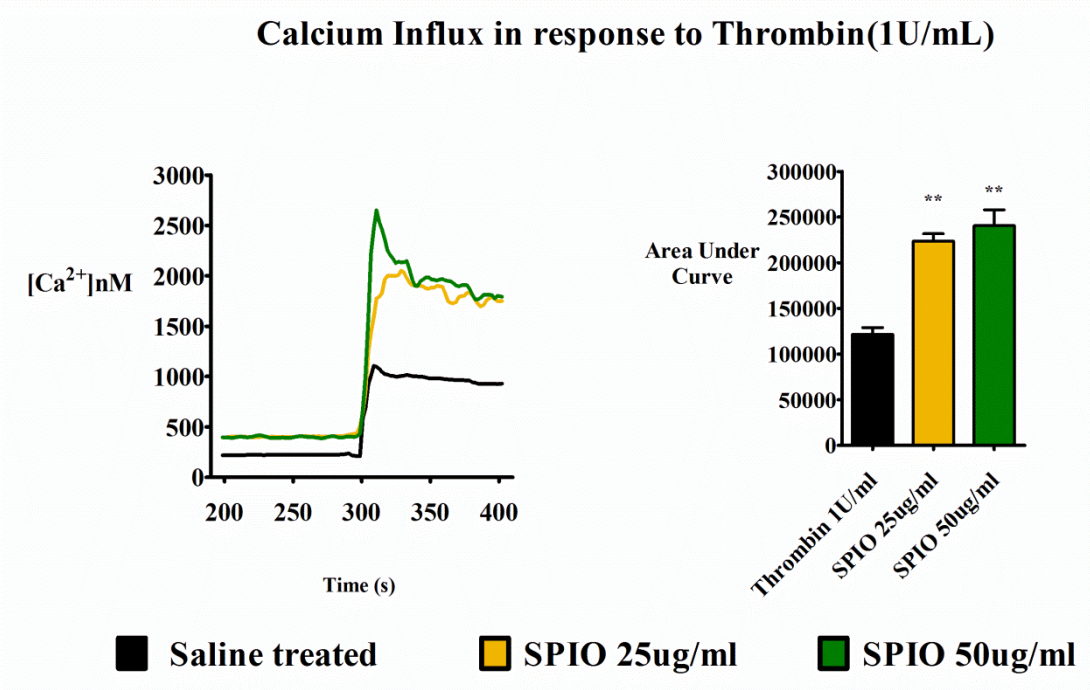

Figure 3-14 Calcium influx. Platelets incubated with SPIO showed increased sensitivity to thrombin measured by calcium influx. The increases were significant when compared to platelets incubated with saline alone. Data represent mean ± sem, n=3.

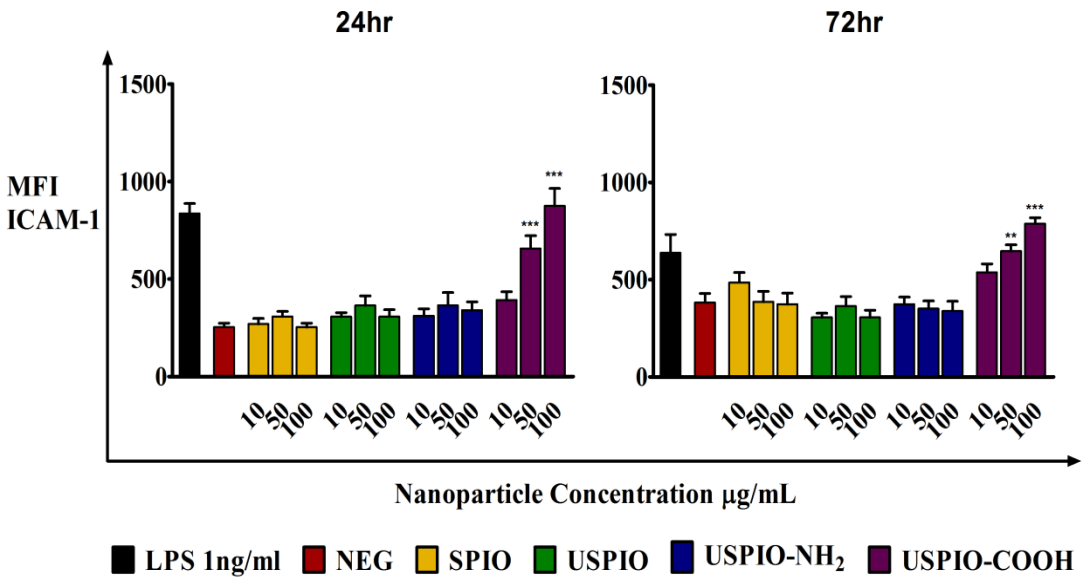

Figure 3-15 ICAM-1 Expression in monocyte derived macrophage cells after treatment with iron-oxide nanoparticles after 24 and 72 hours. Treatment with the carboxylated iron-oxide nanoparticles caused an increase in ICAM-1 which persisted over 72hours. Data represent mean±sem, n=4, $p<0.01$ **, $p<0.001$ ***.

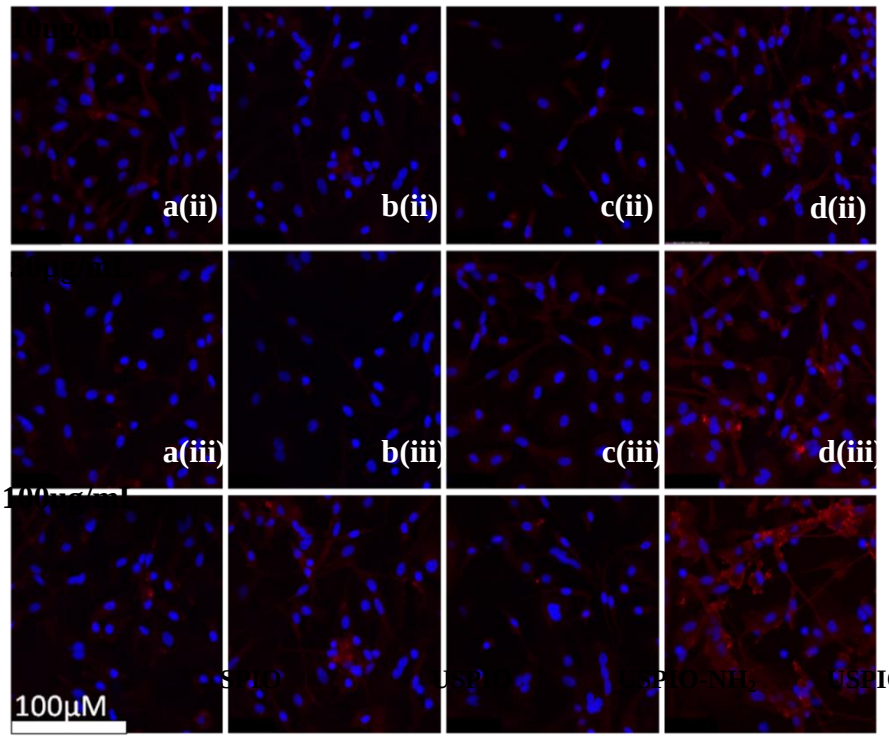

Figure 3-16 Confocal Microscopy ICAM-1 Expression at 24hrs. A dose dependent increase in ICAM-1 fluorescence can be seen (d(i), d(ii)) in the USPIO-COOH treated cells which is not apparent with any of the other treatments.

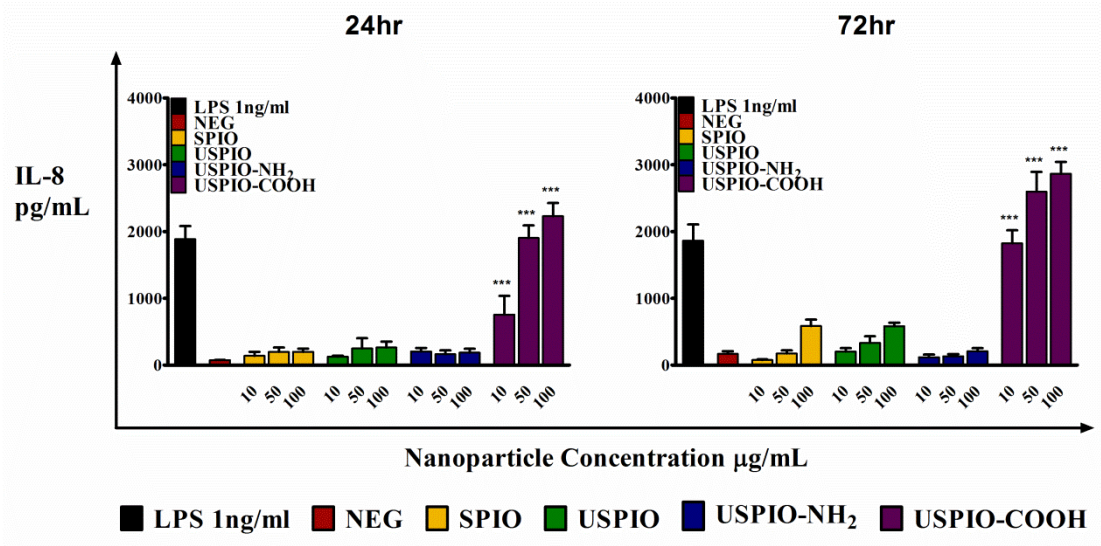

Figure 3-17 IL-8 pg/mL at 24hrs in cell culture supernatants. Treatment with the carboxylated iron-oxide nanoparticles caused an increase in IL-8 in cell culture supernatants. This effect persisted over 72-hours and was specific to the carboxylic nanoparticles. Data represent mean±SEM, n=4, $p<0.001$ ***.

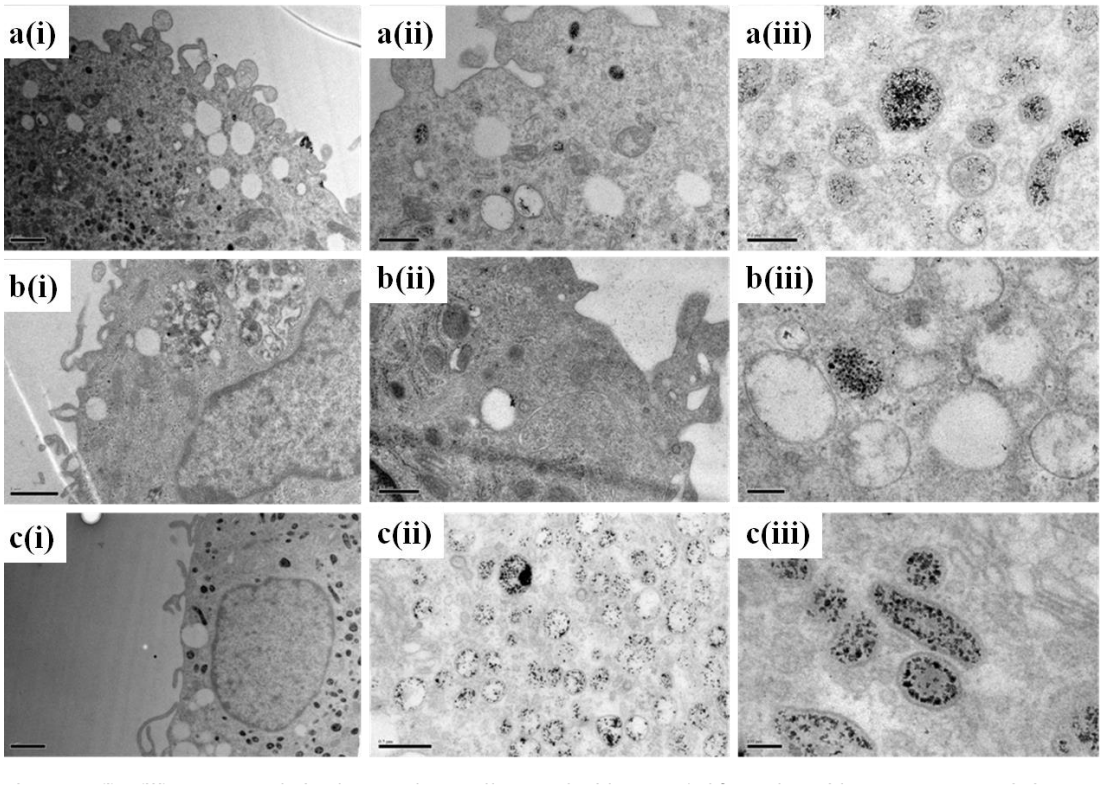

Figure 3-18.Transmission electron micrographs showing nanoparticle uptake in MDMØ cells (increasing magnification from left to right)**.** Row a) SPIO, row b) USPIO-NH_2, row c) USPIO-COOH.

3.5 *Discussion*

In recent years considerable effort and creativity have been applied to the development and study of ENP surfaces with the aim of understanding and controlling their interactions with bio-macromolecules. From a chemist's point of view, although challenging, most ENPs can be functionalised with a variety of ligands increasing their utility in clinical medicine; however there are many aspects of particle functionalisation that need to be addressed in their translation from bench-to-bedside. Persuasive evidence exists in the literature that surface modification of non-metallic ENPs plays a role in platelet activation (McGuinnes, Duffin, Brown, Mills, Megson, MacNee, Johnston, Lu, Tran, Li, Wang, Newby, & Donaldson 2011).

Here, it was demonstrated, *in vitro,* that the surface charge and functionalisation of ENPs can activate platelets and induce an inflammatory response in monocyte derived macrophages.

It was found that positively charges ENPs were more potent activators of platelets, inducing the formation of platelet-leukocyte binding, up-regulation of platelet surface p-selectin and PAC-1, and triggered platelet aggregation. As well as having effects directly on platelets all ENPs tested made platelets more sensitive to known agonists TRAP-6 and thrombin. The negatively charged carboxylated USPIO activated monocyte derived macrophage cells

causing them to release pro-inflammatory cytokine IL-8 and up-regulated ICAM-1 protein expression.

Recently it has been shown that the surface functionalisation of ENPs determines their behaviour in post-ischaemic tissue with amine modified ENPs causing enhanced microvascular permeability and it is hypothesised that the interaction of aminated ENPs with cell membranes could be mediated by electrostatic forces which have been previously reported for cationic molecules and negatively charged cell membranes (Rehberg et al. 2010;Rehberg et al. 2012b).

Platelet-monocyte aggregates are heterotypic complexes found circulating in the peripheral blood in response to platelet activation (Passacquale, Vamadevan, Pereira, Hamid, Corrigall, & Ferro 2011) and have been shown to be a more sensitive assessment of platelet activation than traditional measures of platelet activation like p-selectin, which is readily shed from their surfaces (Michelson et al. 1996). Interactions between monocytes and platelets are predominantly mediated by divalent cation-dependent interactions between platelet p-selectin and p-selectin glycoprotein ligand-1 expressed on monocytes.

Platelet-monocyte complexes have been shown to be important in inflammatory diseases such as atherosclerosis (Barnard et al. 2003;Freedman and Loscalzo 2002). Here positively charged ENPs were

more potent activators of platelets than negatively charged ENPs. Positively charged ENPs significantly increased platelet surface p-selectin expression and the formation of platelet-monocyte aggregates. Given the relevance of circulating platelet-monocyte aggregates to cardiovascular disease and their correlation with patients with ACS (Freedman & Loscalzo 2002) platelet-monocyte aggregation could be used as a quick standard method for screening ENPs intended for clinical use; identifying those which could have the potential to promote inflammation and exacerbate atherothrombotic disease (Passacquale, Vamadevan, Pereira, Hamid, Corrigall, & Ferro 2011).

The response of platelets to the agonist TRAP-6 was measured after incubation with SPION, USPION-NH_2 and USPION-COOH. In comparison with the negative control TRAP-6 did not cause a significant elevation in platelet activation. The same dose of TRAP-6 when added to platelets incubated with ENPs caused significant increases in both CD62P expression and Pac-1 binding showing that incubation with ENPs causes platelets to lower their threshold of activation or become hyper-reactive. Calcium mobilisation plays an important role in platelet activation and aggregation mediating cytoskeletal changes and secretion (Allison et al. 2006). Thrombin was used to induce calcium influx and increase intracellular calcium ion concentration in platelets. When this was repeated in platelets incubated with increasing doses of SPIO intracellular calcium was significantly increased in a dose dependent manner compared to saline treated platelets. Taken together these results suggest that surface functionalisation has a bearing on

platelet activation, the positively charged ENPs being more potent activators of platelets than negatively charged particles but it seems that exposure to ENPs in general caused platelets to become more responsive to external agonists or become hyper-reactive a condition known to contribute to atherothrombotic disease (Kubik and Richardson 1987).

Intercellular adhesion molecule 1 (ICAM-1) is an important mediator of cell adhesion, immunostimulation and maintenance of the pro-inflammatory environment (Watanabe and Fan 1998). Adhesion molecules such as ICAM-1 are involved in the initial stages of plaque progression involves the recruitment of inflammatory cells from the circulation and their transendothelial migration. The basic science of inflammation biology applied to atherosclerosis has afforded considerable new insight into the mechanisms underlying the recruitment of leukocytes. This process is predominantly mediated by cellular adhesion molecules, which are expressed on the vascular endothelium and on circulating leukocytes in response to several inflammatory stimuli. Two molecules mediating cell-cell adhesive interactions are ICAM-l and the integrin LFA-l (Brown et al. 1993). Persistent up-regulation of adhesion molecules could lead to chronic cell activation, inflammation, and propagation of disease.

Carboxylated ENPs in this study caused significant increases in both ICAM-1 and IL8 pg/mL, which persisted over a 72-hour period. These increases were only seen after treatment with the carboxylated ENPs suggesting it may be a

carboxyl-specific effect potentially driven by increased cellular recognition and uptake of carboxylated ENP as seen by transmission electron microscopy. It has previously been shown that exposure to occupational dusts and particles can cause up-regulation of macrophage ICAM-1 and cause aggregation of alveolar macrophages after pulmonary instillation into a rat model (Brown, Dransfield, Wetherill, & Donaldson 1993) and another study showed that exposure to iron-oxide ENPs caused up-regulation of ICAM-1 and Il-8 in endothelial cells (Zhu et al. 2011b). Up-regulation of ICAM-1 can lead to increased cell binding to vascular endothelium as well as homotypic macrophage binding maintaining and driving the inflammatory environment and potentially exacerbating plaque progression (Libby et al. 2011).

A number of limitations need to be taken into consideration when interpreting this data. As with all *in vitro* studies the conditions are artificial and do not adequately mimic the *in vivo* situation. This may be particularly important for platelets as they are heavily influenced by rheological conditions. Other cell types, such as endothelial cells, which play a central role in cardiovascular disease, may be affected by ENPs and further research is needed into ENP-platelet-endothelial cell interactions. The ENP used in this study, though relevant to clinical use, do not reflect the scope of ENPs in development for intra-venous use.

The data in this study indicate that surface functionalisation plays a critical role in ENP toxicity. Not only that, but toxicity may be different across cell types. As seen here the positively charged aminated particles had a big effect on platelets in vitro while the negatively charged carboxylated USPIOs had a pro-inflammatory effect on monocyte derived macrophages. This study shows that relatively simple *in vitro* techniques could be used to determine the potential for ENPs to cause platelet activation and induce cellular inflammation.

Chapter 4 **Ex-Vivo Effects of Engineered Nanoparticles**

4.1 *Abstract*

ENPs designed for medical use share certain properties with CDNPs and may exert similar pro-thrombotic effects. In this study a well validated model of thrombosis, the Badimon chamber, was used to investigate whether ENPs induce thrombosis in flowing blood subjected to then. As this was the first time the Badimon chamber was used for such a study its utility as an appropriate model was also under investigation. Flow cytometry was used to assess platelet activation and a cytometric bead array was used to detect inflammatory cytokines sampled from the chamber.

In a randomised, double-blind, cross-over study Feraheme®, Poly-NH_2 and Poly-COOH nanoparticles were added extracorporeally to native whole blood. The higher dose of Feraheme® (300µg/mL) caused significant ($p=0.002$) increase in thrombus formation under high shear but not low shear conditions. No platelet activation was detected compared to the saline control. The negatively charged Poly-COOH caused significant increases in platelet surface p-selectin, PAC-1, $p<0.05$ for all, but this did not translate into an increase in thrombus formation.

The Badimon chamber showed promise as a model for testing the effect of ENPs on thrombus formation and resolves some of the limitations of the *in vitro* toxicology studies.

4.2 *Introduction*

Platelet activation and thrombosis are critical determinants of the clinical outcome following atheromatous plaque rupture, which often results in thrombotic coronary artery occlusion, myocardial infarction and sudden cardiovascular death. A variety of ENPs are under development for imaging atherothrombotic vascular disease and for the delivery of targeted therapeutic ENPs to the unstable plaque.

Using a carefully characterised exposure system, we have previously shown that exposure to combustion-derived ENPs in dilute diesel exhaust causes an impairment of vascular and fibrinolytic function (Mills et al. 2005), and induces asymptomatic myocardial ischemia in patients with coronary heart disease (Mills, Tornqvist, Gonzalez, Vink, Robinson, Soderberg, Boon, Donaldson, Sandstrom, Blomberg, & Newby 2007b). More recently we have demonstrated using a Badimon chamber that inhalation exposure to diesel exhaust increases platelet activation and thrombus formation in man (Lucking, Lundback, Mills, Faratian, Barath, Pourazar, Cassee, Donaldson, Boon, Badimon, Sandstrom, Blomberg, & Newby 2008). These pro-thrombotic effects may well be mediated by a direct effect of circulating ENPs on platelet function.

ENP contrast agents that specifically target unstable atheromatous plaques have the potential to assist in both the diagnosis and treatment of vascular lesions (Nahrendorf et al. 2009b). However, because they are delivered directly into the blood they also have to the potential to activate platelets and thus adversely affect clinical outcome (McGuinnes, Duffin, Brown, Mills, Megson, MacNee, Johnston, Lu, Tran, Li, Wang, Newby, & Donaldson 2011). As yet there are no published studies addressing whether the direct intravascular infusion of these ENP contrast agents exert adverse effects on platelet or vascular function. The ex-vivo evaluation of nanoparticulates, and test particles with differing physicochemical properties, will help to determine the characteristics of nanoparticulates that influence platelet function and thrombosis. These studies are an essential part of the development of safe medical imaging and therapeutic nanoparticulates.

4.3 *Aims and Hypothesis*

We hypothesise that medical ENPs designed for intravenous use could have similar pro-thrombotic effects as inhaled CDNPs due to the physical similarities they share such as size and surface area and that the Badimon chamber could be used as an ex-vivo model to assess the pro-thrombotic nature of ENPs designed for biomedical use, specifically those intended for intravenous injection.

Our preliminary investigations suggest that ENM surface charge may be an important determinant in their thrombogenicity. Using the Badimon chamber as an ex-vivo we aimed to mimic more realistic conditions of thrombus formation and the potential for ENPs to influence this.

The aim of this study is to investigate the effects of ENP contrast agents on platelet function and thrombogenesis *ex vivo*. ENPs designed for atheroma imaging were compared with ENPs of known activity in assays of platelet activation as detailed in Chapter 3.

4.4 Methods

4.4.1 **The Badimon Chamber**

The Badimon chamber is an *ex vivo* model of deep arterial injury and thrombus formation used previously to study the effects of diesel exhaust ENP inhalation on thrombosis in man (Lucking, Lundback, Mills, Faratian, Barath, Pourazar, Cassee, Donaldson, Boon, Badimon, Sandstrom, Blomberg, & Newby 2008;Lundback, Mills, Lucking, Barath, Donaldson, Newby, Sandstrom, & Blomberg 2009). The chamber permits an assessment of thrombus formation in whole blood without the need for anti-coagulants or exposure of the patient to the compounds being tested. While principally used to assess the impact of novel antithrombotic agents it can be readily modified to assess the effects of ENM on thrombosis by adding them into the extracorporeal blood flow at a defined concentration and assessing the impact on thrombosis compared to untreated blood. A pump is used to draw blood from the ante-cubital vein through the chambers, maintained at 37°C in a water bath. The rheological conditions in the first chamber simulate those of patent coronary arteries (low-shear rate), whereas those in the second and third chambers simulate those of stenosed coronary artery (high-shear rate) (Lucking, Lundback, Mills, Faratian, Barath, Pourazar, Cassee, Donaldson, Boon, Badimon, Sandstrom, Blomberg, & Newby 2008). The thrombus formed in the low shear chamber is fibrin and macrophage- rich whereas the thrombus formed in high shear conditions is platelet- rich

(Lucking, Lundback, Mills, Faratian, Barath, Pourazar, Cassee, Donaldson, Boon, Badimon, Sandstrom, Blomberg, & Newby 2008). This powerful technique permits the dynamic formation of thrombus to be observed and allows the assessment of thrombotic and anti-thrombotic interventions. The chamber is therefore potentially able to assess ENP interactions with specific blood cells and types of thrombus.

The Badimon chamber was custom made at Edinburgh University based on an original Badimon chambers obtained from the designer of the chamber. The chamber themselves are Plexiglas blocks through which a cylindrical hole has been bored. This mimics the typical cylindrical shape of vasculature. The bore size is either 0.2 or 0.1 cm diameter modelling low and high shear stress respectively. Portions of these channels are left open in order to expose the flowing blood to a biological or prosthetic surface. Another Plexiglas block is placed on top of this block, on top of the non-exposed side of the test surface and screwed into place to create a leak free system.

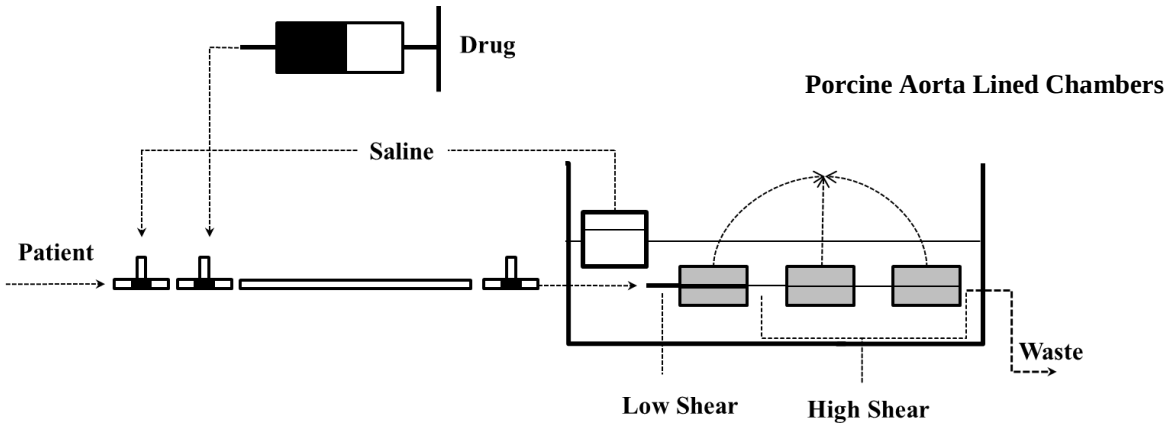

Figure 4-1 Badimon Chamber Set-up

Schematic of Badimon chamber set-up showing from left to right the flow of blood from the patient through the tubing where the blood mixes with the extra-corporeal drug, in this case particles, then across the three chambers lined with denuded porcine aorta and on to the effluent container.

Table 4-1 Flow characteristics of perfusion chambers

Tubular diameter (cm)	**Blood flow rate (mL/min)**	**Blood wall shear rate (1/s)**
0.2	**5** **10** **20** **30** **40**	**105** **212** **425** **640** **850**
0.1	**5** **10** **20** **30** **40**	**840** **1,680** **3,360** **5,040** **6,720**

(Badimon et al. 2012)

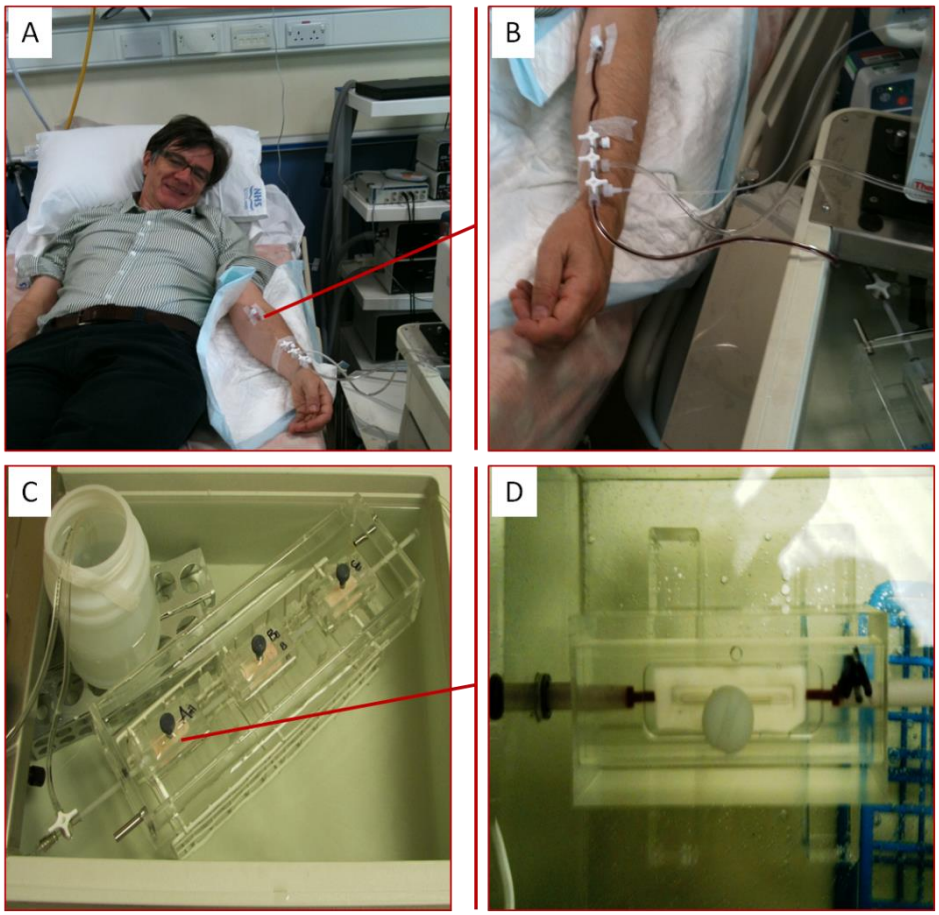

Figure 4-2 Badimon chamber set-up with volunteer

Images of Badimon chamber in action showing blood flowing from the subject (A-B) and across the porcine aorta lined chambers (C-D).

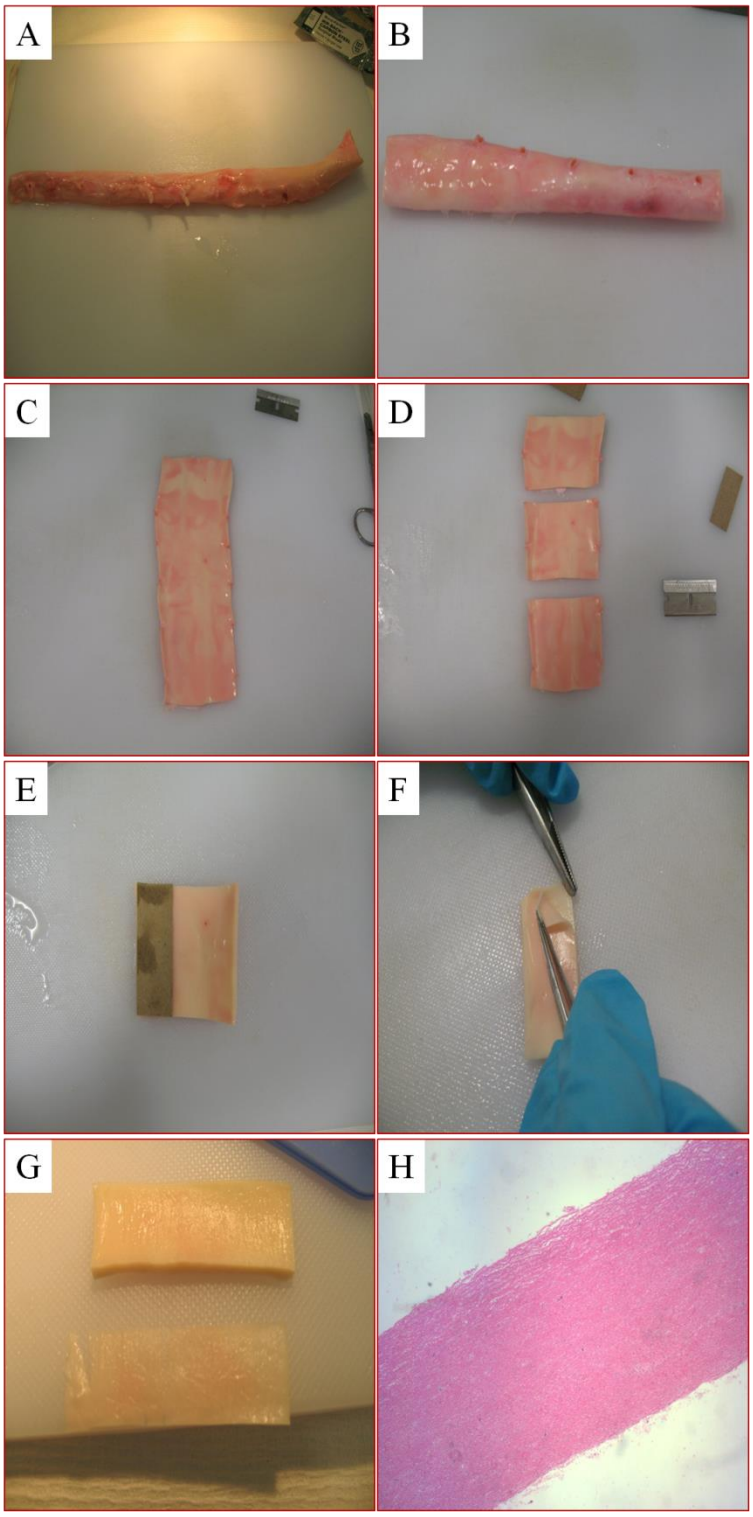

Figure 4-3 Preparation of Porcine Aortic Strips

Images showing the steps in the preparation of the porcine aortic strips for use in the Badimon chamber. Image A shows the whole untouched aorta as supplied by the company (Pel-Freez® Biologicals). The aorta is first trimmed of its excess fat and the remainder of the aortic arch is removes (B). The aorta is cut along the branches (C) and then cut into sections lengthways so as to fit in the chamber (D). The edges of the sections are squared off and cut into strips using a template (E). The top corner of the strip is marked to show from which end the strip was denuded. Strips are denuded from thick end to thin by making a small incision in the top corner and then gently peeling back the endothelial layer and a small amount of the underlying intimal layer (F). The layer of tissue that's removed should be as thin as possible and come away in one piece (G). It is important to go over the surface of the strip with forceps ensuring there are no loose flaps of tissue, as this would cause the formation of a false clot on the surface of the aorta.

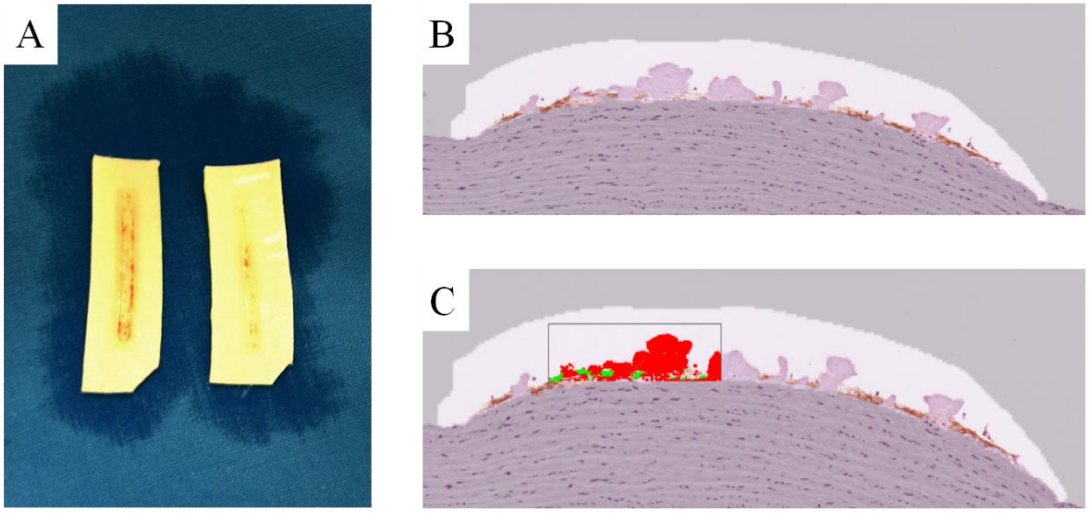

Figure 4-4 Quantification of Thrombus Area

Thrombus is formed along the entire length of the exposed substrate (equal to the window of the flow channel [2 cm]). Images were acquired at X20 magnification, and the thrombus area was measured using an Ariol image acquisition system (Applied Imaging, USA) by a blinded operator. Results from at least six sections were averaged to determine thrombus area for each chamber (μm^2) (Images courtesy of Dr Andrew Lucking).

4.4.2 **Study Design**

Healthy volunteers (n=12) attended the clinical research facility at the Edinburgh Royal Infirmary on two occasions for a series of Badimon chamber perfusion studies. A 27-guage intravenous cannula was placed in a large antecubital fossa vein. A peristaltic pump drew blood from the antecubital vein through a series of perfusion chambers maintained at 37˚C in a water bath as described above. During the first visit saline (control) or suspensions of ENPs were infused to achieve local concentrations of 0.15 mg/mL and 0.3mg/mL in the extracorporeal circuit of the Badimon Chamber. The order of extra-corporeal infusions was randomized using a balanced block design. All studies were performed in a temperature controlled clinical research facility by staff blinded to exposure allocation.

The primary end point was thrombus area (high and low shear conditions) with secondary endpoints including platelet-monocyte aggregation, plasma markers of inflammation and platelet activation determined by flow cytometry.

4.4.3 **Nanoparticle Panel**

4.4.3.1 Feraheme®

Feraheme® was prepared at the following concentrations: diluted 1:10 (3 mg/mL) or diluted 1:20 (1.5mg/mL) in sterile isotonic saline (0.9%) and bath sonicated for 5 min prior to perfusion. Feraheme® solutions were infused at a rate of 1mL/min in the extra-corporeal circuit and mixed with 50 mL of blood drawn through the perfusion chamber at 10 mL per minute over 5 mins reaching a final concentration of 150µg/mL or 300µg/mL in blood.

4.4.3.2 Model Engineered Nanoparticles

Carboxylated and aminated ENPs (50nm) *(Polysciences Inc.*, *Sigma-Aldrich*®, respectively) were supplied at 25 mg/mL and diluted 1:8.3 in sterile isotonic saline (0.9%) to achieve a stock solution at 3 mg/mL and bath sonicated for 5 min prior to perfusion. ENP solution was infused at a rate of 1mL/min into the extra-corporeal circuit and mixed with 50 mL of blood drawn through the perfusion chamber at 10 mL per minute over 5 mins reaching a final concentration of 0.3mg/mL in the extracorporeal circuit.

4.4.4 **Visit 1**

During visit one; subjects underwent three Badimon chamber perfusion studies in a randomised order with the addition of either normal saline or Feraheme® USPION at a final concentration of 0.15 mg/mL or 0.3 mg/mL. 0.15 mg/mL is based on the concentration of USPION found in the systemic circulation following intravenous infusion of 4mg/kg USPION in previous clinical trials 20 minutes after infusion (Landry et al. 2005). The *ex-vivo* study included two concentrations of USPION; 0.15 mg/mL to reflect concentrations delivered during a continuous infusion over 30 mins of 4mg/kg USPION, and as the purpose of the study is to determine the safety of the USPIONs we included a dose two fold higher than a patient would ever be exposed to in a clinical situation.

4.4.5 **Visit 2**

During visit two, subjects underwent three Badimon chamber perfusion studies in a randomised order with the addition of either normal saline or positively charged aminated latex beads or negatively charged carboxylated latex beads at a final concentration of 0.3 mg/mL. These charged model ENPs have been shown to consistently cause platelet aggregation and platelet-monocyte binding at this concentration (McGuinnes, Duffin, Brown,

Mills, Megson, MacNee, Johnston, Lu, Tran, Li, Wang, Newby, & Donaldson 2011).

4.4.6 **Subjects**

Twelve healthy, non-smoking subjects, age 18-65 year old were identified from the healthy volunteer database. Subjects with previous medical history or on regular medication including the oral contraceptive pill and non-steroidal anti-inflammatory agents with anti-platelet activity were excluded. All subjects underwent a general examination including height, weight, heart rate, and blood pressure. To exclude subclinical haematological, renal or hepatic disease routine haematological (full blood count) and clinical chemistry (urea and electrolytes, liver function,) tests were measured prior to enrolment.

4.4.7 **Inflammatory Measures**

Effluent was collected from the chamber and analysed for plasma IL-1ß, IL-12p70, IL-10, IL-6, IL-8 and TNF-αusing a BD™ human inflammatory cytometric bead array (BD Biosciences).

4.4.8 **Platelet Activation**

Effluent was also analysed for platelet-monocyte aggregation and platelet activation by flow cytometry including p-selectin, PAC-1 binding and platelet surface CD36.

4.4.9 **ICPMS**

Iron content by inductively coupled plasma mass spectrometry (ICPMS). Whole blood Iron content was measured by inductively coupled plasma mass spectrometry (ICPMS) in effluent from the Badimon chamber to ensure the addition system is working as expected.

Blood was also collected from healthy volunteers taking part in a separate study (11/MRE00/5) in which healthy volunteers were directly infused with Feraheme® at baseline and 24-hours post infusion to validate the extracorporeal doses.

4.5 *Statistics*

Statistical analysis of data will be performed using GraphPad Prism. Primary and secondary end-points following each infusion will be compared with

saline control with data analysed using repeated measures 1-way analysis of variance. Statistical significance will be taken at $P<0.05$.

4.6 *Results*

4.6.1 **Subjects**

Subjects recruited were considered healthy volunteers, average age 38±3, all subjects were male and did not differ significantly with respect to gender, age, height, and weight (Table 4-1) all subjects attended for two studies and reported no adverse effects having taken part.

4.6.2 **Inflammatory Markers**

There was a heterogeneous response in inflammatory cytokines in serum sampled from the chamber with the addition of either Feraheme® (Table 4-4), beads (Table 4-5) compared to the saline control.

4.6.3 **ICPMS**

Iron concentration in Badimon effluent correlated well with the estimated addition (Table 4-3). The net iron value for the lower dose was 116.91±12.55 µg/mL and the higher dose was 240.75±8.83 µg/mL. The higher dose was roughly double the lower dose as expected and closely matched the C_{max}

previously reported in the literature, 126.0±32.6 µg/mL, (Landry, Jacobs, Davis, Shenouda, & Bolton 2005). To validate the calculated extracorporeal doses used blood was collected from healthy volunteers taking part in a separate MRI study that were receiving Feraheme®. Blood was sampled at baseline pre-Feraheme®, and 24-hours post Feraheme®. The *in vivo* iron concentrations correlated well with the estimated concentrations, 71.56±11.5 µg/mL 24-hours post.

4.6.4 **Platelet Activation**

There were no significant increases in platelet-monocyte aggregates, platelet surface p-selectin, PAC-1 or CD36 following the addition of the lower or higher doses of Feraheme® when compared to the saline control.

The Poly-COOH beads increased platelet surface p-selectin ($p=0.003$), CD36 ($p=0.002$) and PAC-1 (0.0003) whereas the Poly-NH_2 had no such effects compared to saline control. Neither of the charged beads significantly increased platelet-monocyte aggregation.

4.6.5 **Thrombus Formation**

Thrombus formation in the high-shear chamber increased following addition of both doses of Feraheme® though the lower dose did not reach significance whereas the higher dose did ($p=0.002$). No increase in thrombus was seen in the low-shear chamber. Surprisingly the addition of Poly-NH_2 and Poly-COOH caused a significant decrease in thrombus formation $p=0.02$, $p=0.0076$ respectively.

Table 4-2 Baseline Characteristics of Healthy Volunteers. Data represent mean ± SEM n=12

	Value
Age	38±3
Height (m)	1.75±0.02
Body mass index (kg/m^2)	26±0.9
Heart rate	65±3
Systolic blood pressure (mmHg)	134±3
Diastolic blood pressure (mmHg)	81±3

Table 4-3 Inductively Coupled Plasma Mass Spectrometry from extracorporeal study. Data represent mean ± SEM n=12

Extracorporeal Drug	Total Iron Concentration in Effluent (mg/L)
Saline	418.67±8.14
Feraheme® 150µg/mL	535.58±12.56
Feraheme® 300µg/mL	659.42±8.83

Table 4-4 Inductively Coupled Plasma Mass Spectrometry from healthy volunteers receiving intra-venous Feraheme®. Data represent mean ± SEM, n=6.

Drug	Total Iron concentration in whole blood from healthy volunteers (mg/L)
Pre-Feraheme®	467.94±19.1
24-hour Post Feraheme®	539.5±11.5

Table 4-5 Inflammatory cytokine levels after the addition of Feraheme® to the extracorporeal circuit. Data represent mean ± SEM n=12

Cytokine (pg/mL)	Saline	Feraheme® 150µg/mL	Feraheme® 300µg/mL
IL-12p70	0±0	2.8 ±1.8	2.3±2.2
TNF-α	9.5±2.3	10.9±2.6	10.2±2.5
IL-10	0±0	0.5±0.5	0±0
IL-6	1.3±0.8	1.3±0.8	0.9±0.6
IL-1β	6.2±1.3	5.4±1.3	5.6±1.2
IL-8	4.5±1.3	3.4±1.2	3.3±0.9

Table 4-6 Inflammatory cytokine levels after the addition of Polystyrene beads to the extracorporeal circuit. Data represent mean ± SEM n=12

Cytokine (pg/mL)	Saline	Positive bead	Negative bead
IL-12p70	0±0	4.3±2.8	7.3±3.2
TNF-α	9.5±2.3	12.5±2.9	14.5±2.8
IL-10	0±0	1.9±1.0	2.6±1.0
IL-6	1.3±0.8	1.7±0.9	0.9±0.6
IL-1β	6.2±1.3	9.3±1.5	7.5±1.2
IL-8	4.5±1.3	7.1±1.0	6.8±1.3

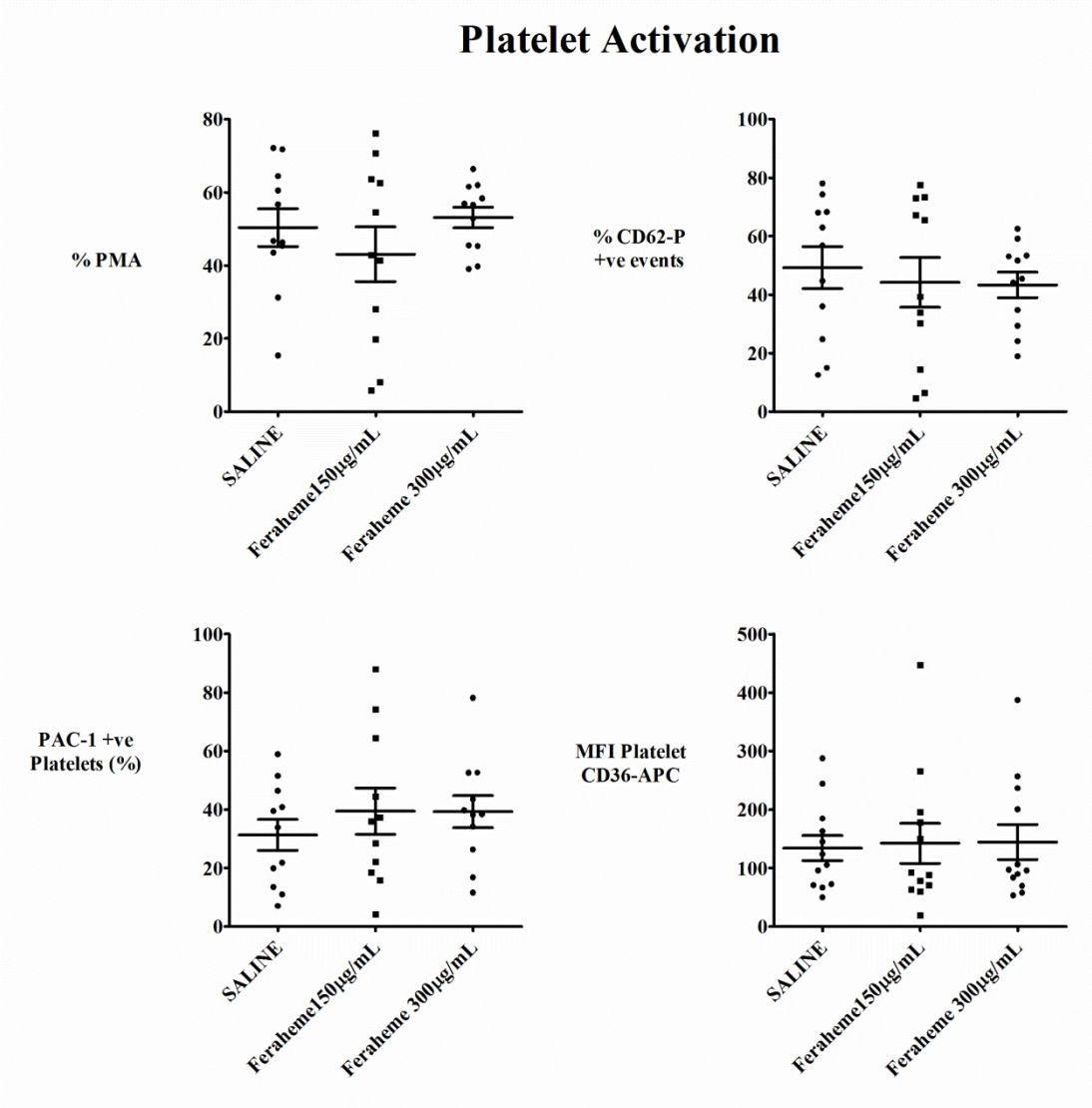

Figure 4-5 Platelet activation markers measured in whole blood sampled from the Badimon chamber after the addition of Feraheme®. No increase in platelet activation was seen for either dose of Feraheme®. Parameter assessed included platelet monocyte aggregation, platelet surface p-selectin, PAC-1 and CD36. Data represent mean±sem, n=11-12.

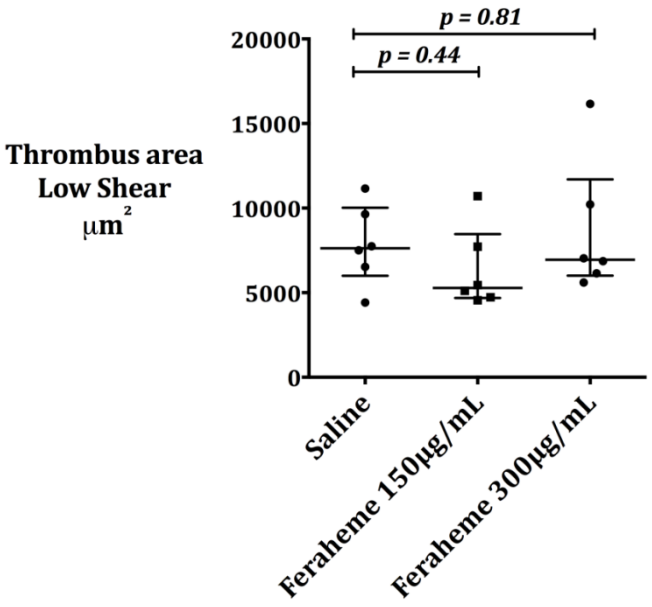

Figure 4-5 Thrombus formation under low shear with the addition of Feraheme®. No increase in thrombus was seen for either concentration of Feraheme® under low shear conditions. Data represent mean ± SEM n=6

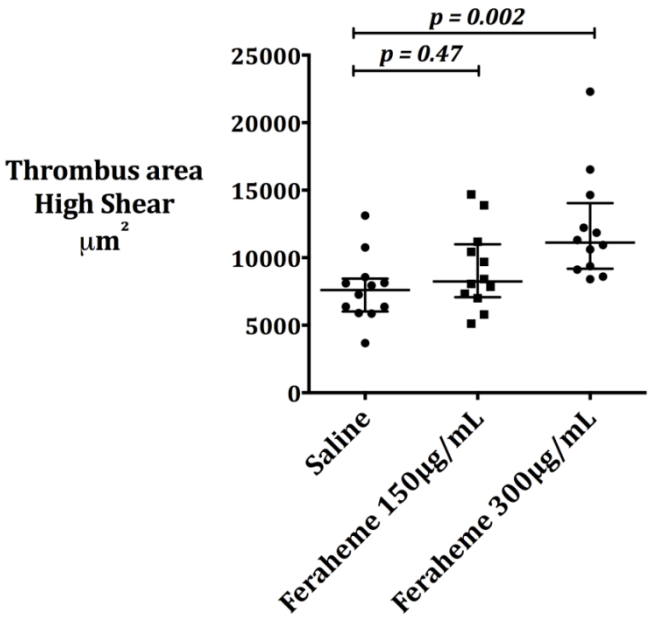

Figure 4-6. Thrombus formation under high shear with the addition of Feraheme®. While no increase in thrombus area was seen with the lower dose of Feraheme® a significant (p=0.002) increase in thrombus was seen with the higher dose of Feraheme®. Data represent mean ± SEM n=12

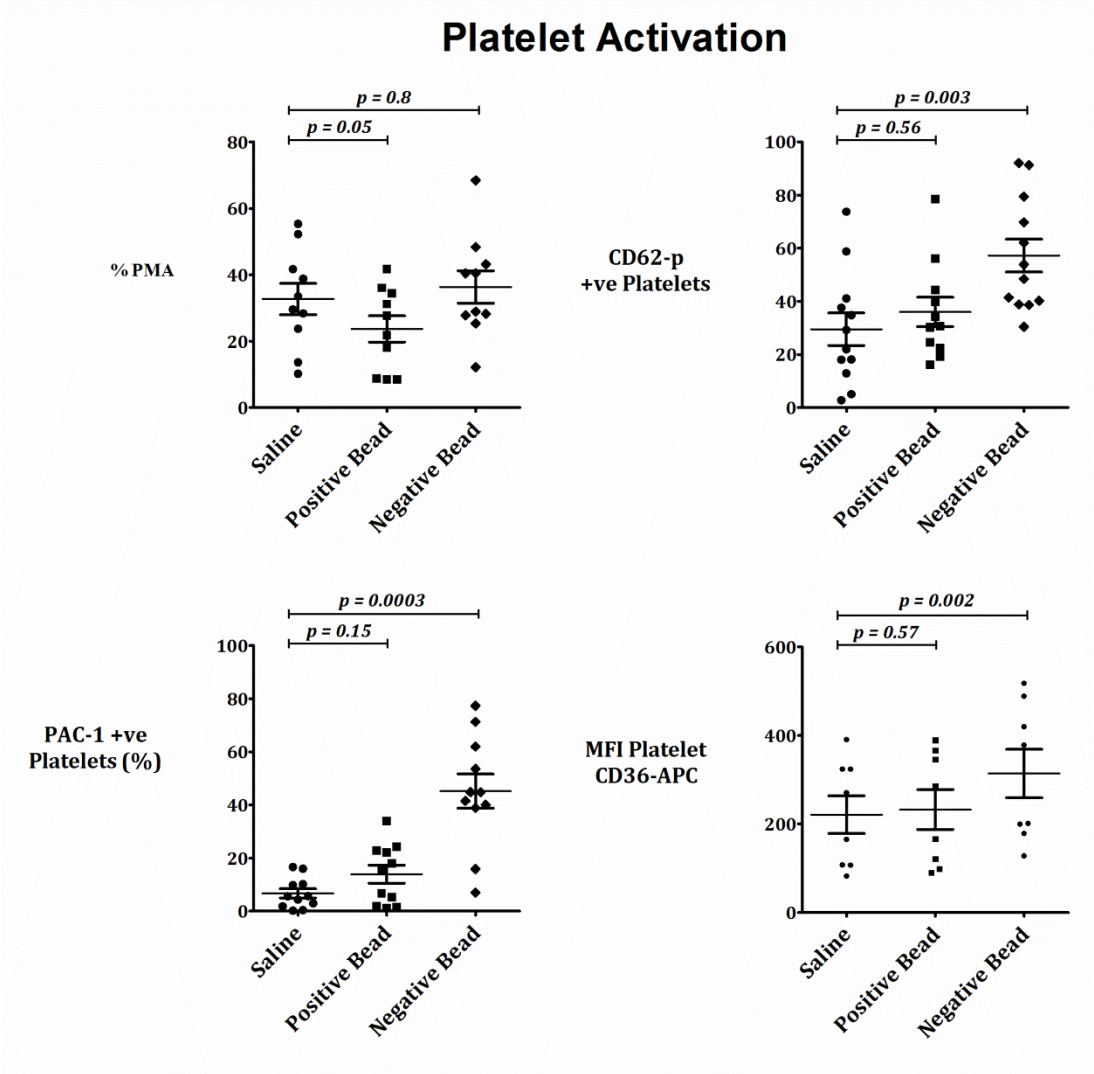

Figure 4-6. Platelet activation markers measured in whole blood sampled from the Badimon chamber after the addition of positively or negatively charged beads. An increase in markers of platelet activation could not be detected after the addition of aminated beads however the carboxylated beads resulted in increases in platelet p-selectin, PAC-1 and CD36. Data represent mean±sem, n=8-12.

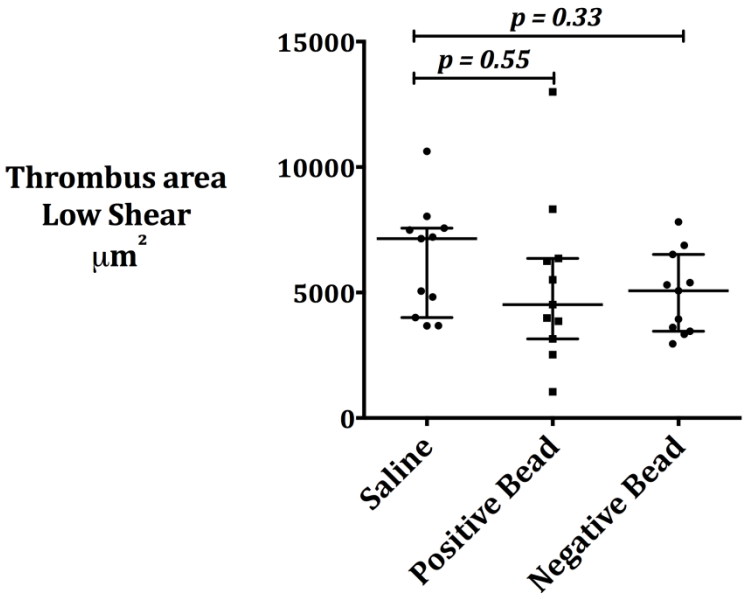

Figure 4-10 Thrombus formation under low shear with the addition of positively or negatively charged polystyrene beads. The low shear chamber is predominantly characterised by macrophage rich thrombus which was not increased by the addition of charged beads. Data represent mean±sem, n=11.

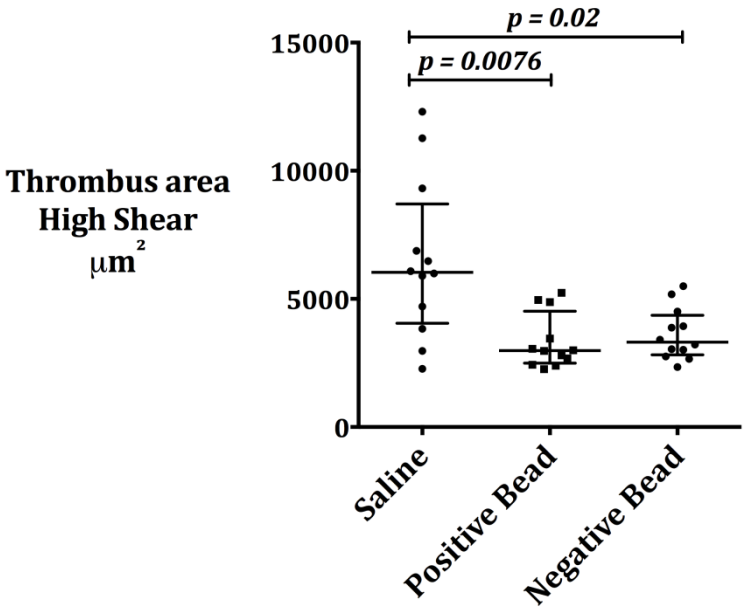

Figure 4-11 Thrombus formation under high shear with the addition of positively or negatively charged latex beads. No increase in thrombus are was observed despite the beads known ability to activate platelets in vitro.Data represent mean ± SEM, n=12.

4.7 *Discussion*

The process of thrombosis is heavily influenced by the local rheological conditions and endothelial integrity. The Badimon chamber has many advantages over other models of thrombosis. It is designed to retain the cylindrical shape typical of vasculature; and is capable of simulating a broad range of flow conditions through altering the flow rate into the chamber as well as allowing both laminar and nonparallel streamline flows. The chamber allows for the addition of a variety of substances, extracorporeally, assessing their effect on thrombus formation in native whole blood. No studies have been carried out to determine the potential for intravenous medical ENPs to exacerbate atherothrombotic disease despite their similarities to CDNPs, now shown to be the most likely mediator of the adverse health effects of air pollution, (Mills, Miller, Lucking, Beveridge, Flint, Boere, Fokkens, Boon, Sandstrom, Blomberg, Duffin, Donaldson, Hadoke, Cassee, & Newby 2011) (Donaldson 2006).

In this study we hypothesised that the Badimon chamber could be used as an ex-vivo model to assess the pro-thrombotic nature of ENPs designed for clinical use, specifically those intended for intravenous injection. Twelve healthy volunteers were recruited and attended the clinical research facility on two separate occasions. On each visit three runs of the Badimon chamber, lasting 5 minutes each, were carried out; 1 saline control run and 2 runs where ENPs were added to the blood before it entered the chamber.

Two separate studies were carried out the first was to determine whether an FDA approved USPION Feraheme® could increase thrombus formation in the Badimon chamber at the physiologically relevant dose of 150µg/mL (Landry, Jacobs, Davis, Shenouda, & Bolton 2005) and as the purpose of the study was to determine the safety profile of the USPIONs we included a dose two fold higher than the final serum concentration but theoretically a dose that could be reached locally at some sites during administration of the bolus (300µg/mL). The second study was to determine a potential mechanism behind the impact of ENPs on thrombus formation. We did this with manufactured latex beads of known size and surface functionalisation.

This study demonstrates that the Badimon chamber could be a useful model to test the thrombogenicity of ENPs designed for medical use. Thrombus was significantly increased under high shear with stress the addition of the higher dose of Feraheme®. However with the charged ENPs, which activated platelets *in vitro* and *ex* vivo, significantly reduced thrombus in the high shear chamber. No increases in inflammatory markers were detected compared to saline control. In order to verify whether or not the addition system was working efficiently whole blood was sampled from the chamber during each USPION/saline run then analysed for iron content using ICPMS. The results indicated an increase in blood iron content consistent with the addition of both the lower and higher dose of Feraheme®. Thus we could be confident that the ENPs were mixing with the blood thoroughly and we were delivering our theorised doses with very little being lost on tubing or in the chambers.

A range of inflammatory cytokines (IL-1ß, IL-12p70, IL-10, IL-6, IL-8 and TNF-α) were analysed in serum sampled from the chamber effluent both before and after addition of the ENPs. There were no increase in the cytokines tested but that is not altogether surprising given the very short (5 minutes) time frame over which the experiment took place. Even some of the most potent inducers of cytokine production e.g. lipopolysaccharide (LPS) can take up to 20 minutes to stimulate measurable increases in TNF-α production from monocyte/macrophage cells (Lacy and Stow 2011).

We observed an increase in thrombus formation in the high shear chambers after the addition of Feraheme® at both at both the lower and higher dose the latter reaching significance. No increases in thrombus were seen in the low shear chamber suggesting any increases seen are most likely due to platelet activation (Lucking, Lundback, Mills, Faratian, Barath, Pourazar, Cassee, Donaldson, Boon, Badimon, Sandstrom, Blomberg, & Newby 2008).

Platelet–monocyte binding is principally dependent on p-selectin but, despite the increase in platelet rich thrombus in the high shear chamber, we did not observe an increase in the platelet surface expression of p-selectin or platelet-monocyte aggregation with either the low or high dose of Feraheme®. There was no increase in platelet surface activated gpIIßIIIα (PAC-1) or platelet surface CD36, which plays a role binding thrombospondin-1 and oxidised LDL cholesterol (Nergiz-Unal et al. 2011). Given the very short amount of time the platelets have to interact with

Feraheme® it is not surprising that there is not widespread platelet activation but rather localised increased thrombus formation in the presence of the extra stimulus of the denuded porcine aorta, suggesting the platelets may be more prone to activation after exposure to the Feraheme® but not directly activated by it. Thrombus formation under flow is a tightly controlled process that takes place in the microenvironment around the vascular wall and plays a role in normal and pathological haemostasis and thrombosis. It is therefore not wholly surprising that there was not an overall increase in platelet activation in chamber effluent.

Charged latex particles were used in the study as we thought they would be good candidates as a positive control for thrombus formation in the chamber as they caused significant platelet activation and aggregation in *in vitro (Chapter 3)* (McGuinnes, Duffin, Brown, Mills, Megson, MacNee, Johnston, Lu, Tran, Li, Wang, Newby, & Donaldson 2011). The negatively charged carboxylated beads caused significant increases in platelet activation (CD62-p, Pac-1, CD36), however this did not translate to an increase in thrombus formation in either the low or high shear chambers. In fact in the high shear chamber there was a significant decrease in thrombus formation with the infusion of both beads. This could be due to the platelets being activated upon contact with the beads before entering the chamber and passing straight through and so no longer prone to further activation by the collagen surface within the chamber resulting in a false reduction in thrombus formation. This is an important factor to take into consideration when using

the chamber; taken at face value the data could be wrongly interpreted as showing that the charged latex beads reduced thrombus formation within the chamber. Any future studies using the Badimon chamber with charged particles should consider using a lower dose of the charged particles.

As a model for testing the pro-thrombotic nature of ENPs the Badimon chamber is a promising technique but does have a number of limitations. This study used only one type of clinical nanoparticle; future studies would need to use a range of ENPs with of varying sizes, compositions and surface functionalisations to further validate it as a suitable technique to determine its usefulness as an *ex-vivo* model for testing the thrombogenicity of ENPs. The very short time the ENPs have to interact with the blood is another limitation of the technique; currently in this model the ENPs mix for a matter of seconds before it enters the chamber and does not fully reflect in *in vivo* situation where these ENPs have been shown to have a blood half-life of 9.3 to 14.5 h (Landry, Jacobs, Davis, Shenouda, & Bolton 2005) so has much more time to interact with platelets and other cells of the circulatory system.

This study showed that an FDA approved drug designed for iron-replacement therapy, but also under investigation as a nanoparticulate contrast agent, can increase thrombus formation in an *ex vivo* model of thrombus formation in healthy volunteers. While the Badimon technique needs further validation the study highlights the need for more thorough testing of ENP- based drugs for intravenous administration to ensure the full range of their potential side

effects and possible clinical consequences are known before being used in patients. ENPs are dealt with by the body differently from traditional drugs and are often retained in the body for a prolonged period of time. Particular care and attention should be paid to ENPs designed to interact with certain cells or those designed for prolonged retention in the circulatory system. Ultimately this study demonstrates that ENPs have unique toxicity profiles often not accommodated by traditional toxicity testing. To ensure the continued and safe use of this technology, more thorough testing of ENPs designed for medical used should be undertaken at the development stages before widespread clinical use.

Chapter 5 *In Vitro* Effects of Engineered Nanoparticles

5.1 *Abstract*

This study was designed to determine whether intra-venous Feraheme® increases thrombus in patients with cardiovascular disease.

Patients with abdominal aortic aneurysms were recruited for a larger study monitoring disease progression with USPIO Feraheme® and MRI scanning. Thrombus formation, coagulation, platelet activation, and inflammatory markers were measured in a cohort of 8 patients both before and 1-hour after administering the Feraheme®. Thrombus formation was measured using the Badimon ex vivo perfusion chamber. Platelet activation was assessed by flow cytometry.

Compared with baseline, Feraheme® infusion increased thrombus formation under high-shear conditions (p=0.03), and caused platelet activation with increased p-selectin (p=0.02) and CD36 (p=0.02). No increase in thrombus under low shear conditions was observed.

Here it is shown for the first time that ENPs delivered directly into the blood may also have adverse prothrombotic effects in patients with cardiovascular

disease the clinical consequences of these findings are unknown but warrant further investigation.

5.2 *Introduction*

5.2.1 **Abdominal Aortic Aneurysms**

Abdominal aortic aneurysms (AAA) frequently occur in patients with atherosclerosis and the two disease processes share several common risk factors. The formation, growth and rupture of aneurysm is now recognised to be the result of a complex interplay between biological and biomechanical factors (Weintraub 2009).

Aneurysm tissue is abdominal aorta that is surgically removed and is characterised by excessive medial neovascularisation, infiltration of inflammatory cells (principally macrophages and B-lymphocytes) and irreversible remodelling of the extracellular matrix. These pathological processes do not affect the aorta uniformly but are focal in nature. Shear wall stress varies spatially within the aneurysm and tensile strength varies in different parts of the aneurysm sac. Focal neovascularisation is present at the site of rupture only and its presence corresponds to the degree of inflammation. These biological ‘hotspots’ represent sites of potential rupture and are potential targets of developing imaging strategies to assess the aneurysmal expansion rates and the risk of rupture (Michel et al. 2011;Nchimi et al. 2010)

Patients with asymptomatic AAA are observed in a surveillance programme involving serial ultrasound measurements of the antero-posterior diameter of the aneurysm. The threshold at which intervention is considered for asymptomatic aneurysms is generally 55 mm reference. Whilst the risk of rupture increases with diameter reference, the absolute diameter of the aneurysm is not the sole determinant of the risk of rupture reference and up to a fifth of ruptured AAA are <55 mm in diameter reference, reference. MRI is emerging as a useful investigation for cardiovascular disease offering high-resolution images without exposure to ionising radiation. In atherosclerotic disease, MRI can distinguish different plaque components including the fibrous cap, the lipid core and areas of calcification (van et al. 2011).

In recent years, advances in magnetic resonance (MR) scanning have led to the development of novel nanoparticulate contrast agents to enhance cardiovascular imaging (Amirbekian, Lipinski, Briley-Saebo, Amirbekian, Aguinaldo, Weinreb, Vucic, Frias, Hyafil, Mani, Fisher, & Fayad 2007a). Ultra-small paramagnetic iron oxide (USPIO) ENPs can be taken up by macrophage in atheroma and detected by MRI imaging in animal models of disease (Sigovan, Boussel, Sulaiman, Sappey-Marinier, Alsaid, sbleds-Mansard, Ibarrola, Gamondes, Corot, Lancelot, Raynaud, Vives, Lacledere, Violas, Douek, & Canet-Soulas 2009).

5.3 *Hypothesis and Aims*

A variety of ENPs are under development for imaging AAA and for the delivery of targeted therapies to the unstable plaque (Yilmaz, Rosch, Klingel, Kandolf, Helluy, Hiller, Jakob, & Sechtem 2011a). As yet there are no published studies addressing whether the direct intravascular infusion of these ENP contrast agents exert adverse effects on platelet or vascular function in patients with underlying cardiovascular disease.

I have previously demonstrated that ENPs increase thrombus and platelet activation *ex vivo* in healthy volunteers therefore:

I hypothesise that ENPs, when delivered systemically will activate platelets and exert a pro-thrombotic effect in susceptible with atherothrombotic disease increasing cardiovascular risk.

5.4 *Methods*

5.4.1 **Study Design**

The study was performed with the approval of local research Ethics Committees, in accordance with the Declaration of Helsinki and the written informed consent of all participants. The study was performed with the approval of local research Ethics Committees, in accordance with the Declaration of Helsinki [REC 05/S1104/26].

5.4.2 **Nanoparticle Panel**

Feraheme® was supplied by Advanced Magnetics, Inc., Cambridge, MA. As supplied, each vial contains 510 mg of elemental iron in 17 mL (30 mg/mL). It was administered via a peripheral venous cannula at a dose of 4 mgFe/kg body weight at a rate of up to 1 mL/sec. This dose had been safely administered before and equates to 8% of total body iron for males and 9.5% for females, or about the same amount of iron as is contained in 1-2 units of blood.

Subjects underwent MRI of the AAA before and 24-36 hours after administration of USPION; Feraheme®. Administration was performed by a

member of the research team or a qualified research nurse, in the Clinical Research Facility at the Royal Infirmary of Edinburgh. Non-invasive physiological monitoring (continuous ECG monitoring, oxygen saturation probe, non-invasive blood pressure, and temperature and nurse observation) was performed during Feraheme® administration.

5.4.3 **Inclusion criteria**

Patients with an AAA >40 mm on ultrasound scanning.

5.4.4 **Exclusion criteria**

Any medical history or clinically relevant abnormality identified on the screening medical examination, vital sign measurement, or clinical laboratory examination.

Subjects with planned AAA surgery.

- Renal impairment with eGFR of <30 mls/min at screening, history of kidney transplant or history of contrast nephropathy.
- Women of childbearing potential without contraception collagen-vascular disease.
- Inability to undergo magnetic resonance or computed tomography scanning.

Contraindication to MRI scanning (as assessed by local MRI safety questionnaire) which includes but not limited to:

- Intracranial aneurysm clips (except Sugita) or other metallic objects,
- History of intra- orbital metal fragments that have not been removed, Pacemakers, implantable cardiac defibrillators and non-MR compatible heart valves,
- Inner ear implants,
- History of claustrophobia in MRI.

5.5 *Inflammation*

Venous blood was drawn at screening and/or during the study to measure biochemical markers of inflammation using a BD™ human inflammatory cytometric bead array (BD Biosciences).

5.6 *Platelet Activation*

Effluent from the chamber was analysed for platelet-monocyte aggregation and platelet activation by flow cytometry including p-selectin, PAC-1 binding and platelet surface CD36.

5.7 *Badimon Study*

AAA patients (n=8) attended on one occasion for a series of Badimon chamber perfusion studies before and after USPION infusion. A 27-guage intravenous cannula was placed in a large antecubital fossa vein. A peristaltic pump drew blood from the antecubital vein through a series of perfusion chambers maintained at 37˚C in a water bath as described in detail in Chapter 4. The primary end point was thrombus area (high and low shear conditions).

5.8 *Statistics*

Statistical analysis of data was performed using GraphPad Prism. Primary and secondary end-points following each infusion will be compared with saline control with data analysed using paired student's t-test. Statistical significance will be taken at $P<0.05$.

5.9 *Results*

Patients were recruited as part of an on-going imaging study [REC 05/S1104/26]. All 8 patients returned for the two visits and reported no adverse effects as a result of the Feraheme®.

5.9.1 **Inflammation**

There were no increases in inflammatory markers 1-hour post Feraheme® administration compared to saline control (Table 5-2).

5.9.2 **Platelet Activation**

Neither platelet-monocyte aggregation nor PAC-1 was increased 1-hour post-Feraheme®. P-selectin, and CD36 however were increased 1-hour post Feraheme® compared to the baseline levels p=0.02 for both indicating systemic platelet activation most likely as a result of the direct administration of Feraheme. The effect of MRI on platelet activation was considered but discounted as there is no literature to date to suggest a magnetic field has any effect on platelet activation (Sagdiyev, 2012).

5.9.3 **Thrombus Formation**

Thrombus formation was increased 1-hour post Feraheme® in the high-shear chamber compared with the baseline pre-Feraheme® values, p=0.03. No such increase were seen in the low-shear chambers suggesting this is a platelet driven effect which correlates well with the increase in platelet activation markers p-selectin and CD36.

Table 5-1 Baseline characteristics of AAA patients which participated in the study. (Data represent mean ± SEM n=8)

	Value
Age	75±1
Weight	75±5
Pulse	65±4
Systolic Pressure	148±5
Diastolic Pressure	80±3

Table 5-2 Inflammatory cytokine detection using cytometric bead array pre- and 1-hour post- Feraheme® administration in AAA patients. Data represent Data represent mean ± SEM n=8

	Before Administration	1hr + administration
IL-12p70	2.2±0.7	1.9±0.6
TNF-α	11.1±0.9	15.25±0.9
IL-10	-	-
IL-6	1.6±0.3	1.3±0.3
IL-1ß	9.95±0.4	7.75±0.7
IL-8	9.35±0.6	8.4±0.5

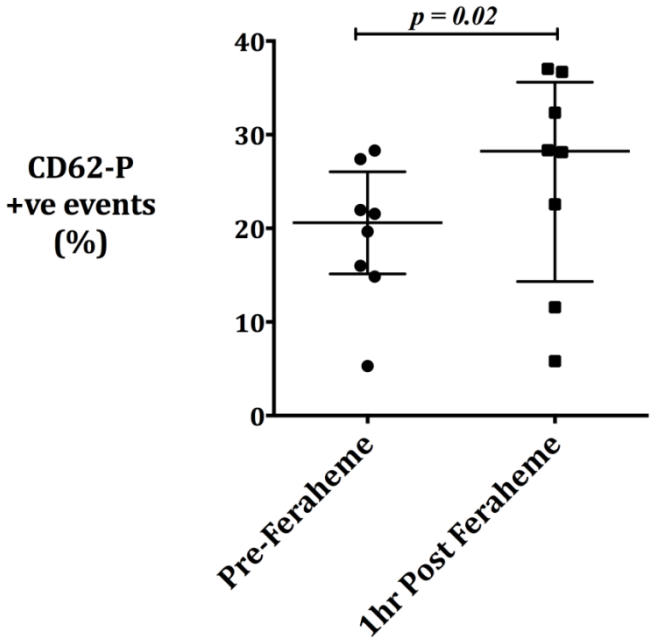

Figure 5-1 Platelet surface p-selectin expression in whole blood sampled from the Badimon chamber pre- and 1-hour post- Feraheme®. Data represent mean ± SEM n=8

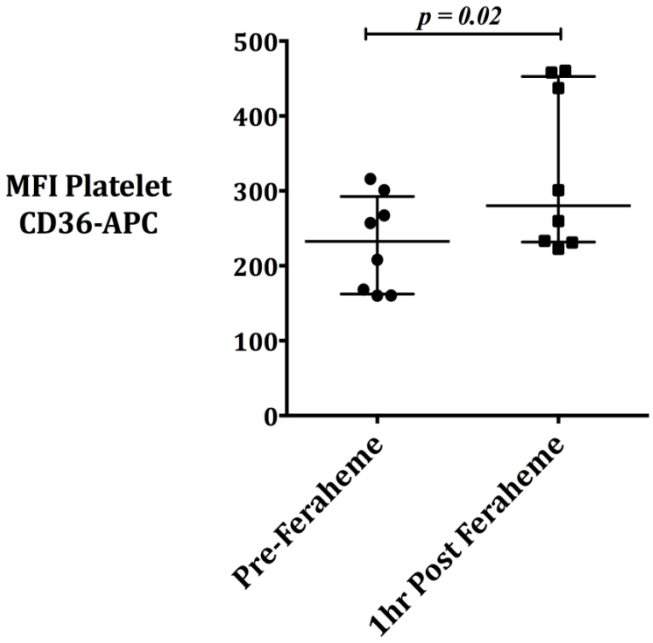

Figure 5-2 Platelet surface CD36 expression in whole blood sampled from the Badimon chamber pre- and 1-hour post- Feraheme® Data represent mean ± SEM n=8

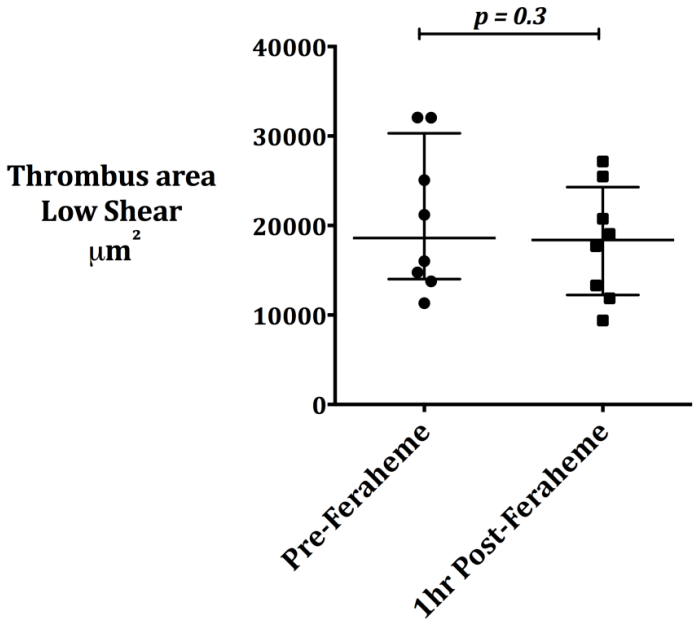

Figure 5-3 Thrombus formation under low shear pre- and 1-hour post-Feraheme®. Data represent mean ± SEM, n=8

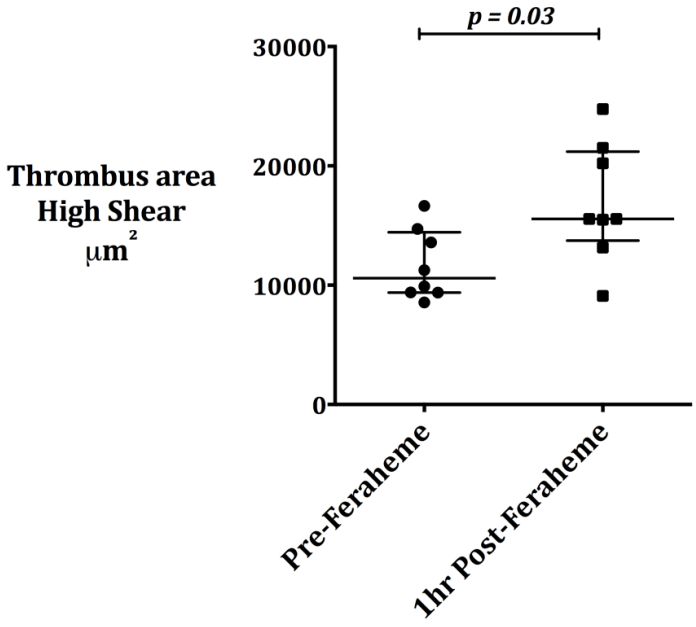

Figure 5-4 Thrombus formation under high shear pre- and 1-hour post-Feraheme® administration in AAA patients. Data represent mean±SEM, n=8.

5.10 *Discussion*

Recently a novel class of MRI contrast agents containing SPIONs have been developed which provide additional biological and functional information through the detection of cellular inflammation within tissues. Ultrasmall SPIO (USPIO), with particle sizes in the range 10-30 nm, escape immediate recognition by the RES and persist in the bloodstream allowing them to be used to assess the accumulation of macrophages within vascular and lymphatic tissues (Richards, Semple, Macgillivray, Gray, Langrish, Williams, Dweck, Wallace, McKillop, Chalmers, Garden, & Newby 2011).

Developing a reproducible in vivo model of thrombosis for use in human studies is challenging. The Badimon chamber is a validated ex vivo model of arterial injury and thrombosis (Badimon et al. 1999). It has previously been used to evaluate the effects of novel antithrombotic regimes (Osende et al. 2001) and exposure to CDNPs (Lucking, Lundback, Mills, Faratian, Barath, Pourazar, Cassee, Donaldson, Boon, Badimon, Sandstrom, Blomberg, & Newby 2008) on thrombosis and has a number of advantages over other techniques.

This is the first in man study to demonstrate that intra-venous infusion of ENPs can cause up-regulation of surface markers of platelet activation 1-

hour post infusion and increased the thrombogenicity of blood in an *ex vivo* model of thrombus formation; the Badimon chamber.

The Badimon chamber has previously been used as an *ex vivo* model of arterial injury and thrombosis after exposure to inhaled dilute diesel exhaust. Here we employed the model to assess the effect of intra-vascular ENPs on thrombosis. Thrombus area was significantly increased under high-shear 1-hour post infusion of Feraheme®. Not only does this correlate well with the high-shear thrombus formation following extra-corporeal addition of Feraheme® to the chamber (Chapter 4) it goes some way to validating the model as a good candidate to take forward to look at new intra-vascular ENP formulations and contrast agents on thrombus formation in man.

The flow cytometric data showed significant increases in platelet surface p-selectin and CD36, 1-hour post infusion, both markers of activation. This correlates well with the increase in platelet-rich thrombus area in the high-shear chamber. The increased time the Feraheme® had to interact with platelets in this study (1-hour) compared to the extracorporeal addition (<30sec) is the most likely explanation for the differences in significance. No increase in platelet-monocyte aggregates or inflammatory markers could be detected 1-hour post infusion.

Previous studies have successfully used the Badimon chamber to investigate the effects of smoking, blood glucose, platelet function, anti-platelet therapy, and exposure to diesel exhaust on thrombosis (Lucking, Lundback, Mills, Faratian, Barath, Pourazar, Cassee, Donaldson, Boon, Badimon, Sandstrom, Blomberg, & Newby 2008)(Badimon, Lettino, Toschi, Fuster, Berrozpe, Chesebro, & Badimon 1999)(Sambola et al. 2003). The results of this study correlate well with previous Badimon studies in susceptible patients. These susceptible populations have increased risk of acute cardiovascular events it is plausible that the effects seen in this study could translate into clinical events when these agents are used more widely.

If the Badimon chamber is to be developed as a tool to model the pro-thrombotic nature of intra-vascular ENP formulations future studies should include longer time-points. The results from this study are promising, demonstrating increased platelet-driven thrombus formation in combination with systemic platelet activation in man but only one relatively short time-point was assessed. The effects seen here could be transient and whether or not it can be related to adverse clinical outcomes is unknown but warrant further investigation.

Chapter 6 **Final Comments**

6.1 *Summary*

ENM are likely to have a big impact on diagnostic assays, medical imaging, and targeted therapeutics in the near future. Characteristics of these ENPs, such as size, surface area, charge and surface chemistry as well as the method by which they are delivered will determine their distribution, efficacy and potential toxicity. ENPs designed for medical use are usually derived from materials deemed biologically safe, but it remains unclear how we define a 'biologically safe' material and in particular what investigations should be mandatory in the development of these materials. Unfortunately the behaviour of ENPs cannot be determined from their bulk properties; when relatively inert or safe materials in their bulk form are presented in the nano-scale they may exert previously unseen harmful effects on cells and systems. If we are to maximise the potential of nanotechnologies in the field of medicine we must ensure that novel nanomaterials are rigorously tested before introduction to the clinic or any other arena where they can enter the body.

The nanotechnology industry has exploded over the past twenty years the graph below demonstrates the number of publications relating to the word ENP on PubMed versus the number of publications mentioning toxicity and ENP.

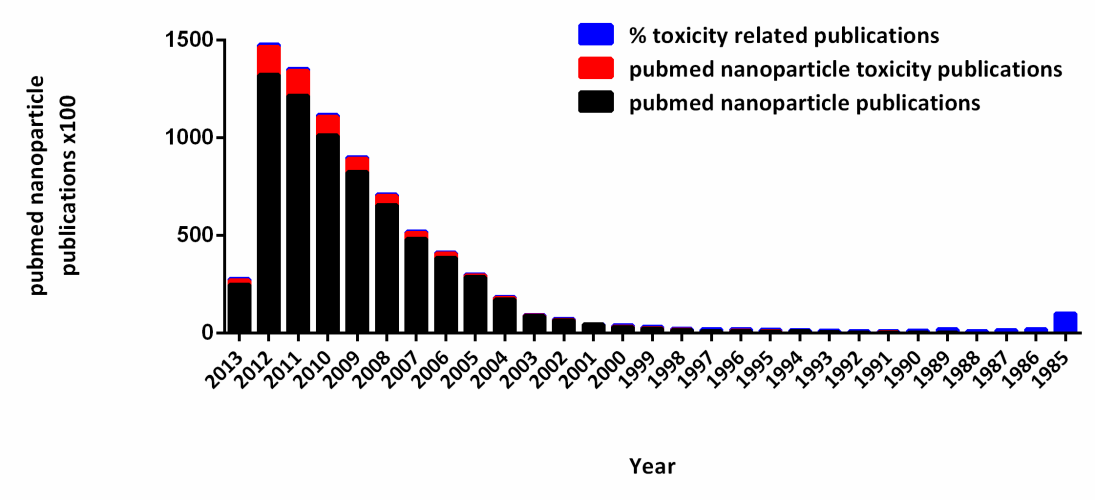

Figure 6-1 Breakdown of ENP Publications in PubMed (20.02.13)

It's obvious that the number of ENP being produced outstrips the rate at which their toxicity is being tested. It has been shown that inhaled ENPs from air pollution are associated with increases in cardiovascular morbidity and mortality with deaths due to ischemia, arrhythmia and heart failure [Brook *et al.*, 2004]. These associations are strongest for fine particulate air pollutants, of which combustion-derived particulate in diesel exhaust is an important component. Whilst the mechanisms responsible for these associations are only partly understood, observational studies suggest that exposure to air pollution may worsen symptoms of angina, exacerbate exercise induced myocardial ischemia, and trigger acute myocardial infarction [Peters *et al.,* 2006]. Currently the thinking is that whilst a certain proportion of these ENPs will translocate across the lung blood barrier the majority will be taken up by phagocytic cells in the lung causing an inflammatory response which in turn can activate the endothelium and trigger an adverse cardiovascular event (Mills, Miller, Lucking, Beveridge, Flint, Boere, Fokkens, Boon, Sandstrom, Blomberg, Duffin, Donaldson, Hadoke, Cassee, & Newby 2011;Shaw,

Robertson, Miller, Duffin, Tabor, Donaldson, Newby, & Hadoke 2011). While most medical ENPs are designed to be introduced into the body intravenously by -passing the lungs and uptake by alveolar macrophages, question have been raised about the safety of introducing huge amounts of ENPs directly into the blood of people with underlying CV disease when CDNP in the lung exacerbates it (Donaldson & Seaton 2007). We hypothesized that ENPs designed for clinical use could activate platelets and have prothrombotic effects when introduced into the blood.

6.2 *In Vitro Effects of Engineered Nanoparticles*

A series of *in vivo* tests were designed to determine how ENPs interacted with platelets and $MDM_{\varnothing}$. Platelets play a key role in thrombosis forming blood clots with fibrin at sites of injury around the body. Any abnormality in the coagulation of blood increases the risk of thrombosis and adverse cardiac events. Flow cytometry was used to measure the surface expression of platelet and leucocyte activation markers as well as platelet–leucocyte aggregates, a technique increasingly recognized as the gold standard measure of in vivo platelet activation, in patients with CV disease (Freedman & Loscalzo 2002). Aminated polystyrene and iron oxide ENPs activated platelets *in vitro* up-regulating platelet surface p-selectin, Pac-1 binding, platelet-monocyte aggregation and platelet-neutrophil aggregation. Confocal microscopy was used to visualise the platelet-monocyte aggregates which

showed the aminated ENPs affiliation for the platelets suggesting the ENPs interact first with the platelets activating them which in turn mediates their binding to monocytes and neutrophils (Barnard, Krueger, Frelinger, III, Furman, & Michelson 2003;Freedman & Loscalzo 2002). The toxicity of aminated or cationic ENPs to platelets has been reported in the literature (Jones et al. 2012a;Jones, Campbell, Franks, Gibson, Thiagarajan, Vieira-de-Abreu, Sukavaneshvar, Mohammad, Li, Ghandehari, Weyrich, Brooks, & Grainger 2012b). Here we demonstrated that cationic ENPs are more potent platelet activators when compared to anionic ENPs which we suggest is mediated by electrostatic interactions between the cationic platelet membranes and anionic amine groups on the ENP surface. These findings underline the need to fully characterise the adverse effects of amine terminated ENPs on platelets and their potential to cause toxicity.

Platelet responsiveness shows marked individual variation with some people displaying high baseline platelet activity including response to agonists (Bray 2007;Natarajan et al. 2008;Yee et al. 2006). This remains an important cardiovascular risk factor. Platelets incubated with various iron oxide ENPs showed significant increases in surface p-selectin and Pac-1 by flow cytometry to submaximal concentrations of known agonist TRAP-6 as well as an increase in calcium influx in response to thrombin. The hyper-reactive state induced was not ENP specific indicating a more global effect and the possibility that exposure of platelets to ENPs share common signalling pathways which make them more reactive to lower doses of agonists.

The use of iron oxide ENPs in clinical imaging has been well documented (Amirbekian et al. 2007b;Schmitz, Winterhalter, Schiffler, Gust, Wagner, Kresse, Coupland, Semmler, & Wolf 2002;Yilmaz, Rosch, Klingel, Kandolf, Helluy, Hiller, Jakob, & Sechtem 2011b) however most research on SPIONs has been dedicated to the synthesis, characterization, and surface properties of ENPs rather than their biological impact.

Whilst iron-oxide ENPs may not be particularly toxic this study demonstrated that depending on their surface functionalisation they could have pro-inflammatory effects. Monocyte derived macrophage cells showed increase ICAM-1 expression as well as IL-8 protein in cell culture supernatants. Both of these have been implicated in the initiation and propagation of atherosclerotic disease mediating endothelial cell dysfunction and cell recruitment (Apostolakis et al. 2009;Galkina and Ley 2007). The unmodified and aminated ENPs had no pro-inflammatory effects on the $_{MDM\emptyset}$ suggesting the carboxylation activated specific pathways on in the cell.

The *in vitro* work carried out demonstrates that ENPs can behave very differently depending on their surface modifications and are not universally toxic or pro-inflammatory across all cell lines but act specifically depending on the functionalisation.

6.3 *Ex-Vivo Effects of Engineered Nanoparticles*

Shear forces generated by flowing blood have significant impact on platelet adhesion and thrombus propagation. Such effects aren't taken into account in many *in vitro* techniques, such as aggregometry. To factor this into our platelet studies we used a parallel flow chamber to carry out experiments under well controlled conditions of time, thrombogenic surface and flow rate.

The objective of this study was to use an established model of *ex-vivo* thrombus formation to determine the pro-thrombotic potential of clinical ENPs. In a double blind randomised cross-over study healthy male volunteers attended the clinical research facility at the Edinburgh Royal Infirmary on two occasions where they underwent three runs of the Badimon chamber at each visit. For the volunteers the study involved no more than a blood donation as at no point were they in contact with the ENPs.

During each run either a control (saline) or ENP formulation was added, extracorporeally, to the blood before it entered the chamber. The addition of the iron-oxide ENP Feraheme® to the chamber (300µg/mL) resulted in a significant increase in the chamber compared to the saline control. The lower dose (150µg/mL) caused an increase in thrombus though this did not reach significance.

In the *in vitro studies* it was demonstrated that exposure of platelets to ENP caused them to become hyper-reactive and more responsive to the agonists TRAP-6 and thrombin. Based on these observations it is likely that the platelets become sensitised or primed upon contact with the Feraheme® ENPs and the subsequent contact with the sub-endothelial matrix, combined with the high shear stress (1680 s^{-1}) in the second and third chambers causes their arrest, adhesion, and thrombus formation.

The latex beads used in the study were selected as they caused *in vitro* increases in platelet activation however when added to the Badimon chamber an overall decrease in thrombus was observed; as expected an increase in markers of platelet activation was observed. Due to the highly agonistic activity of these beads it could be that the platelets are simply activating and forming aggregates before they come in contact with the denuded aorta and passing straight through the chamber.

The Badimon shows potential for use as an *ex vivo* model of thrombus formation with the extra-corporeal addition of ENPs that show little *in vitro* platelet activation but may cause problems *in vivo* where other forces such as blood flow or stenosis come into play.

6.4 *In Vivo Effects of Engineered Nanoparticles*

As a complimentary investigation to the *ex vivo* extracorporeal Feraheme® study patients with AAA were assessed for platelet activation and thrombus formation using the Badimon chamber both before and 1-hour after receiving Feraheme®. At 1-hour post Feraheme® both platelet activation and thrombus area were significantly increased. From pharmacokinetic studies carried out the circulating concentration of Feraheme® 1-hour post infusion has been found to be 150µg/mL (Landry, Jacobs, Davis, Shenouda, & Bolton 2005); this is the lower of the two doses used in the healthy volunteer, extracorporeal study (study 2). Whilst this dose did increase thrombus formation in study 2 it did not reach significance whereas when given *in vivo* to patients with underlying cardiovascular disease, significant increases in *ex vivo* thrombus were seen. This could be due to the underlying cardiovascular disease making the AAA patients inherently more susceptible to the effects of IV ENPs or the fact the ENPs had more time to interact with the blood (1-hour) and activate circulating platelets. Whatever the mechanism it took half the dose of ENPs to cause similar increases in thrombus formation in AAA patients as opposed to healthy volunteers.

Whether or not the platelet activation and thrombus formation seen in this study translate into clinical events or are merely a transient side-effect that clinicians should be aware of is unknown but what is clear is that medical

ENPs need more thorough safety profiling in susceptible populations in particular in patients with atherothrombotic disease.

6.5 *Future Directions*

These studies aimed to resolve a potentially important paradox in medical imaging and therapeutics: CDNPs are toxic to the cardiovascular system even at relatively low concentrations, yet in the quest to enhance cardiovascular imaging the cardiovascular community propose direct intravascular infusion of nanoparticles with similar structural properties at high concentrations in patients with unstable atherothrombotic disease. As this field develops more attention should be given to assay the potential toxicity of novel imaging agents and engineered nanoparticles.

Given their importance in the outcome of cardiovascular disease a reliable method of assessing the effect of ENPs on platelet function could be a good predictor of their activity *in* vivo. Using readily available flowcytometric techniques it was shown that platelet activation could be detected both in vitro, ex vivo and *in vivo and* correlated well with thrombus formation in the Badimon chamber. Flowcytometry could be a useful technique in assessing the pro-thrombotic nature of ENPs before their introduction into the clinic; its fast, reliable and high throughput. It would rapidly determine which ENP

would directly activate platelets and could also be used for more subtle assessments of platelet biology such as response to agonists. The 96-well plate aggregometry could also be very useful as a fast, consistent measure of platelet activation; though not fully explored in this study there is a lot of scope for this technique to be employed in assessing platelet function testing up to 96 parameters in one experiment with very small amounts of blood.

As well as screening ENP formulations before their introduction into the clinic we have a responsibility to monitor patients that have received those already in use more thoroughly and closely than we have been. From the ex-vivo chamber studies it was shown that 1-hour post infusion of Feraheme® patients had increased markers of platelet activation as well as increased thrombus area in the Badimon chamber. Whether or not this is clinically relevant might be difficult to determine with *in vitro* or *ex-vivo* methods, however it should be our responsibility to monitor any adverse events in these patients over the course of their life compared to patients that didn't receive them. No routine post-marketing safety data is collected despite the novel nature of these drugs. The collection of this data would be relatively straightforward and provide a very meaningful method of monitoring the long-term effects of introducing huge numbers of ENPs into patients with underlying inflammatory conditions such as atherothrombotic disease and go a long way to resolving the paradox.

References

Adamkiewicz, G., Ebelt, S., Syring, M., Slater, J., Speizer, F.E., Schwartz, J., Suh, H., & Gold, D.R. 2004. Association between air pollution exposure and exhaled nitric oxide in an elderly population. *Thorax*, 59, (3) 204-209 available from: PM:14985553

Al-Jamal, W.T., Al-Jamal, K.T., Cakebread, A., Halket, J.M., & Kostarelos, K. 2009. Blood circulation and tissue biodistribution of lipid--quantum dot (L-QD) hybrid vesicles intravenously administered in mice. *Bioconjug.Chem.*, 20, (9) 1696-1702 available from: PM:19655725

Allison, G.L., Lowe, G.M., & Rahman, K. 2006. Aged garlic extract and its constituents inhibit platelet aggregation through multiple mechanisms. *J.Nutr.*, 136, (3 Suppl) 782S-788S available from: PM:16484563

Amirbekian, V., Lipinski, M.J., Briley-Saebo, K.C., Amirbekian, S., Aguinaldo, J.G., Weinreb, D.B., Vucic, E., Frias, J.C., Hyafil, F., Mani, V., Fisher, E.A., & Fayad, Z.A. 2007a. Detecting and assessing macrophages in vivo to evaluate atherosclerosis noninvasively using molecular MRI. *Proc.Natl.Acad.Sci.U.S.A*, 104, (3) 961-966 available from: PM:17215360

Antonini, J.M. 2003. Health effects of welding. *Crit Rev.Toxicol.*, 33, (1) 61-103 available from: PM:12585507

Apostolakis, S., Vogiatzi, K., Amanatidou, V., & Spandidos, D.A. 2009. Interleukin 8 and cardiovascular disease. *Cardiovasc.Res.*, 84, (3) 353-360 available from: PM:19617600

Armstrong, P.C., Dhanji, A.R., Truss, N.J., Zain, Z.N., Tucker, A.T., Mitchell, J.A., & Warner, T.D. 2009. Utility of 96-well plate aggregometry and measurement of thrombi adhesion to determine aspirin and clopidogrel effectiveness. *Thromb.Haemost.*, 102, (4) 772-778 available from: PM:19806265

Badimon, J.J., Lettino, M., Toschi, V., Fuster, V., Berrozpe, M., Chesebro, J.H., & Badimon, L. 1999. Local inhibition of tissue factor reduces the thrombogenicity of disrupted human atherosclerotic plaques: effects of tissue factor pathway inhibitor on plaque thrombogenicity under flow conditions. *Circulation*, 99, (14) 1780-1787 available from: PM:10199872

Badimon, L., Padro, T., & Vilahur, G. 2012. Extracorporeal assays of thrombosis. *Methods Mol.Biol.*, 788, 43-57 available from: PM:22130699

Barlow, P.G., Clouter-Baker, A., Donaldson, K., Maccallum, J., & Stone, V. 2005. Carbon black nanoparticles induce type II epithelial cells to release chemotaxins for alveolar macrophages. *Part Fibre.Toxicol.*, 2, 11 available from: PM:16332254

Barnard, M.R., Krueger, L.A., Frelinger, A.L., III, Furman, M.I., & Michelson, A.D. 2003. Whole blood analysis of leukocyte-platelet aggregates. *Curr.Protoc.Cytom.*, Chapter 6, Unit available from: PM:18770779

Beduneau, A., Ma, Z., Grotepas, C.B., Kabanov, A., Rabinow, B.E., Gong, N., Mosley, R.L., Dou, H., Boska, M.D., & Gendelman, H.E. 2009. Facilitated monocyte-macrophage uptake and tissue distribution of superparmagnetic iron-oxide nanoparticles. *PLoS.One.*, 4, (2) e4343 available from: PM:19183814

Behndig, A.F., Mudway, I.S., Brown, J.L., Stenfors, N., Helleday, R., Duggan, S.T., Wilson, S.J., Boman, C., Cassee, F.R., Frew, A.J., Kelly, F.J., Sandstrom, T., & Blomberg, A. 2006. Airway antioxidant and inflammatory responses to diesel exhaust exposure in healthy humans
11. *Eur.Respir.J*, 27, (2) 359-365 available from: PM:16452593

Berry, C.C., Wells, S., Charles, S., & Curtis, A.S. 2003. Dextran and albumin derivatised iron oxide nanoparticles: influence on fibroblasts in vitro. *Biomaterials*, 24, (25) 4551-4557 available from: PM:12950997

Bihari, P., Holzer, M., Praetner, M., Fent, J., Lerchenberger, M., Reichel, C.A., Rehberg, M., Lakatos, S., & Krombach, F. 2010. Single-walled carbon nanotubes activate platelets and accelerate thrombus formation in the microcirculation. *Toxicology*, 269, (2-3) 148-154 available from: PM:19698757

Bray, P.F. 2007. Platelet hyperreactivity: predictive and intrinsic properties. *Hematol.Oncol.Clin.North Am.*, 21, (4) 633-6vi available from: PM:17666282

Briley-Saebo, K.C., Mani, V., Hyafil, F., Cornily, J.C., & Fayad, Z.A. 2008. Fractionated Feridex and positive contrast: in vivo MR imaging of atherosclerosis. *Magn Reson.Med.*, 59, (4) 721-730 available from: PM:18383304

Brook, R.D., Brook, J.R., & Rajagopalan, S. 2003. Air pollution: the "Heart" of the problem. *Curr.Hypertens.Rep.*, 5, (1) 32-39 available from: PM:12530933

Brook, R.D., Brook, J.R., Urch, B., Vincent, R., Rajagopalan, S., & Silverman, F. 2002. Inhalation of fine particulate air pollution and ozone causes acute arterial vasoconstriction in healthy adults. *Circulation*, 105, (13) 1534-1536 available from: PM:11927516

Brown LM, Collings N, Harrison RM, Maynard, A. D., & Maynard RL. Ultrafine particles in the atmosphere
182. 2003. London, Imperial College Press.

Brown, D.M., Dransfield, I., Wetherill, G.Z., & Donaldson, K. 1993. LFA-1 and ICAM-1 in homotypic aggregation of rat alveolar macrophages: organic dust-mediated aggregation by a non-protein kinase C-dependent pathway. *Am.J.Respir.Cell Mol.Biol.*, 9, (2) 205-212 available from: PM:8101715

Buchanan, J.R., Burka, L.T., & Melnick, R.L. 1997. Purpose and guidelines for toxicokinetic studies within the National Toxicology Program. *Environ.Health Perspect.*, 105, (5) 468-471 available from: PM:9222127

Campen, M.J., Lund, A.K., Knuckles, T.L., Conklin, D.J., Bishop, B., Young, D., Seilkop, S., Seagrave, J., Reed, M.D., & McDonald, J.D. 2010. Inhaled diesel emissions alter atherosclerotic plaque composition in ApoE(-/-) mice. *Toxicol.Appl.Pharmacol.*, 242, (3) 310-317 available from: PM:19891982

Castranova, V. 2011. Overview of current toxicological knowledge of engineered nanoparticles. *J.Occup.Environ.Med.*, 53, (6 Suppl) S14-S17 available from: PM:21606847

Cho, W.S., Duffin, R., Thielbeer, F., Bradley, M., Megson, I.L., MacNee, W., Poland, C.A., Tran, C.L., & Donaldson, K. 2012. Zeta potential and solubility to toxic ions as mechanisms of lung inflammation caused by metal/metal oxide nanoparticles. *Toxicological Sciences*, 126, (2) 469-477 available from: PM:22240982

Cormode, D.P., Skajaa, T., Fayad, Z.A., & Mulder, W.J. 2009. Nanotechnology in medical imaging: probe design and applications. *Arterioscler.Thromb.Vasc.Biol.*, 29, (7) 992-1000 available from: PM:19057023

De Jong, W.H., Hagens, W.I., Krystek, P., Burger, M.C., Sips, A.J., & Geertsma, R.E. 2008. Particle size-dependent organ distribution of gold nanoparticles after intravenous administration. *Biomaterials*, 29, (12) 1912-1919 available from: PM:18242692

Delfino, R.J., Sioutas, C., & Malik, S. 2005. Potential role of ultrafine particles in associations between airborne particle mass and cardiovascular health. *Environ Health Perspect.*, 113, (8) 934-946 available from: PM:16079061

Dick, C.A., Brown, D.M., Donaldson, K., & Stone, V. 2003. The role of free radicals in the toxic and inflammatory effects of four different ultrafine particle types. *Inhal.Toxicol.*, 15, (1) 39-52 available from: PM:12476359

Donaldson, K. 2006. Resolving the nanoparticles paradox. *Nanomed.*, 1, (2) 229-234 available from: PM:17716112

Donaldson, K., Brown, D.M., Mitchell, C., Dineva, M., Beswick, P.H., Gilmour, P., & MacNee, W. 1997. Free radical activity of PM10: Iron-mediated generation of hydroxyl radicals. *Environmental Health Perspectives*, 105, 1285-1289

Donaldson, K. & Seaton, A. 2007. The Janus faces of nanoparticles. *J.Nanosci.Nanotechnol.*, 7, (12) 4607-4611 available from: PM:18283852

Donaldson, K., Stone, V., Tran, C.L., Kreyling, W., & Borm, P.J. 2004. Nanotoxicology. *Occup.Environ Med.*, 61, (9) 727-728 available from: PM:15317911

Donaldson, K., Tran, L., Jimenez, L., Duffin, R., Newby, D.E., Mills, N., MacNee, W., & Stone, V. 2005. Combustion-derived nanoparticles: A review of their toxicology following inhalation exposure
1. *Part Fibre Toxicol.*, 2, (1) 10 available from: PM:16242040

Eck, W., Nicholson, A.I., Zentgraf, H., Semmler, W., & Bartling, S. 2010. Anti-CD4-targeted gold nanoparticles induce specific contrast enhancement of peripheral lymph nodes in X-ray computed tomography of live mice. *Nano.Lett.*, 10, (7) 2318-2322 available from: PM:20496900

Eisen, E.A., Costello, S., Chevrier, J., & Picciotto, S. 2011. Epidemiologic challenges for studies of occupational exposure to engineered nanoparticles; a commentary. *J.Occup.Environ.Med.*, 53, (6 Suppl) S57-S61 available from: PM:21654419

faro-Moreno, E., Nawrot, T.S., Nemmar, A., & Nemery, B. 2007. Particulate matter in the environment: pulmonary and cardiovascular effects. *Curr.Opin.Pulm.Med*, 13, (2) 98-106 available from: PM:17255799

Freedman, J.E. & Loscalzo, J. 2002. Platelet-monocyte aggregates: bridging thrombosis and inflammation. *Circulation*, 105, (18) 2130-2132 available from: PM:11994242

Frohlich, E. 2012. The role of surface charge in cellular uptake and cytotoxicity of medical nanoparticles. *Int.J.Nanomedicine.*, 7, 5577-5591 available from: PM:23144561

Fukukura, Y., Kamiyama, T., Takumi, K., Shindo, T., Higashi, R., & Nakajo, M. 2010. Comparison of ferucarbotran-enhanced fluid-attenuated inversion-recovery echo-planar, T2-weighted turbo spin-echo, T2*-weighted gradient-echo, and diffusion-weighted echo-planar imaging for detection of malignant liver lesions. *J.Magn Reson.Imaging*, 31, (3) 607-616 available from: PM:20187203

Galkina, E. & Ley, K. 2007. Vascular adhesion molecules in atherosclerosis. *Arterioscler.Thromb.Vasc.Biol.*, 27, (11) 2292-2301 available from: PM:17673705

Geiser, M., Rothen-Rutishauser, B., Kapp, N., Schurch, S., Kreyling, W., Schulz, H., Semmler, M., Im, H., V, Heyder, J., & Gehr, P. 2005. Ultrafine particles cross cellular membranes by nonphagocytic mechanisms in lungs and in cultured cells. *Environ Health Perspect.*, 113, (11) 1555-1560 available from: PM:16263511

Grove, E.L. 2012. Antiplatelet effect of aspirin in patients with coronary artery disease. *Dan.Med.J.*, 59, (9) B4506 available from: PM:22951204

Gupta, A.K. & Gupta, M. 2005. Synthesis and surface engineering of iron oxide nanoparticles for biomedical applications
169. *Biomaterials*, 26, (18) 3995-4021 available from: PM:15626447

Hamzah, J., Kotamraju, V.R., Seo, J.W., Agemy, L., Fogal, V., Mahakian, L.M., Peters, D., Roth, L., Gagnon, M.K., Ferrara, K.W., & Ruoslahti, E. 2011. Specific penetration and accumulation of a homing peptide within atherosclerotic plaques of apolipoprotein E-deficient mice. *Proc.Natl.Acad.Sci.U.S.A*, 108, (17) 7154-7159 available from: PM:21482787

Harding, S.A., Din, J.N., Sarma, J., Jessop, A., Weatherall, M., Fox, K.A., & Newby, D.E. 2007. Flow cytometric analysis of circulating platelet-monocyte aggregates in whole blood: methodological considerations. *Thromb.Haemost.*, 98, (2) 451-456 available from: PM:17721630

Harisinghani, M.G., Barentsz, J., Hahn, P.F., Deserno, W.M., Tabatabaei, S., van de Kaa, C.H., de la, R.J., & Weissleder, R. 2003. Noninvasive detection of clinically occult lymph-node metastases in prostate cancer. *N.Engl.J.Med.*, 348, (25) 2491-2499 available from: PM:12815134

Harisinghani, M.G., Saini, S., Slater, G.J., Schnall, M.D., & Rifkin, M.D. 1997. MR imaging of pelvic lymph nodes in primary pelvic carcinoma with ultrasmall superparamagnetic iron oxide (Combidex): preliminary observations. *J.Magn Reson.Imaging*, 7, (1) 161-163 available from: PM:9039609

He, X., Nie, H., Wang, K., Tan, W., Wu, X., & Zhang, P. 2008. In vivo study of biodistribution and urinary excretion of surface-modified silica nanoparticles. *Anal.Chem.*, 80, (24) 9597-9603 available from: PM:19007246

Hirn, S., Semmler-Behnke, M., Schleh, C., Wenk, A., Lipka, J., Schaffler, M., Takenaka, S., Moller, W., Schmid, G., Simon, U., & Kreyling, W.G. 2011. Particle size-dependent and surface charge-dependent biodistribution of gold nanoparticles after intravenous administration. *Eur.J.Pharm.Biopharm.*, 77, (3) 407-416 available from: PM:21195759

Inoue, K. & Takano, H. 2010. Another systemic impact of inhaled diesel exhaust particles. *Toxicological Sciences*, 115, (2) 607-608 available from: PM:20194430

Ishii, H., Hayashi, S., Hogg, J.C., Fujii, T., Goto, Y., Sakamoto, N., Mukae, H., Vincent, R., & van EEDEN, S.F. 2005. Alveolar macrophage-epithelial cell interaction following exposure to atmospheric particles induces the release of mediators involved in monocyte mobilization and recruitment. *Respir.Res.*, 6, 87 available from: PM:16053532

Jacobsen, N.R., Moller, P., Jensen, K.A., Vogel, U., Ladefoged, O., Loft, S., & Wallin, H. 2009. Lung inflammation and genotoxicity following pulmonary exposure to nanoparticles in ApoE-/- mice. *Part Fibre.Toxicol.*, 6, 2 available from: PM:19138394

Jaffer, F.A., Nahrendorf, M., Sosnovik, D., Kelly, K.A., Aikawa, E., & Weissleder, R. 2006a. Cellular imaging of inflammation in atherosclerosis using magnetofluorescent nanomaterials. *Mol.Imaging*, 5, (2) 85-92 available from: PM:16954022

Jaffer, F.A., Sosnovik, D.E., Nahrendorf, M., & Weissleder, R. 2006b. Molecular imaging of myocardial infarction. *J.Mol.Cell Cardiol.*, 41, (6) 921-933 available from: PM:17067633

Jayagopal, A., Russ, P.K., & Haselton, F.R. 2007. Surface engineering of quantum dots for in vivo vascular imaging. *Bioconjug.Chem.*, 18, (5) 1424-1433 available from: PM:17760416

Jendelova, P., Herynek, V., Urdzikova, L., Glogarova, K., Kroupova, J., Andersson, B., Bryja, V., Burian, M., Hajek, M., & Sykova, E. 2004. Magnetic resonance tracking of transplanted bone marrow and embryonic stem cells labeled by iron oxide nanoparticles in rat brain and spinal cord
112. *J Neurosci.Res.*, 76, (2) 232-243 available from: PM:15048921

Jin, S.E. & Kim, C.K. 2012. Long-term stable cationic solid lipid nanoparticles for the enhanced intracellular delivery of SMAD3 antisense oligonucleotides in activated murine macrophages. *J.Pharm.Pharm.Sci.*, 15, (3) 467-482 available from: PM:22974792

Jing, X.H., Yang, L., Duan, X.J., Xie, B., Chen, W., Li, Z., & Tan, H.B. 2008. In vivo MR imaging tracking of magnetic iron oxide nanoparticle labeled, engineered, autologous bone marrow mesenchymal stem cells following intra-articular injection. *Joint Bone Spine*, 75, (4) 432-438 available from: PM:18448377

Jones, C.F., Campbell, R.A., Brooks, A.E., Assemi, S., Tadjiki, S., Thiagarajan, G., Mulcock, C., Weyrich, A.S., Brooks, B.D., Ghandehari, H., & Grainger, D.W. 2012a. Cationic PAMAM dendrimers aggressively initiate blood clot formation. *ACS Nano.*, 6, (11) 9900-9910 available from: PM:23062017

Jones, C.F., Campbell, R.A., Franks, Z., Gibson, C.C., Thiagarajan, G., Vieira-de-Abreu, A., Sukavaneshvar, S., Mohammad, S.F., Li, D.Y., Ghandehari, H., Weyrich, A.S., Brooks, B.D., & Grainger, D.W. 2012b. Cationic PAMAM dendrimers disrupt key platelet functions. *Mol.Pharm.*, 9, (6) 1599-1611 available from: PM:22497592

Kim, B.Y., Rutka, J.T., & Chan, W.C. 2010. Nanomedicine. *N.Engl.J.Med.*, 363, (25) 2434-2443 available from: PM:21158659

Kim, D., Yu, M.K., Lee, T.S., Park, J.J., Jeong, Y.Y., & Jon, S. 2011. Amphiphilic polymer-coated hybrid nanoparticles as CT/MRI dual contrast agents. *Nanotechnology.*, 22, (15) 155101 available from: PM:21389582

Klug, G., Bauer, L., & Bauer, W.R. 2008. Patterns of USPIO deposition in murine atherosclerosis. *Arterioscler.Thromb.Vasc.Biol.*, 28, (9) E157-E159 available from: PM:18716317

Klug, K., Gert, G., Thomas, K., Christan, Z., Marco, P., Elisabeth, B., Volker, H., Rommel, R., Eberhard, E., Peter, J.M., & Wolfgang, B.R. 2009. Murine atherosclerotic plaque imaging with the USPIO Ferumoxtran-10. *Front Biosci.*, 14, 2546-2552 available from: PM:19273218

Kooi, M.E., Cappendijk, V.C., Cleutjens, K.B., Kessels, A.G., Kitslaar, P.J., Borgers, M., Frederik, P.M., Daemen, M.J., & van Engelshoven, J.M. 2003a. Accumulation of ultrasmall superparamagnetic particles of iron oxide in human atherosclerotic plaques can be detected by in vivo magnetic resonance imaging
2. *Circulation*, 107, (19) 2453-2458 available from: PM:12719280

Krombach, G.A., Wendland, M.F., Higgins, C.B., & Saeed, M. 2002a. MR imaging of spatial extent of microvascular injury in reperfused ischemically injured rat myocardium: value of blood pool ultrasmall superparamagnetic particles of iron oxide. *Radiology*, 225, (2) 479-486 available from: PM:12409583

Kubik, M.M. & Richardson, S.G. 1987. A serial study of platelet reactivity throughout the first six months after myocardial infarction: its modification by sulphinpyrazone. *Postgrad.Med.J.*, 63, (739) 351-356 available from: PM:3118351

Lacy, P. & Stow, J.L. 2011. Cytokine release from innate immune cells: association with diverse membrane trafficking pathways. *Blood*, 118, (1) 9-18 available from: PM:21562044

Lamanna, G., Kueny-Stotz, M., Mamlouk-Chaouachi, H., Ghobril, C., Basly, B., Bertin, A., Miladi, I., Billotey, C., Pourroy, G., Begin-Colin, S., & Felder-Flesch, D. 2011. Dendronized iron oxide nanoparticles for multimodal imaging. *Biomaterials*, 32, (33) 8562-8573 available from: PM:21864894

Landry, R., Jacobs, P.M., Davis, R., Shenouda, M., & Bolton, W.K. 2005. Pharmacokinetic study of ferumoxytol: a new iron replacement therapy in normal subjects and hemodialysis patients. *Am.J.Nephrol.*, 25, (4) 400-410 available from: PM:16088081

Langrish, J.P., Mills, N.L., & Newby, D.E. 2008. Air pollution: the new cardiovascular risk factor. *Intern.Med.J.*, 38, (12) 875-878 available from: PM:19120545

Lewinski, N., Colvin, V., & Drezek, R. 2008. Cytotoxicity of nanoparticles. *Small*, 4, (1) 26-49 available from: PM:18165959

Li, S.D. & Huang, L. 2008. Pharmacokinetics and biodistribution of nanoparticles. *Mol.Pharm.*, 5, (4) 496-504 available from: PM:18611037

Li, X.Y., Gilmour, P.S., Donaldson, K., & MacNee, W. 1997. In vivo and in vitro proinflammatory effects of particulate air pollution (PM10). *Environ.Health Perspect.*, 105 Suppl 5, 1279-1283 available from: PM:0009400738

Libby, P., Ridker, P.M., & Hansson, G.K. 2011. Progress and challenges in translating the biology of atherosclerosis. *Nature*, 473, (7347) 317-325 available from: PM:21593864

Libby, P., Ridker, P.M., & Maseri, A. 2002. Inflammation and atherosclerosis 79. *Circulation*, 105, (9) 1135-1143 available from: PM:11877368

Linkov, I., Satterstrom, F.K., & Corey, L.M. 2008. Nanotoxicology and nanomedicine: making hard decisions. *Nanomedicine.*, 4, (2) 167-171 available from: PM:18329962

Lodhia, J., Mandarano, G., Ferris, N., Eu, P., & Cowell, S. 2010a. Development and use of iron oxide nanoparticles (Part 1): Synthesis of iron oxide nanoparticles for MRI. *Biomed.Imaging Interv.J.*, 6, (2) e12 available from: PM:21611034

Lodhia, J., Mandarano, G., Ferris, N., Eu, P., & Cowell, S. 2010b. Development and use of iron oxide nanoparticles (Part 1): Synthesis of iron oxide nanoparticles for MRI. *Biomed.Imaging Interv.J.*, 6, (2) e12 available from: PM:21611034

Lu, S., Duffin, R., Poland, C., Daly, P., Murphy, F., Drost, E., MacNee, W., Stone, V., & Donaldson, K. 2009. Efficacy of simple short-term in vitro assays for predicting the potential of metal oxide nanoparticles to cause pulmonary inflammation. *Environ Health Perspect.*, 117, (2) 241-247 available from: PM:19270794

Lucking, A.J., Lundback, M., Mills, N.L., Faratian, D., Barath, S.L., Pourazar, J., Cassee, F.R., Donaldson, K., Boon, N.A., Badimon, J.J., Sandstrom, T., Blomberg, A., & Newby, D.E. 2008. Diesel exhaust inhalation increases thrombus formation in man. *Eur.Heart J.*, 29, (24) 3043-3051 available from: PM:18952612

Lundback, M., Mills, N.L., Lucking, A., Barath, S., Donaldson, K., Newby, D.E., Sandstrom, T., & Blomberg, A. 2009. Experimental exposure to diesel exhaust increases arterial stiffness in man. *Part Fibre.Toxicol.*, 6, 7 available from: PM:19284640

Mahmoudi, M., Sant, S., Wang, B., Laurent, S., & Sen, T. 2011a. Superparamagnetic iron oxide nanoparticles (SPIONs): development, surface modification and

applications in chemotherapy. *Adv.Drug Deliv.Rev.*, 63, (1-2) 24-46 available from: PM:20685224

Maity, D., Zoppellaro, G., Sedenkova, V., Tucek, J., Safarova, K., Polakova, K., Tomankova, K., Diwoky, C., Stollberger, R., Machala, L., & Zboril, R. 2012. Surface design of core-shell superparamagnetic iron oxide nanoparticles drives record relaxivity values in functional MRI contrast agents. *Chem.Commun.(Camb.)*, 48, (93) 11398-11400 available from: PM:23066527

McCarthy, J.R., Korngold, E., Weissleder, R., & Jaffer, F.A. 2010. A light-activated theranostic nanoagent for targeted macrophage ablation in inflammatory atherosclerosis. *Small*, 6, (18) 2041-2049 available from: PM:20721949

McGuinnes, C., Duffin, R., Brown, S., Mills, L., Megson, I.L., MacNee, W., Johnston, S., Lu, S.L., Tran, L., Li, R., Wang, X., Newby, D.E., & Donaldson, K. 2011. Surface derivatization state of polystyrene latex nanoparticles determines both their potency and their mechanism of causing human platelet aggregation in vitro. *Toxicological Sciences*, 119, (2) 359-368 available from: PM:21123846

Michalska, M., Machtoub, L., Manthey, H.D., Bauer, E., Herold, V., Krohne, G., Lykowsky, G., Hildenbrand, M., Kampf, T., Jakob, P., Zernecke, A., & Bauer, W.R. 2012. Visualization of vascular inflammation in the atherosclerotic mouse by ultrasmall superparamagnetic iron oxide vascular cell adhesion molecule-1-specific nanoparticles. *Arterioscler.Thromb.Vasc.Biol.*, 32, (10) 2350-2357 available from: PM:22879583

Michel, J.B., Martin-Ventura, J.L., Egido, J., Sakalihasan, N., Treska, V., Lindholt, J., Allaire, E., Thorsteinsdottir, U., Cockerill, G., & Swedenborg, J. 2011. Novel aspects of the pathogenesis of aneurysms of the abdominal aorta in humans. *Cardiovasc.Res.*, 90, (1) 18-27 available from: PM:21037321

Michelson, A.D., Barnard, M.R., Hechtman, H.B., MacGregor, H., Connolly, R.J., Loscalzo, J., & Valeri, C.R. 1996. In vivo tracking of platelets: circulating degranulated platelets rapidly lose surface P-selectin but continue to circulate and function. *Proc.Natl.Acad.Sci.U.S.A*, 93, (21) 11877-11882 available from: PM:8876231

Miller, M.R., Borthwick, S.J., Shaw, C.A., McLean, S.G., McClure, D., Mills, N.L., Duffin, R., Donaldson, K., Megson, I.L., Hadoke, P.W., & Newby, D.E. 2009a. Direct impairment of vascular function by diesel exhaust particulate through reduced bioavailability of endothelium-derived nitric oxide induced by superoxide free radicals. *Environ Health Perspect.*, 117, (4) 611-616 available from: PM:19440501

Miller, V.M., Hunter, L.W., Chu, K., Kaul, V., Squillace, P.D., Lieske, J.C., & Jayachandran, M. 2009b. Biologic nanoparticles and platelet reactivity. *Nanomedicine.(Lond)*, 4, (7) 725-733 available from: PM:19839809

Mills, N.L., Donaldson, K., Hadoke, P.W., Boon, N.A., MacNee, W., Cassee, F.R., Sandstrom, T., Blomberg, A., & Newby, D.E. 2008a. Adverse cardiovascular effects of air pollution. *Nat.Clin.Pract.Cardiovasc.Med.* available from: PM:19029991

Mills, N.L., Miller, J.J., Anand, A., Robinson, S.D., Frazer, G.A., Anderson, D., Breen, L., Wilkinson, I.B., McEniery, C.M., Donaldson, K., Newby, D.E., & MacNee, W. 2007a. Increased arterial stiffness in patients with chronic obstructive pulmonary disease; a mechanism for increased cardiovascular risk. *Thorax* available from: PM:18024535

Mills, N.L., Miller, M.R., Lucking, A.J., Beveridge, J., Flint, L., Boere, A.J., Fokkens, P.H., Boon, N.A., Sandstrom, T., Blomberg, A., Duffin, R., Donaldson, K., Hadoke, P.W., Cassee, F.R., & Newby, D.E. 2011. Combustion-derived nanoparticulate induces the adverse vascular effects of diesel exhaust inhalation. *Eur.Heart J.* available from: PM:21753226

Mills, N.L., Robinson, S.D., Fokkens, P.H., Leseman, D.L., Miller, M.R., Anderson, D., Freney, E.J., Heal, M.R., Donovan, R.J., Blomberg, A., Sandstrom, T., MacNee, W., Boon, N.A., Donaldson, K., Newby, D.E., & Cassee, F.R. 2008b. Exposure to concentrated ambient particles does not affect vascular function in patients with coronary heart disease. *Environ Health Perspect.*, 116, (6) 709-715 available from: PM:18560524

Mills, N.L., Tornqvist, H., Gonzalez, M.C., Vink, E., Robinson, S.D., Soderberg, S., Boon, N.A., Donaldson, K., Sandstrom, T., Blomberg, A., & Newby, D.E. 2007b. Ischemic and thrombotic effects of dilute diesel-exhaust inhalation in men with coronary heart disease. *N.Engl.J.Med.*, 357, (11) 1075-1082 available from: PM:17855668

Mills, N.L., Tornqvist, H., Robinson, S.D., Gonzalez, M., Darnley, K., MacNee, W., Boon, N.A., Donaldson, K., Blomberg, A., Sandstrom, T., & Newby, D.E. 2005. Diesel exhaust inhalation causes vascular dysfunction and impaired endogenous fibrinolysis. *Circulation*, 112, (25) 3930-3936 available from: PM:16365212

Moller, P., Mikkelsen, L., Vesterdal, L.K., Folkmann, J.K., Forchhammer, L., Roursgaard, M., Danielsen, P.H., & Loft, S. 2011a. Hazard identification of particulate matter on vasomotor dysfunction and progression of atherosclerosis. *Crit Rev.Toxicol.*, 41, (4) 339-368 available from: PM:21345153

Moller, W., Brown, D.M., Kreyling, W.G., & Stone, V. 2005. Ultrafine particles cause cytoskeletal dysfunctions in macrophages: role of intracellular calcium. *Part Fibre.Toxicol.*, 2, 7 available from: PM:16202162

Morishige, K., Kacher, D.F., Libby, P., Josephson, L., Ganz, P., Weissleder, R., & Aikawa, M. 2010. High-resolution magnetic resonance imaging enhanced with

superparamagnetic nanoparticles measures macrophage burden in atherosclerosis. *Circulation*, 122, (17) 1707-1715 available from: PM:20937980

Mulder, W.J., Strijkers, G.J., Briley-Saboe, K.C., Frias, J.C., Aguinaldo, J.G., Vucic, E., Amirbekian, V., Tang, C., Chin, P.T., Nicolay, K., & Fayad, Z.A. 2007. Molecular imaging of macrophages in atherosclerotic plaques using bimodal PEG-micelles. *Magn Reson.Med.*, 58, (6) 1164-1170 available from: PM:18046703

Nahrendorf, M., Sosnovik, D.E., French, B.A., Swirski, F.K., Bengel, F., Sadeghi, M.M., Lindner, J.R., Wu, J.C., Kraitchman, D.L., Fayad, Z.A., & Sinusas, A.J. 2009a. Multimodality cardiovascular molecular imaging, Part II. *Circ.Cardiovasc.Imaging*, 2, (1) 56-70 available from: PM:19808565

Nahrendorf, M., Zhang, H., Hembrador, S., Panizzi, P., Sosnovik, D.E., Aikawa, E., Libby, P., Swirski, F.K., & Weissleder, R. 2008. Nanoparticle PET-CT imaging of macrophages in inflammatory atherosclerosis. *Circulation*, 117, (3) 379-387 available from: PM:18158358

Natarajan, A., Zaman, A.G., & Marshall, S.M. 2008. Platelet hyperactivity in type 2 diabetes: role of antiplatelet agents. *Diab.Vasc.Dis.Res.*, 5, (2) 138-144 available from: PM:18537103

Nchimi, A., Defawe, O., Brisbois, D., Broussaud, T.K., Defraigne, J.O., Magotteaux, P., Massart, B., Serfaty, J.M., Houard, X., Michel, J.B., & Sakalihasan, N. 2010. MR imaging of iron phagocytosis in intraluminal thrombi of abdominal aortic aneurysms in humans. *Radiology*, 254, (3) 973-981 available from: PM:20177108

Nergiz-Unal, R., Lamers, M.M., Van, K.R., Luiken, J.J., Cosemans, J.M., Glatz, J.F., Kuijpers, M.J., & Heemskerk, J.W. 2011. Signaling role of CD36 in platelet activation and thrombus formation on immobilized thrombospondin or oxidized low-density lipoprotein. *J.Thromb.Haemost.*, 9, (9) 1835-1846 available from: PM:21696539

Neun, B.W. & Dobrovolskaia, M.A. 2011. Method for in vitro analysis of nanoparticle thrombogenic properties. *Methods Mol.Biol.*, 697, 225-235 available from: PM:21116972

Osende, J.I., Fuster, V., Lev, E.I., Shimbo, D., Rauch, U., Marmur, J.D., Richard, M., Varon, D., & Badimon, J.J. 2001. Testing platelet activation with a shear-dependent platelet function test versus aggregation-based tests: relevance for monitoring long-term glycoprotein IIb/IIIa inhibition. *Circulation*, 103, (11) 1488-1491 available from: PM:11257073

Passacquale, G., Vamadevan, P., Pereira, L., Hamid, C., Corrigall, V., & Ferro, A. 2011. Monocyte-platelet interaction induces a pro-inflammatory phenotype in circulating monocytes. *PLoS.One.*, 6, (10) e25595 available from: PM:22022418

Peters, A., von, K.S., Heier, M., Trentinaglia, I., Hormann, A., Wichmann, H.E., & Lowel, H. 2004. Exposure to traffic and the onset of myocardial infarction. *N.Engl.J.Med.*, 351, (17) 1721-1730 available from: PM:15496621

Porter, M., Karp, M., Killedar, S., Bauer, S.M., Guo, J., Williams, D., Breysse, P., Georas, S.N., & Williams, M.A. 2007. Diesel-enriched particulate matter functionally activates human dendritic cells. *Am.J.Respir.Cell Mol.Biol.*, 37, (6) 706-719 available from: PM:17630318

Radomski, A., Jurasz, P., onso-Escolano, D., Drews, M., Morandi, M., Malinski, T., & Radomski, M.W. 2005. Nanoparticle-induced platelet aggregation and vascular thrombosis
3. *Br.J Pharmacol.*, 146, (6) 882-893 available from: PM:16158070

Rehberg, M., Leite, C.F., Mildner, K., Horstkotte, J., Zeuschner, D., & Krombach, F. 2012a. Surface chemistry of quantum dots determines their behavior in postischemic tissue. *ACS Nano.*, 6, (2) 1370-1379 available from: PM:22243127 Rehberg, M., Praetner, M., Leite, C.F., Reichel, C.A., Bihari, P., Mildner, K., Duhr, S., Zeuschner, D., & Krombach, F. 2010. Quantum dots modulate leukocyte adhesion and transmigration depending on their surface modification. *Nano.Lett.*, 10, (9) 3656-3664 available from: PM:20695477

Renshaw, P.F., Owen, C.S., McLaughlin, A.C., Frey, T.G., & Leigh, J.S., Jr. 1986. Ferromagnetic contrast agents: a new approach. *Magn Reson.Med.*, 3, (2) 217-225 available from: PM:3713487

Renwick, L.C., Brown, D., Clouter, A., & Donaldson, K. 2004. Increased inflammation and altered macrophage chemotactic responses caused by two ultrafine particle types. *Occup.Environ Med.*, 61, (5) 442-447 available from: PM:15090666

Richards, J.M., Semple, S.I., Macgillivray, T.J., Gray, C., Langrish, J.P., Williams, M., Dweck, M., Wallace, W., McKillop, G., Chalmers, R.T., Garden, O.J., & Newby, D.E. 2011. Abdominal aortic aneurysm growth predicted by uptake of ultrasmall superparamagnetic particles of iron oxide: a pilot study. *Circ.Cardiovasc.Imaging*, 4, (3) 274-281 available from: PM:21304070

Rosner, M.H. & Auerbach, M. 2011a. Ferumoxytol for the treatment of iron deficiency. *Expert.Rev.Hematol.*, 4, (4) 399-406 available from: PM:21801130

Ruehm, S.G., Goyen, M., Barkhausen, J., Kroger, K., Bosk, S., Ladd, M.E., & Debatin, J.F. 2001a. Rapid magnetic resonance angiography for detection of atherosclerosis
82. *Lancet*, 357, (9262) 1086-1091 available from: PM:11297960

Sambola, A., Osende, J., Hathcock, J., Degen, M., Nemerson, Y., Fuster, V., Crandall, J., & Badimon, J.J. 2003. Role of risk factors in the modulation of tissue factor

activity and blood thrombogenicity. *Circulation*, 107, (7) 973-977 available from: PM:12600909

Sanz, J. & Fayad, Z.A. 2008. Imaging of atherosclerotic cardiovascular disease. *Nature*, 451, (7181) 953-957 available from: PM:18288186

Schladt, T.D., Schneider, K., Schild, H., & Tremel, W. 2011. Synthesis and bio-functionalization of magnetic nanoparticles for medical diagnosis and treatment. *Dalton Trans.* available from: PM:21359397

Schmitz, S.A., Taupitz, M., Wagner, S., Wolf, K.J., Beyersdorff, D., & Hamm, B. 2001a. Magnetic resonance imaging of atherosclerotic plaques using superparamagnetic iron oxide particles. *J.Magn Reson.Imaging*, 14, (4) 355-361 available from: PM:11599058

Schmitz, S.A., Winterhalter, S., Schiffler, S., Gust, R., Wagner, S., Kresse, M., Coupland, S.E., Semmler, W., & Wolf, K.J. 2001b. USPIO-enhanced direct MR imaging of thrombus: preclinical evaluation in rabbits. *Radiology*, 221, (1) 237-243 available from: PM:11568346

Schmitz, S.A., Winterhalter, S., Schiffler, S., Gust, R., Wagner, S., Kresse, M., Coupland, S.E., Semmler, W., & Wolf, K.J. 2002. USPIO-enhanced direct thrombus MRI. *Acad.Radiol.*, 9 Suppl 2, S339-S340 available from: PM:12188268

Semmler-Behnke, M., Kreyling, W.G., Lipka, J., Fertsch, S., Wenk, A., Takenaka, S., Schmid, G., & Brandau, W. 2008. Biodistribution of 1.4- and 18-nm gold particles in rats. *Small*, 4, (12) 2108-2111 available from: PM:19031432

Shaw, C.A., Robertson, S., Miller, M.R., Duffin, R., Tabor, C.M., Donaldson, K., Newby, D.E., & Hadoke, P.W. 2011. Diesel exhaust particulate-exposed macrophages cause marked endothelial cell activation. *Am.J.Respir.Cell Mol.Biol.*, 44, (6) 840-851 available from: PM:20693402

Shaw, S. & Murthy, P.V. 2010. Magnetic targeting in the impermeable microvessel with two-phase fluid model--non-Newtonian characteristics of blood. *Microvasc.Res.*, 80, (2) 209-220 available from: PM:20478317

Sigovan, M., Boussel, L., Sulaiman, A., Sappey-Marinier, D., Alsaid, H., sbleds-Mansard, C., Ibarrola, D., Gamondes, D., Corot, C., Lancelot, E., Raynaud, J.S., Vives, V., Lacledere, C., Violas, X., Douek, P.C., & Canet-Soulas, E. 2009. Rapid-clearance iron nanoparticles for inflammation imaging of atherosclerotic plaque: initial experience in animal model. *Radiology*, 252, (2) 401-409 available from: PM:19703881

Slevin, M., Wang, Q., Font, M.A., Luque, A., Juan-Babot, O., Gaffney, J., Kumar, P., Kumar, S., Badimon, L., & Krupinski, J. 2008. Atherothrombosis and plaque

heterology: different location or a unique disease? *Pathobiology*, 75, (4) 209-225 available from: PM:18580067

Song, S., Qin, Y., He, Y., Huang, Q., Fan, C., & Chen, H.Y. 2010. Functional nanoprobes for ultrasensitive detection of biomolecules. *Chem.Soc.Rev.*, 39, (11) 4234-4243 available from: PM:20871878

Sosnovik, D.E., Nahrendorf, M., & Weissleder, R. 2008. Magnetic nanoparticles for MR imaging: agents, techniques and cardiovascular applications. *Basic Res.Cardiol.*, 103, (2) 122-130 available from: PM:18324368

Stark, D.D., Moseley, M.E., Bacon, B.R., Moss, A.A., Goldberg, H.I., Bass, N.M., & James, T.L. 1985. Magnetic resonance imaging and spectroscopy of hepatic iron overload. *Radiology*, 154, (1) 137-142 available from: PM:3964933

Stone, V., Johnston, H., & Clift, M.J. 2007. Air pollution, ultrafine and nanoparticle toxicology: cellular and molecular interactions. *IEEE Trans.Nanobioscience.*, 6, (4) 331-340 available from: PM:18217626

Sun, J., Wang, S., Zhao, D., Hun, F.H., Weng, L., & Liu, H. 2011. Cytotoxicity, permeability, and inflammation of metal oxide nanoparticles in human cardiac microvascular endothelial cells : Cytotoxicity, permeability, and inflammation of metal oxide nanoparticles. *Cell Biol.Toxicol.* available from: PM:21681618

Tang, T.Y., Howarth, S.P., Miller, S.R., Graves, M.J., King-Im, J.M., Li, Z.Y., Walsh, S.R., Patterson, A.J., Kirkpatrick, P.J., Warburton, E.A., Varty, K., Gaunt, M.E., & Gillard, J.H. 2008. Correlation of carotid atheromatous plaque inflammation using USPIO-enhanced MR imaging with degree of luminal stenosis. *Stroke*, 39, (7) 2144-2147 available from: PM:18451355

Taylor, A. & Sansom, M.S. 2010. Studies on viral fusion peptides: the distribution of lipophilic and electrostatic potential over the peptide determines the angle of insertion into a membrane. *Eur.Biophys.J.*, 39, (11) 1537-1545 available from: PM:20499059

Thu, M.S., Najbauer, J., Kendall, S.E., Harutyunyan, I., Sangalang, N., Gutova, M., Metz, M.Z., Garcia, E., Frank, R.T., Kim, S.U., Moats, R.A., & Aboody, K.S. 2009. Iron labeling and pre-clinical MRI visualization of therapeutic human neural stem cells in a murine glioma model. *PLoS.One.*, 4, (9) e7218 available from: PM:19787043

Tornqvist, H., Mills, N.L., Gonzalez, M., Miller, M.R., Robinson, S.D., Megson, I.L., MacNee, W., Donaldson, K., Soderberg, S., Newby, D.E., Sandstrom, T., & Blomberg, A. 2007. Persistent endothelial dysfunction in humans after diesel exhaust inhalation. *Am.J.Respir.Crit Care Med.*, 176, (4) 395-400 available from: PM:17446340

Trivedi, R., King-Im, J., & Gillard, J. 2003a. Accumulation of ultrasmall superparamagnetic particles of iron oxide in human atherosclerotic plaque. *Circulation*, 108, (19) e140 available from: PM:14610003

Trivedi, R.A., King-Im, J.M., Graves, M.J., Cross, J.J., Horsley, J., Goddard, M.J., Skepper, J.N., Quartey, G., Warburton, E., Joubert, I., Wang, L., Kirkpatrick, P.J., Brown, J., & Gillard, J.H. 2004. In vivo detection of macrophages in human carotid atheroma: temporal dependence of ultrasmall superparamagnetic particles of iron oxide-enhanced MRI. *Stroke*, 35, (7) 1631-1635 available from: PM:15166394

Uppal, R. & Caravan, P. 2010. Targeted probes for cardiovascular MRI. *Future.Med.Chem.*, 2, (3) 451-470 available from: PM:20539821

Uppal, R., Catana, C., Ay, I., Benner, T., Sorensen, A.G., & Caravan, P. 2011. Bimodal thrombus imaging: simultaneous PET/MR imaging with a fibrin-targeted dual PET/MR probe--feasibility study in rat model. *Radiology*, 258, (3) 812-820 available from: PM:21177389

van Gils, J.M., Zwaginga, J.J., & Hordijk, P.L. 2009. Molecular and functional interactions among monocytes, platelets, and endothelial cells and their relevance for cardiovascular diseases. *J.Leukoc.Biol.*, 85, (2) 195-204 available from: PM:18948548

van Tilborg, G.A., Strijkers, G.J., Pouget, E.M., Reutelingsperger, C.P., Sommerdijk, N.A., Nicolay, K., & Mulder, W.J. 2008. Kinetics of avidin-induced clearance of biotinylated bimodal liposomes for improved MR molecular imaging. *Magn Reson.Med.*, 60, (6) 1444-1456 available from: PM:19025910

van, W.C., Wong, J., Morant, K., Jennings, A., Austin, P.C., Jetty, P., & Forster, A.J. 2011. The influence of incidental abdominal aortic aneurysm monitoring on patient outcomes. *J.Vasc.Surg.*, 54, (5) 1290-1297 available from: PM:21803526

Viera, A.J. & Sheridan, S.L. 2010. Global risk of coronary heart disease: assessment and application. *Am.Fam.Physician*, 82, (3) 265-274 available from: PM:20672791

Voura, E.B., Jaiswal, J.K., Mattoussi, H., & Simon, S.M. 2004. Tracking metastatic tumor cell extravasation with quantum dot nanocrystals and fluorescence emission-scanning microscopy. *Nat.Med.*, 10, (9) 993-998 available from: PM:15334072

Walker, N.J. & Bucher, J.R. 2009. A 21st century paradigm for evaluating the health hazards of nanoscale materials? *Toxicol.Sci.*, 110, (2) 251-254 available from: PM:19468057

Wang, H., Zhao, Y., Wu, Y., Hu, Y.L., Nan, K., Nie, G., & Chen, H. 2011. Enhanced anti-tumor efficacy by co-delivery of doxorubicin and paclitaxel with amphiphilic

methoxy PEG-PLGA copolymer nanoparticles. *Biomaterials* available from: PM:21807411

Wang, T.J. 2011. Assessing the role of circulating, genetic, and imaging biomarkers in cardiovascular risk prediction. *Circulation*, 123, (5) 551-565 available from: PM:21300963

Watanabe, T. & Fan, J. 1998. Atherosclerosis and inflammation mononuclear cell recruitment and adhesion molecules with reference to the implication of ICAM-1/LFA-1 pathway in atherogenesis. *Int.J.Cardiol.*, 66 Suppl 1, S45-S53 available from: PM:9951802

Weidner, A.M., van Lin, E.N., Dinter, D.J., Rozema, T., Schoenberg, S.O., Wenz, F., Barentsz, J.O., & Lohr, F. 2011. Ferumoxtran-10 MR lymphography for target definition and follow-up in a patient undergoing image-guided, dose-escalated radiotherapy of lymph nodes upon PSA relapse. *Strahlenther.Onkol.*, 187, (3) 206-212 available from: PM:21347637

Weintraub, N.L. 2009. Understanding abdominal aortic aneurysm. *N.Engl.J.Med.*, 361, (11) 1114-1116 available from: PM:19741234

Yang, S.H., Heo, D., Park, J., Na, S., Suh, J.S., Haam, S., Park, S.W., Huh, Y.M., & Yang, J. 2012. Role of surface charge in cytotoxicity of charged manganese ferrite nanoparticles towards macrophages. *Nanotechnology.*, 23, (50) 505702 available from: PM:23164999

Yang, X., Hong, H., Grailer, J.J., Rowland, I.J., Javadi, A., Hurley, S.A., Xiao, Y., Yang, Y., Zhang, Y., Nickles, R.J., Cai, W., Steeber, D.A., & Gong, S. 2011. cRGD-functionalized, DOX-conjugated, and (6)(4)Cu-labeled superparamagnetic iron oxide nanoparticles for targeted anticancer drug delivery and PET/MR imaging. *Biomaterials*, 32, (17) 4151-4160 available from: PM:21367450

Yee, D.L., Bergeron, A.L., Sun, C.W., Dong, J.F., & Bray, P.F. 2006. Platelet hyperreactivity generalizes to multiple forms of stimulation. *J.Thromb.Haemost.*, 4, (9) 2043-2050 available from: PM:16961612

Yilmaz, A., Rosch, S., Klingel, K., Kandolf, R., Helluy, X., Hiller, K.H., Jakob, P.M., & Sechtem, U. 2011a. Magnetic resonance imaging (MRI) of inflamed myocardium using iron oxide nanoparticles in patients with acute myocardial infarction - Preliminary results. *Int.J Cardiol.* available from: PM:21689857

Zhao, Y., Zhao, L., Zhou, L., Zhi, Y., Xu, J., Wei, Z., Zhang, K.X., Ouellette, B.F., & Shen, H. 2010. Quantum dot conjugates for targeted silencing of bcr/abl gene by RNA

interference in human myelogenous leukemia K562 cells. *J.Nanosci.Nanotechnol.*, 10, (8) 5137-5143 available from: PM:21125862

Zhu, M.T., Wang, B., Wang, Y., Yuan, L., Wang, H.J., Wang, M., Ouyang, H., Chai, Z.F., Feng, W.Y., & Zhao, Y.L. 2011a. Endothelial dysfunction and inflammation induced by iron oxide nanoparticle exposure: Risk factors for early atherosclerosis. *Toxicol.Lett.*, 203, (2) 162-171 available from: PM:21439359

Zhu, M.T., Wang, Y., Feng, W.Y., Wang, B., Wang, M., Ouyang, H., & Chai, Z.F. 2010. Oxidative stress and apoptosis induced by iron oxide nanoparticles in cultured human umbilical endothelial cells. *J.Nanosci.Nanotechnol.*, 10, (12) 8584-8590 available from: PM:21121369

APPENDIX I: Cytotoxicity Data Superparamagnetic Iron Oxide Nanoparticles and Polystyrene Beads

A range of cytotoxicity tests were carried out using the SPIO/USPIO from this study all with the conclusion that these particles can be considered low toxicity. The following data demonstrates the ENPs biocompatibility with a range of cell types, including platelets and $_{MDM\emptyset}$. Whilst not all the particles used were put through all the cytotoxicity tests I feel confident that USPIO/SPIO designed for medical purposes would demonstrate similar cytotoxicity profiles.

Calcein-am staining was performed on platelets that had been incubated with ENPs for 30min and analysed by flow cytometry. Calcein-am is taken up by cells and cleaved by intracellular esterases to fluorescent calcein. This process can only be carried out by viable cells.

Figure A

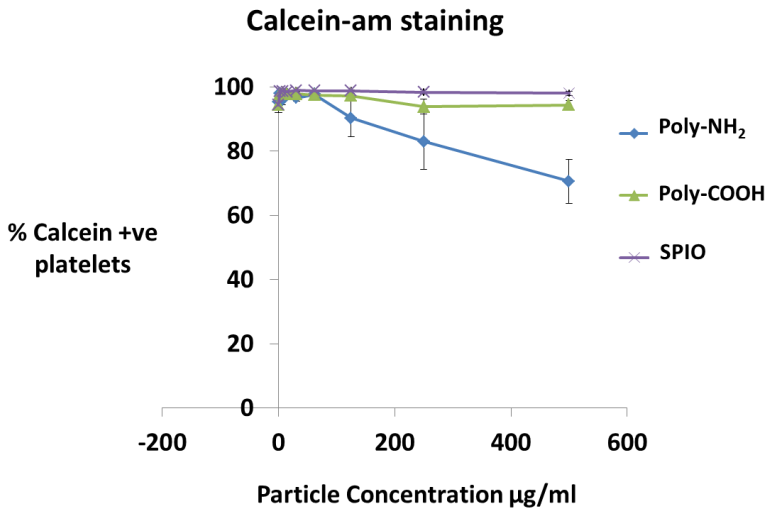

Here it can be seen that the amine beads caused a 30% reduction in platelet viability after 30-mins whereas the Poly-COOH and SPIO had no such

effects. This is most likely due to the negatively charged platelet membranes being disrupted by the positively charged beads.

Monocyte derived macrophage viability was determined using AnnexinV/Propidium iodide (PI) staining. $_{MDM\emptyset}$ cells were incubated for up to 72-hours with iron-oxide ENPs then stained for apoptosis (annexin V) and necrosis (PI). Any cells that didn't stain were considered viable (Figure B)

Figure B

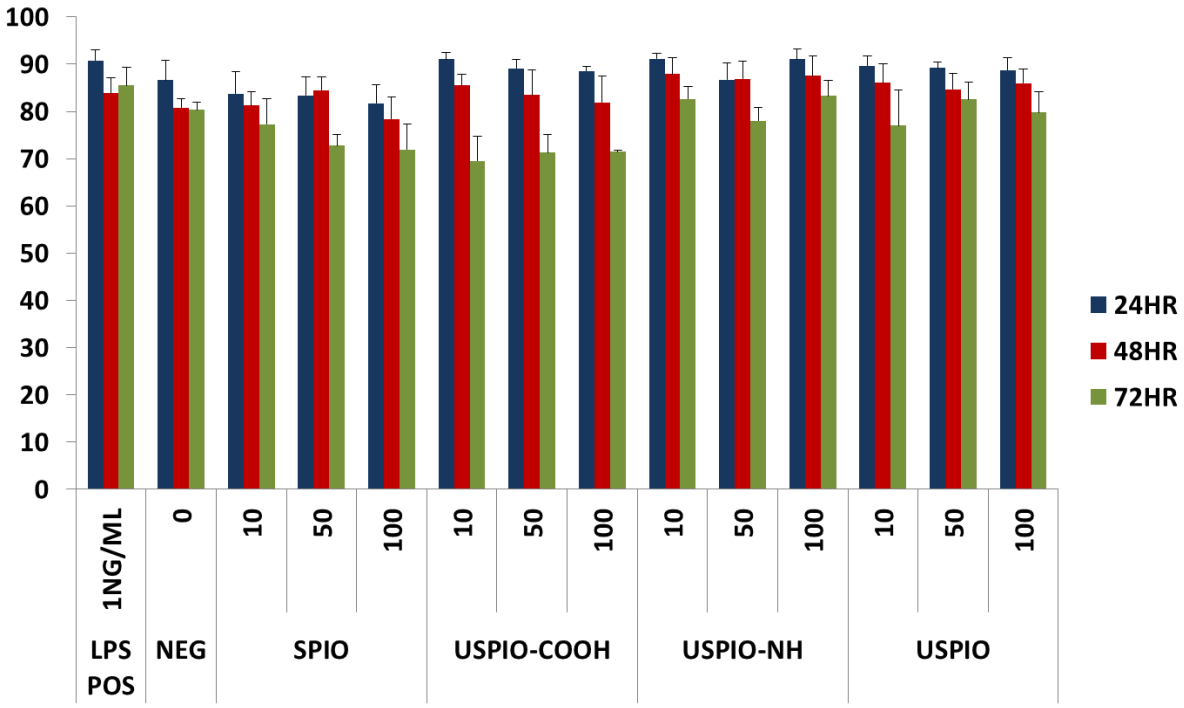

It can be seen that although there is a reduction in cell viability over the 72-hour period it is not significant. Overall the ENPs were well tolerated by the cells.

Haemolysis was used to determine the toxicity of the Poly-Beads. Haemolysis was performed in washed red blood cells (RBC). RBC and ENPs were incubated for 30-mins and haemoglobin release was measured using light absorbance.

Figure C

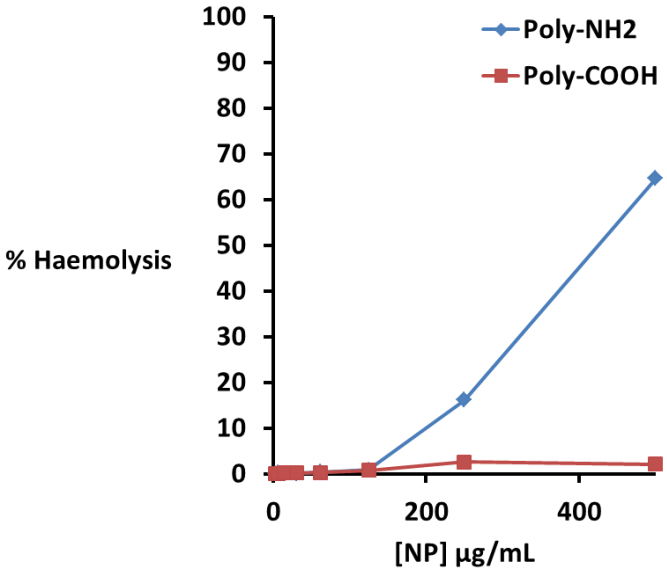

Figure C clearly demonstrates that the positively charged amine beads were very haemolytic suggesting they readily disrupt cell membranes whereas the carboxylated beads do not.

Cytotoxicity was not the focus of this study but is a necessary part of any work carried out with nanoparticles in vitro in vivo and ex vivo. While the SPION/USPIO and the Poly-COOH beads used in this study could be considered minimally toxic the aminated Poly-NH_2 displayed considerable toxicity after just 30-mins in platelets and RBC. The effects the Poly-NH_2 beads have on cell membranes most likely accounts for the in vitro effects seen in platelets (chapter 3). Considering the toxicological profile of the

SPIO/USPIO demonstrated here I am confident they effects seen in vitro and ex vivo were not mediated by cell injury or death.

Appendix II: Papers and Publications

ADVERSE EFFECTS OF ENGINEERED NANOMATERIALS

EXPOSURE, TOXICOLOGY, AND IMPACT ON HUMAN HEALTH

ADVERSE EFFECTS OF ENGINEERED NANOMATERIALS

EXPOSURE, TOXICOLOGY, AND IMPACT ON HUMAN HEALTH

Edited by

BENGT FADEEL
Division of Molecular Toxicology
Institute of Environmental Medicine, Karolinska Institute,
Stockholm, Sweden

ANTONIO PIETROIUSTI
Department of Biopathology
Tor Vergata University
Rome, Italy

ANNA SHVEDOVA
Pathology and Physiology Research Branch
Health Effects Laboratory Division
National Institute for Occupational Safety and Health
Morgantown, WV, USA

ELSEVIER

AMSTERDAM • BOSTON • HEIDELBERG • LONDON
NEW YORK • OXFORD • PARIS • SAN DIEGO
SAN FRANCISCO • SINGAPORE • SYDNEY • TOKYO
Academic Press is an imprint of Elsevier

Academic Press is an imprint of Elsevier
32 Jamestown Road, London NW1 7BY, UK
225 Wyman Street, Waltham, MA 02451, USA
525 B Street, Suite 1800, San Diego, CA 92101-4495, USA

First edition 2012

British Library Cataloguing-in-Publication Data
A catalogue record for this book is available from the British Library

Library of Congress Cataloging-in-Publication Data
A catalog record for this book is available from the Library of Congress

ISBN : 978-0-12-386940-1

For information on all Academic Press publications
visit our website at elsevierdirect.com

Typeset by TNQ Books and Journals Pvt Ltd.
www.tnq.co.in

Printed and bound in United States of America

12 13 14 15 16 10 9 8 7 6 5 4 3 2 1

Contents

Preface

Should one ban aspirin? Most would say no – aspirin has helped to stave off disease in innumerable patients. Yet, this drug has also causes thousands of deaths due to gastrointestinal bleeding and severe disabilities due to hemorrhagic stroke. However, its benefits largely outweigh the costs of these adverse effects. In some way, this reasoning is even more true for engineered nanomaterials (ENM), if we consider that the enormous benefits to humans by their industrial and biomedical applications are certain, whereas their expected adverse effects are probably largely preventable. We have the duty, however, to develop a careful understanding of these effects in order to minimize them as much as possible. This book, focusing essentially on the disease potential of ENM, by examining systematically their possible effects on different organs and systems, on the basis of the experimental evidence and of plausible pathogenetic pathways, may provide a useful guide in this endeavor.

The chapters, written by acknowledged experts in the field, attempt a translation from experimental data to human disease in order to address the question: what nanomaterial-induced diseases might potentially occur in humans? The book provides up-to-date information on occupational exposure and adverse health effects of ENM, and also discusses their biomedical applications, the other side of the coin.

The first part of the book includes six chapters, aimed at giving the reader the possibility of a correct interpretation of the reported data. More specifically, the first chapter of the book gives a general overview of the interaction of the ENM with the human body, describing basic phenomena such as corona formation, oxidative stress and inflammation, which may lead to adverse outcomes in different organs and conditions (from cancer, to atherosclerosis, to fetal maldevelopment). The following two chapters describe the assessment of ENM in the occupational setting and how ENM can be managed. Hence, Chapter 2 discusses exposure to ENM in different settings, methods of exposure evaluation, and available protective measures, and Chapter 3 the existence and development of reliable – and possibly specific – biological markers for health surveillance. Chapters 4 and 5 deal with the complex case of *in vivo* and *in vitro* assessments of ENM toxicity and they describe two possible solutions to the problem: on the one hand, the selection of the most appropriate *in vitro* (cell culture-based) and *in vivo* (live animal) tests and the correct interpretation of the findings (Chapter 4), and on the other, the development of predictive computer-generated models (Chapter 5). The two approaches are not mutually exclusive, since the performance of correctly designed experiments is the prerequisite for the development of reliable computational models.

The first section of the book ends with the exhaustive description of the competences

and decisions of the most important EU and US regulatory and governmental agencies, aimed at the legislative safeguarding of workers, consumers, and patients from the potential risk of inadvertent or deliberate exposure to ENM.

The second part includes a series of eight chapters addressing the pathogenic potential of ENM for specific organ and tissues. Chapter 7 describes the possible adverse effects on the respiratory system, one of the most important routes of entry of ENM, whereas other organ system-specific chapters are devoted to ENM effects on the cardiovascular system (Chapter 8), neurological system (Chapter 9), skin (Chapter 11) and the gastrointestinal tract (Chapter 12). The body of evidence for the disease potential of ENM is substantial: the possibility of pulmonary fibrosis, malignant mesothelioma and atherosclerotic disease should be considered, at least for some ENM. In other cases, the link with human diseases is much more speculative, such as for neurodegenerative disorders or with Crohn's disease, an inflammatory disease of the intestines. It should be considered, however, that the amount of research on the possible pulmonary and cardiovascular effects is much higher than on neurological and gastrointestinal adverse effects. For example, nothing is known on the process of corona formation and transformation, and of the biological consequences of this process, for ENM traveling through the various compartments of the gastrointestinal lumen. The skin seems perhaps the most insensitive organ to the possible injurious action of ENM, although they might cause damage at distal sites in other, more susceptible organs if they cross the skin barrier. Chapters 10 and 14 deal with the possible impact of ENM on the immune system and on our genetic material, respectively. Both report plausible evidence of damage, a finding which may have profound implications for human health, since alterations of the immunologic and genetic integrity underpin numerous disease processes, including the development of cancer. Chapter 13 focuses on a very recently reported possible adverse effect of ENM, i.e. reproductive toxicology. This is of particular concern, for obvious reasons.

In the third and final section of the book, two chapters focusing on diagnostic (Chapter 15) and therapeutic (Chapter 16) applications of ENM are included. Although the book is oriented towards adverse effects, the positive health implications of ENM should not be ignored. The chapter on diagnostics is focused on cancer, since this represents the most relevant application and because other uses, such as diagnostic tools, are discussed in the context of some of the other chapters (in particular, Chapters 4 and 8). Chapter 16 provides a comprehensive overview of nanomaterials for drug delivery including a critical discussion of various classes of nano-scale drug carriers that are already in clinical use or are currently in clinical trials or show promise for therapeutic and/or theranostic applications.

The annex provides information on various routes of synthesis of various classes of nanomaterials. This is not an esoteric topic of interest only to material scientists; a detailed understanding of the synthesis of ENM is needed as this may impact on biological interactions and, hence, on disease processes. For instance, the presence of contaminants can sometimes explain cytotoxic effects. Finally, the glossary at the end of the book provides an explanation of the most relevant terms used in the book.

This book is a state-of-the-art presentation of relevant research on adverse effects of engineered nanomaterials on human health. We are indebted to all the colleagues who have participated in this project. We hope that this volume will serve as a useful guide for students and researchers in the field and for clinicians, policymakers, and regulators with an interest in nanosafety and human health.

Bengt Fadeel

Karolinska Institutet, Antonio Pietroiusti, University of Rome "Tor Vergata", Aruna Shvedova, National Institute for Occupational Safety and Health

List of Contributors

Christoph Alexiou Department of Oto-Rhino-Laryngology, Head and Neck Surgery, Section for Experimental Oncology and Nanomedicine, Erlangen, Germany

Giuseppe Bardi Center for Nanotechnology Innovation @ NEST, Istituto Italiano di Tecnologia, Pisa, Italy

Antonio Bergamaschi Institute of Occupational Medicine, Università Cattolica del Sacro Cuore Roma, Rome, Italy

Enrico Bergamaschi Laboratory of Industrial Toxicology, University of Parma Medical School, Parma, Italy

Diana Boraschi Institute of Biomedical Technologies of the National Research Council, Pisa, Italy

Cyrill Bussy Nanomedicine Laboratory, Center for Drug Delivery Research, The School of Pharmacy, University of London, London, UK

Luisa Campagnolo Department of Public Health and Cell Biology, University of Tor Vergata, Rome, Italy

Sandra Ceccatelli Department of Neuroscience, Karolinska Institutet, Stockholm, Sweden

Chunying Chen National Centre for Nanoscience and Technology, Beijing, China

Kai Cheng Molecular Imaging Program at Stanford (MIPS), Canary Center at Stanford for Cancer Early Detection, Department of Radiology and Bio-X Program, School of Medicine, Stanford University, Stanford, CA, USA

Zhen Cheng Molecular Imaging Program at Stanford (MIPS), Canary Center at Stanford for Cancer Early Detection, Department of Radiology and Bio-X Program, School of Medicine, Stanford University, Stanford, CA, USA

Renato Colognato Clinical Pharmacology Unit, "L. Sacco" University Hospital, Milano, Italy

Sara Correia Carreira BIRCH, Biophysics Research Unit, Department of Medical Physics & Bioengineering, University Hospitals Bristol NHS Foundation Trust, St Michael's Hospital, Bristol, UK

Wim H. De Jong National Institute for Public Health and the Environment, Laboratory for Health Protection Research, Bilthoven, The Netherlands

Shareen H. Doak Institute of Life Science, College of Medicine, Swansea University, Swansea, Wales, UK

Ken Donaldson Queen's Medical Research Institute, University of Edinburgh, Edinburgh, UK

Rodger Duffin Centre for Inflammation Research, Edinburgh University, Edinburgh, UK

Albert Duschl University of Salzburg, Department of Molecular Biology, Salzburg, Austria

Maria Dusinska NILU-Norwegian Institute for Air Research, Health Effects Laboratory, Departments of CEE and Environmental Chemistry, Kjeller, Norway

Vidana Epa CSIRO Materials Science & Engineering, Parkville, Australia

Maureen R. Gwinn US Environmental Protection Agency, Washington, DC, USA

Karin Sørig Hougaard National Research Center for the Working Environment, Copenhagen, Denmark

Ivo Iavicoli Institute of Occupational Medicine, Università Cattolica del Sacro Cuore Roma, Rome, Italy

Mark A. Jepson School of Biochemistry, University of Bristol, Bristol, UK

Vadim G. Kessler Department of Chemistry, SLU BioCenter, Uppsala, Sweden

Kostas Kostarelos Nanomedicine Laboratory, Center for Drug Delivery Research, The School of Pharmacy, University of London, London, UK

Francesca Larese Filon Unit of Occupational Medicine, University of Trieste, Trieste, Italy

Ying Liu National Centre for Nanoscience and Technology, Beijing, China

Andrea Magrini Department of Biopathology and Imaging, University of Rome "Tor Vergata", Rome, Italy

Laura Methven Nanomedicine Laboratory, Center for Drug Delivery Research, The School of Pharmacy, University of London, London, UK

Nicholas L. Mills Centre for Cardiovascular Science, Edinburgh University, Edinburgh, UK

Nancy A. Monteiro-Riviere North Carolina State University-CVM Department of Clinical Sciences & Joint Biomedical Engineering at NCSU & UNC Chapel Hill Center for Chemical Toxicology Research and Pharmacokinetics, Raleigh, NC, USA

Andreas M. Nyström The Swedish Medical Nanoscience Center, and the Department of Neuroscience Karolinska Institutet, SE-171 77 Stockholm, Sweden

Margriet V.D.Z. Park Maastricht University, Department of Toxicogenomics, Maastricht; National Institute for Public Health and the Environment, Laboratory for Health Protection Research, Bilthoven, The Netherlands

Robby A. Petros Department of Chemistry, University of North Texas, Denton, TX, USA

Craig Poland Institute of Occupational Medicine, Edinburgh, UK

Jennifer B. Raftis Centre for Inflammation Research, Edinburgh University, Edinburgh, UK

Elise Rundén-Pran NILU-Norwegian Institute for Air Research, Health Effects Laboratory, Departments of CEE and Environmental Chemistry, Kjeller, Norway

Margaret Saunders BIRCH, Biophysics Research Unit, Department of Medical Physics & Bioengineering, University Hospitals Bristol NHS Foundation Trust, St Michael's Hospital, Bristol, UK

Kai Savolainen Nanosafety Research Centre, Finnish Institute of Occupational Health, Helsinki, Finland

Gulaim A. Seisenbaeva Department of Chemistry, SLU BioCenter, Uppsala, Sweden

Birgit Sokull-Klüttgen European Commission, Joint Research Centre, Institute for Health and Consumer Protection, Unit I05 Nanobiosciences, Ispra, Italy

Muhammet S. Toprak KTH Royal Institute of Technology, Functional Materials Division, Kista-Stockholm, Sweden

Lang Tran Institute of Occupational Medicine, Research Avenue North, Edinburgh, UK

Peter Wick Empa, Swiss Federal Laboratories for Materials Science and Technology, Laboratory for Materials-Biology Interactions, St Gallen, Switzerland

Dave Winkler CSIRO Materials Science & Engineering, Clayton, Australia; Monash Institute of Pharmaceutical Science, Parkville, Australia

CHAPTER

8

c0008

Cardiovascular System

Jennifer B. Raftis[1], *Nicholas L. Mills*[2], *Rodger Duffin*[1]

[1]Centre for Inflammation Research, Edinburgh University, Edinburgh, UK

[2]Centre for Cardiovascular Science, Edinburgh University, Edinburgh, UK

OUTLINE

INTRODUCTION

s0010
p0010

Nanotechnology aims for the development of nanoparticles (NP; particles with at least one dimension less than 100 nm) and other nanomaterials with novel properties, which cannot be obtained through use of the same material in bulk or molecular form. It is currently being applied in all manner of commercial industries to confer unique properties on products or improve existing ones [1]. Some of the most significant applications are likely to occur in the field of medicine. Many engineered nanoparticles and nanosurfaces have already been evaluated in the clinic [2] and it is likely nanomaterials will have a major impact in areas such as diagnostics, medical imaging and therapeutics.

Adverse Effects of Engineered Nanomaterials
DOI: 10.1016/B978-0-12-386940-1.00008-8

10008-FADEEL-9780123869401

p0015 While the nanotechnologies develop novel engineered NPs, we are already exposed to numerous NPs in the environment through inhalation of ambient particles (particles less than 10 μm in diameter; PM_{10}) from combustion, industrial and occupational sources and through the ingestion of contaminated food and water. Epidemiological and experimental studies have identified a range of adverse health effects related to PM_{10}, and the key components and underlying mechanisms responsible are beginning to emerge [3–7]. Interestingly the "ultrafine" or nanoparticulate component of PM_{10} is considered to have the greatest potential for toxicity and harm. Findings from environmental research and particle toxicology studies have been extrapolated and used to guide our approach to the risk assessment of engineered nanoparticles. Combustion derived nanoparticles (CDNPs) share some characteristics with engineered NPs, such as size, charge and surface area that influence toxicity. Exposure to CDNPs has been shown to impair vascular function [8], promote myocardial ischemia [9], and induce prothrombotic changes in the circulation in humans [10] and may directly contribute to the formation of atherosclerotic plaque [11]. These observations highlight an important paradox between the harmful effects of CDNP and the potential for engineered NPs to be used in clinical applications; especially for those NPs designed for intravenous administration in medical imaging.

p0020 In this chapter, we review the clinical applications of engineered NPs focusing on currently available NPs with diagnostic and therapeutic roles in cardiovascular medicine (for a discussion of other diagnostic and therapeutic applications of NPs, see Chapters 15 and 16). The chemical and physical properties that are functionally important for each particle and application are outlined, and strategies to optimize performance through modification of these properties identified. We also highlight the potential for engineered NPs adversely to affect cellular function and have relevant adverse biological effects on the cardiovascular system.

s0015 DIAGNOSTIC APPLICATIONS IN CARDIOVASCULAR DISEASE

p0025 Atherothrombosis remains the leading cause of death in developed countries. Successful therapies and strategies for prevention are dependent on identification of at risk individuals using clinical risk scores based on age, sex, blood pressure, serum cholesterol and cigarette smoking [12,13]. While these risk scores are used widely and identification of traditional risk factors is the basis of most primary prevention screening policies, these calculators are imperfect; the majority of persons presenting with an adverse cardiac event have no prior history or any established risk factors [12]. The converse is also true, many patients with risk factors for cardiovascular disease do not go onto develop atherothrombosis or have an acute cardiovascular event.

p0030 An alternative and perhaps preferable strategy would be to identify individuals with early atherosclerotic disease in an attempt to modify the course of the disease and prevent the clinical consequences of plaque rupture, thrombosis and infarction. Clinical and experimental research has focused on the identification of novel biomarkers that could indicate the early development of atherothrombotic disease. Before a biomarker is introduced to the clinic as a diagnostic tool, it must satisfy the following criteria: it must be highly specific, easy to measure, provide novel information about the disease, and reflect disease burden accurately

10008-FADEEL-9780123869401

helping the clinician decide on an appropriate course of treatment (see also Chapter 3 for an extensive discussion on biomarkers). These basic criteria are not easily met for a heterogeneous condition like atherothrombosis.

p0035 Atherothrombosis is a complex inflammatory disease and is classified according to plaque composition [14]. Plaque rupture and subsequent thrombosis involve a number of inflammatory processes including endothelial dysfunction, leukocyte recruitment and migration, platelet activation, matrix metalloproteinase activity, and degradation of the fibrous cap resulting in plaque rupture and thrombosis [15]. Imaging strategies that target these pathological processes in atherosclerotic plaque development may provide more sensitive methods to monitor disease progression, permit early detection of the disease, and have a role in the assessment of treatment efficacy. The ability to identify plaque structure and function/activity would allow the clinician to identify those individuals at highest risk of plaque rupture.

s0020 ENGINEERED NANOMATERIALS

p0040 Nanoparticles are unique in terms of their size and structure. Their small size allows them to interact with the body on a molecular level and confers upon them a high ratio of surface area to volume. They can be engineered to have different shapes, sizes, structures, surface functionalization and coatings, allowing them to be specifically targeted to a biomarker of disease [16]. The ability to understand and manipulate the properties of nanomaterials will ultimately determine their usefulness in nanomedicine [17].

p0045 Table 8.1 adapted from [18], gives examples of nanomaterials intended for clinical use (see also Chapter 15 for an extensive discussion of nanomaterials used for imaging).

p0050 Nanomaterial synthesis has progressed rapidly in recent years and has generated complex state-of-the-art nano-scale structures with diverse and complex functionalities [17]. The ability to construct such nanomaterials has led to the development of multimodal and multifunctional nanoparticles to facilitate magnetic resonance imaging (MRI), computed tomography (CT) and positron emission tomography (PET) imaging (see also Chapters 4 and 15 for a discussion of these diagnostic imaging techniques) or for targeted drug delivery [19]. The development of such nanoparticles has led to the terms "theragnostic" or "theranostic" to describe a nanoparticle that can be used both for diagnostic and therapeutic applications [17,20].

s0025 Superparamagnetic Iron Oxide Nanoparticles (SPIONs)

p0055 In 1985, Stark et al. used MRI to determine the quantitative relationship between relaxation rates and iron levels in patients with iron overload [21] and it was quickly deduced that the increase in T2 relaxation rates in these patients could be artificially replicated and used to provide contrast in magnetic resonance imaging [22]. MRI imaging is used routinely to assess the extent of damage after a myocardial infarct or to monitor the extent of peripheral vascular disease [23]. SPIONs were originally used to provide contrast when imaging liver [24], spleen [25] and lymph nodes [26] as this is where these particles naturally accumulated. With improvements in nanoparticle production, iron-oxide nanoparticles were designed to

10008-FADEEL-9780123869401

t0010 TABLE 8.1 Nanomaterials in Clinical Use and Development for Imaging, Diagnosis and Therapy

Nanomaterial	Commercial Name	Application	Target	Adverse Effects	Manufacturer	Current Status
Metallic						
Iron oxide	Feridex	MRI	Liver	Back pain, vasodilation	Bayer Schering	FDA approved
	Resovist	MRI	Liver	None	Bayer Schering	FDA approved
	Combidex	MRI	Lymph nodes	None	Advanced Magnetics	In phase 3 clinical trials
	NanoTherm	Cancer therapy	Various	Acute urinary retention	MagForce	In phase 3 clinical trials
	Ferahеme	Iron replacement therapy	RES macrophages of the liver, spleen and bone marrow	Diarrhea, nausea, dizziness, hypotension, constipation, peripheral edema anaphylactic-type reactions, cardiac arrest, Tachycardia, angioedema, ischemic myocardial events.	AMAG Pharmaceuticals	FDA approved
Gold	Verigene	In vitro diagnostics	Genetic	N/A	Nanosphere	FDA approved
	Aurimmune	Cancer therapy	Various	Fever	Cytimmune Sciences	In phase 2 clinical trials
Nanoshells	Auroshell	Cancer therapy	Head and Neck	Under investigation	Nanospectra Biosciences	In phase 1 clinical trials
Semiconductor						
Quantum dot	Qdots, EviTags, semiconductor nanocrystals	Fluorescent contrast In vitro diagnostics	Tumors, cells, tissues and molecular sensing structures	N/A	Life Technologies, eBioscience, Nanoco, CrystalPlex, Cytodiagnostics	Research use only
Organic						
Protein	Abraxane	Cancer therapy	Breast	Cytopenia	Abraxis Bioscience	FDA approved
Liposome	DoxilCaelyx	Cancer therapy	Various	Hand-foot syndrome, stomatitis	Ortho Biotech	FDA approved
Polymer	Oncaspar	Cancer therapy	Acute lymphoblastic leukemia	Urticaria, rash	Rhône-Poulenc Rorer	FDA approved
	CALAA-01	Cancer therapy	Various	Mild renal toxicity	Calando	In phase 2 clinical trials
Dendrimer	VivaGel	Microbicide	Cervicovaginal	Abdominal pain, dysuria	Starpharma	In phase 2 clinical trials
Micelle	Genexol-PM	Cancer therapy	various	Peripheral sensory neuropathy, neutropenia	Samyang	For phase 4 clinical trials

10008-FADEEL-9780123869401

be more biocompatible with increased circulation times to assist with MRI imaging [27]. Particle size and surface coating can be modified to target SPIONs to different sites. Larger particles, 50–150 nm in diameter, predominantly produce a signal decrease and are used as contrast media for imaging the liver and spleen. Smaller particles, less than 20 nm, are distributed more widely *in vivo* and can improve the identification of lymph nodes [28,29] or assist in the characterization of vulnerable atherothrombotic plaque. SPIONs have been used to enhance plaque imaging in a number of experimental models of atherosclerosis [30–33], however, the clinical studies published to date are less consistent [34–37].

p0060 Macrophages are the most common target for molecular imaging agents as there is a large body of evidence implicating them in the disease and, as a naturally phagocytic cell, they tend to scavenge foreign material without much manipulation. Several experimental studies have demonstrated that SPIONs or ultra-small paramagnetic iron oxide nanoparticles (USPIONs) can locate to atherosclerotic plaques and can be used to evaluate its metabolic state [31,35,38–40]. Targeted molecular imaging has been shown to result in localization of engineered nanoparticles within macrophages in atherosclerotic plaque [39,41,42].

p0065 Other applications of SPIONs include the assessment of myocardial perfusion [27,43] and characterization of aortic aneurysm formation as demonstrated in Figure 8.1 [35].

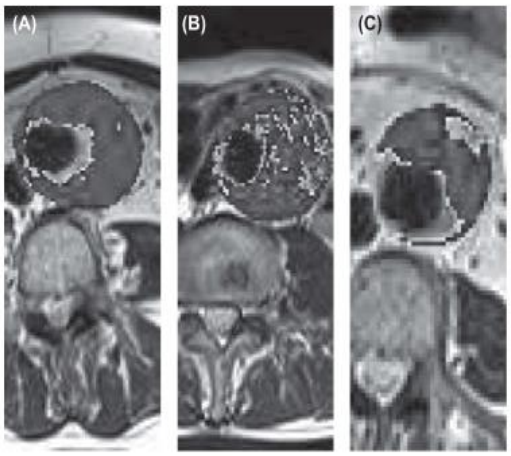

f0010 FIGURE 8.1 Representative abdominal aortic aneurysm (AAA) slices from patients showing differential patterns of uptake of 20-nm dextran-coated iron oxide nanoparticles corresponding to sites of cellular inflammation in sufficient amounts to cause a drop out in signal on an MRI scan. *Reproduced from [35] with permission from the American Heart Association.*

10008-FADEEL-9780123869401

p0070 SPIONs with a modified coat have also been used in molecular imaging, such as receptor-directed imaging [44], cell labeling for *in-vivo* monitoring of stem cell migration [45], and in labeling gene constructs for localization in gene therapy studies [46].

p0075 Examples of SPIONs in development or clinical use are given in Table 8.2 (adapted from [47]).

s0030 Lipid-Based Nanoparticles

p0080 Although more commonly associated with drug delivery, a number of studies have assessed the diagnostic potential of lipid-based nanoparticles [27,48,49]. Liposomes contain amphiphilic molecules, which have both hydrophobic and hydrophilic groups that self-assemble in water resulting in the formation of a hydrophilic core, whereas a micelle is a single layer of amphiphilic molecules with a hydrophobic core (Figure 8.2).

p0085 These constructs can be "loaded" with drugs, contrast agents, such as gadolinium, or gases for *in vivo* imaging [48,50,51]. Amirbekian et al. demonstrated that micelles containing gadolinium (Gd-micelles:100 nm) and targeted to the macrophage scavenging receptor CD204 enhanced MR imaging of atheroma compared to untargeted Gd-micelles, with increases in signal intensity directly related to the macrophage content of atheromatous plaque [52].

t0015 TABLE 8.2 Iron-Oxide Based Nanomaterialsin Clinical, Pre-Clinical and Development for Diagnosis and Therapy

Name	Status	Application	Administration	Relaxivities $mmol^{-1}sec^{-1}$	Coating	Core size (nm)
Lumirem and Gastromark	USA and Europe	GI	Oral	T2-72 T1-3.2	Silica	300
Abdoscan	Europe	GI	Oral	N/A	Polystyrene	300
Endorem/ Feriedex	USA	Liver/Spleen	IV	T2-98.3 T1-23.9	Dextran	5.6
Resovist	Withdrawn from some markets	Liver/Spleen	IV	T2-151.0 T1-25.4	Carbo-Dextran	4.2
Sinerem/ Combidex	Clinical trial	Lymph node Bone Marrow	IV	T2-44.1 T1-21.6	Dextran	4-6
Clariscan	Discontinued	Perfusion/ angiography	IV	T2-35 T1-20	Carbohydrate-PEG	5-7
Supravist	Preclinical	Perfusion Lymph node Bone Marrow	IV	T2-57 T1-7.3	Carbo-Dextran	3-5
MION 46	Preclinical	Angiography Lymph node Tumour Infarction	IV	N/A	Dextran	4-6
Feraheme	USA	Iron replacement therapy	IV	N/A	Polyglucose sorbitol carboxymethylether	2-10

10008-FADEEL-9780123869401

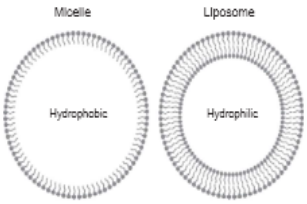

f0015 **FIGURE 8.2** Lipid-based nano-constructs.

Briley-Saebo et al. used lipid-coated USPIONs and SPIONs functionalized to target oxidized phospholipids or malondialdehyde-lysine for plaque imaging and demonstrated signal loss on T2* weighted MR images of atherosclerotic lesions with preferential accumulation of the epitope-targeted PEG-nanoparticles within lipid-rich macrophage foam cells [49]. The authors suggest this was due to binding of particles to extracellular oxidized low density lipoproteins (LDL) at these sites, or binding to oxidized LDL on macrophage scavenger receptors and enhanced uptake. They conclude that these particles may provide a platform to target vulnerable atherosclerotic plaques [49]. Combining nanoparticle technologies may yield more versatile particles with both diagnostic and therapeutic applications.

s0035 Gold

p0090 Certain metal nanoparticles, such as gold, with the application of light, generate a strong surface plasmon field by oscillating electrons around the metal surface. The field strength may depend upon the metal type, particle size and the wavelength of light. Gold is a metal of interest as it is considered chemically inert and can generate an intense surface plasmon field. Therefore, several protocols have been generated in order to obtain optimal dispersion, size and shape of gold nanoparticles for diagnostic purposes. At present, most colloidal synthesis protocols are based around the reduction of chloroauric acid, $HauCl_4$, in the presence of citrate to produce monodisperse particles with controlled equivolume diameters of 10 to 60 nm [53]. Different reduction agents are used if other shaped nanoparticles are desired. Rod-shaped gold nanoparticles are useful for near-infrared imaging and in combination with photoacoustic imaging show promise in detection and diagnosis of cardiovascular disease [54]. van Schooneveld et al. developed a tri-modal gold nanoparticle for enhanced imaging using MRI, CT and FI of macrophage cells *in vitro* and in the liver *in vivo* [55] with potential applications for imaging chronic inflammatory diseases.

s0040 PARTICOKINETICS OF NANOMATERIALS FOR DIAGNOSTIC USE

p0095 Understanding the particokinetics of engineered nanomaterials is a critical consideration when designing them for biomedical uses (see also Chapter 1 for a discussion on this subject).

10008-FADEEL-9780123869401

Engineered nanoparticles accumulate differentially throughout the body depending on their physiochemical properties; characteristics of the NP such as size, surface area, charge and surface chemistry as well as the method by which they are introduced (intravenous infusion, subdermal injection, inhalation or ingestion) determine the ultimate fate of the NP once inside the body.

p0100 Surface characteristics are important in determining whether or not a particle will be cleared by the recticuloendothelial system after intravenous administration [56]. When hydrophobic nanoparticles are injected directly into the circulation, they rapidly become opsonized by blood serum proteins and are cleared by the reticuloendothelial system. However, this opsonization and first pass clearance can be limited by alteration of the surface coatings of the nanoparticles. The most common method of prolonging circulation is conjugation of the nanoparticle with polyethylene glycol (PEG) polymer, providing the particle with steric hindrance to opsonization or phagocytosis [57] and allowing the PEGylated form to remain in the circulation for much longer, increasing interaction with blood components. A number of studies have demonstrated altered distribution patterns based on modification of the surface coating. Beduneau [25] covalently conjugated IgG molecules to the surface of SPIONs showing accelerated uptake by monocytes and enhanced retention *in vivo* without affecting monocyte viability. This technique could be very useful in the monitoring and tracking of disease progression. It is clear that surface modification has the ability to alter the distribution and clearance patterns of nanoparticles in the body, with small changes in surface moiety resulting in major differences in behavior of these particles in the body [58,59].

p0105 Hydrodynamic size also determines distribution [60]. Normally, in a healthy individual, the endothelium is very effective at preventing extravasation of nanoparticles due to the presence of tight gap junctions (<2 nm in diameter). However, when the endothelium is compromised, as is the case in atherosclerosis, these normally tight junctions become leaky and could potentially allow passage of nanoparticles to the underlying basement membrane. The final destination of particles in the body has been reported to be directly related to their size; larger particles, greater than 100 nm in diameter, deposit in the spleen due to its discontinuous endothelium with large fenestrations and smaller particles, less than 100 nm in diameter, deposit in the liver passing through the fenestrated endothelium and finally residing in the underlying parenchymal cells. Kinetic studies with gold nanoparticles have shown their pattern of distribution to be size dependent [61]. De Jong et al. [60] intravenously administered gold nanoparticles in rats and found that the biodistribution was dependent on particle size with the smallest particles (10 nm) having the most widespread organ distribution. Table 8.3 illustrates the size-dependent biodistribution of systemic nanoparticles.

s0045 ADVERSE EFFECTS OF COMBUSTION DERIVED NANOPARTICLES IN CARDIOVASCULAR DISEASE

p0110 While nanotechnology aims to develop new engineered NPs with novel properties, there are numerous sources of NPs in the environment from natural and anthropogenic sources. There have been many epidemiological, *in vitro*, *in vivo* and *ex vivo* studies demonstrating

10008-FADEEL-9780123869401

t0020 TABLE 8.3 Size Based Biodistribution of Nanomaterials

Hydrodynamic Diameter	Tissue Uptake	Renal Excretion
>30nm	Rapidly cleared by reticuloendothelial system (RES)	Not excreted by kidneys, excretion involves degradation of NP in RES tissue
10-30nm	Longer circulation time leads to increased uptake by non RES tissues.	Little, <5%, excretion by renal system excretion involves degradation of NP in RES tissue
4-10nm	Longer circulation time leads to increased uptake by non RES tissues.	Renal clearance increases as particle size decreases.
<4nm	Uptake in most cell types for particles not excreted by kidneys	Rapid clearance of nanoparticles by kidneys with retention of between 5-10% of injected dose

the adverse health effects of PM_{10} with the majority of investigators identifying the "ultrafine"' or nanoparticulate component as the most toxic of airborne pollutants [5–7,62–65]. These studies have raised concerns about the potential for engineered NPs to exert similar adverse health effects. Exposure to ambient particles is associated with more hospitalizations with acute cardiovascular events and an increase in cardiovascular deaths [66–69]. These effects are thought to be mediated by particle-induced oxidative stress and inflammation leading to vascular dysfunction, impaired fibrinolysis, and changes in the autonomic regulation of heart rate and rhythm [69,70]. Combustion derived nanoparticles (CDNPs) have been shown to be prothrombotic [9] and may contribute to the formation of atherosclerotic plaques. While CDNPs differ greatly in chemical composition compared to engineered nanoparticles, they share similarities in other characteristics considered toxicologically significant, such as size and surface area. It is therefore plausible that engineered nanoparticles will exert similar pro-inflammatory and prothrombotic effects; especially those manufactured for direct intravenous administration as a contrast agent in medical imaging [71,72].

B. ENGINEERED NANOMATERIALS: IMPACT ON HUMAN HEALTH

10008-FADEEL-9780123869401

p0115 Given the huge amount of published data implicating CDNPs in the pathogenesis of cardiovascular diseases [73], an understanding of the toxicology of nanoparticles intended for medical use is central to their future use. Mills et al. [3] provide an overview of the most widely accepted mechanisms for the adverse cardiovascular effects of CDNP.

s0050

TOXICITY OF ENGINEERED NANOPARTICLES IN CARDIOVASCULAR DISEASE

p0120 It is not surprising that a number of recent reviews focusing on the effects of occupational exposure to engineered nanomaterials have raised concerns that they could have similar health implications as CDNP [74–76]. Resolution of these issues will require a collaborative approach between industry, government, academic researchers and clinicians. In addition to occupational exposure to engineered nanomaterials, the direct exposures to engineered nanoparticles through medical use in susceptible populations is of immediate concern. Engineered nanomaterials unlike novel pharmacological therapies are not routinely tested to determine their effect on the cardiovascular system prior to clinical use. Tables 8.1 and 8.2 highlight the many different nanoparticles being developed for clinical use. All of these nanoparticles, not just those intended for the diagnosis and treatment of cardiovascular disease, have the potential to interact with cells associated with the progression of cardiovascular disease. To date, there are no observational studies linking exposure to engineered nanomaterials and cardiovascular events, however, a number of preclinical studies have reported that exposure to engineered nanomaterials, directly or indirectly, can cause endothelial dysfunction and platelet activation, and may plausibly contribute to ischemic heart disease [77–80]. The schematic diagrams depicted in Figure 8.3 and Figure 8.4 identify mechanisms and potential targets for engineered nanoparticles in circulation.

s0055

In vitro Studies

p0125 Cardiovascular disease is a complex and dynamic process with many contributing factors and therefore a single *in vitro* model to study the adverse effects of engineered nanomaterials on cardiovascular system is unlikely to emerge. However, platelets, platelet–monocyte aggregation and the vascular endothelium have emerged as useful *in vitro* systems given their key role in the pathogenesis of coronary and ischemic heart disease [81,82].

p0130 Compatibility of nanoparticles with blood components is important and a number of studies have employed assays of hemolysis [83], platelet aggregation and activation [84] and platelet–leukocyte aggregation [77]. Direct and indirect toxicity to the cardiovascular system can be determined using cell lines with assays of oxidative stress, inflammation and cell death [85]. Whether observations from these *in vitro* models apply *in vivo* or in the clinic is uncertain and, in the absence of any standards for the assessment of the cardiovascular toxicity of engineered nanomaterials, the role of *in vitro* assessments remains controversial.

p0135 Recent studies have shown that engineered nanoparticles can interact with platelets causing activation, aggregation [77,84,86] and hyperreactivity (unpublished observations). Surface charge is thought to be a critical determinant in platelet–nanoparticle activation [77].

10008-FADEEL-9780123869401

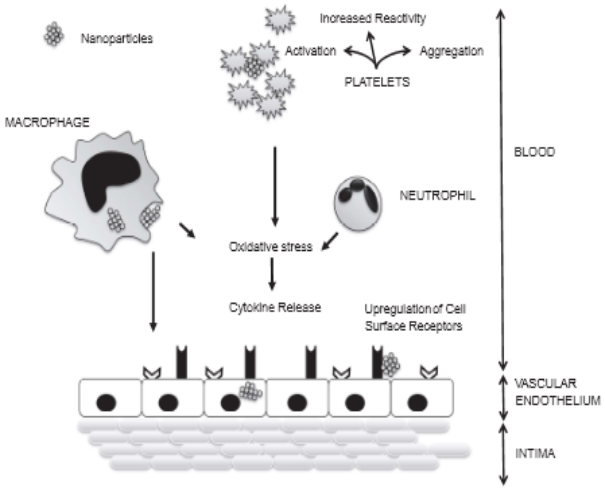

f0020 FIGURE 8.3 Overview of interactions of blood-borne engineered nanoparticles.

f0025 FIGURE 8.4 Pathways of nanoparticle-mediated cardiovascular morbidity and death.

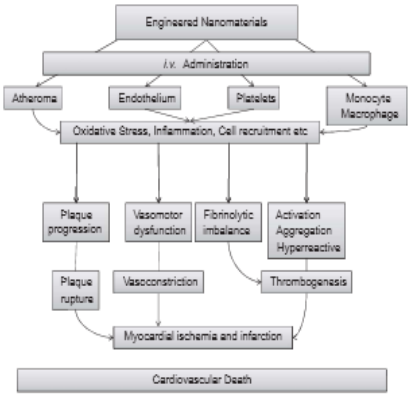

10008-FADEEL-9780123869401

When studying the impact of engineered nanomaterials on a complex multisystem disease, it is important to take into consideration potential downstream, indirect effects as well as direct toxicity. Shaw et al. [87] demonstrated that CDNP induce moderate toxicity and inflammatory effects on endothelial cells following direct incubation, these effects were amplified when endothelial cells were exposed to conditioned supernatant from monocyte-derived macrophages exposed to CDNP due to the release of cytokines from CDNP laden macrophages. This approach utilizing co-culture and other techniques that model the secondary effects of CDNP [88–90] could be very useful in studying the cardiovascular effects of engineered nanomaterials. Nanomaterials are increasingly being used in cell tracking to monitor disease progression [43,91,92]. It is no longer sufficient to assess the potential toxicity of engineered nanoparticles on the cell carriers alone; it is essential that these cells do not become "time bombs" capable of releasing vast quantities of pro-inflammatory mediators in a vulnerable atherosclerotic plaque. This mechanism may be equally important in the occupational setting where inhalation of nanomaterials has been shown to have systemic effects on the cardiovascular system [93–97].

s0060 *In vivo* Studies

p0140 *In vivo* studies carried out in susceptible animals have contributed significantly to our understanding of cardiovascular disease. In the ApoE knock-out mouse, CDNP instilled into the lungs increases atherogenesis [10,98,99]. Indeed, engineered nanomaterials such as carbon nanotubes and titanium dioxide can accelerate plaque progression in susceptible animal models [74]. Mills et al. exposed healthy human volunteers to dilute diesel exhaust, pure carbon nanoparticles, filtered diesel exhaust, or filtered air, in a randomized double blind cross-over study demonstrating that the adverse vascular effects of diesel exhaust could be attributed mainly to the nanoparticulate component and not to the associated gaseous pollutants [100]. Observations *in vivo* were replicated *in vitro* using wire-myography providing a rationale for testing the effects of engineered nanomaterials on vascular function before introduction to the clinic.

s0065 *Ex vivo* Studies

p0145 *Ex vivo* studies have been very informative in modeling the effects of CDNP on cardiovascular disease and have potential use in determining the effects of engineered nanomaterials on cardiovascular disease. They allow measurements to be taken in tissues or artificial environments outside the organism but with as little as possible deviation from natural conditions with no risk to the patient. *Ex vivo* techniques have not been used widely to study the effects of engineered nanomaterials on the cardiovascular system due to the need for specialist equipment, training, and the high cost involved, however, given the potential to generate meaningful data in the near patient setting, these systems are worth consideration. *Ex vivo* techniques also side-step possible ethical issues associated with exposing healthy or disease populations to the unknown effects of engineered nanoparticles. Traditional *ex vivo* models have assessed the direct effects of CDNP in isolated vessels to assess vasomotor dysfunction. This chapter does not intend to review previous studies as they have largely focused on CDNP, however, this topic is very well covered by many comprehensive reviews

10008-FADEEL-9780123869401

(see Møller et al. [74]) and the findings could easily be applied to the study of the adverse effects of engineered nanomaterial [74].

p0150 A recent *ex vivo* study used the Langendorff heart as a model system to study the cardiovascular effects of engineered nanoparticles [101]. The isolated heart is a well-established method of modeling cardiac dysfunction and is used extensively to monitor electrophysiological parameters after exposure to investigational products. This model assesses the direct effects of engineered nanoparticles on the intact heart without the contribution from other systemic effects [74]. The authors report that silicon dioxide and titanium dioxide nanoparticles, as well as engineered nanoparticles made of flame soot, caused a significant dose-dependent increase in heart rate and promoted cardiac arrhythmia [101]. They hypothesize that the nanoparticle-induced increase in heart rate might be caused by the release of catecholamines from the sympathetic nerve endings in the heart, which was supported by studies using β1-receptor antagonism post-excision and by depleting catecholamine stores in the neurons pre-excision.

p0155 As many medical nanoparticles in development are for use in populations considered particularly vulnerable, it would be desirable to model this *ex vivo*. The Badimon chamber is an *ex vivo* model of deep arterial injury and thrombus formation used previously to study the effects of diesel exhaust inhalation on thrombosis in humans [10,102]. The chamber permits an assessment of thrombus formation in whole native blood without the need for anticoagulants or exposure of the patient to the compounds being tested. While principally used to assess the impact of novel antithrombotic agents, it can just as easily be used to assess the effects of engineered nanomaterials on thrombosis. A pump is used to draw blood from an ante-cubital vein through the chambers maintained at 37°C in a water bath. The rheological conditions in the first chamber simulate those of patent coronary arteries (low-shear rate), whereas those in the second and third chambers simulate those of stenosed coronary artery (high-shear rate) [10]. The thrombus formed in the low shear chamber is macrophage rich whereas the thrombus formed in high shear conditions is platelet rich [10] (Figure 8.5). The chamber is therefore potentially able to assess nanoparticle interactions with specific

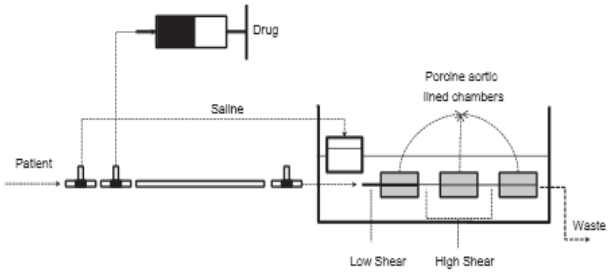

f0030 **FIGURE 8.5** Schematic of Badimon chamber set-up.

10008-FADEEL-9780123869401

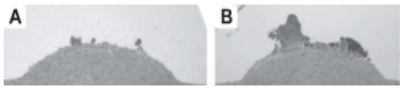

f0035 FIGURE 8.6 Porcine aortic strips from the Badimon chamber. Strip A represents a saline control run. Strip B represents a run with PEGylated quantum dots. Magnification: ×100.

cells and types of thrombus. Our preliminary investigations suggest that engineered nanomaterials may increase thrombus formation and that surface charge may be an important determinant (Figure 8.6).

s0070

TAKE-HOME MESSAGES

p0160 Engineered nanomaterials are likely to have a big impact on diagnostic assays, medical imaging and targeted therapeutics in the near future. Characteristics of these nanoparticles, such as size, surface area, charge and surface chemistry, as well as the method by which they are delivered, will determine their distribution, efficacy and potential toxicity. Nanoparticles designed for medical use are usually derived from materials deemed biologically safe, but it remains unclear how we define a "biologically safe"' material and, in particular, what investigations should be mandatory in the development of these materials. Unfortunately, the behavior of nanoparticles cannot be determined from their bulk properties; when relatively inert or safe materials in their bulk form are presented in the nano-scale they may exert previously unseen harmful effects on cells and systems. Several potential adverse effects on the cardiovascular system are indeed possible, as suggested by available *in vitro*, *in vivo* and *ex vivo* studies. If we are to maximize the potential of nanotechnologies in the field of medicine, we must ensure that novel nanomaterials are rigorously tested before introduction to the clinic.

References

[1] Medina C, Santos-Martinez MJ, Radomski A, Corrigan OI, Radomski MW. Nanoparticles: pharmacological and toxicological significance. Br J Pharmacol 2007;150:552–8.
[2] Linkov I, Satterstrom FK, Corey LM. Nanotoxicology and nanomedicine: making hard decisions. Nanomedicine 2008;4:167–71.
[3] Mills NL, Donaldson K, Hadoke PW, et al. Adverse cardiovascular effects of air pollution. Nat Clin Pract Cardiovasc Med 2008.
[4] Mills NL, Robinson SD, Fokkens PH, et al. Exposure to concentrated ambient particles does not affect vascular function in patients with coronary heart disease. Environ Health Perspect 2008;116:709–15.
[5] Donaldson K, Brown DM, Mitchell C, et al. Free radical activity of PM10: Iron-mediated generation of hydroxyl radicals. Environ Health Perspect 1997;105:1285–9.
[6] Renwick LC, Brown D, Clouter A, Donaldson K. Increased inflammation and altered macrophage chemotactic responses caused by two ultrafine particle types. Occup Environ Med 2004;61:442–7.
[7] Barlow PG, Clouter-Baker A, Donaldson K, Maccallum J, Stone V. Carbon black nanoparticles induce type II epithelial cells to release chemotaxins for alveolar macrophages. Part Fibre Toxicol 2005;2:11.
[8] Barath S, Mills NL, Lundback M, et al. Impaired vascular function after exposure to diesel exhaust generated at urban transient running conditions. Part Fibre Toxicol 2010;7:19.

[AQ1]

10008-FADEEL-9780123869401

[9] Mills NL, Tornqvist H, Gonzalez MC, et al. Ischemic and thrombotic effects of dilute diesel-exhaust inhalation in men with coronary heart disease. N Engl J Med 2007;357:1075–82.
[10] Lucking AJ, Lundback M, Mills NL, et al. Diesel exhaust inhalation increases thrombus formation in man. Eur Heart J 2008;29:3043–51.
[11] Hoffmann B, Moebus S, Kroger K, et al. Residential exposure to urban air pollution, ankle-brachial index, and peripheral arterial disease. Epidemiology 2009;20:280–8.
[12] Wang TJ. Assessing the role of circulating, genetic, and imaging biomarkers in cardiovascular risk prediction. Circulation 2011;123:551–65.
[13] Viera AJ, Sheridan SL. Global risk of coronary heart disease: assessment and application. Am Fam Physician 2010;82:265–74.
[14] van Gils JM, Zwaginga JJ, Hordijk PL. Molecular and functional interactions among monocytes, platelets, and endothelial cells and their relevance for cardiovascular diseases. J Leukoc Biol 2009;85:195–204.
[15] Slevin M, Wang Q, Font MA, et al. Atherothrombosis and plaque heterology: different location or a unique disease? Pathobiology 2008;75:209–25.
[16] Song S, Qin Y, He Y, Huang Q, Fan C, Chen HY. Functional nanoprobes for ultrasensitive detection of biomolecules. Chem Soc Rev 2010;39:4234–43.
[17] Cormode DP, Skajaa T, Fayad ZA, Mulder WJ. Nanotechnology in medical imaging: probe design and applications. Arterioscler Thromb Vasc Biol 2009;29:992–1000.
[18] Kim BY, Rutka JT, Chan WC. Nanomedicine. N Engl J Med 2010;363:2434–43.
[19] Kim D, Yu MK, Lee TS, Park JJ, Jeong YY, Jon S. Amphiphilic polymer-coated hybrid nanoparticles as CT/MRI dual contrast agents. Nanotechnology 2011;22:155101.
[20] Schladt TD, Schneider K, Schild H, Tremel W. Synthesis and bio-functionalization of magnetic nanoparticles for medical diagnosis and treatment. Dalton Trans 2011.
[21] Stark DD, Moseley ME, Bacon BR, et al. Magnetic resonance imaging and spectroscopy of hepatic iron overload. Radiology 1985;154:137–42.
[22] Renshaw PF, Owen CS, McLaughlin AC, Frey TG, Leigh Jr JS. Ferromagnetic contrast agents: a new approach. Magn Reson Med 1986;3:217–25.
[23] Uppal R, Caravan P. Targeted probes for cardiovascular MRI. Future Med Chem 2010;2:451–70.
[24] Fukukura Y, Kamiyama T, Takumi K, Shindo T, Higashi R, Nakajo M. Comparison of ferucarbotran-enhanced fluid-attenuated inversion-recovery echo-planar, T2-weighted turbo spin-echo, T2*-weighted gradient-echo, and diffusion-weighted echo-planar imaging for detection of malignant liver lesions. J Magn Reson Imaging 2010;31:607–16.
[25] Beduneau A, Ma Z, Grotepas CB, et al. Facilitated monocyte-macrophage uptake and tissue distribution of superparmagnetic iron-oxide nanoparticles. PLoS One 2009;4:e4343.
[26] Weidner AM, van Lin EN, Dinter DJ, et al. Ferumoxtran-10 MR lymphography for target definition and follow-up in a patient undergoing image-guided, dose-escalated radiotherapy of lymph nodes upon PSA relapse. Strahlenther Onkol 2011;187:206–12.
[27] Krombach GA, Wandland MF, Higgins CB, Saeed M. MR imaging of spatial extent of microvascular injury in reperfused ischemically injured rat myocardium: value of blood pool ultrasmall superparamagnetic particles of iron oxide. Radiology 2002;225:479–86.
[28] Harisinghani MG, Barentsz J, Hahn PF, et al. Noninvasive detection of clinically occult lymph-node metastases in prostate cancer. N Engl J Med 2003;348:2491–9.
[29] Harisinghani MG, Saini S, Slater GJ, Schnall MD, Rifkin MD. MR imaging of pelvic lymph nodes in primary pelvic carcinoma with ultrasmall superparamagnetic iron oxide (Combidex): preliminary observations. J Magn Reson Imaging 1997;7:161–3.
[30] Klug G, Bauer L, Bauer WR. Patterns of USPIO deposition in murine atherosclerosis. Arterioscler Thromb Vasc Biol 2008;28:E157–9.
[31] Klug K, Gert G, Thomas K, et al. Murine atherosclerotic plaque imaging with the USPIO Ferumoxtran-10. Front Biosci 2009;14:2546–52.
[32] Sigovan M, Boussel L, Sulaiman A, et al. Rapid-clearance iron nanoparticles for inflammation imaging of atherosclerotic plaque: initial experience in animal model. Radiology 2009;252:401–9.
[33] Briley-Saebo KC, Mani V, Hyafil F, Cornily JC, Fayad ZA. Fractionated Feridex and positive contrast: in vivo MR imaging of atherosclerosis. Magn Reson Med 2008;59:721–30.

10008-FADEEL-9780123869401

[34] Morishige K, Kacher DF, Libby P, et al. High-resolution magnetic resonance imaging enhanced with superparamagnetic nanoparticles measures macrophage burden in atherosclerosis. Circulation 2010;122:1707–15.
[35] Richards JM, Semple SI, Macgillivray TJ, et al. Abdominal aortic aneurysm growth predicted by uptake of ultrasmall superparamagnetic particles of iron oxide: a pilot study. Circ Cardiovasc Imaging 2011;4:274–81.
[36] Tang TY, Howarth SP, Miller SR, et al. Correlation of carotid atheromatous plaque inflammation using USPIO-enhanced MR imaging with degree of luminal stenosis. Stroke 2008;39:2144–7.
[37] Yilmaz A, Rosch S, Klingel K, et al. Magnetic resonance imaging (MRI) of inflamed myocardium using iron oxide nanoparticles in patients with acute myocardial infarction – Preliminary results. Int J Cardiol 2011. [AQ3]
[38] Trivedi RA, King-Im JM, Graves MJ, et al. In vivo detection of macrophages in human carotid atheroma: temporal dependence of ultrasmall superparamagnetic particles of iron oxide-enhanced MRI. Stroke 2004;35:1631–5.
[39] Kooi ME, Cappendijk VC, Cleutjens KB, et al. Accumulation of ultrasmall superparamagnetic particles of iron oxide in human atherosclerotic plaques can be detected by in vivo magnetic resonance imaging 2. Circulation 2003;107:2453–8.
[40] Schmitz SA, Taupitz M, Wagner S, Wolf KJ, Beyersdorff D, Hamm B. Magnetic resonance imaging of atherosclerotic plaques using superparamagnetic iron oxide particles. J Magn Reson Imaging 2001;14:355–61.
[41] Trivedi R, King-Im J, Gillard J. Accumulation of ultrasmall superparamagnetic particles of iron oxide in human atherosclerotic plaque. Circulation 2003;108:e140.
[42] Ruehm SG, Goyen M, Barkhausen J, et al. Rapid magnetic resonance angiography for detection of atherosclerosis. Lancet 2001;357:1086–91.
[43] Jing XH, Yang L, Duan XJ, et al. In vivo MR imaging tracking of magnetic iron oxide nanoparticle labeled, engineered, autologous bone marrow mesenchymal stem cells following intra-articular injection. Joint Bone Spine 2008;75:432–8.
[44] Eck W, Nicholson AI, Zentgraf H, Semmler W, Bartling S. Anti-CD4-targeted gold nanoparticles induce specific contrast enhancement of peripheral lymph nodes in X-ray computed tomography of live mice. Nano Lett 2010;10:2318–22.
[45] Thu MS, Najbauer J, Kendall SE, et al. Iron labeling and pre-clinical MRI visualization of therapeutic human neural stem cells in a murine glioma model. PLoS One 2009;4:e7218.
[46] Zhao Y, Zhao L, Zhou L, et al. Quantum dot conjugates for targeted silencing of bcr/abl gene by RNA interference in human myelogenous leukemia K562 cells. J Nanosci Nanotechnol 2010;10:5137–43.
[47] Lodhia J, Mandarano G, Ferris N, Eu P, Cowell S. Development and use of iron oxide nanoparticles (Part 1): Synthesis of iron oxide nanoparticles for MRI. Biomed Imaging Interv J 2010;6:e12.
[48] Liu Z, Lammers T, Ehling J, et al. Iron oxide nanoparticle-containing microbubble composites as contrast agents for MR and ultrasound dual-modality imaging. Biomaterials 2011;32:6155–63.
[49] Briley-Saebo KC, Cho YS, Shaw PX, et al. Targeted iron oxide particles for in vivo magnetic resonance detection of atherosclerotic lesions with antibodies directed to oxidation-specific epitopes. J Am Coll Cardiol 2011;57:337–47.
[50] Yang F, Li L, Li Y, Chen Z, Wu J, Gu N. Superparamagnetic nanoparticle-inclusion microbubbles for ultrasound contrast agents. Phys Med Biol 2008;53:6129–41.
[51] Mulder WJ, Strijkers GJ, Briley-Saboe KC, et al. Molecular imaging of macrophages in atherosclerotic plaques using bimodal PEG-micelles. Magn Reson Med 2007;58:1164–70.
[52] Amirbekian V, Lipinski MJ, Briley-Saebo KC, et al. Detecting and assessing macrophages in vivo to evaluate atherosclerosis noninvasively using molecular MRI. Proc Natl Acad Sci USA 2007;104:961–6.
[53] Khlebtsov N, Dykman L. Biodistribution and toxicity of engineered gold nanoparticles: a review of in vitro and in vivo studies. Chem Soc Rev 2011;40:1647–71.
[54] Pan D, Pramanik M, Senpan A, Wickline SA, Wang LV, Lanza GM. A facile synthesis of novel self-assembled gold nanorods designed for near-infrared imaging. J Nanosci Nanotechnol 2010;10:8118–23.
[55] van Schooneveld MM, Cormode DP, Koole R, et al. A fluorescent, paramagnetic and PEGylated gold/silica nanoparticle for MRI, CT and fluorescence imaging. Contrast Media Mol Imaging 2010;5:231–6.
[56] Al-Jamal WT, Al-Jamal KT, Cakebread A, Halket JM, Kostarelos K. Blood circulation and tissue biodistribution of lipid–quantum dot (L-QD) hybrid vesicles intravenously administered in mice. Bioconjug Chem 2009;20:1696–702.

10008-FADEEL-9780123869401

[57] Li SD, Huang L. Pharmacokinetics and biodistribution of nanoparticles. Mol Pharm 2008;5:496–504.
[58] van Tilborg GA, Strijkers GJ, Fouget EM, et al. Kinetics of avidin-induced clearance of biotinylated bimodal liposomes for improved MR molecular imaging. Magn Reson Med 2008;60:1444–56.
[59] Jayagopal A, Russ PK, Haselton FR. Surface engineering of quantum dots for in vivo vascular imaging. Bioconjug Chem 2007;18:1424–33.
[60] De Jong WH, Hagens WI, Krystek P, Burger MC, Sips AJ, Geertsma RE. Particle size-dependent organ distribution of gold nanoparticles after intravenous administration. Biomaterials 2008;29:1912–9.
[61] Hirn S, Semmler-Behnke M, Schleh C, et al. Particle size-dependent and surface charge-dependent biodistribution of gold nanoparticles after intravenous administration. Eur J Pharm Biopharm 2011;77:407–16.
[62] Mills NL, Robinson SD, Fokkens PH, et al. Exposure to concentrated ambient particles does not affect vascular function in patients with coronary heart disease. Environ Health Perspect 2008;116:709–15.
[63] Geiser M, Rothen-Rutishauser B, Kapp N, et al. Ultrafine particles cross cellular membranes by nonphagocytic mechanisms in lungs and in cultured cells. Environ Health Perspect 2005;113:1555–60.
[64] Moller W, Brown DM, Kreyling WG, Stone V. Ultrafine particles cause cytoskeletal dysfunctions in macrophages: role of intracellular calcium. Part Fibre Toxicol 2005;2:7.
[65] Brown LM, Collings N, Harrison RM, Maynard AD, Maynard RL. Ultrafine particles in the atmosphere. London: Imperial College Press; 2003.
[66] Brook RD, Brook JR, Urch B, Vincent R, Rajagopalan S, Silverman F. Inhalation of fine particulate air pollution and ozone causes acute arterial vasoconstriction in healthy adults. Circulation 2002;105:1534–6.
[67] Delfino RJ, Sioutas C, Malik S. Potential role of ultrafine particles in associations between airborne particle mass and cardiovascular health. Environ Health Perspect 2005;113:934–46.
[68] Mills NL, Miller JJ, Anand A, et al. Increased arterial stiffness in patients with chronic obstructive pulmonary disease; a mechanism for increased cardiovascular risk. Thorax 2007.
[69] Mills NL, Donaldson K, Hadoke PW, et al. Adverse cardiovascular effects of air pollution. Nat Clin Pract Cardiovasc Med 2009;6:36–44.
[70] Langrish JP, Mills NL, Newby DE. Air pollution: the new cardiovascular risk factor. Intern Med J 2008;38:875–8.
[71] Donaldson K. Resolving the nanoparticles paradox. Nanomedicine 2006;1:229–34.
[72] Donaldson K, Seaton A. The Janus faces of nanoparticles. J Nanosci Nanotechnol 2007;7:4607–11.
[73] Donaldson K, Tran L, Jimenez L, et al. Combustion-derived nanoparticles: A review of their toxicology following inhalation exposure 1. Part Fibre Toxicol 2005;2:10.
[74] Møller P, Mikkelsen L, Vesterdal LK, et al. Hazard identification of particulate matter on vasomotor dysfunction and progression of atherosclerosis. Crit Rev Toxicol 2011;41:339–68.
[75] Eisen EA, Costello S, Chevrier J, Picciotto S. Epidemiologic challenges for studies of occupational exposure to engineered nanoparticles; a commentary. J Occup Environ Med 2011;53:S57–61.
[76] Castranova V. Overview of current toxicological knowledge of engineered nanoparticles. J Occup Environ Med 2011;53:514–7.
[77] McGuinnes C, Duffin R, Brown S, et al. Surface derivatization state of polystyrene latex nanoparticles determines both their potency and their mechanism of causing human platelet aggregation in vitro. Toxicol Sci 2011;119:359–68.
[78] Zhu MT, Wang B, Wang Y, et al. Endothelial dysfunction and inflammation induced by iron oxide nanoparticle exposure: Risk factors for early atherosclerosis. Toxicol Lett 2011;203:162–71.
[79] Zhu MT, Wang Y, Feng WY, et al. Oxidative stress and apoptosis induced by iron oxide nanoparticles in cultured human umbilical endothelial cells. J Nanosci Nanotechnol 2010;10:8584–90.
[80] Sun J, Wang S, Zhao D, Hun FH, Weng L, Liu H. Cytotoxicity, permeability, and inflammation of metal oxide nanoparticles in human cardiac microvascular endothelial cells: Cytotoxicity, permeability, and inflammation of metal oxide nanoparticles. Cell Biol Toxicol 2011.
[81] Neun BW, Dobrovolskaia MA. Method for in vitro analysis of nanoparticle thrombogenic properties. Meth Mol Biol 2011;697:225–35.
[82] Bihari P, Holzer M, Praetner M, et al. Single-walled carbon nanotubes activate platelets and accelerate thrombus formation in the microcirculation. Toxicology 2010;269:148–54.
[83] Lu S, Duffin R, Poland C, et al. Efficacy of simple short-term in vitro assays for predicting the potential of metal oxide nanoparticles to cause pulmonary inflammation. Environ Health Perspect 2009;117:241–7.

B. ENGINEERED NANOMATERIALS: IMPACT ON HUMAN HEALTH

10008-FADEEL-9780123869401

[84] Radomski A, Jurasz P, onso-Escolano D, et al. Nanoparticle-induced platelet aggregation and vascular thrombosis 3. Br J Pharmacol 2005;146:882–93.
[85] Dick CA, Brown DM, Donaldson K, Stone V. The role of free radicals in the toxic and inflammatory effects of four different ultrafine particle types. Inhal Toxicol 2003;15:39–52.
[86] Miller VM, Hunter LW, Chu K, et al. Biologic nanoparticles and platelet reactivity. Nanomedicine (Lond) 2009;4:725–33.
[87] Shaw CA, Robertson S, Miller MR, et al. Diesel exhaust particulate-exposed macrophages cause marked endothelial cell activation. Am J Respir Cell Mol Biol 2011;44:840–51.
[88] Inoue K, Takano H. Another systemic impact of inhaled diesel exhaust particles. Toxicol Sci 2010;115:607–8.
[89] Ishii H, Hayashi S, Hogg JC, et al. Alveolar macrophage-epithelial cell interaction following exposure to atmospheric particles induces the release of mediators involved in monocyte mobilization and recruitment. Respir Res 2005;6:87.
[90] Porter M, Karp M, Killedar S, et al. Diesel-enriched particulate matter functionally activates human dendritic cells. Am J Respir Cell Mol Biol 2007;37:706–19.
[91] Jendelova P, Herynek V, Urdzikova L, et al. Magnetic resonance tracking of transplanted bone marrow and embryonic stem cells labeled by iron oxide nanoparticles in rat brain and spinal cord. J Neurosci Res 2004;76:232–43.
[92] Voura EB, Jaiswal JK, Mattoussi H, Simon SM. Tracking metastatic tumor cell extravasation with quantum dot nanocrystals and fluorescence emission-scanning microscopy. Nat Med 2004;10:993–8.
[93] Adamkiewicz G, Ebalt S, Syring M, et al. Association between air pollution exposure and exhaled nitric oxide in an elderly population. Thorax 2004;59:204–9.
[94] Antonini JM. Health effects of welding. Crit Rev Toxicol 2003;33:61–103.
[95] Behndig AF, Mudway IS, Brown JL, et al. Airway antioxidant and inflammatory responses to diesel exhaust exposure in healthy humans 11. Eur Respir J 2006;27:359–65.
[96] Brook RD, Brook JR, Rajagopalan S. Air pollution: the "Heart" of the problem. Curr Hypertens Rep 2003;5:32–9.
[97] Faro-Moreno E, Nawrot TS, Nemmar A, Nemery B. Particulate matter in the environment: pulmonary and cardiovascular effects. Curr Opin Pulm Med 2007;13:98–106.
[98] Tornqvist H, Mills NL, Gonzalez M, et al. Persistent endothelial dysfunction in humans after diesel exhaust inhalation. Am J Respir Crit Care Med 2007;176:395–400.
[99] Jacobsen NR, Moller P, Jensen KA, et al. Lung inflammation and genotoxicity following pulmonary exposure to nanoparticles in ApoE-/- mice. Part Fibre Toxicol 2009;6:2.
[100] Mills NL, Miller MR, Lucking AJ, et al. Combustion-derived nanoparticulate induces the adverse vascular effects of diesel exhaust inhalation. Eur Heart J 2011. [AQ6]
[101] Stampfl A, Maier M, Radykewicz R, Reitmeir P, Gottlicher M, Niessner R. Langendorff heart: a model system to study cardiovascular effects of engineered nanoparticles. ACS Nano 2011. [AQ7]
[102] Lundback M, Mills NL, Lucking A, et al. Experimental exposure to diesel exhaust increases arterial stiffness in man. Part Fibre Toxicol 2009;6:7.

10008-FADEEL-9780123869401

176 © Schattauer 2012 New Technologies, Diagnostic Tools and Drugs

Lyophilised reconstituted human platelets increase thrombus formation in a clinical *ex vivo* model of deep arterial injury

Nikhil Vilas Joshi[1]; Jennifer B. Raftis[2]; Andrew J. Lucking[1]; Amanda H. Hunter[1]; Mike Millar[3]; Mike Fitzpatrick[4]; Giora Z. Feuerstein[4]; David E. Newby[1]

[1]Centre for Cardiovascular Sciences, University of Edinburgh, UK; [2]Centre for Inflammation Research, University of Edinburgh, UK; [3]Centre for Reproductive Health, University of Edinburgh, UK; [4]Cellphire INC., Rockville, Maryland, USA

Summary

Platelets are the principal component of the innate haemostatic system that protect from traumatic bleeding. We investigated whether lyophilised human platelets (LHPs) could enhance clot formation within platelet-free and whole blood environments using an *ex vivo* model of deep arterial injury. Lyophilised human platelets were produced from stored human platelets and characterised using conventional, fluorescent and electron microscopic techniques. LHPs were resuspended in platelet-free plasma (PFP) obtained from citrated whole human blood to form final concentrations of 0, 20 and 200 x 10^9 LHPs/L. LHPs with recalcified PFP or whole blood were perfused through the chamber at low (212 s^{-1}) and high (1,690 s^{-1}) shear rates with porcine aortic tunica media as thrombogenic substrate. LHPs shared morphological characteristics with native human platelets and were incorporated into clot generated from PFP or whole blood. Histomorphometrically measured mean thrombus area increased in a dose-dependent manner following the addition of LHPs to PFP under conditions of high shear [704 $\mu m^2 \pm$ 186 μm^2 (mean ± SEM), 1,511 $\mu m^2 \pm$ 320 μm^2 and 2,378 $\mu m^2 \pm$ 315 μm^2, for LHPs at 0, 20 and 200 x 10^9/l, respectively ($p = 0.012$)]. Lyophilised human platelets retain haemostatic properties when reconstituted in both PFP and whole blood, and enhance thrombus formation in a model of deep arterial injury. These data suggest that LHPs have the potential to serve as a therapeutic intervention during haemorrhage under circumstances of trauma, and platelet depletion or dysfunction.

Keywords

Bleeding disorders, haemostasis, lyophilised human platelets, platelet substitutes

Correspondence to:
Dr. Nikhil Vilas Joshi
SU 305, Chancellors Building
University/BHF Centre for Cardiovascular Science
Little France Crescent, Edinburgh, UK
Tel.: +44 131 242 6515, Fax: +44 131 242 6422
E-mail: nikhil.joshi@ed.ac.uk

Financial support:
The study was supported by an unrestricted research grant by Cellphire Inc. NVJ is supported by Chief Scientist Office (ETM/160) and BMA's Josephine Lansdell Award (2011).

Received: February 1, 2012
Accepted after major revision: April 1, 2012
Prepublished online: May 25, 2012
doi:10.1160/TH12-02-0059
Thromb Haemost 2012; 108: 176–182

Introduction

Platelets play a key role in achieving haemostasis during bleeding and are crucial in preventing excessive blood loss. Patients with thrombocytopaenia, disordered platelet function and traumatic injuries are at substantial risk of haemorrhage and frequently require donor platelet transfusion. Platelet concentrates for transfusion have been available for routine clinical use for more than four decades: more than 1·5 million platelets transfusions are undertaken in the US and 2.9 million in Europe each year (1). Use of fresh or stored human platelets requires storage at 22°C, and have a mandated shelf life of 5–7 days due to the risk of sepsis and other reactions that increase in frequency and severity with the length of storage (2). Furthermore, compared to fresh platelets, stored platelets are less effective at controlling acute haemorrhage due to altered functional integrity and structure (3). Further barriers for the use of fresh human platelets are their limited availability in rural hospitals and front line military combat zones, where there are no means to obtain, store and deliver fresh platelets. This is particularly relevant, as trauma-related haemorrhage remains the single most important cause of death in the pre-hospital civilian and miliary setting (4, 5). The total costs of obtaining and making platelets ready for transfusion may exceed one billion dollars annually in the US alone (6).

The development of a novel platelet product is an increasingly important scientific and clinical endeavor. A haemostatically effective product could eventually replace, supplement, or serve as an adjunct to the use of standard allogeneic platelets transfusion (7). Various methods to develop more stable platelet-derived products have been employed. However, this approach has yet to be materialised (8). We here describe a lyophilised human platelet (LHP) product that shows considerable therapeutic promise with demonstrable and persistent haemostatic activity (9, 10).

Characterisation of LHPs (Thrombosomes, Cellphire Inc., Rockville, MD, USA) has been performed and data regarding surface marker presentation, size, thrombin generation, and *in vivo*

safety and efficacy has been previously reported (9, 10). These LHPs have shown high *in vitro* Annexin V binding, with ability to adhere spontaneously, when perfused over collagen-coated glass capillaries (10). However, it remains unclear whether LHPs are efficacious in conditions where platelets are deficient or dysfunctional, and whether they can contribute to haemostasis in humans.

The investigation of dynamic *in situ* thrombus formation in humans is challenging because of the ethical and technical challenges that this presents. The Badimon chamber is an *ex vivo* model of thrombosis that is suitable for use in clinical studies and has a number of important advantages over other techniques including the ability to assess thrombus formation on a pathophysiologically relevant substrate and under conditions of continuous flow (11–14). Using this model, we sought to characterise and investigate whether LHPs have the potential to contribute to human clot formation within platelet-depleted or whole blood environments.

Methods

Healthy volunteers

Blood was collected from healthy non-smoking volunteers, aged between 18 and 35 years who did not have evidence of coagulopathy or any clinically significant illness. The study was performed according to the Declaration of Helsinki, with the approval of the local research ethics committee and the written informed consent of all subjects.

Platelet-free plasma (PFP)

Blood (250 ml) was collected using a 17 G needle and citrated using 25 ml of 3.8% sodium citrate (1/10 dilution; v/v). Citrated blood was centrifuged at 200 g for 20 minutes (min) (MSE Mistral 3000i, DJB Labcare, Buckinghamshire, UK)), without brake at 25°C to obtain platelet-rich plasma (PRP). PRP was carefully aspirated and further centrifuged at 750 g without brake or acceleration for 20 min to obtain platelet-poor plasma (PPP). This was filtered initially using a 0.44 µm (Millex-GP, Millipore, Billerica, MA, USA) and then by a 0.22 µm (Millex-GP, Millipore) syringe-driven filter to obtain PFP. The absence of platelets was confirmed by a Coulter counter (Multisiser™ 3 Coulter Counter®, Beckman Coulter, Brea, CA, USA).

Lyophilised human platelets

Cryo-lyophilised human platelets are presented in vacuum-sealed vials after being manufactured by lyophilisation of human in date-stored platelets (hIDSP) as a source material by proprietary process developed by Cellphire Inc. (Thrombosomes®; Cellphire Inc.) (9, 10). This process results in a LHP concentration of 2.0 ± 0.3 x 10^9/ml in a physiological buffer that can be reconstituted in 5 min by the addition sterile water. Lyophilised human platelets were then re-suspended in PFP or whole blood to achieve a final volume of 60 ml at 20 or 200 x10^9/l to be drawn into the Badimon chamber.

The Badimon chamber

Thrombus formation was measured using the Badimon chamber (▶Fig. 1) as described previously (15–17). In brief, a peristaltic pump (Alaris Asena GH; Cardinal Health, San Diego, CA, USA) was used to draw PFP, or whole blood directly from the subject, through a series of three cylindrical perfusion chambers maintained at 37°C in a water bath. Carefully prepared strips of porcine aorta (Pel-Freez Biologicals, Rogers, AR, USA), from which the

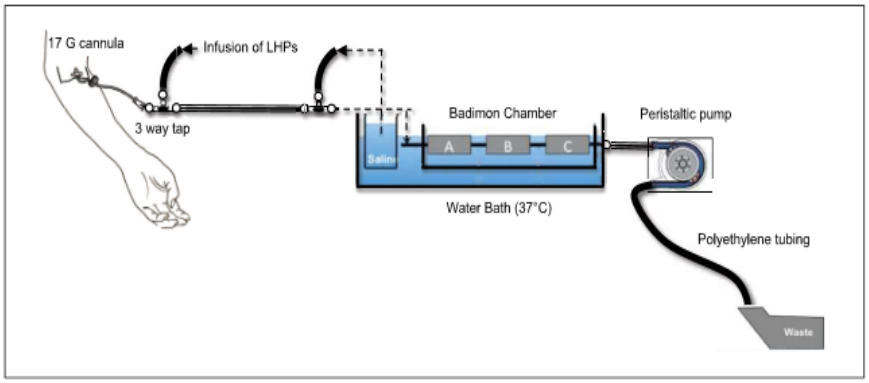

Figure 1: The Badimon chamber. Schematic illustration of the Badimon chamber with extra-corporeal infusion of lyophilised human platelets (LHPs).

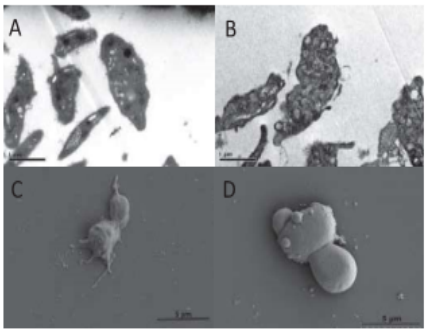

Figure 2: Electron microscopy. A) Transmission electron microscopy of fresh human platelets. B) Transmission electron microscopy of lyophilised human platelets. Dense granules and alpha-granules were less distinct than fresh platelets suggesting loss of cytoplasmic architecture and granule integrity. C) Scanning electron microscopy of fresh human platelets. D) Scanning electron microscopy of lyophilised human platelets. Morphology consistent with activated platelets.

intima and a thin layer of media had been removed, acted as the thrombogenic substrate as a model of deep arterial injury (13). The rheological conditions in the first chamber simulate those of patent coronary arteries (low shear rate, approx. 212 s^{-1}), while those in the second and third chambers simulate those of mildly stenosed coronary arteries (high shear rate, approx. 1,690 s^{-1}).

Each study lasted for 5 min during which flow was maintained at a constant rate of 10 ml/min using a peristaltic pump (Masterflex model 7013, Cole-Palmer Instruments, Vernon Hills, IL, USA) positioned distal to the chambers. Following perfusion, the chambers were flushed with 0.9% saline for one minute under the same rheological conditions.

Tissue histology

Immediately after each study, the porcine strips with thrombus attached were carefully removed and fixed in 4% paraformaldehyde for 72 hours (h). Each strip was subsequently paraffin-wax embedded and 5 µm sections were prepared. Sections were stained with Masson's trichrome stain to detect total thrombus area. For immunohistochemical staining of glycoprotein IIb/IIIa receptor, sections were stained using a Leica Vision Biosystems Bond x immunostaining robot. Briefly after blocking in peroxide for 10 min, sections were incubated with the mouse anti-human integrin alpha-2b/beta-3a monoclonal antibody (Thermo Fisher Scientific, Rockford, IL, USA) at a final dilution of 1:1,000 for 120 min at room temperature. All incubation steps were followed by washing in TBS/Tween sections were incubated for 15 min with prepolymer/post primary block, 15 min with polymer (HRP) prior to DAB (3,3'-Diaminobenzidine) visualisation and haematoxylin counterstain as per manufacturer's instructions. Sections were dehydrated in graded ethanol, cleared in xylene before coverslipping in Pertex. Images were taken on a Zeiss Axioskop2 fitted with an Axiocam MRc digital camera using Axiovision software.

Electron microscopy

Native platelets and LHPs were suspended in a 3% glutaraldehyde solution with 0.1 M cacodylate buffer at pH 7.4 for at least 1 h. After fixation, cells were centrifuged and re-suspended in sterile water before being pelleted and overlaid with platelet-free plasma and 0.1 M cacodylate buffer. For transmission electron microscopy, cell pellets were post-fixed in 1% osmium tetra-oxide, embedded in araldite resin and cut into ultra-thin sections (60 nm thick) before viewing on a Philips CM12 transmission electron microscope (Philips Electronic Instruments Inc., Mahwah, NJ, USA). For scanning electron microscopy, platelets were allowed to settle on glass coverslips, rinsed and then stained with osmium tetra-oxide before critical point drying and sputter coating with gold before viewing on a Hitachi S-2600N digital scanning electron microscope (Oxford Instruments, Oxfordshire, UK).

Study protocol

PFP studies

To assess whether LHPs contributed to thrombus formation under conditions of shear stress in the absence of platelets, LHPs were re-suspended in PFP to give a final concentration of 0, 20 and 200 x 10^9 particles/l. To counteract the effect of citrate in the plasma, 1.2 ml of 1 M $CaCl_2$ added to every 60 ml of plasma, just prior to entry into the Badimon chamber.

Ex vivo whole blood studies

To assess whether LHPs contribute to thrombus formation in whole human blood, a pump was used to draw blood from an antecubital vein to generate *ex vivo* thrombus in the Badimon chamber. Fluorescein isothiocyanate (FITC) anti-glycoprotein IIb/IIIa labelled LHPs (Thrombosomes®; Cellphire Inc.) were added to the extracorporeal circuit with a calibrated syringe driver (Alaris Asena GH; Cardinal Health), and allowed to mix prior to entering the perfusion chambers as previously described (15, 16). After 24 h fixation in 4% paraformaldehyde the strips were paraffin- wax embedded. As paraffin processing destroys the FITC fluorescence, the samples were then sectioned and stained with anti-FITC antibody to identify the LHPs as described above.

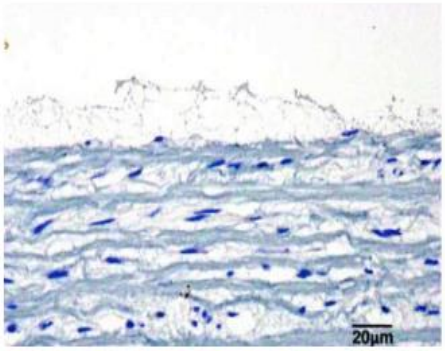

A

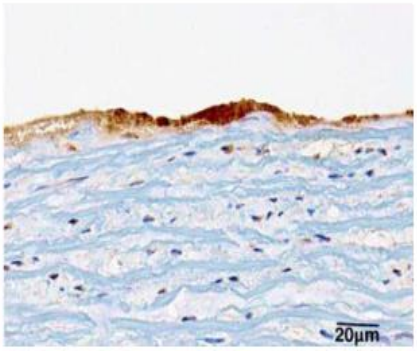

B

Figure 3: Immunohistochemistry in platelet-free plasma (PFP) system. Glycoprotein IIb/IIIa receptor staining, sections incubated with the mouse anti-human integrin alpha-2b/beta-3 monoclonal antibody, counterstained with hematoxylin. A) Representative image of thrombus generated in PFP; high shear chamber. Thrombus is stained with background hematoxylin stain only confirming absence of glycoprotein IIb/IIIa receptor expression (40x magnification). B) Thrombus generated by lyophilised human platelets in PFP; high shear chamber. There is intense dark stain indicative of glycoprotein IIb/IIIa receptor expression (40x magnification).

Statistical analysis

Continuous variables are reported as mean ± standard error of the mean. Statistical analysis was performed with GraphPad Prism (GraphPad Software, La Jolla, CA, USA) by one-way ANOVA with post-hoc tests (Dunn's multiple comparison test). Statistical significance was taken at two-sided $p < 0.05$.

Results

Characterisation of LHPs

Scanning electron microscopy identified that LHPs assumed morphology consistent with activated platelets (▶ Fig. 2). On transmission electron microscopy, dense granules and alpha-granules were less distinct than with normal platelets suggesting some changes of cytoplasmic architecture and granule morphology.

Histology

Histological sections from the porcine aortic strips in the Badimon chamber identified uptake of LHPs into thrombus generated by PFP, and this was confirmed by immunohistochemistry staining of a platelet specific surface fibrinogen receptor GPIIb/IIIa complex (▶ Fig. 3).

The platelet count of subjects at the time of *ex vivo* studies was 327 ± 82 x 10^9/l. LHPs contributed towards thrombus formation in whole human blood as evidenced by incorporation of fluorescent-labelled LHPs into the thrombus in the *ex vivo* extracorporeal system (▶ Fig. 4).

Thrombus area

Given that LHPs would compete with normal competent platelets for thrombus formation in whole human blood, we wished to assess the effect of LHPs on thrombus formation in a platelet-free system. We therefore assessed thrombus formation in PFP in the presence and absence of LHPs. In the low shear chamber total thrombus area for the PFP which was 4,962 ± 961 µm². This appeared to increase further with the addition of LHPs at concentrations of 20 and 200 x 10^9/l: thrombus area 6,170 ± 866 µm² and 7,504 ± 1416 µm², respectively (one-way ANOVA, $P = 0.05$; ▶ Fig. 5). In the high shear chamber, the mean thrombus area with PFP increased from 704 ± 186 µm² to 1,511 ± 320 µm² and 2,378 ± 315 µm² respectively (one-way ANOVA, $p = 0.01$; ▶ Fig. 4) when LHPs were introduced in the same concentrations.

Discussion

Our study demonstrates the therapeutic potential of LHPs. We have shown that the LHPs are morphologically intact and share external appearances consistent with activated platelets. For the first time, we demonstrate that LHPs are actively incorporated within thrombus generated by human PFP and whole blood. Moreover, under conditions of platelet depletion, LHPs enhance thrombus formation under conditions of low and high-shear stress.

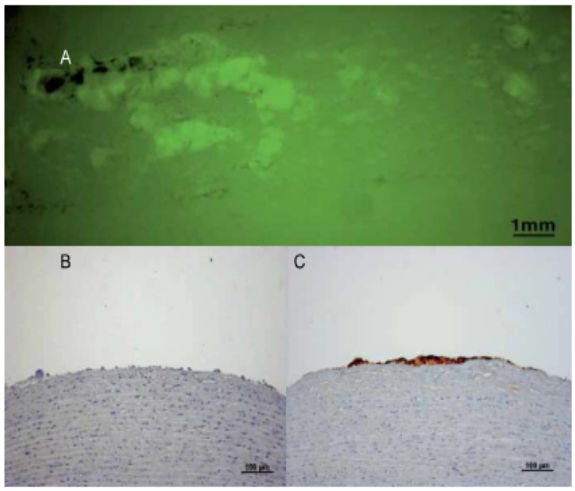

Figure 4: Fluorescence microscopy in an *ex vivo* whole blood system. A) Morphology of fresh thrombus formed on aortic strip in a high shear chamber after infusing FITC-labelled anti-glycoprotein IIb/IIIa LHPs into the *ex vivo* extra-corporal circuit. Image taken with confocal microscope using Yellow Fluorescent Protein filter settings (490–510 nm) to excite FITC-labelled lyophilised human platelets demonstrating native blood thrombus (non fluorescent and dark) integrating with fluorescent thrombus formed by lyophilised human platelets. B) Anti-FITC staining of thrombus in the absence of lyophilised human platelets. Negative control (10x magnification). C) Anti-FITC staining of FITC-labelled lyophilised human platelets with hematoxylin counter stain. The dark brown staining confirms the incorporation of LHPs into the thrombus (10x magnification).

Scanning and transmission electronic microscopy demonstrated that LHPs maintain the anatomical integrity and assume morphological characteristics of native activated human platelets. Although some loss of cytoplasmic definition is noted, there are significant structural similarities between fresh platelets and LHPs with comparable subcellular organelle distribution, membrane integrity and cytoskeletal structure, as suggested by previous studies (18, 19).

Our work is consistent with previously reported *in vitro* and animal studies on lyophilised platelets developed with different method of platelet preservation (18, 20–22). Lyophilised platelets are incorporated into the haemostatic plug at the site of injury and normalise prolonged bleeding time in a thrombocytopenic animal model (18). In a porcine liver injury model, there is reduced bleeding, improved haemodynamics, diminished lactate concentrations and markedly increased survival after infusion of LHPs (20). The safety of LHPs has been observed in several animal models including baboons (23), rabbits (21) and dogs (18), although one study has using a porcine liver injury model (20) has reported thrombotic complications with LHPs. More importantly, we have conducted extensive safety studies in canine and rabbit models where doses as high as 100 times the anticipated clinical dose (in humans) were infused with no adverse events noted including no evidence of either macroscopic or microscopic clots or haemorrhages (10).

One of the major limitations of the studies to date has been the lack of a consistent translational model to assess potential clinical efficacy (2, 24, 25). An *in vivo* model of thrombosis for use in clinical studies presents significant concerns and does not currently exist. We used the Badimon chamber as it represents a well established *ex vivo* model of deep arterial injury and thrombosis in humans. The Badimon chamber enables assessment in both low and high arterial shear stress conditions. We have previously demonstrated that fibrin is the main component of thrombus in the low-shear chamber and the platelets predominate in the high-shear chamber (13). Indeed, anti-platelet therapies have a predominant effect on thrombus burden in the high-shear chamber (11, 12, 26). To mimic a platelet-deplete state, we used human PFP to re-suspend the LHPs. This platelet depletion was successfully achieved and modified the size and constituents of the thrombus that is formed in the chamber. Indeed, we observed that the thrombus size was smaller in the high- compared to the low-shear chamber, which is the inverse of that seen with whole blood, and is consistent with the absence of platelets in PFP.

It has been suggested that there is glycoprotein IIb/IIIa receptor antigen loss during the process of lyophilisation using a different method of LHP production (27, 28). However, the *in vitro* data

What is known about this topic?

- Platelet concentrates for transfusion are available for routine clinical use, but their short-term shelf life means availability is limited in rural hospitals and front line combat zones.
- Lyophilised human platelets have shown promise as a platelets substitute and previous *in vivo* and animal studies have demonstrated their efficacy.

What does this paper add?

- Lyophilised human platelets actively contribute to thrombus formation in conditions of high shear and continuous flow in humans.
- These advanced haemostatic infusion products have therapeutic potential in patients with haemorrhage under circumstances of trauma, or platelet depletion or dysfunction.

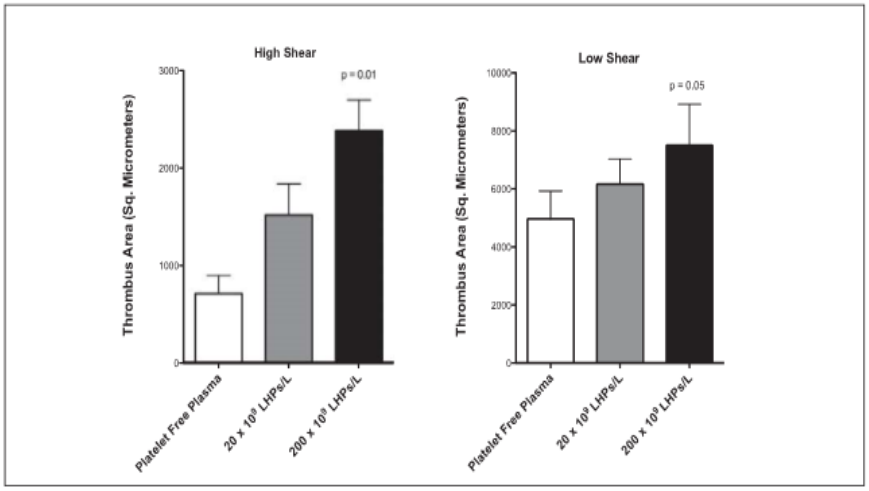

Figure 5: Total thrombus area within the high and low shear chamber. Data shown are mean ± SEM (n=18).

show that virtually all LHPs express glycoprotein IIb/IIIa receptors antigen on their surface (unpublished data, Cellphire Inc.). In our study, the glycoprotein IIb/IIIa receptor antigen was not detected by immunohistochemistry in the thrombus generated during the platelet-deplete state. In contrast, the addition of LHPs was accompanied by immunohistochemical expression of the glycoprotein IIb/IIIa receptor confirming the presence of this key platelet antigen on LHPs as well as the incorporation of the LHPs into the thrombus.

By using an extra-corporeal circuit and infusing fluorescent-labelled LHPs at a constant rate, we could demonstrate the incorporation of LHPs into thrombus generated from native whole blood. This ability to integrate with native thrombus in a complex dynamic flow environment akin to injured arterial tissue confirms our observations further.

Study limitations

We acknowledge several limitations of our study. Due to the innate nature of any haemostatic product, LHPs may compete against, be additive to, or even synergise with normal platelets during the process of thrombus formation. We also acknowledge that the current assessment of LHPs is limited to acute thrombus formation on a denuded endothelial surface in a thrombocytopenic state. Finally, we have yet to assess the tolerability and *in vivo* efficacy of intravenous administration of LHPs in phase I clinical trials or indeed phase II clinical trials of patients with thrombocytopenia or massive blood loss.

Conclusion

In conclusion, our study demonstrates the ability of LHPs to adhere rapidly to exposed extra-cellular matrix of endothelial-denuded arterial blood vessels under conditions of high shear and contribute actively to thrombus formation. This supports the possibility that LHPs could serve as an advanced haemostatic agent in bleeding disorders and suggests that further work to investigate the functional properties of this rehydrated lyophilised infusible haemostatic platelet product is warranted.

Acknowledgements

We are grateful to the Wellcome Trust Clinical Research Facility and the Queen's Medical Research Institute for their help with this study.

Conflicts of interest

MF is employed by and has equity ownership in Cellphire Inc. GF is a consultant of Cellphire Inc. DEN has received a research grant from Cellphire Inc. None of the other authors declares any conflicts of interest.

References

1. Stroneck DF, Rebulla P. Platelet transfusions. Lancet 2007; 370: 427–438.
2. Blajchman M. Substitutes and alternatives to platelet transfusions in thrombocytopenic patients. J Thromb Haemost 2003; 1: 1637–1641.
3. Holme S, Heaton A. In vitro platelet ageing at 22 degrees C is reduced compared to in vivo ageing at 37 degrees C. Br J Haematol 1995; 91: 212–218.
4. Sauaia A, Moore FA, Moore EE, et al. Epidemiology of trauma deaths: a reassessment. J Trauma 1995; 38: 185–193.

5. Holcomb JB, McMullin NR, Pearse L, et al. Causes of death in U.S. Special Operations Forces in the global war on terrorism: 2001–2004. Ann Surg 2007; 245: 986–991.
6. Heal JM, Blumberg N. Optimizing platelet transfusion therapy. Blood Rev 2004; 18: 149–165.
7. Blajchman MA. Novel platelet products, substitutes and alternatives. Transfus Clin Biol 2001; 8: 267–271.
8. Bode AP, Fischer TH. Lyophilized platelets: fifty years in the making. Artif Cells Blood Substit Immobil Biotechnol 2007; 35: 125–133.
9. Fitzpatrick G, Agashe H, Dee J. Trehalose stabilized freeze dried human platelets, Thrombosomes, reduce blood loss in thrombocytopenic rabbit ear bleed model by as much as 89.5%. International Society of Blood Transfusion. Vox Sanguinis 2010; 99 (Suppl 1): Abstract P-0452.
10. Fitzpatrick M, Dee J, Koh A, et al. Characterization of a novel lyophilized platelet derivative (LPDH) which exhibits in vitro hemostatic function, and in vivo safety and efficacy in trauma induced uncontrolled bleeding in nonhuman primate. ASH Annual Meeting Abstracts 2011. Blood 2011; 118: Abstract 719.
11. Zafar MU, Farkouh ME, Osende J, et al. Potent arterial antithrombotic effect of direct factor-Xa inhibition with ZK-807834 administered to coronary artery disease patients. Thromb Haemost 2007; 97: 487–492.
12. Wahlander K, Eriksson-Lepkowska M, Nystrom P, et al. Antithrombotic effects of ximelagatran plus acetylsalicylic acid (ASA) and clopidogrel plus ASA in a human ex vivo arterial thrombosis model. Thromb Haemost 2006; 95: 447–453.
13. Lucking AJ, Chelliah R, Trotman AD, et al. Characterisation and reproducibility of a human ex vivo model of thrombosis. Thromb Res 2010; 126: 431–435.
14. Vilahur G, Pena E, Padro T, et al. Protein disulphide isomerase-mediated LA419–NO release provides additional antithrombotic effects to the blockade of the ADP receptor. Thromb Haemost 2007; 97: 650–657.
15. Chelliah R, Lucking A, Tattersall L, et al. P selectin antagonism reduces thrombus formation in humans. J Thromb Haemost 2009; 7: 1915–1919.
16. Lucking A, Visvanathan A, Philippou H, et al. Effect of the small molecule plasminogen activator inhibitor 1 (PAI 1) inhibitor, PAI 749, in clinical models of fibrinolysis. J Thromb Haemost 2010; 8: 1333–1339.
17. Lucking AJ, Lundback M, Mills NL, et al. Diesel exhaust inhalation increases thrombus formation in man. Eur Heart J 2008; 29: 3043–3051.
18. Read MS, Reddick RL, Bode AP, et al. Preservation of hemostatic and structural properties of rehydrated lyophilized platelets: potential for long-term storage of dried platelets for transfusion. Proc Natl Acad Sci USA 1995; 92: 397–401.
19. Read MS, Bode AP. Platelet storage: efforts to extend the shelf life of platelet concentrates. Mol Med Today 1995; 1: 322–328.
20. Hawksworth J, Elster E, Fryer D, et al. Evaluation of lyophilized platelets as an infusible hemostatic agent in experimental non compressible hemorrhage in swine. J Thromb Haemost 2009; 7: 1663–1671.
21. Bode A, Blajchman M, Bardossy L, et al. Hemostatic properties of human lyophilized platelets in a thrombocytopenic rabbit model and a simulated bleeding time device. Blood 1994; 84 (Suppl 1): 464a.
22. Bode AP, Read MS, Reddick RL. Activation and adherence of lyophilized human platelets on canine vessel strips in the Baumgartner perfusion chamber* 1,* 2,* 3. J Lab Clin Med 1999; 133: 200–211.
23. Valeri C, MacGregor H, Barnard M, et al. Survival of baboon biotin X N hydroxysuccinimide and 111In oxine labelled autologous fresh and lyophilized reconstituted platelets. Vox Sang 2005; 88: 122–129.
24. Blajchman MA. Substitutes for success. Nat Med 1999; 5: 17–18.
25. Lee DH, Blajchman MA. Novel platelet products and substitutes. Transfus Med Rev 1998; 12: 175–187.
26. Dangas G, Badimon JJ, Coller BS, et al. Administration of abciximab during percutaneous coronary intervention reduces both ex vivo platelet thrombus formation and fibrin deposition: implications for a potential anticoagulant effect of abciximab. Arterioscl Thromb Vasc Biol 1998; 18: 1342.
27. Fischer TH, Merricks EP, Bode AP, et al. Thrombus formation with rehydrated, lyophilized platelets. Hematology 2002; 7: 359–369.
28. Bode AP, Read MS. Lyophilized platelets: continued development. Transfusion Sci 2000; 22: 99–105.

REVIEW

For reprint orders, please contact: reprints@futuremedicine.com

Nanoparticles and the cardiovascular system: a critical review

Nanoparticles (NPs) are tiny particles with a diameter of less than 100 nm. Traffic exhaust is a major source of combustion-derived NPs (CDNPs), which represent a significant component in urban air pollution. Epidemiological, panel and controlled human chamber studies clearly demonstrate that exposure to CDNPs is associated with multiple adverse cardiovascular effects in both healthy individuals and those with pre-existing cardiovascular disease. NPs are also manufactured from a large range of materials for industrial use in a vast array of products including for use as novel imaging agents for medical use. There is currently little information available on the impacts of manufactured NPs in humans, but experimental studies demonstrate similarities to the detrimental cardiovascular actions of CDNPs. This review describes the evidence for these cardiovascular effects and attempts to resolve the paradox between the adverse effects of the unintentional exposure of CDNPs and the intentional delivery of manufactured NPs for medical purposes.

KEYWORDS: atherosclerosis · atherothrombosis · cardiovascular · combustion · engineered · inflammation · lungs · manufactured · nanoparticles

Ken Donaldson*[1], Rodger Duffin[2], Jeremy P Langrish[3], Mark R Miller[3], Nicholas L Mills[3], Craig A Poland[4], Jennifer Raftis[1], Anoop Shah[3], Catherine A Shaw[3] & David E Newby[3]

[1]*Centre for Inflammation Research, Queens Medical Research Institute, University of Edinburgh, Edinburgh, UK*
[2]*CXR Biosciences, Dundee, UK*
[3]*University/BHF Centre for Cardiovascular Sciences, University of Edinburgh, Edinburgh, UK*
[4]*Institute of Occupational Medicine, Research Avenue North, Riccarton Edinburgh, UK*
**Author for correspondence: Tel.: +44 131 242 6580 ken.donaldson@ed.ac.uk*

There is a long history of research demonstrating that inhalation of a variety of environmental and occupational particles can lead to lung disease after they become airborne in workplaces or the environment and get inhaled into the lungs [1]. Particles can be categorized in various ways, however, the classification on the basis of size is a useful one, especially because the toxicity (on a mass basis) of particles increases as their size decreases [2]. The terms nanoparticles (NPs) and ultrafine particles describe particles in the same size range (less than 100 nm), but the former can be defined as manufactured and ultrafine particles are sometimes defined as those arising in ambient air; in this review they are viewed as interchangeable depending on the context. NPs or ultrafine particles are defined as particles with at least two dimensions less than 100 nm; NPs have three dimensions less than 100 nm and nanofibers have two dimensions less than 100 nm and the third dimension can be tens or hundreds of microns in length. In general this review deals with NPs, not nanofibers. Particle size affects the aerodynamic behavior of particles and, therefore, is an important factor influencing the deposition of particles in the lung, and specifically, the region of deposition. Fine (~0.1–2.5 μm) and coarse (~2.5–10 μm) compact particles deposit by sedimentation or impaction, while NPs (<0.1 μm) deposit in the lung by diffusion. Particles with median diameters <0.1 μm have a deposition fraction of approximately 20–50% in the pulmonary region, although this falls off as the NPs become smaller [3]. NPs aggregate into larger chains and clusters and so their aerodynamic size is greater than the primary particle size. NPs inhaled into the lungs deposit with moderate efficiency throughout the lungs, including beyond the ciliated airways in the fragile and slow-clearing alveolar parts of the lung. In this region, close to the air–blood interface, they are cleared slowly by macrophages, as are other conventionally respirable particles.

NPs can be present in the air in a number of scenarios and can be inhaled into the lungs 'accidentally'; they can also enter the body intentionally by injection or by inhalation in the form of nanomedicines or nanodiagnostics (Table 1). NPs can also be given orally as nanomedicine, but this review is confined to the delivery of NPs into the blood for imaging and therapy in cardiovascular disease.

Combustion-derived NPs (CDNPs) from traffic sources are carbon centered and normally represent the predominant particle by number in urban air pollution. Along with NPs derived from atmospheric chemistry (e.g., sulfates and nitrates) these were hitherto known as ultrafine particles in the ambient air; in other words, they were <100 nm in diameter or $PM_{0.1}$. $PM_{0.1}$ defines the sampling convention that measures particulate material by mass with 50% efficiency for particles with an aerodynamic diameter of 0.1 μm.

Future Medicine part of fsg

10.2217/NNM.13.16 © 2013 Future Medicine Ltd *Nanomedicine* (2013) **8**(3), 403–423 ISSN 1743-5889

Table 1. Main types of nanoparticle dealt with in the review and the evidence regarding cardiovascular effects.

Nanoparticle	Exposure	Example	Available data	Evidence of adverse effects on the cardiovascular system	
				Human	*Animal*
Combustion	Released into the general environment leading to inhalation	Diesel exhaust particles	Large amounts of epidemiology and explanatory toxicology	Y	Y
Bulk	Released into the workplace environment initially and eventually may reach the general environment leading to inhalation	TiO_2	Little or no epidemiology but large amounts of toxicology	N	Y
Naturally occurring	Released into the environment leading to inhalation exposure	Nanoclay	Little epidemiology and little toxicology	Y, asbestos	Y, asbestos
Nanomedicine	Injected or delivered into the human body under sterile conditions	SPIONs	Some in use, toxicology only partially established	N	N

N: No; SPION: Superparamagnetic iron oxide nanoparticle; Y: Yes.

The development of nanotechnologies has given rise to a huge array of different synthetic NPs with uses ranging from electronics to imaging and therapeutics in nanomedicine. The risks that are posed by NPs will depend on their composition, physicochemical nature and properties, their mode and extent of exposure, and distribution and handling by the body (Table 1).

It was not until the 1980s that the term ultrafine began to be used in connection with particle aerosols in mainstream particle toxicology [4–6]. By the early 1990s, poorly soluble, low-toxicity particles such as TiO_2 that were relatively harmless as micron-sized particles had been reported to be more pathogenic in the form of ultrafine particles/NPs [7]. The extra toxicity of the ultrafine forms of poorly soluble, low toxicity materials was found to be a consequence of their high surface area producing oxidative stress and their tendency to enter the interstitium of the lungs in rat studies, initiating inflammation as well as overloading clearance mechanisms in the rat lung if they accumulated to very high lung burdens [7–9].

Air pollution has long been a major source of particulate exposure in the wider population. Recognition that ultrafine/NP fraction of air pollution ($PM_{0.1}$) played a major role in the adverse effects of particulate matter (PM) led to a considerable research effort into the toxicology of CDNPs [10–12]. Surprisingly, it became apparent that the cardiovascular system was the site of the major adverse health impact of PM in terms of overall mortality and morbidity and this led to a major research effort to understand how particles depositing in the lungs could impact the blood vessels and the heart. Diesel exhaust particles (DEPs) have become the model particle for studying the adverse effect of CDNPs on the cardiovascular system because of the high proportion of NPs in the emission, their ubiquity and evidence that they have extra potential to cause cellular injury and inflammation in the lungs. They are also capable of having profound effects on the cardiovascular system [13–15].

While air pollution is the major source of anthropogenic particles for the wider public, in the occupational setting, workers can be exposed to a far greater variety of particles. In terms of NPs, the mass production of industrially important commodities such as carbon black and TiO_2 have provided a range of exposure scenarios for workers involved in production and use since the middle of the last century. In the intervening years, there has been an increase in the production and use of such manufactured

NPs (MNPs) raising the potential for worker exposure. In light of the data regarding NPs in the environment (i.e., CDNPs) there has been concern regarding adverse health effects in MNP-exposed workers. Specifically, the rise of the nanotechnologies have produced a whole new science of particles, leading to novel designs for particles useful in industry and medicine. As well as the concern over the potential negative impact of such NPs on the cardiovascular system, there is also considerable hope and effort within the scientific community to utilize NPs in therapeutic and diagnostic approaches for combating cardiovascular disease [16]. This apparent paradox has not gone unnoticed and questions have been raised as to whether NPs used in therapeutics such as drug delivery might pose the same risks as environmental NPs [17–19]. This review describes what is currently known about the cardiovascular toxicology of both CDNPs and MNPs, describing mechanisms for the cardiovascular effects of NPs after the inhalation–exposure scenario and the purposeful introduction of NPs into the body for medical reasons.

When NPs enter tissue, similar to all particles, they are taken up by cells whose function is to deal with 'foreign' material. In the lungs and other tissues, these cells are leukocytes called macrophages, and in the blood they are called monocytes, which are cells of the same lineage as macrophages. FIGURES 1 & 2 provide examples of the essential features of CDNPs and MNPs as they appear in transmission and scanning electron microscopy and when they are deposited in the lungs or are inside cells.

Epidemiological evidence for impacts of the CDNPs in ambient PM on the cardiovascular system

Combustion-derived pollutants remain a significant contributory source of outdoor air pollution, with United Nations estimates of approximately 1.3 million premature deaths per year from outdoor air pollution [20]. The exemplar CDNP is DEP. DEPs are in the primary size range of 40–80 nm, have a carbon core and associated organics from unburnt fuel and lube oil, as well as metals such as iron that are present in the raw fuel and are present on the soot particles following combustion. This section will discuss the epidemiological associations of particulate matter and specific cardiovascular conditions. The majority of these studies are based on ambient PM, which is measured by sampling conventions that are size based. A few of the studies involve measurement of only the NP fraction ($PM_{0.1}$), however the fine fraction ($PM_{2.5}$) is enriched with CDNPs. The justification for the argument that the adverse effects of PM are due to the NPs lies in:

- The generally greater effects of $PM_{2.5}$ (see below) compared with the same mass of coarser (PM_{10}) particles;
- Chamber studies where controlled CDNP exposure has greater adverse cardiovascular system effects than PM_{10} or $PM_{2.5}$ (see 'Chamber studies' section);
- The toxicological data highlighting the importance of composition in the proinflammatory effects of CDNPs [10].

The evidence for these effects are found in short-term, time-series studies that examine the relationship between adverse health effects and pollution levels over the previous few hours to days and long-term studies that examine mortality and morbidity rates in populations where the levels of pollution differ.

Long-term exposure to particulate pollution & cardiovascular disease

Ambient air pollution has a long-standing and close temporal relationship with adverse health effects from the extreme episodes of the Meuse Valley fog in 1930 [21] and the London fog incident in 1952 [22] to recent epidemiological evidence implicating PM as a major perpetrator [23]. More recently, several epidemiological studies have investigated long-term exposure to particulate matter and cardiovascular events. Miller *et al.* demonstrated that a 10 $\mu g/m^3$ increment in $PM_{2.5}$ was associated with a 24% (hazard ratio: 1.24; 95% CI: 1.09–1.41) increased risk of a cardiovascular event in a large cohort of post-menopausal women [24]. Two further studies, the American Cancer Society cohort and the Harvard Six Cities studies demonstrated similar positive associations with fine particulate matter [25,26].

Interestingly, long-term particulate exposure studies have also considered development and progression of cardiovascular disease. Schwartz demonstrated a proportional relationship in the white cell count, fibrinogen levels and platelet counts per interquartile increment in PM_{10} levels [27], while another study demonstrated an increase in carotid intima-media thickness, a marker of subclinical atherosclerosis, of 5.9% (95% CI: 1.0–11.0) with every 10 $\mu g/m^3$ increment in $PM_{2.5}$ [28].

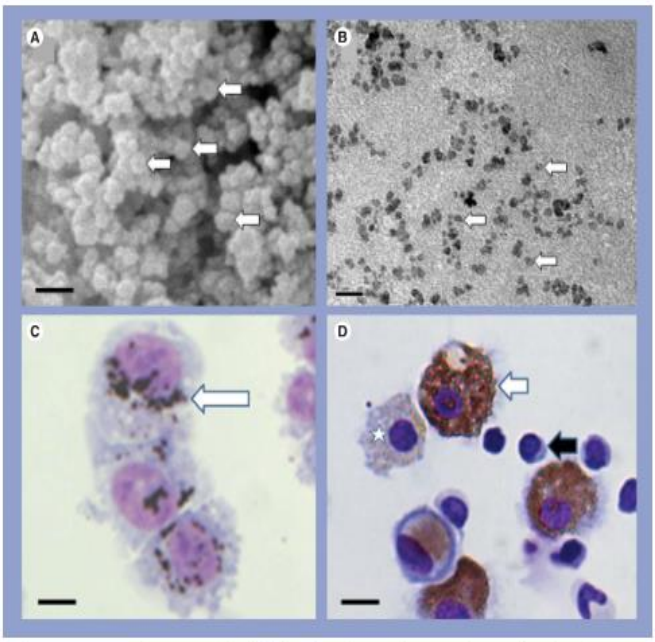

Figure 1. Images of nanoparticles. (A) Scanning electron microscope image of combustion-derived nanoparticles in the form of diesel exhaust particles; individual nanoparticles are indicated by arrows. **(B)** Transmission electron microscope image of superfine paramagnetic iron oxide nanoparticles (SPIONs); the SPIONs are the dark bodies dotted over the image (white arrows). **(C)** Endothelial cells in culture exposed to diesel exhaust particles with ingested diesel exhaust particles indicated by the white arrow. **(D)** White blood cells exposed to SPIONs; the large cells are monocytes that have taken up the SPIONs to varying degrees; the white arrow indicates a heavily loaded monocyte and the star indicates a more lightly loaded monocyte; the black arrow indicates a lymphocyte. Scale bars represent **(A)** 200 nm, **(B)** 20 nm, **(C)** 10 µm and **(D)** 15 µm.

Short-term exposure to particulate pollution & cardiovascular disease

Several recent studies discussed below, utilizing time-series and case-crossover study designs, have investigated the association of particulate pollution and adverse cardiovascular events. Short-term exposure studies are more sensitive to daily fluctuations in a particular outcome and ambient pollution and allow greater control of potential confounders providing a more accurate insight into the real impact of pollution on adverse health events. This section will concentrate on short-term particulate exposure and myocardial infarction, heart failure and stroke.

Short-term exposure to particulate pollution & myocardial infarction

Myocardial infarction still remains one of the main causes of cardiovascular death with nearly half of all men and a third of all women suffering from coronary heart disease. A recent meta-analysis has demonstrated significant association with an increase in the risk of myocardial infarction for both $PM_{2.5}$ (2.5%; 95% CI: 1.5–3.6) and PM_{10} (0.6%; 95% CI: 0.2–0.9) per 10 µg/m^3 increment [29]. Additionally in subgroup analysis, $PM_{2.5}$ showed a continued and delayed association with a 1.7% (95% CI: 0.2–3.3) increase in the risk of myocardial infarction seen at 1-day lag between exposures and events. Peters *et al.* further supported this association with a near threefold increase (odds ratio: 2.92; 95% CI: 2.06–3.61) in the likelihood of being in traffic in the hours before a myocardial infarction [30].

Particulate pollution is an important trigger for myocardial infarction and is comparable to well-known individual triggers such as physical exertion, alcohol intake and negative emotions, such as anger [31]. Recent risk assessment has demonstrated that a 30 µg/m^3 increment in

particulate matter is attributable to a 4.8% risk of triggering myocardial infarction, while exposure to traffic was attributable to a 7.4% risk of incident myocardial infarction [31].

Short-term exposure to particulate pollution & heart failure

Heart failure is an escalating public health issue affecting nearly 5.7 million individuals and contributing to one in nine deaths in the USA [32]. It affects 2–3% of the general population with an increasing prevalence in the elderly; it has an annual hospitalization rate of 2% and a 1-year mortality following hospitalization rate of 30% [32]. Heart failure ranks as the most frequent reason for hospitalization and rehospitalization in older Americans, accounting for 4.7% of total hospital discharge diagnoses [33].

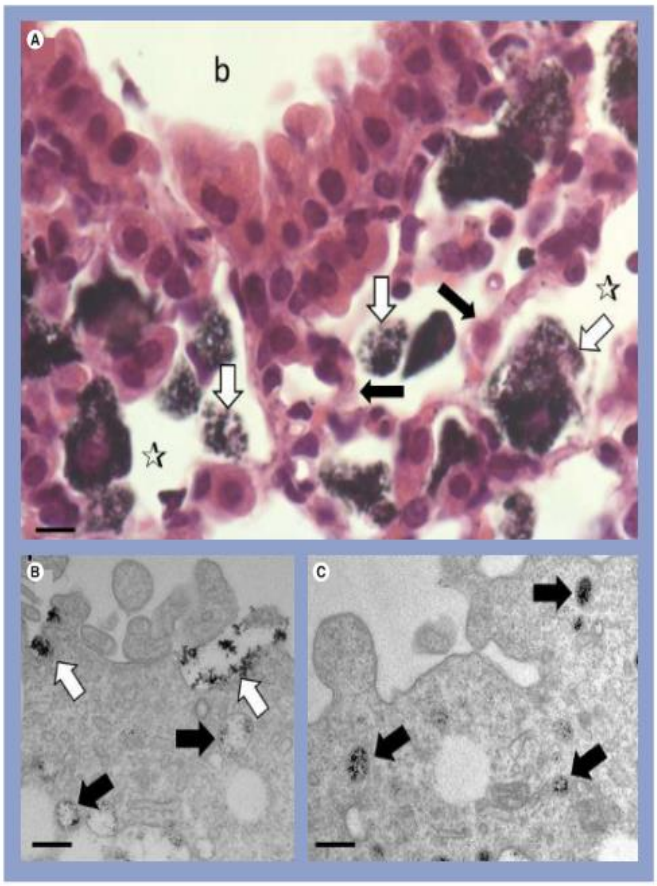

Figure 2. Images of nanoparticles. (A) Lungs of a mouse following exposure to diesel exhaust particles. Particle-laden macrophages (white arrows) are visible in alveolar spaces (stars) close to a small bronchiole (b). Note the close proximity of the particle-laden macrophages to alveolar septae (black arrows) that are richly endowed with blood capillaries. **(B)** Transmission electron microscope image of a human monocyte that had been exposed to superfine paramagnetic iron oxide nanoparticles, which are being phagocytosed and are present in invaginations in the plasma membrane (white arrow) that are destined to become particle-loaded phagosomes (black arrows). **(C)** Transmission electron microscope image of a human monocyte showing complete uptake of superfine paramagnetic iron oxide nanoparticles into loaded phagosomes in the cytoplasm of the monocyte (black arrows). Scale bars represent **(A)** 10 µm, **(B)** 200 nm and **(C)** 200 nm.

Several large studies have examined the effect of particulate pollution on heart failure hospitalizations and mortality. A few studies merit further discussion. Dominici *et al.* looked at nearly a million heart failure admissions across the USA and found a 1.28% (95% CI: 0.78–1.78) increase in risk per 10 μg/m³ increment in $PM_{2.5}$ [34]. More interestingly, the association was the strongest compared with other cardiopulmonary conditions, pointing toward increased adverse effects of particulate matter in patients with chronic congestive cardiac failure [34]. The majority of hospitalizations in patients with heart failure are due to cardiorespiratory causes, primarily due to decompensated heart failure and dysrhythmias. A smaller proportion of patients with heart failure are hospitalized owing to coexisting myocardial infarction and pulmonary pathologies. It is probable that coexisting comorbidities result in patients with heart failure being more vulnerable to pollutant exposure.

Several studies have also demonstrated positive associations between particulate exposure and cardiac failure death (see [35]). Over 80% of all heart failure mortality is either due to pump failure or sudden death, of which over 50% of all deaths are secondary to sudden death. Studies have already shown an association between particulate pollution and risk of sudden cardiac arrest [36].

Short-term exposure to particulate pollution & stroke

Stroke remains an important condition contributing significantly to both morbidity and mortality, affecting nearly one in ten individuals, with a higher incidence with increasing age in men. It remains the third leading cause of death despite significant reduction in death rate over the past few decades [37].

Compared with other cardiovascular end points, namely acute myocardial infarction and heart failure, it appears that the evidence of air pollution on stroke admissions is the weakest [38]. A recent large case-crossover study showed a 0.81% (95% CI: 0.30–1.32) increase in incident stroke per 10 μg/m³ increment in $PM_{2.5}$ [38]. The effect of PM_{10} was weaker at a 0.4% (95% CI 0–0.8%) increase per 10 μg/m³ increment, which was bordering on significant [38].

Chamber studies & panel studies on cardiovascular impacts of CDNP

While the epidemiological associations are compelling, such studies can merely describe an association and allow us to hypothesize the underlying pathophysiological mechanisms. Alternative approaches are required to investigate these underlying mechanisms and to test the plausibility of these associations. One such approach is the use of panel studies assessing groups of patients or volunteers studied repeatedly in different exposure conditions, although such studies are at the mercy of environmental conditions and exposure may vary widely throughout the study period. An alternative is human studies using controlled exposure to PM air pollutants, either in isolation or in combination with additional gaseous air pollutants, such as concentrated ambient particles (CAPs) or diesel exhaust [15,39]. These studies allow the controlled delivery of air pollutants to a well-characterized patient or volunteer population and the detailed investigation of the pathophysiological mechanisms that may underlie the epidemiological observations.

In the first-reported human exposure study, Brook and colleagues exposed 25 healthy adults to CAPs at approximately 150 μg/m³ with O_3 at 120 parts per billion or filtered air for 2 h in a randomized double-blind crossover study [40]. They demonstrated that exposure led to acute vasoconstriction in the brachial artery, detectable immediately after the exposure, without significant changes in vascular endothelial function assessed using flow-mediated dilatation or blood pressure [40]. In further studies, the same group demonstrated that a similar exposure to CAPs and O_3 combined was associated with increases in blood pressure during the exposure [41], which can be attributed purely to the PM component of the exposure and not the O_3 [42]. Similar changes in arterial tone [43] and central arterial stiffness [44] have been demonstrated following exposure to dilute diesel exhaust, as a model of urban CDNP air pollution. The mechanism underlying these observations remains unclear, although they may be due to acute changes in autonomic tone and activity of the autonomic nervous system. Indeed, epidemiological studies have repeatedly demonstrated an association between PM exposure and a reduction in heart rate variability [45–47], a surrogate marker of autonomic nervous system activity [48]. Interestingly, the evidence for short-term exposure to PM air pollution and a reduction in heart rate variability from controlled exposure studies is less convincing and heterogeneous. Diesel exhaust exposure does not appear to result in a change in measures of heart rate variability [49], while exposure to CAPs or

in fact gaseous air pollutants, such as SO_2, have been shown to reduce heart rate variability [50,51]. This distinction is probably due to the important differences in the chemical composition of the different exposures [52], with exposures to CAPs having higher concentrations of transition metals that may interact directly with autonomic fibers or reflexes to influence cardiac vagal and sympathetic tone [53]. Along with changes in vascular tone, arterial stiffness, blood pressure and autonomic tone, acute exposure to dilute diesel exhaust has been shown to increase electrocardiographic measures of myocardial ischemia in men with coronary heart disease, where ST segment depression and total ischemic burden increase during the exposure itself [54].

Following exposure to dilute diesel exhaust, vascular endothelial function is impaired compared with exposure to filtered air [55]. The mechanism of this impairment remains unclear, but initial studies suggested that this may be a result of increases in the local release of endothelin-1 [43], a potent endogenous vasoconstrictor that has been implicated in the vascular responses to cigarette smokers and in those with hypertension [56]. Further investigation did not support this proposal and instead suggested that this is driven by a reduction in nitric oxide (NO) bioavailability [57]. The adverse effect on vascular vasomotor function appears to be driven entirely by the nanoparticulate component of the diesel exhaust and not the gases, as exposure to filtered exhaust did not result in changes in endothelial function [58]. Furthermore, these effects are highly dependent on the composition of the PM itself, and indeed a CAP exposure in Edinburgh (UK) – where the majority of the ambient PM consists of salt due to the maritime location – did not affect vascular function [59], and neither did elemental carbon NPs in isolation [58]. Similarly, attenuation of vascular vasomotor function has been demonstrated using flow-mediated dilatation at 24 h following exposure to CAPs in Toronto (Canada) but not in Ann Arbor (MI, USA) which the authors suggest is probably due to the differing chemical composition of PM in the two locations [12,42].

Exposure to dilute diesel exhaust also increases the formation of blood clots in an *ex vivo* model of arterial thrombosis in response to arterial injury. This was also associated with increases in platelet activation [60] and a reduction in the stimulated release of the endogenous fibrinolytic enzyme tissue plasminogen activator [55].

The central mechanism linking all these observations is thought to be oxidative stress and local and systemic inflammatory responses. While oxidative stress is difficult to measure *in vivo*, there is increasing evidence that there is an increase in markers of oxidative stress following exposure to PM air pollution from observational and panel studies, controlled exposure studies in humans, as well as *in vitro* and animal studies [61].

Together these observations help to provide biological plausibility to the epidemiological associations between exposure to particulate air pollution and acute cardiovascular events (Figure 3). Following exposure, vascular endothelial function is impaired, a recognized precursor to the development of atherosclerotic

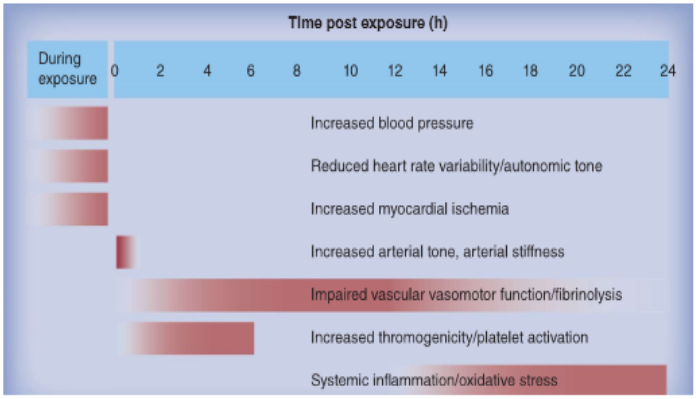

Figure 3. Summary of the cardiovascular effects of short-term exposure to dilute diesel exhaust and concentrated ambient particles in controlled human studies.

plaques, and there are increases in local oxidative stress and inflammation. These mechanisms may induce lipid oxidation, and the formation and progression of atherosclerotic plaques. Acute exposure to PM also influences blood pressure, arterial tone and autonomic function, which may promote acute plaque rupture in the coronary arteries, and subsequent thrombus formation via increased platelet activation. The adaptive responses to this impending vessel closure, such as vascular vasodilatation and release of endogenous fibrinolytic enzymes, are impaired and this may lead to the triggering of acute myocardial events. Furthermore, changes in the autonomic control of the heart rate may result in an increase in subsequent arrhythmic events. Therefore, a clear route is apparent through which the combined actions of PM can increase cardiovascular morbidity and mortality.

CDNPs in models of cardiovascular disease

In vitro studies

Although the epidemiological link between exposure to air pollution and cardiovascular disease is now well established, the underlying mechanism(s) have not yet been fully defined. Owing to the fact that atherosclerosis evolves on a background of vascular inflammation and oxidative stress, experimental studies *in vitro* generally focus on how CDNPs (and their constituents) contribute to these processes in cell types critical to atherogenesis, particularly endothelial cells and inflammatory cells. NPs are taken up by alveolar macrophages and are reported to be able to cross the epithelium and enter the interstitium, both within macrophages and freely, where they come into close contact with endothelial cells [7]. The effects of NPs on macrophages and endothelial cells in relation to proinflammatory events in the vessel wall are, therefore, potentially important in understanding vascular inflammation and the cardiovascular consequences of NP exposure.

When exposed to CDNPs *in vitro* endothelial cells are activated to mount a proinflammatory response. PM_{10} and ultrafine particles from various sources, including diesel engines, cause upregulation of multiple proinflammatory genes, including E-selectin, *MIP-2α* and *MCP-1*, at the mRNA level [62], and increased secretion of inflammatory cytokines such as IL-6, IL-8 and MCP-1 [62,63]. A critical event during atherosclerosis is the recruitment and retention of inflammatory cells, such as monocytes and macrophages, in the subendothelial space, where they contribute to atherosclerotic plaque formation. CDNPs contribute to this process by inducing expression of the adhesion molecules, ICAM-1 and VCAM-1, on the surface of endothelial cells [64–67], which results in adhesion of monoctyes to the endothelial monolayer [67]. Expression of many proinflammatory and proatherogenic genes is governed by redox-sensitive transcription factors, for example NF-κB, which can be activated by particle-induced oxidative stress. CDNPs have the capacity to intrinsically generate free radicals [61] and to induce oxidative stress in cells and tissues. Motorcycle exhaust and DEPs induce NF-κB activation via oxidative stress in human umbilical vein endothelial cells resulting in ICAM-1 and VCAM-1 expression [64], which is attenuated by the antioxidants vitamin C and desferrioxamine [64,67]. Similarly, ultrafine particles from diesel engines cause increased superoxide formation in human aortic endothelial cells resulting in upregulation of tissue factor and the antioxidant enzyme heme oxygenase-1 via activation of MAPK and JNK. These effects were inhibited by both the antioxidant *N*-acetylcysteine and by a JNK inhibitor [68].

Although these effects can be observed *in vitro*, they require relatively high concentrations of particles to be administered directly to endothelial cells. It is currently unclear whether particles deposited in the lung are able to translocate in sufficient numbers to reach such concentrations in endothelial cells *in vivo*. Recent studies have demonstrated that CDNPs may alter the expression of tight junction proteins, disrupting the intercellular junctions that normally restrict endothelial permeability. For example, DEPs cause the redistribution of vascular endothelial cadherin from the cell membrane to an intracellular location [69,70], downregulate the tight junction protein ZO-1 [71] and increase transendothelial resistance [72]. All of these alterations result in increased endothelial cell permeability, hypothetically increasing particle (or their soluble constituents) translocation to the circulation. However, the evidence for particle translocation remains controversial with some studies reporting significant direct translocation of inhaled carbon-based particles from the lung to the circulation [73], while others have been unable to demonstrate this in humans [74]. Similar studies using noncarbon particles have concluded that translocation occurs only to a limited extent [75].

An alternative hypothesis to explain how CDNPs can contribute to cardiovascular disease

is indirectly via the activation of alveolar macrophages in the lung. PM from various sources is well documented to cause increased production of reactive oxygen species and inflammatory cytokines, particularly TNF-α, in macrophages via NF-κB signaling [10]. A series of recent studies have demonstrated that the inflammatory milieu elaborated from particle-exposed macrophages can activate endothelial cells indirectly, often with more potent effects than those generated by treating endothelial cells with particles directly. The particle-free conditioned medium from DEP-exposed macrophages can induce TNF-α-dependent expression of adhesion molecules [76] and vastly amplify the production of MCP-1 [77] in endothelial cells compared with direct particle treatment. Additionally, DEP treatment of macrophage–endothelial cocultures causes greater increases in the expression of MCP-1 and NO synthase compared with endothelial cells alone [78]. Using a novel translational approach, Channell *et al.* have recently demonstrated that following a controlled DEP exposure, plasma from healthy human volunteers increases expression of VCAM-1 in cultured primary human coronary artery endothelial cells [79]. This suggests that soluble proinflammatory factors are present in the circulation following an inhalation exposure to CDNPs [79].

Although there is now strong evidence that CDNPs can cause proinflammatory and proatherogenic effects, the exact components of the DEP that mediate these effects has currently not been identified. Research is now focused on elucidating whether the carbon core or the many organic chemicals and transition metal ions present on the surface of particles are responsible for the observed biological effects. However, identifying the key biologically active constituents is experimentally challenging owing to the complex chemical fractionation required to separate constituent components. Using organic solvents such as dichloromethane to separate the organic and aqueous soluble phases of DEPs, the organic fraction containing the polyaromatic hydrocarbons and quinones has been proposed as the reactive fraction [80,81]. Using DEPs collected from engines operating under different load conditions, Li *et al.* have demonstrated that DEPs with the highest levels of redox-active organic compounds and metals generate the most potent proinflammatory response [82] and induce greater permeability [68] in endothelial cells. However, identifying the key biologically active constituents of CDNPs is experimentally challenging owing to the complex chemical fractionation required to separate a vast array of constituent components, and further research is needed to achieve this aim.

Animal studies

Vasculature & atherosclerosis

Exposure of rodents to both urban air pollution and from vehicle exhaust is associated with an impaired vascular function, generally manifesting as proconstriction and/or decreased relaxation of blood vessels [61,83]. Similar to controlled exposures in humans, these exposures are associated with increased blood pressure. Therefore, these pollutants have the capacity to impair both small resistance arteries (that control blood pressure) as well as large conductance arteries (that regulate the distribution of blood to organs, and are the site of atherosclerotic vascular disease) without confinement to a specific vascular bed (e.g., levels of impairment do not necessarily appear to be greater in pulmonary vasculature than systemic vascular beds). Vascular function is impaired *in situ* and *ex vivo* (in isolated vessels) following *in vivo* exposure to vehicular exhaust or the particulates alone, and, interestingly, after direct *in vitro* exposure of isolated blood vessels to CDNPs [84]. These findings have several important implications. First, CDNPs themselves, rather than the gaseous and semi-volatile copollutants can induce vascular dysfunction, although there may be some synergism between these different constituents [85]. Second, vascular effects of CDNPs are long lived, persisting after the isolation of blood vessels in the absence of neuroendocrine regulation. Third, CDNPs alone have the capacity to impair vascular function (albeit, requiring high concentrations to do so *in vitro*) without prior interaction with the lung, in the absence of neural regulations and without circulating mediators and inflammatory cells.

These observations provide weight to the possibility that particles may translocate from the lung and directly impair vascular function. In light of this, several studies have used *in vitro* exposure of blood vessels to determine the cellular mechanisms involved. These include endothelial cell dysfunction, inhibition of NO pathways and enhanced responsiveness to vasoconstrictors [86]. Particle-induced oxidative stress may be a common mechanism for these effects and certainly multiple studies have provided evidence of oxygen-derived free radicals in blood vessels after both *in vivo* and *in vitro* exposure to CDNPs [61].

The acute vascular actions of CDNPs can easily be linked to the chronic processes involved in vascular disease atherosclerosis and the formation of lipid- and inflammatory cell-rich lesions on the inner surface of blood vessels that underlies the majority of cardiovascular conditions. Endothelial dysfunction, dysregulation of antioxidant enzymes, expression of adhesion markers and inflammatory cell accumulation are the hallmarks of early atherosclerosis. Furthermore, inflammation, oxidative stress and attenuation of the numerous protective effects of NO will promote the later stages of plaque development such as plaque expansion, remodeling and instability. Accordingly, there is now considerable evidence that exposure to CDNPs or urban PM increases the size and promotes the development of atherosclerosis in animal models [83,85]. Interestingly, the ultrafine component of urban PM exerts a greater proatherosclerotic effect than the fine particulate, suggesting PM from combustion (e.g., vehicular exhaust) is especially harmful in this regard [87].

Oxidative stress and inflammation once again feature as prime candidates for the proatherosclerotic effects of CDNPs [61]. Several studies in both rabbit and mouse models of atherosclerosis have demonstrated that repeated exposure to PM leads to plaques with a high inflammatory cell content [88–90]. PM exposure is also associated with a notable increase in oxygen-derived free radicals in both the vascular wall and plaques of CDNP-treated animals. DEP has been shown to oxidatively modify low-density lipoprotein (oxidation of low-density lipoprotein is believed to be preferentially taken up by monocytes leading to rapid plaque expansion) [91]. PM has significantly greater actions in atherosclerosis-prone animals fed a high-fat diet as opposed to that of a normal chow diet [92,93], highlighting the synergism of the combined insult of high lipids, oxidative stress and inflammation. Finally, acute cardiovascular events (e.g., stroke and heart attack) are usually caused by plaque rupture, leading to thrombotic occlusion of blood vessels. Even in the absence of an animal model of plaque rupture, CDNP exposure of animals is associated with changes in the composition of the plaque that is believed to promote instability (i.e., more prone to rupture), including high lipid and inflammatory cell content [90,93], matrix metalloproteinase expression [94] and tissue factor expression [89].

The animal models have been used to demonstrate that CDNPs can exacerbate structural changes to the myocardium. For example, $PM_{2.5}$ increases the degree of cardiac remodeling in response to prolonged angiotensin-II-induced hypertension [95] and ultrafine PM, exacerbated the extent of myocardial infarction induced by myocardial ischemia/reperfusion [96]. Myocardial damage and necrosis is mediated through local infiltration of neutrophils and oxidative damage, among others, and both these mechanisms were greater in infarcted regions of CDNP-treated animals. However, currently it is not clear if this is a direct cause of particle translocation to the myocardium, or indirectly through a systemic inflammatory response or increase in autonomic activation.

The blood

Similar to early epidemiological studies, rodent exposure to $PM_{2.5}$ and DEPs is associated with increases in plasma fibrinogen [97,98]. Raised fibrinogen concentrations do not necessarily confer greater blood coagulability and, as an acute phase protein, fibrinogen has a complex relationship with inflammatory mediators. However, more recently, animal studies have demonstrated that several types of PM modify an extensive range of coagulation/thrombotic factors, including factors VII, VIII and VX, D-dimers, endothelial von Willebrand factor and several markers of platelet activation [24]. CDNP exposure of animals also impairs fibrinolysis through an increased release of PAI-1 [99]. Therefore, there is a general consensus that CDNPs promote a prothrombotic blood state and, certainly *in vivo* models of thrombus formation in artificially damaged blood vessels, show that prior PM exposure leads to a greater and more rapid formation of thrombosis (see [99]).

The mechanisms underlying these effects are less clear. A 'spillover' of inflammatory mediators from the lung to the blood is one of the primary mechanisms believed to explain the cardiovascular effects of inhaled particles. Numerous studies have supported this hypothesis, however, a lack of consistency between different parameters and studies leaves this a matter of debate that is beyond the scope of this review. Nevertheless, there is often a relationship between the inflammatory factors in the blood and thrombogenicity following PM exposure [100]. Interestingly, direct addition of CDNPs to isolated blood decreases clotting time, in other words, blood clots more readily [101]. Platelet activation, in particular, has been proposed to mediate these direct effects of PM on the blood [102].

MNPs in models of cardiovascular disease

The rising concern regarding MNPs produced by nanotechnological processes originated in large part because of the evidence outlined above that NPs were responsible for the adverse effects of environmental PM. MNPs come in a remarkable range of sizes and compositions, but typically they are <100 nm in primary size and are composed of metal oxides (e.g., TiO_2 and SiO_2) and carbon (e.g., carbon black and carbon nanotubes [CNTs]). The emphasis on the effects of PM_{10} on the cardiovascular system stimulated research into potential effects of MNPs on the cardiovascular system. Currently, there are no epidemiological data addressing the effects of MNPs on the cardiovascular system, which is unsurprising given the relative infancy of the nanotechnology industry and the relatively short length of time that there has been potential for human exposure to these new materials. Such studies have been proposed, but results from these are not likely in the near future [103]. Therefore, in terms of understanding the cardiovascular risks of exposure to NPs, we must look towards toxicological studies in model systems to inform us of the likely impacts upon which to base worker protection measures.

MNPs & atherosclerosis models

Several studies have examined the effect of MNPs on atherosclerosis in the ApoE-deficient mouse model of experimental atherosclerosis. In the study by Kang *et al.* ApoE mice were exposed to relatively low levels of nickel hydroxide NPs (79 μg nickel/m³) via whole body inhalation for 5 h per day, 5 days a week for 1 week or 5 months [104]. The exposure to the nickel NPs induced oxidative stress and inflammation in both the lungs and in extrapulmonary organs. The atherosclerotic lesions demonstrated significant progression in the animals exposed to the nickel NPs, accompanied by an increase in oxidative mitochondrial DNA damage in the aorta and the induction of an acute phase response. Vesterdal *et al.* [105] used Printex 90® (Evonik, Antwerp, Germany) carbon black NPs delivered to ApoE mice by two consecutive intratracheal doses of 0.5 mg/kg. In contrast to the prior study with nickel NPs, no effects were seen on the progression of atherosclerotic plaques or the expression of adhesion molecules on the endothelium. Another low toxicity NP TiO_2 was investigated by Mikkelsen *et al.* [106]. Exposure was by intratracheal installation at 0.5 mg/kg body weight and no effects were observed on the vasodilatory function of the vessels or on adhesion molecules in the endothelium. However, the exposure to NP TiO_2 was associated with a modest increase in plaque progression in the aorta. In the study by Li *et al.* a single intratracheal installation of wall CNT produced evidence of oxidative stress in the heart and the aorta as evidenced by increases in glutathione expression and mitochondrial DNA damage [107]. In addition, the single CNT exposure resulted in accelerated plaque formation.

Effects on the microcirculation

LeBlanc *et al.* examined the effect of TiO_2 NP inhalation on the coronary microvascular system [108]. The exposed animals showed impairment of endothelium-dependent vasoreactivity in the coronary arterioles, presumed to be due to oxidative stress in the microvascular system since catalase ameliorated the impairment in vasodilation.

Effects on platelet aggregation & thrombosis

Owing to the possibility that NPs can enter the circulation and directly change the coagulant state by influencing platelet adhesion and activation, several studies have explored the direct action of NPs on platelet activation. Radomski *et al.* demonstrated that a range of MNPs could influence platelet aggregation *in vitro* and vascular thrombosis *in vivo* [102]. Carbon NPs and single- and multi-walled CNTs all directly increased platelet aggregation and accelerated the rate of vascular thrombosis in a model of ferric chloride-induced hemostasis. This was accompanied by an upregulation of GPIIb/IIIa in the platelets. Interestingly particle-induced aggregation was inhibited by prostacyclin but not by aspirin. In a study by Khandoga *et al.*, mice received a 24 h exposure to filtered air or nanoparticulate carbon black and intravital fluorescence microscopy was then carried out on the hepatic microcirculation [109].

Exposure to the nanoparticulate carbon particles caused platelet accumulation in the microvasculature, but leukocyte recruitment and sinusoidal perfusion did not change compared with the control exposures. Fibrinogen deposition was detected by immunochemistry in both hepatic and cardiac microvessels from the NP carbon-exposed mice. There were no changes in the plasma levels of cytokines nor blood cells following

exposure to the nanoparticulate carbon. These results suggest that the thrombogenic effect in the microcirculation following inhalation of carbon NPs was independent of inflammation. To examine the role of surface derivatization on NP activity, McGuinnes *et al.* examined the effect of variously derivatized polystyrene latex NP (PLNP) [110]. This study assumed that the NP would reach the blood and examined the direct effect on platelet aggregation. Whereas carboxylated PLNP and aminated PLNP caused platelet aggregation, the unmodified PLNP did not. In addition, whereas carboxylated PLNP caused aggregation by classical upregulation of adhesion receptors, aminated PLNP did not upregulate adhesion receptors and appeared to act by perturbation of the platelet membrane revealing anionic lipids. The study clearly demonstrates that NPs composed of insoluble low toxicity materials are significantly altered in their potency in causing platelet aggregation by altering the surface chemistry, and that different surface modifications can cause aggregation by different mechanisms.

Corbalan *et al.* examined the direct effect of amorphous silica NPs on human platelets [111]. Exposure to the amorphous silica NP induced platelet aggregations with a low ratio of NO to peroxynitrite, suggestive of superoxide radical generation. Burke *et al.* assessed the ability of multiwall CNT (MWCNT) to activate the intrinsic pathway of coagulation as measured by the activated partial thromboplastin time [112]. Functionalization of the CNT by amidation or carboxylation enhanced the procoagulant activity and the pathway was activated by a nonclassical mechanism strongly dependent on factor IX. The study also examined the ability of the MWCNT to activate platelets *in vitro*. Aminated MWCNT caused greater platelet activation than carboxylated or pristine MWCNT. However, systemic injection of pristine MWCNT decreased platelet counts, increased von Willebrand factor and decreased D-dimers, suggesting an important role of the graphene surface of MWCNT. Surprisingly, carboxylated and aminated MWCNT had little or no procoagulant effect *in vivo*, highlighting the difficulties in translating *in vitro* results to an *in vivo* scenario. Finally, the study by Singh *et al.* demonstrated that pristine graphene oxide was highly thrombogenic in mice and invoked aggregatory responses in human platelets [113]. By contrast, aminated graphene had absolutely no stimulatory effect on platelets, nor did it induce pulmonary thromboembolism following intravenous administration. These findings again highlight the importance of surface chemistry on NP activity, especially with regards to their procoagulant actions. Erdely *et al.* examined the effect of pharyngeal aspiration of carbon nanotubes and reported clear evidence of an acute phase response in the blood and increased levels of complement up to 28 days following exposure [114]. The authors concluded that the response in the lung to CNTs produced systemic changes that led to cardiovascular outcomes. These changes included increased adhesion receptors such as E-selectin, endothelial dysfunction and disturbance to the plasminogen activator/inactivator balance leading to a change in thrombotic potential and induction of a procoagulant state.

Medical NPs in models of cardiovascular disease

The enthusiasm for the use of engineered NPs in medicine, especially medical imaging, could be considered surprising in light of the clear detrimental actions of CDNPs and some existing MNPs. However, the types of nanomaterials used in nanomedicine have several distinct properties from those used in manufacturing industries. Medical NPs are typically composed of biodegradeable materials such as macromolecular proteins, carbohydrates and lipids, in the form of polymers, dendrimers and lipid micelles. Most current medical NPs are injected into the systemic circulation, and the dosimetry is very different from inhalation scenarios. The dose within the blood is very high at the point of injection, thus coagulation represents an important hazard end point for evaluation.

Superparamagnetic iron oxide NPs (SPIONs) or ultrasmall SPIONs (USPIONs), are used for imaging in the cardiovascular system using MRI. Their uptake by inflammatory cells also provides additional biological and functional information through the detection of cellular inflammation where SPION-loaded leukocytes accumulate. USPIONs have particle sizes in the range 10–30 nm and are often stabilized by the hydrophilic polymer dextran. Their small size allows them to evade opsonization, escape immediate recognition by the reticuloendothelial system and persist in the bloodstream for longer than larger particles [115], allowing USPIONs to be used to assess the accumulation of macrophages within vascular and lymphatic tissues [116]. Current preparations are biodegradable and deemed safe for clinical

use. Ferumoxytol has been proposed for use in the imaging of atherosclerosis, and ferumoxtran-10 (Sinerem®; Guerbet Laboratories, France), have been demonstrated to be useful for the detection of carotid atheroma. In clinical studies with ferumoxtran-10, T2*-weighted MRI signal decrease has been demonstrated within the carotid plaques of patients prior to endarterectomy. Furthermore, the intensity of the USPION MRI signal appears to correlate with the propensity for plaque rupture. Indeed, postsurgery histology confirmed the presence of intracellular USPIONs in macrophage-derived cells of atherosclerotic samples. Similar findings have been obtained in hyperlipidemic rabbits administered with ferumoxtran-10.

Nanotechnology has advanced rapidly and is now a platform for many medical applications, such as drug delivery [117], imaging [118] and diagnosis of disease [119]. However, a number of questions have been raised regarding the safety of introducing large numbers of NPs to potentially vulnerable patients [120]. NPs currently under development for medical applications need to be thoroughly tested, taking into consideration what has already been established with regards to the toxicology profile of existing MNPs. The diversity of medical NPs with respect to size, surface area, composition and surface properties, and the rapid pace of their development and commercialization, poses significant challenges to traditional toxicity testing paradigms. Pre-clinical strategies have adopted traditional pharmacological testing methods in evaluating the toxicity of NPs for clinical use. However, with so many variables and no agreed standards for safety, full characterization of the effects of NP is a lengthy, but arguably essential, procedure.

The direct exposures to engineered NPs for medical use is of immediate concern, especially with regards to whether there are, as yet unknown, susceptible populations. Unlike novel pharmacological therapies, MNPs do not undergo rigorous testing to determine their cardiovascular effects prior to clinical use. Bearing in mind the clear cardiovascular actions of CDNPs, all NPs, not just those intended for the diagnosis and treatment of cardiovascular disease, have the potential to impact on elements of the cardiovascular system and promote the progression of cardiovascular disease. Presently, there are no observational studies linking exposure to engineered nanomaterials and cardiovascular events, however, a number of preclinical studies have raised pressing concerns that exposure to engineered nanomaterials, directly or indirectly, can cause endothelial dysfunction, platelet activation and may plausibly contribute to ischemic heart disease [110,121,122].

Cardiovascular disease is a complex and dynamic process with many contributing factors and, therefore, a single *in vitro* model to study the adverse effects of medical nanomaterials on the cardiovascular system is unlikely to emerge. However, platelets, platelet–monocyte aggregation and the endothelial cells/isolated blood vessels have emerged as useful *in vitro* systems to determine potential adverse effects of NPs. While the relevance of the dose of NPs employed *in vitro* models requires justification in some instances, these studies are useful from a mechanistic perspective, and high doses are employed for injection of medical NPs. Compatibility of medical NPs with blood components is important and a number of studies have employed assays of hemolysis [123], platelet aggregation/activation [102] and platelet-leukocyte binding [110]. Direct and indirect toxicity to the cardiovascular system can be determined using cell lines, accompanied by assays for oxidative stress, inflammation and cell death [124]. Whether observations from these *in vitro* models apply *in vivo* or in the clinic is uncertain, and in the absence of any standards for the assessment of the cardiovascular toxicity of engineered nanomaterials the relevance of *in vitro* models requires further investigation.

Recent studies have demonstrated that engineered NPs can interact with platelets causing activation, aggregation [102,110] and hyper-reactivity [Raftis J. Unpublished Data]. Surface charge is thought to be a critical determinant in platelet-NP activation [110] and, therefore, should be taken into account when designing novel MNPs. Exploration of engineered nanomaterials in complex multisystem disease models requires consideration of potential downstream effects as well as direct toxicity. Nanomaterials are increasingly being used in cell tracking to monitor disease progression [125,126]. It is no longer sufficient to assess the potential toxicity of engineered NPs on the cell carriers alone, for example, could MNP-loaded inflammatory cells represent 'time bombs', capable of releasing proinflammatory mediators within a vulnerable atherosclerotic plaque?

Platelets play a critical role in thrombosis and maintaining homeostasis in the blood, and can contribute to acute coronary syndrome or, alternatively, a reduction in their

responsiveness could lead to hemorrhage. There is very little literature available regarding the impact of engineered nanomaterials on hematocompatibility and even less on their platelet function. Since many MNP preparations in development are for intravenous use, platelet interaction is inevitable and, therefore, it is important to assess whether these particles are directly altering platelet function or are indirectly affecting their activity in the body. Platelet activation and thrombosis are critical determinants of the clinical outcome following atheromatous plaque rupture, with thrombotic coronary artery occlusion resulting in myocardial infarction and sudden cardiovascular death. A variety of engineered NPs are under development for imaging atherothrombotic vascular disease and for the delivery of targeted therapies to the unstable plaque. Therefore, we need to ensure that our new nanomedicines are not actually causing clandestine harm.

Conclusion on mechanisms

Mechanism of cardiovascular effects following inhalation

The mechanisms of the adverse cardiovascular effects have been alluded to in the above account, and, although not fully understood, some conclusions can be drawn. Initially it was puzzling that the lead adverse effect of PM exposure should be cardiovascular, but in the last 20 or so years considerable advances have been made in understanding the link between deposition of CDNPs in the lungs and subsequent adverse effects in the cardiovascular system. The impairments to the cardiovascular system that follow deposition of CDNPs and MNPs in the lungs in epidemiological and experimental studies are shown in Figure 4. There are, in general, three mechanistic pathways whereby NP deposition in the lungs might bring about these impairments (Figure 5). These are via inflammation, translocation of NPs into the cardiovascular system, especially into atherosclerotic plaques, and via the autonomic nervous system.

Inflammation

The classical, or 'indirect' hypothesis is that inhaled particles cause an inflammatory response in the lung that leads to spillover of inflammatory mediators into the circulation that induce parallel inflammation-induced damage to the cardiovascular system [127,128]. Inflammation and oxidative stress are virtually inseparable during particle-induced inflammation, and cytokines and oxidants generated in the lungs following deposition of NPs could have effects away from the lungs [10,129]. The idea that inflammation in the lungs can have adverse effects in the cardiovascular system is not confined to air pollution but is well documented in other situations. Cytokines could enhance inflammatory events in the vessel wall and the endothelium leading to decreased plaque stability while oxidants such as superoxide could scavenge NO leading to endothelial dysfunction. Arguably, this remains the most widely accepted hypothesis for the cardiopulmonary link, providing both a means by which the systemic actions of inhaled particles are amplified and prolonged, with measurable mediators in both systems. However, this mechanism alone is unlikely to account for all cardiovascular effects of inhaled particles owing to inconsistencies in the levels of inflammatory mediators even within different studies using similar experimental set-ups. Furthermore, dissociations in the time courses of pulmonary and blood cytokines provide additional doubt, especially with regards to the rapid cardiovascular effects of inhaled particles occurring within the first few hours after exposure.

Translocation

More recently, a 'direct' action of particles on the cardiovascular system has been proposed via particle translocation. Owing to the small size of NPs, it is possible that NPs penetrate through the alveolar–capillary barrier [130] to become blood-borne and directly damage the cardiovascular cells. It has been fairly well established that particles can penetrate into several layers of the alveolar epithelium [7] and cross similar structural barriers, for example, that of the olfactory bulb [131]. There are also isolated reports that have been able to estimate levels of translocation in blood [132], although at present it has not been possible to perform similar experiments with CDNPs. Furthermore, there is some doubt as to whether enough particles are able to translocate to account for the magnitude of the cardiovascular effects observed.

Autonomic nervous system

The third hypothesis is the involvement of the autonomic nervous system. Here, particles are hypothesized to stimulate sensory receptors within the lung, which signal to the CNS leading to cardiovascular actions via changes in the activity of the autonomic nervous

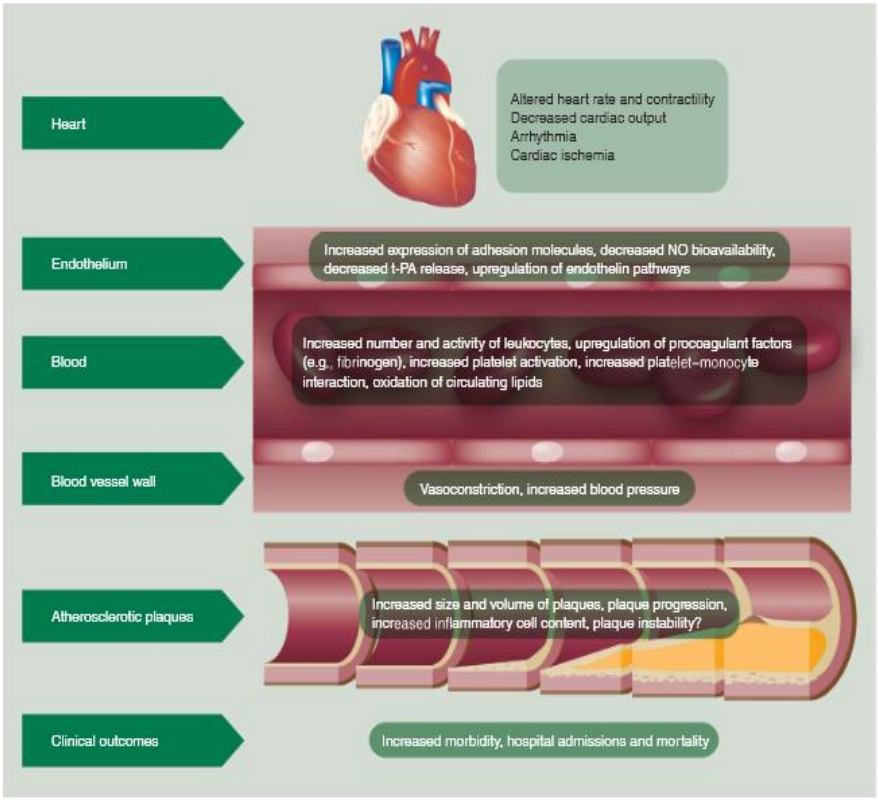

Figure 4. Cardiovascular impairments associated with pulmonary deposition of nanoparticles in epidemiological and experimental studies. These are discussed at various points in the text.
NO: Nitric oxide; t-PA: Tissue plasminogen activator.

system [42]. This is perhaps the most clearly defined hypothesis, with a clear mechanistic route from lung to cardiovascular system, and the only hypothesis currently able to explain the rapid (within 1–4 h) effects of air pollution. The evidence for this link is relatively consistent in terms of the effects of CDNPs on the heart and, for example, heart rate variability; however, the relevance of this pathway for the vascular and blood effects is more obscure.

It is apparent that the research community have some way to go to reach a definitive answer to the question of mechanism. Undoubtedly, the lack of a coherent answer is in part due to it being unfeasible that a simple single pathway is responsible for such complex, varied and diverse adverse outcomes. It is possible that all three pathways play a role affecting some parts of the cardiovascular system but not others. Furthermore, there is great potential for interaction between the proposed pathways, for example, potential for inflammatory cells to aid particle translocation by increasing alveolar permeability or actively carrying particles into the blood, amplification of the actions of blood-borne particles by circulating inflammatory cells or stimulation of sensory receptors in the lung by the particle-induced inflammatory response rather than by the particles themselves.

Mechanism after injection of medical NPs into the circulation

There are no diseases associated with the injection of medical NPs, but minor effects of some NP types on elements of the blood at high doses have been detected. Further work is required to identify whether injection of high doses of these NPs might impact on the procoagulant state

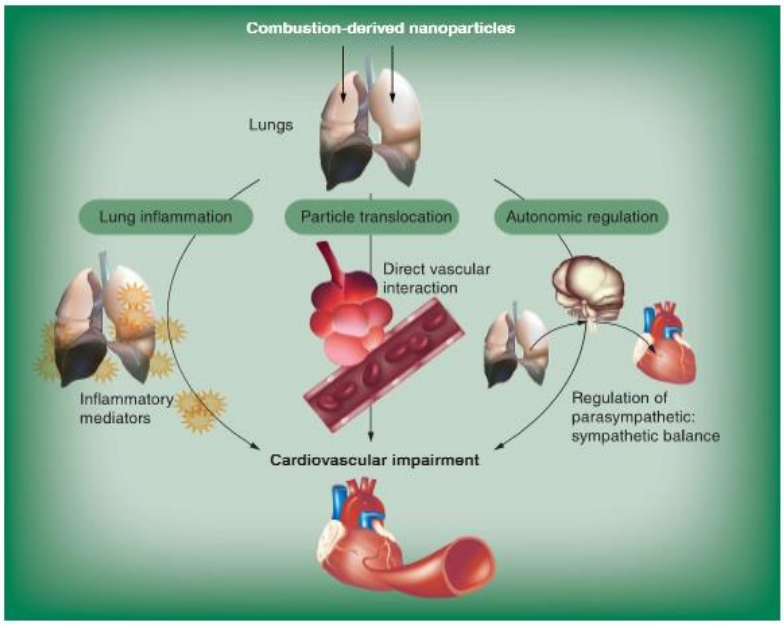

Figure 5. Three hypothetical pathways whereby nanoparticles that deposit in the lungs could impact the cardiovascular system and cause the impairments shown in Figure 4.

of the blood. SPION locate to atherosclerotic plaques which can be used for imaging but also provides a pathogenic mechanism for rupture of plaques if their presence in the plaque initiates inflammation. More research is needed into this aspect of the uses of medical NPs.

Conclusion

Exposure to CDNPs in air pollution is linked to adverse cardiovascular actions in both healthy individuals and, especially, individuals with pre-existing cardiovascular disease. Epidemiological studies have demonstrated evidence of both acute (within hours to days) and chronic (years) effects. Controlled chamber studies exposing volunteers to ultrafine fractions of ambient particles (usually urban in source) and diesel exhaust, the major source of NPs in the urban particle cloud, back up these observations. The measurable clinical effects associated with CDNP exposure include endothelial dysfunction, increased blood pressure, dysrhythmia, myocardial ischemia and procoagulant changes.

Cell culture and animal models have provided much insight into the underlying processes occurring in cells and tissues following exposure. In animal models there are clear effects consistent with human observations, including impaired vascular function, autonomic-induced changes to cardiac function, procoagulant actions through interactions with inflammatory mediators and exacerbation of atherosclerosis. Both animal and cell experiments have implicated the following mechanisms for the cardiovascular actions of CDNPs: oxidative stress, loss of NO bioavailability, proinflammatory changes in endothelial cell function (e.g., adhesion receptor upregulation) and release of inflammatory cytokines into the systemic circulation. The relative roles of the signaling pathways responsible for the cardiovascular effects of CDNP inhalation (e.g., inflammation vs translocation vs neurohumoral activity) and the constituents of CDNPs that mediate these effects (e.g., transition metals and surface organics) requires further investigation.

Similar effects are described in animal and cell models exposed to MNPs, particularly in relation to a proinflammatory and procoagulant effect of MNPs, although there is also evidence for detrimental actions on the microcirculation and atherosclerosis. However, at present there are essentially no scientific data available on the

effects of either high levels of exposure of MNPs in occupational settings, or epidemiological data on low chronic exposure of MNPs on the wider population, owing to the relatively recent large-scale use of these materials. Nevertheless, medical uses of NPs are increasing, especially for imaging purposes, and vigilance is needed to ensure resolution of the apparent paradox of using NPs in conditions where other classes of NP would have potent toxicological effects (e.g., injection into the blood).

In summary, CDNP exposure is associated with a multitude of detrimental cardiovascular effects, therefore, it is essential that all new NP medicinal products are fully tested, with particular regard to the cardiovascular system, to ensure that accidental occupational or prolonged environment exposure to these nanomaterials is not associated with similar cardiovascular toxicity.

Future perspective

Over the next 10–15 years we can look forward to two major developments in this area: an increased understanding of the mechanism of cardiovascular effects of NPs that might enable interventional strategies; and sufficient data for a structure–toxicity model for the toxicity of MNPs that would allow benign-by-design NPs to be developed. For the foreseeable future there will be ongoing environmental exposure to CDNPs, with a cardiovascular impact that can be deemed modifiable if the mechanism was known. Additional interventions can be considered other than nonspecific reductions in PM that require changes to legislation, which are slow to put in place and often difficult to enforce. This modification could be at the level of emission-reduction technologies, which would seek to decrease the most toxicologically potent component of the particles (e.g., metals), if this were known. Alternatively, if sufficient knowledge of pathophysiology were to emerge, then intervention could be at the level of the individual's biochemistry through a type of dietary supplement, for example. With regards to MNPs, a fuller understanding of the NP structures that dictate toxic potency would allow at least the potential for manufacturers to make safer NPs. A qualifier of this is that decreasing the most harmful structural characteristics must not decrease the utility of the NP for its particular industrial use. Therefore, while there is a clear disparity between the recognized toxicity of CDNPs and the widespread development of novel engineered nanomaterials, our ever increasing understanding of nanotoxicity should allow for the design of safe nanomaterials for wide-ranging applications, even for the identification and treatment of disease itself.

Financial & competing interests disclosure

The authors have no relevant affiliations or financial involvement with any organization or entity with a financial interest in or financial conflict with the subject matter or materials discussed in the manuscript. This includes employment, consultancies, honoraria, stock ownership or options, expert testimony, grants or patents received or pending, or royalties.

No writing assistance was utilized in the production of this manuscript.

Executive summary

- There is strong epidemiological evidence suggesting that increased exposure to combustion-derived nanoparticles (CDNPs) in the form of diesel exhaust particles is associated with increased adverse cardiovascular effects readily detectable in populations in cities. The effects seen are mortality and morbidity in the short- and long-term from cardiovascular-related conditions, primarily myocardial infarction, heart failure and stroke.
- Chamber studies support the epidemiological evidence. In chamber studies, human subjects are exposed to concentrated CDNPs or particulate material under controlled conditions, and these have shown a variety of pathophysiological end points related to the cardiovascular system, such as impaired endothelial function, increased thrombogenicity and altered vasomotor function.
- In experimental toxicology models of cardiovascular effects following CDNP exposures in both *in vitro* and *in vivo* systems, the adverse effects seen in human populations are largely reproduced. This has allowed mechanisms to be studied in these systems. Relevant cells exposed to CDNPs *in vitro* show a range of responses that are relevant to adverse cardiovascular effects, including proinflammatory effects. In animal models, particle exposures cause marked adverse effects on the vasculature, the heart itself and the blood.
- Manufactured nanoparticles have been less well studied than CDNPs, but show effects consistent with those seen with CDNPs in both *in vivo* and *in vitro* models and have been particularly studied with regards to direct thrombogenic effects on platelets.
- Medical nanoparticles pose a particular problem since they can be injected into the blood intentionally for therapeutic or imaging purposes in individuals with cardiovascular disease and so pose a special risk of, for example, thrombogenicity, and are under study.
- Over the next 10 years, a better general understanding of the structural characteristics of particles that affect their toxicity should enable rational approaches to be adopted that ameliorate the adverse cardiovascular effects of nanoparticles and allow their safe use in nanomedicine.

References

Papers of special note have been highlighted as:
▪ of interest
▪▪ of considerable interest

1 Donaldson K, Seaton A. A short history of the toxicology of inhaled particles. *Part. Fibre Toxicol.* 9, 13 (2012).

2 Brown DM, Wilson MR, MacNee W, Stone V, Donaldson K. Size-dependent proinflammatory effects of ultrafine polystyrene particles: a role for surface area and oxidative stress in the enhanced activity of ultrafines. *Toxicol. Appl. Pharmacol.* 175, 191–199 (2001).

3 Kreyling WG, Moller W, Semmler-Behnke M, Oberdorster G. Particle dosimetry: deposition and clearance from the respiratory tract and translocaton to extra-pulmonary sites. In: *Particle Toxicology.* Donaldson K, Borm P (Eds). CRC Press, FL, USA, 47–74 (2007).

4 Yu CP, Hu JP. Diffusional deposition of ultrafine particles in the human lung. In: *Aerosols in the Mining and Industrial Work Environments.* Marple VA, Liu VYH (Eds). Ann Arbor Sciences, MI, USA, 139–149 (1983).

5 Sun JD, Wolff RK, Kanapilly GM, McClellan RO. Lung retention and metabolic fate of inhaled benzo(a)pyrene associated with diesel exhaust particles. *Toxicol. Appl. Pharmacol.* 73, 48–59 (1984).

6 Lam HF, Conner MW, Rogers AE, Fitzgerald S, Amdur MO. Functional and morphologic changes in the lungs of guinea pigs exposed to freshly generated ultrafine zinc oxide. *Toxicol. Appl. Pharmacol.* 78, 29–38 (1985).

7 Ferin J, Oberdorster G, Penney DP. Pulmonary retention of ultrafine and fine particles in rats. *Am. J. Respir. Cell Mol. Biol.* 6, 535–542 (1992).

8 Brown DM, Stone V, Findlay P, MacNee W, Donaldson K. Increased inflammation and intracellular calcium caused by ultrafine carbon black is independent of transition metals or other soluble components. *Occup. Environ. Med.* 57, 685–691 (2000).

9 Tran CL, Buchanan D, Cullen RT, Searl A, Jones AD, Donaldson K. Inhalation of poorly soluble particles. II. Influence of particle surface area on inflammation and clearance. *Inhal. Toxicol.* 12, 1113–1126 (2000).

10 Donaldson K, Tran L, Jimenez L *et al.* Combustion-derived nanoparticles: a review of their toxicology following inhalation exposure. *Part. Fibre Toxicol.* 2, 10 (2005).

11 Stoeger T, Takenaka S, Frankenberger B *et al.* Deducing *in vivo* toxicity of combustion-derived nanoparticles from a cell-free oxidative potency assay and metabolic activation of organic compounds. *Environ. Health Perspect.* 117, 54–60 (2009).

12 Neumann HG. Health risk of combustion products: toxicological considerations. *Chemosphere* 42, 473–479 (2001).

13 Donaldson K, Mills N, MacNee W, Robinson S, Newby D. Role of inflammation in cardiopulmonary health effects of PM. *Toxicol. Appl. Pharmacol.* 207, 483–488 (2005).

14 Mills NL, Donaldson K, Hadoke PW *et al.* Adverse cardiovascular effects of air pollution. *Nat. Clin. Pract. Cardiovasc. Med.* 6(1), 36–44 (2008).

15 Langrish JP, Mills NL, Newby DE. Air pollution: the new cardiovascular risk factor. *Intern. Med. J.* 38, 875–878 (2008).

16 Gupta AS. Nanomedicine approaches in vascular disease: a review. *Nanomedicine* 7, 763–779 (2011).

17 Donaldson K, Seaton A. The Janus faces of nanoparticles. *J. Nanosci. Nanotechnol.* 7, 4607–4611 (2007).

18 Borm PJ, Muller-Schulte D. Nanoparticles in drug delivery and environmental exposure: same size, same risks? *Nanomedicine (Lond.)* 1, 235–249 (2006).

19 Donaldson K. Resolving the nanoparticles paradox. *Nanomedicine* 1, 229–234 (2006).

20 WHO. Exposure to air pollution:a major public health concern. In: *Preventing Disease Through Healthy Environments.* WHO, Geneva, Switzerland (2010).

21 Nemery B, Hoet PH, Nemmar A. The Meuse Valley fog of 1930: an air pollution disaster. *Lancet* 357, 704–708 (2001).

22 Stone R. Air pollution. Counting the cost of London's killer smog. *Science* 298, 2106–2107 (2002).

23 Brunekreef B, Holgate ST. Air pollution and health. *Lancet* 360, 1233–1242 (2002).

24 Miller KA, Siscovick DS, Sheppard L *et al.* Long-term exposure to air pollution and incidence of cardiovascular events in women. *N. Engl. J. Med.* 356, 447–458 (2007).

25 Dockery DW, Pope CA, Xu XP *et al.* An association between air-pollution and mortality in six U.S. cities. *N. Engl. J. Med.* 329(24), 1753–1759 (1993).

26 Pope CA, Thun MJ, Namboodiri MM *et al.* Particulate air pollution as a predictor of mortality in a prospective study of U.S. adults. *Am. J. Respir. Crit. Care Med.* 151(3 Pt 1), 669–674 (1995).

27 Schwartz J. Air pollution and blood markers of cardiovascular risk. *Environ. Health Perspect.* 109(Suppl. 3), 405–409 (2001).

▪ **Ground-breaking study demonstrating the relationship between particle exposure and cardiovascular effects.**

28 Kunzli N, Jerrett M, Mack WJ *et al.* Ambient air pollution and atherosclerosis in Los Angeles. *Environ. Health Perspect.* 113, 201–206 (2005).

▪ **Key study demonstrating the contribution of air pollution to atherosclerosis development.**

29 Mustafic H, Jabre P, Caussin C *et al.* Main air pollutants and myocardial infarction: a systematic review and meta-analysis. *JAMA* 307, 713–721 (2012).

30 Peters A, von Klot S, Heier M *et al.* Exposure to traffic and the onset of myocardial infarction. *N. Engl. J. Med.* 351, 1721–1730 (2004).

31 Nawrot TS, Perez L, Kunzli N, Munters E, Nemery B. Public health importance of triggers of myocardial infarction: a comparative risk assessment. *Lancet* 377, 732–740 (2011).

32 Roger VL, Go AS, Lloyd-Jones DM *et al.* Executive summary: heart disease and stroke statistics – 2012 update: a report from the American Heart Association. *Circulation* 125, 188–197 (2012).

33 Jencks SF, Williams MV, Coleman EA. Rehospitalizations among patients in the medicare fee-for-service program. *N. Engl. J. Med.* 360, 1418–1428 (2009).

34 Dominici F, McDermott A, Zeger SL, Samet JM. On the use of generalized additive models in time-series studies of air pollution and health. *Am. J. Epidemiol.* 156, 193–203 (2002).

35 Ueda K, Nitta H, Ono M. Effects of fine particulate matter on daily mortality for specific heart diseases in Japan. *Circ. J.* 73, 1248–1254 (2009).

36 Silverman RA, Ito K, Freese J *et al.* Association of ambient fine particles with out-of-hospital cardiac arrests in New York City. *Am. J. Epidemiol.* 172, 917–923 (2010).

37 Jemal A, Ward E, Hao Y, Thun M. Trends in the leading causes of death in the United States, 1970-2002. *JAMA* 294(10), 1255–1259 (2005).

38 Committee on the Medical Effects of Air Pollutants. *Cardiovascular disease and air pollution. 2006.* Department of Health, London, UK, 1–215 (2006).

39 Ghio AJ, Huang YC. Exposure to concentrated ambient particles (CAPs): a review. *Inhal. Toxicol.* 16, 53–59 (2004).

40 Brook RD, Brook JR, Urch B, Vincent R, Rajagopalan S, Silverman F. Inhalation of fine particulate air pollution and ozone causes acute arterial vasoconstriction in healthy adults. *Circulation* 105, 1534–1536 (2002).

41 Urch B, Silverman F, Corey P *et al.* Acute blood pressure responses in healthy adults

during controlled air pollution exposures. *Environ. Health Perspect.* 113, 1052–1055 (2005).

42 Brook RD, Urch B, Dvonch JT *et al.* Insights into the mechanisms and mediators of the effects of air pollution exposure on blood pressure and vascular function in healthy humans. *Hypertension* 54, 659–667 (2009).

43 Peretz A, Sullivan JH, Leotta DF *et al.* Diesel exhaust inhalation elicits acute vasoconstriction *in vivo*. *Environ. Health Perspect.* 116, 937–942 (2008).

44 Lundback M, Mills NL, Lucking A *et al.* Experimental exposure to diesel exhaust increases arterial stiffness in man. *Part. Fibre Toxicol.* 6, 7 (2009).

45 Chang LT, Tang CS, Pan YZ, Chan CC. Association of heart rate variability of the elderly with personal exposure to PM 1, PM 1–2.5, and PM 2.5–10. *Bull. Environ. Contam. Toxicol.* 79, 552–556 (2007).

46 Arito H, Takahashi M, Iwasaki T, Uchiyama I. Age-related changes in ventilatory and heart rate responses to acute ozone exposure in the conscious rat. *Ind. Health* 35, 78–86 (1997).

47 Park SK, O'neill MS, Vokonas PS, Sparrow D, Schwartz J. Effects of air pollution on heart rate variability: the VA normative aging study. *Environ. Health Perspect.* 113, 304–309 (2005).

48 Heart rate variability: standards of measurement, physiological interpretation and clinical use. Task Force of the European Society of Cardiology and the North American Society of Pacing and Electrophysiology. *Circulation* 93(5), 1043–1065 (1996).

49 Mills NL, Finlayson AE, Gonzalez MC *et al.* Diesel exhaust inhalation does not affect heart rhythm or heart rate variability. *Heart* 97, 544–550 (2011).

50 Devlin RB, Ghio AJ, Kehrl H, Sanders G, Cascio W. Elderly humans exposed to concentrated air pollution particles have decreased heart rate variability. *Eur. Respir. J. Suppl.* 40, 576–580 (2003).

51 Routledge HC, Chowdhary S, Townend JN. Heart rate variability – a therapeutic target? *J. Clin. Pharm. Ther.* 27, 85–92 (2002).

52 de Hartog JJ, Lanki T, Timonen KL *et al.* Associations between PM2.5 and heart rate variability are modified by particle composition and beta-blocker use in patients with coronary heart disease. *Environ. Health Perspect.* 117, 105–111 (2009).

53 Campen MJ, Nolan JP, Schladweiler MC, Kodavanti UP, Costa DL, Watkinson WP. Cardiac and thermoregulatory effects of instilled particulate matter-associated transition metals in healthy and cardiopulmonary-compromised rats. *J. Toxicol. Environ. Health A* 65, 1615–1631 (2002).

54 Mills NL, Tornqvist H, Gonzalez MC *et al.* Ischemic and thrombotic effects of dilute diesel-exhaust inhalation in men with coronary heart disease. *N. Engl. J. Med.* 357, 1075–1082 (2007).

** **Demonstrates that acute exposure to dilute diesel exhaust increases electrocardiographic measures of myocardial ischemia in men with coronary heart disease.**

55 Mills NL, Tornqvist H, Robinson SD *et al.* Diesel exhaust inhalation causes vascular dysfunction and impaired endogenous fibrinolysis. *Circulation* 112, 3930–3936 (2005).

** **Important paper demonstrating that inhalation of diesel particles impairs endothelial function in normal human subjects.**

56 Cardillo C, Campia U, Kilcoyne CM, Bryant MB, Panza JA. Improved endothelium-dependent vasodilation after blockade of endothelin receptors in patients with essential hypertension. *Circulation* 105, 452–456 (2002).

57 Langrish JP, Unosson B, Bosson J. Diesel exhaust inhalation induced vascular dysfunction: the role of nitric oxide. *Am. J. Resp. Crit. Care Med.* 57(14), E1429 (2011).

58 Mills NL, Miller MR, Lucking AJ *et al.* Combustion-derived nanoparticulate induces the adverse vascular effects of diesel exhaust inhalation. *Eur. Heart J.* 32, 2660–2671 (2011).

* **Important study demonstrating that particles, not gases, mediate the adverse vascular impacts of diesel exhaust.**

59 Mills NL, Robinson SD, Fokkens PH *et al.* Exposure to concentrated ambient particles does not affect vascular function in patients with coronary heart disease. *Environ. Health Perspect.* 116, 709–715 (2008).

60 Lucking AJ, Lundback M, Mills NL *et al.* Diesel exhaust inhalation increases thrombus formation in man. *Eur. Heart J.* 29, 3043–3051 (2008).

61 Miller MR, Shaw CA, Langrish JP. From particles to patients: oxidative stress and the cardiovascular effects of air pollution. *Future Cardiol.* 8, 577–602 (2012).

62 Aung HH, Lame MW, Gohil K *et al.* Comparative gene responses to collected ambient particles *in vitro*: endothelial responses. *Physiol. Genomics* 43, 917–929 (2011).

63 Karoly ED, Li Z, Dailey LA, Hyseni X, Huang YC. Up-regulation of tissue factor in human pulmonary artery endothelial cells after ultrafine particle exposure. *Environ. Health Perspect.* 115, 535–540 (2007).

64 Lee CC, Huang SH, Yang YT, Cheng YW, Li CH, Kang JJ. Motorcycle exhaust particles up-regulate expression of vascular adhesion molecule-1 and intercellular adhesion molecule-1 in human umbilical vein endothelial cells. *Toxicol. In Vitro* 26, 552–560 (2012).

65 Forchhammer L, Loft S, Roursgaard M *et al.* Expression of adhesion molecules, monocyte interactions and oxidative stress in human endothelial cells exposed to wood smoke and diesel exhaust particulate matter. *Toxicol. Lett.* 209, 121–128 (2012).

66 Frikke-Schmidt H, Roursgaard M, Lykkesfeldt J, Loft S, Nojgaard JK, Moller P. Effect of vitamin C and iron chelation on diesel exhaust particle and carbon black induced oxidative damage and cell adhesion molecule expression in human endothelial cells. *Toxicol. Lett.* 203, 181–189 (2011).

67 Montiel-Davalos A, Alfaro-Moreno E, Lopez-Marure R. PM2.5 and PM10 induce the expression of adhesion molecules and the adhesion of monocytic cells to human umbilical vein endothelial cells. *Inhal. Toxicol.* 19(Suppl. 1), 91–98 (2007).

68 Li R, Ning Z, Cui J *et al.* Ultrafine particles from diesel engines induce vascular oxidative stress via JNK activation. *Free Radic. Biol. Med.* 46, 775–782 (2009).

69 Chao MW, Po IP, Laumbach RJ, Koslosky J, Cooper K, Gordon MK. DEP induction of ROS in capillary-like endothelial tubes leads to VEGF-A expression. *Toxicology* 297, 34–46 (2012).

70 Chao MW, Kozlosky J, Po IP *et al.* Diesel exhaust particle exposure causes redistribution of endothelial tube VE-cadherin. *Toxicology* 279, 73–84 (2011).

71 Li R, Ning Z, Cui J, Yu F, Sioutas C, Hsiai T. Diesel exhaust particles modulate vascular endothelial cell permeability: implication of ZO1 expression. *Toxicol. Lett.* 197, 163–168 (2010).

72 Sumanasekera WK, Ivanova MM, Johnston BJ *et al.* Rapid effects of diesel exhaust particulate extracts on intracellular signaling in human endothelial cells. *Toxicol. Lett.* 174, 61–73 (2007).

73 Nemmar A, Hoet PH, Vanquickenborne B *et al.* Passage of inhaled particles into the blood circulation in humans. *Circulation* 105, 411–414 (2002).

74 Mills N, Amin N, Robinson S *et al.* Do inhaled carbon nanoparticles translocate directly into the circulation in humans? *Am. J. Resp. Crit. Care Med.* 173(4), 426–431 (2006).

75 Kreyling WG, Semmler M, Erbe F *et al.* Translocation of ultrafine insoluble iridium particles from lung epithelium to

extrapulmonary organs is size dependent but very low. *J. Toxicol. Environ. Health A* 65, 1513–1530 (2002).

76 Kristovich R, Knight DA, Long JF. Macrophage-mediated endothelial inflammatory responses to airborne particulates: impact of particulate physicochemical properties. *Chem. Res. Toxicol.* 17, 1303–1312 (2004).

77 Shaw CA, Robertson S, Miller MR *et al.* Diesel particulate-exposed macrophages cause marked endothelial cell activation. *Am. J. Respir. Cell Mol. Biol.* 44(6), 840–851 (2010).

78 Weldy CS, Wilkerson HW, Larson TV, Stewart JA, Kavanagh TJ. DIESEL particulate exposed macrophages alter endothelial cell expression of eNOS, iNOS, MCP1, and glutathione synthesis genes. *Toxicol. In Vitro* 25, 2064–2073 (2011).

79 Channell MM, Paffett ML, Devlin RB, Madden MC, Campen MJ. Circulating factors induce coronary endothelial cell activation following exposure to inhaled diesel exhaust and nitrogen dioxide in humans: evidence from a novel translational *in vitro* model. *Toxicol. Sci.* 127, 179–186 (2012).

80 Siegel PD, Saxena RK, Saxena QB *et al.* Effect of diesel exhaust particulate (DEP) on immune responses: contributions of particulate versus organic soluble components. *J. Toxicol. Environ. Health A* 67, 221–231 (2004).

81 Yin XJ, Dong CC, Ma JY, Roberts JR, Antonini JM, Ma JK. Suppression of phagocytic and bactericidal functions of rat alveolar macrophages by the organic component of diesel exhaust particles. *J. Toxicol. Environ. Health A* 70, 820–828 (2007).

82 Li R, Ning Z, Majumdar R *et al.* Ultrafine particles from diesel vehicle emissions at different driving cycles induce differential vascular pro-inflammatory responses: implication of chemical components and NF-kappaB signaling. *Part. Fibre Toxicol.* 7, 6 (2010).

83 Møller P, Mikkelsen L, Vesterdal LK *et al.* Hazard identification of particulate matter on vasomotor dysfunction and progression of atherosclerosis. *Crit. Rev. Toxicol.* 41, 339–368 (2011).

84 Miller MR, Borthwick SJ, Shaw CA *et al.* Direct impairment of vascular function by diesel exhaust particulate through reduced bioavailability of endothelium-derived nitric oxide induced by superoxide free radicals. *Environ. Health Perspect.* 117, 611–616 (2009).

** **Demonstrates the mechanism for impact of exposure to nanoparticles on nitric oxide-dependent vascular function.**

85 Quan C, Sun Q, Lippmann M, Chen LC. Comparative effects of inhaled diesel exhaust and ambient fine particles on inflammation, atherosclerosis, and vascular dysfunction. *Inhal. Toxicol.* 22, 738–753 (2010).

86 Mills N, Miller MR. Particles and the vascular endothelium. In: *Cardiovascular Effects of Inhaled Ultrafine and Nanosized Particles.* Cassee F, Mills N, Newby D (Eds). J Wiley & Sons Inc, NJ, USA, 379–402 (2011).

87 Araujo JA, Barajas B, Kleinman M *et al.* Ambient particulate pollutants in the ultrafine range promote early atherosclerosis and systemic oxidative stress. *Circ. Res.* 102, 589–596 (2008).

88 Campen MJ, Lund AK, Knuckles TL *et al.* Inhaled diesel emissions alter atherosclerotic plaque composition in *ApoE*$^{(-/-)}$ mice. *Toxicol. Appl. Pharmacol.* 242, 310–317 (2010).

89 Sun Q, Yue P, Kirk RI *et al.* Ambient air particulate matter exposure and tissue factor expression in atherosclerosis. *Inhal. Toxicol.* 20, 127–137 (2008).

90 Ying Z, Kampfrath T, Thurston G *et al.* Ambient particulates alter vascular function through induction of reactive oxygen and nitrogen species. *Toxicol. Sci.* 111, 80–88 (2009).

91 Ikeda M, Shitashige M, Yamasaki H, Sagai M, Tomita T. Oxidative modification of low density lipoprotein by diesel exhaust particles. *Biol. Pharm. Bull.* 18, 866–871 (1995).

92 Gong KW, Zhao W, Li N *et al.* Air-pollutant chemicals and oxidized lipids exhibit genome-wide synergistic effects on endothelial cells. *Genome Biol.* 8, R149 (2007).

93 Sun Q, Wang A, Jin X *et al.* Long-term air pollution exposure and acceleration of atherosclerosis and vascular inflammation in an animal model. *JAMA* 294, 3003–3010 (2005).

94 Lund AK, Lucero J, Lucas S *et al.* Vehicular emissions induce vascular MMP-9 expression and activity associated with endothelin-1-mediated pathways. *Arterioscler. Thromb. Vasc. Biol.* 29, 511–517 (2009).

95 Ying Z, Yue P, Xu X *et al.* Air pollution and cardiac remodeling: a role for RhoA/Rho-kinase. *Am. J. Physiol. Heart Circ. Physiol.* 296, H1540–H1550 (2009).

96 Cozzi E, Hazarika S, Stallings HW 3rd *et al.* Ultrafine particulate matter exposure augments ischemia-reperfusion injury in mice. *Am. J. Physiol. Heart Circ. Physiol.* 291, H894–H903 (2006).

97 Yan YH, Chou CC, Lee CT, Liu JY, Cheng TJ. Enhanced insulin resistance in diet-induced obese rats exposed to fine particles by instillation. *Inhal. Toxicol.* 23, 507–519 (2011).

98 Emmerechts J, Alfaro-Moreno E, Vanaudenaerde BM, Nemery B, Hoylaerts MF. Short-term exposure to particulate matter induces arterial but not venous thrombosis in healthy mice. *J. Thromb. Haemost.* 8, 2651–2661 (2010).

99 Emmerechts J, Hoylaerts MF. The effect of air pollution on haemostasis. *Hamostaseologie* 32, 5–13 (2012).

100 Nemmar A, Nemery B, Hoet PH, Vermylen J, Hoylaerts MF. Pulmonary inflammation and thrombogenicity caused by diesel particles in hamsters: role of histamine. *Am. J. Respir. Crit. Care Med.* 168, 1366–1372 (2003).

101 Nemmar A, Zia S, Subramaniyan D, Fahim MA, Ali BH. Exacerbation of thrombotic events by diesel exhaust particle in mouse model of hypertension. *Toxicology* 285, 39–45 (2011).

102 Radomski A, Jurasz P, Alonso-Escolano D *et al.* Nanoparticle-induced platelet aggregation and vascular thrombosis. *Br. J. Pharmacol.* 146, 882–893 (2005).

103 Schulte PA, Trout DB. Nanomaterials and worker health: medical surveillance, exposure registries, and epidemiologic research. *J. Occup. Environ. Med.* 53, S3–S7 (2011).

104 Kang GS, Gillespie PA, Gunnison A, Moreira AL, Tchou-Wong KM, Chen LC. Long-term inhalation exposure to nickel nanoparticles exacerbated atherosclerosis in a susceptible mouse model. *Environ. Health Perspect.* 119, 176–181 (2011).

105 Vesterdal LK, Folkmann JK, Jacobsen NR *et al.* Pulmonary exposure to carbon black nanoparticles and vascular effects. *Part. Fibre Toxicol.* 7, 33 (2010).

106 Mikkelsen L, Sheykhzade M, Jensen KA *et al.* Modest effect on plaque progression and vasodilatory function in atherosclerosis-prone mice exposed to nanosized TiO(2). *Part. Fibre Toxicol.* 8, 32 (2011).

107 Li Z, Hulderman T, Salmen R *et al.* Cardiovascular effects of pulmonary exposure to single-wall carbon nanotubes. *Environ. Health Perspect.* 115, 377–382 (2007).

108 LeBlanc AJ, Cumpston JL, Chen BT, Frazer D, Castranova V, Nurkiewicz TR. Nanoparticle inhalation impairs endothelium-dependent vasodilation in subepicardial arterioles. *J. Toxicol. Environ. Health A* 72, 1576–1584 (2009).

109 Khandoga A, Stampfl A, Takenaka S *et al.* Ultrafine particles exert prothrombotic but not inflammatory effects on the hepatic microcirculation in healthy mice *in vivo*. *Circulation* 109, 1320–1325 (2004).

110 McGuinnes C, Duffin R, Brown S *et al.* Surface derivatization state of polystyrene latex nanoparticles determines both their potency and their mechanism of causing

human platelet aggregation *in vitro*. *Toxicol. Sci.* 119, 359–368 (2011).

111 Corbalan JJ, Medina C, Jacoby A, Malinski T, Radomski MW. Amorphous silica nanoparticles aggregate human platelets: potential implications for vascular homeostasis. *Int. J. Nanomedicine* 7, 631–639 (2012).

112 Burke AR, Singh RN, Carroll DL *et al.* Determinants of the thrombogenic potential of multiwalled carbon nanotubes. *Biomaterials* 32, 5970–5978 (2011).

113 Singh SK, Singh MK, Kulkarni PP, Sonkar VK, Gracio JJ, Dash D. Amine-modified graphene: thrombo-protective safer alternative to graphene oxide for biomedical applications. *ACS Nano* 6, 2731–2740 (2012).

114 Erdely A, Hulderman T, Salmen R *et al.* Cross-talk between lung and systemic circulation during carbon nanotube respiratory exposure. Potential biomarkers. *Nano Lett.* 9, 36–43 (2009).

115 Pai AB, Nielsen JC, Kausz A, Miller P, Owen JS. Plasma pharmacokinetics of two consecutive doses of ferumoxytol in healthy subjects. *Clin. Pharmacol. Ther.* 88, 237–242 (2010).

116 Richards JM, Semple SI, Macgillivray TJ *et al.* Abdominal aortic aneurysm growth predicted by uptake of ultrasmall superparamagnetic particles of iron oxide: a pilot study. *Circ. Cardiovasc. Imaging* 4, 274–281 (2011).

117 Wang H, Zhao Y, Wu Y *et al.* Enhanced anti-tumor efficacy by co-delivery of doxorubicin and paclitaxel with amphiphilic methoxy PEG–PLGA copolymer nanoparticles. *Biomaterials* 32, 8281–8290 (2011).

118 Yilmaz A, Rosch S, Klingel K *et al.* Magnetic resonance imaging (MRI) of inflamed myocardium using iron oxide nanoparticles in patients with acute myocardial infarction – preliminary results. *Int. J. Cardiol.* doi:10.1016/j.ijcard.2011.06.004 (2011) (Epub ahead of print).

119 Hamzah J, Kotamraju VR, Seo JW *et al.* Specific penetration and accumulation of a homing peptide within atherosclerotic plaques of apolipoprotein E-deficient mice. *Proc. Natl Acad. Sci. USA* 108, 7154–7159 (2011).

120 Rosner MH, Auerbach M. Ferumoxytol for the treatment of iron deficiency. *Expert Rev. Hematol.* 4, 399–406 (2011).

121 Zhu MT, Wang Y, Feng WY *et al.* Oxidative stress and apoptosis induced by iron oxide nanoparticles in cultured human umbilical endothelial cells. *J. Nanosci. Nanotechnol.* 10, 8584–8590 (2010).

122 Zhu MT, Wang B, Wang Y *et al.* Endothelial dysfunction and inflammation induced by iron oxide nanoparticle exposure: risk factors for early atherosclerosis. *Toxicol. Lett.* 203, 162–171 (2011).

123 Lu S, Duffin R, Poland C *et al.* Efficacy of simple short-term *in vitro* assays for predicting the potential of metal oxide nanoparticles to cause pulmonary inflammation. *Environ. Health Perspect.* 117, 241–247 (2009).

124 Dick CA, Brown DM, Donaldson K, Stone V. The role of free radicals in the toxic and inflammatory effects of four different ultrafine particle types. *Inhal. Toxicol.* 15, 39–52 (2003).

125 Jendelova P, Herynek V, Urdzikova L *et al.* Magnetic resonance tracking of transplanted bone marrow and embryonic stem cells labeled by iron oxide nanoparticles in rat brain and spinal cord. *J. Neurosci. Res.* 76, 232–243 (2004).

126 Jing XH, Yang L, Duan XJ *et al.* *In vivo* MR imaging tracking of magnetic iron oxide nanoparticle labeled, engineered, autologous bone marrow mesenchymal stem cells following intra-articular injection. *Joint Bone Spine* 75, 432–438 (2008).

127 Seaton A, MacNee W, Donaldson K, Godden D. Particulate air-pollution and acute health-effects. *Lancet* 345, 176–178 (1995).

128 Van ES, Leipsic J, Paul Man SF, Sin DD. The relationship between lung inflammation and cardiovascular disease. *Am. J. Respir. Crit. Care Med.* 186, 11–16 (2012).

129 Hubbs AF, Mercer RR, Benkovic SA *et al.* Nanotoxicology – a pathologist's perspective. *Toxicol. Pathol.* 39, 301–324 (2011).

130 Geiser M, Rothen-Rutishauser B, Kapp N *et al.* Ultrafine particles cross cellular membranes by nonphagocytic mechanisms in lungs and in cultured cells. *Environ. Health Perspect.* 113, 1555–1560 (2005).

131 Oberdorster G, Sharp Z, Elder AP, Gelein R, Kreyling W, Cox C. Translocation of inhaled ultrafine particles to the brain. *Inhal. Toxicol.* 16, 437–445 (2004).

132 Moller W, Kreyling WG, Schmid O, Semmler-Behnke M, Schulz H. Deposition, retention and clearance and translocation of inhaled fine and nano-sized particles in the respiratory tract. In: *Particle–Lung Cell Interactions (2nd Edition)*. Gehr P, Muhlfeld C, Rothen-Rutishauser B, Blank F (Eds). Informa Healthcare, NY, USA, 79–107 (2010).